Title
Multicomponent Diffusion of Interacting, Nonionic Micelles with Hydrophobic Solutes

Author
Alexander, Nathan

Publication Date
2021

Peer reviewed|Thesis/dissertation

Multicomponent Diffusion of Interacting, Nonionic Micelles with Hydrophobic Solutes

By

NATHAN PERRY ALEXANDER

DISSERTATION

Submitted in partial satisfaction of the requirements for the degree of

DOCTOR OF PHILOSOPHY

in

Chemical Engineering

in the

OFFICE OF GRADUATE STUDIES

of the

UNIVERSITY OF CALIFORNIA

DAVIS

Approved:

Stephanie R. Dungan, Chair

Ronald J. Phillips

Roland Faller

Robert L. Powell

Committee in Charge

2021

Acknowledgements

I would like to thank my research advisors Prof. Stephanie Dungan and Prof. Ronald Phillips for their guidance, support, and contribution to the work presented in this thesis. I feel very fortunate to have been mentored by them, and their commitment to rigorous, fundamental analysis has significantly influenced my philosophy and approach toward scientific research, for which I am grateful. In addition, I would like to thank the remaining members of my dissertation committee, Prof. Robert Powell and Prof. Roland Faller, for their support and contribution to my professional development.

Jen Staton, Andrew Karman, Joel Christenson, and other members of the Dungan and Phillips groups, past and present, have all contributed to my wellbeing during my time in Davis. I appreciate our discussions and time spent outside of the lab.

I would like to thank my family for their support and for encouraging me to pursue my interests.

Finally, I gratefully acknowledge funding by the National Science Foundation (CBET1506474) and a Jastro-Shields fellowship from the University of California at Davis.

Abstract

In this thesis, we examine diffusion in ternary, aqueous solutions of the nonionic surfactant decaethylene glycol monododecyl ether ($C_{12}E_{10}$) and a hydrophobic solute, either decane or limonene. In solution, the surfactant molecules self-assemble to form micelles swollen by hydrophobic solutes, with essentially no free hydrophobic solute or surfactant monomer in the surrounding solvent. The diffusive behavior of this system is very interesting in that surfactant-solute interactions are strong, and result in a highly non-diagonal diffusivity matrix [**D**], which depends in part on how strongly micelles grow with an increasing amount of solubilizate along the diffusion pathway. This behavior is distinct from that of colloidal dispersions comprised of polydisperse rigid hard particles, which are unable to reassemble on a molecular level to lower the system free energy as they diffuse. The goal of this work is to present experimental data and develop rigorous theoretical results that capture the influence of self-assembly on the ternary diffusion coefficient matrix [**D**], and on the time and static correlation functions that are commonly used to analyze light scattering data in these mixtures.

In Chapter 1, ternary diffusion coefficient matrices [**D**] and morphological parameters, such as the micelle aggregation number, hydrodynamic radius, and hydration index, were measured using the Taylor dispersion method and static and dynamic light scattering techniques, respectively, for $C_{12}E_{10}$/decane/water solutions. The matrix [**D**] for this system was found to be highly non-diagonal, and concentration dependent, over a broad domain of solute to surfactant molar ratios, and micelle volume fractions up to $\phi \approx 0.25$. Measurements for the average micelle radius and aggregation number indicate a weak dependence on the micelle volume fraction but a strong linear increase with the solute-to-surfactant molar ratio. Furthermore, a

theoretical model, based on Batchelor's theory for gradient diffusion in dilute, polydisperse mixtures of interacting spheres is developed and effectively used to predict [**D**] with no adjustable parameters. In this model, a Poisson distribution of solute molecules among micelles was assumed with a one-to-one correspondence between the number of solute to surfactant molecules distinguishing each micelle species.

In Chapter 2, experimental data for the ternary diffusion coefficient matrices [**D**] are presented for crowded ternary mixtures of $C_{12}E_{10}$ surfactant with either decane or limonene solute. Our theoretical model for [**D**], which was introduced in Chapter 1, is simplified by neglecting local polydispersity. Even though the model originates from dilute theory that incorporates pairwise hydrodynamic and thermodynamic interactions, the theoretical results were in surprisingly good agreement with experimental data for concentrated mixtures, with volume fractions up to $\phi \approx 0.47$. This agreement suggests that the effects of many-particle hydrodynamic and thermodynamic interactions cancel, resulting in experimental and theoretical predictions that are nearly linear over the entire range of concentration. In addition, the theory predicts eigenvalues D_- and D_+ that correspond to long-time self and gradient diffusion coefficients, respectively, for monodisperse spheres, in reasonable agreement with experimental data.

The third and final chapter of this thesis involves the development of model equations for the Rayleigh ratio and the mode amplitudes of the normalized electric field autocorrelation function, which are commonly used to analyze time averaged and photon correlation spectroscopy data, respectively. These theoretical results were derived using thermodynamic fluctuation theory applied to crowded solute-containing micellar solutions and microemulsions

with negligible molecular species and polydispersity. This theory invokes nonequilibrium thermodynamics and enforces local equilibrium between molecular solute, surfactant, and the various micellar species, in order to support the influence of self-assembly on the light scattering functions for the first time. We find that micelle growth effects along the diffusion path in these mixtures, which were shown to drive strong multicomponent diffusion effects, expressed via the ternary diffusivity matrix $[\mathbf{D}]$, do not affect the scattering functions in the limit of zero local polydispersity. Hence, theoretical predictions for the Rayleigh ratio and the field autocorrelation function for ternary mixtures of solute-containing, locally monodisperse micellar solutions are identical to those developed for binary mixtures of monodisperse, colloidal hard spheres. However, micelle growth effects are predicted to influence the thermodynamic driving forces and eigenmodes for diffusion. In support of our theoretical results, measurements for the Rayleigh ratio and the field autocorrelation function for ternary aqueous solutions of decaethylene glycol monododecyl ether ($C_{12}E_{10}$) with either decane or limonene solute were performed for several molar ratios and volume fractions up to $\phi \approx 0.25$, and for binary mixtures of $C_{12}E_{10}$/water up to $\phi \approx 0.5$. Excellent agreement between our light scattering theory and experimental data is achieved for low to moderate volume fractions ($\phi < 0.3$) and at higher concentration when our volume fraction calculations are corrected to account for micelle dehydration.

Contents

Outline

In Chapter 1, ternary diffusion coefficient matrices [**D**] and morphological parameters, such as the micelle aggregation number, hydrodynamic radius, and hydration index, are presented as a function of either volume fraction or the solute to surfactant molar ratio for $C_{12}E_{10}$/decane/water solutions. A theoretical model, based on Batchelor's theory for gradient diffusion in dilute, polydisperse mixtures of interacting spheres is developed. In this model, a Poisson distribution of solute molecules among micelles was assumed with a one-to-one correspondence between the number of solute to surfactant molecules distinguishing each micelle species.

In Chapter 2, experimental data for the ternary diffusion coefficient matrices [**D**], acquired using the Taylor dispersion method, are presented for crowded ternary mixtures of $C_{12}E_{10}$ surfactant with either decane or limonene solute. Our theoretical model for [**D**], which was introduced in Chapter 1, is simplified by neglecting local polydispersity.

Finally, in Chapter 3, model equations for the Rayleigh ratio and the normalized time correlation function for the scattered electric field are derived using thermodynamic fluctuation theory applied to crowded solute-containing micellar solutions and microemulsions with negligible molecular species and polydispersity. In addition, measurements for the Rayleigh ratio and the field autocorrelation function for ternary aqueous solutions of decaethylene glycol monododecyl ether ($C_{12}E_{10}$) with either decane or limonene solute were performed for several molar ratios and volume fractions up to $\phi \approx 0.25$, and for binary mixtures of $C_{12}E_{10}$/water up to $\phi \approx 0.5$.

Chapter 1

Multicomponent Diffusion in Aqueous Solutions of Nonionic Micelles and Decane

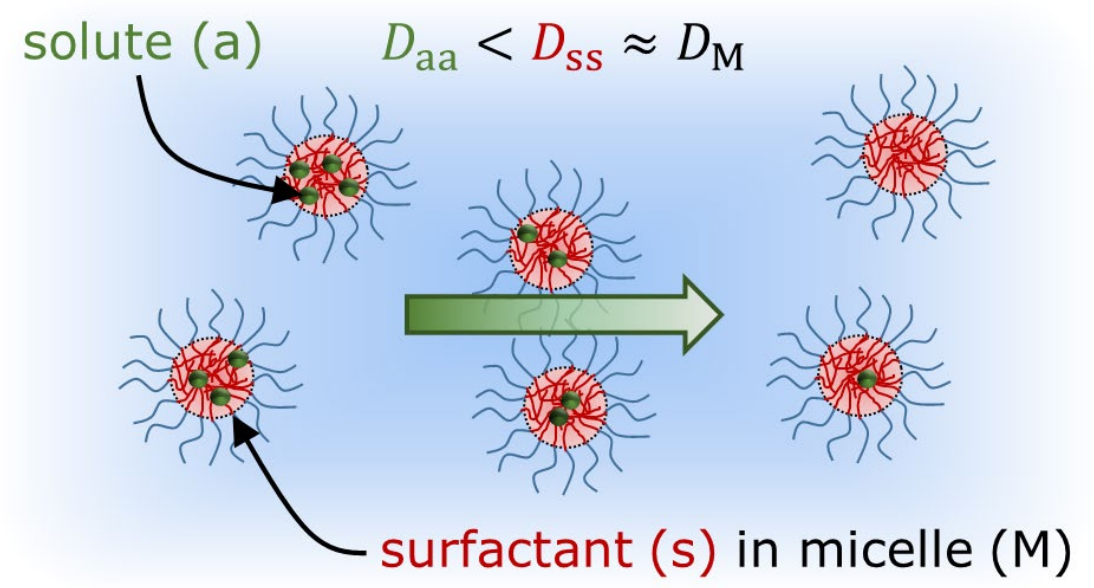

LANGMUIR Article
Cite This: Langmuir 2019, 35, 13595−13606 pubs.acs.org/Langmuir

Multicomponent Diffusion in Aqueous Solutions of Nonionic Micelles and Decane

Nathan P. Alexander,[†] Ronald J. Phillips,[†] and Stephanie R. Dungan*[,†,‡]

[†]Department of Chemical Engineering and [‡]Department of Food Science and Technology, University of California at Davis, Davis, California 95616 United States

ABSTRACT: Taylor dispersion and dynamic light scattering techniques were used to measure the ternary diffusivity matrix [**D**] and the micelle gradient diffusion coefficient, respectively, in crowded aqueous solutions of decaethylene glycol monododecyl ether ($C_{12}E_{10}$) and decane. The results indicate that $C_{12}E_{10}$ diffused down its own gradient with the micelle gradient diffusivity while decane diffused down a decane gradient at a much slower rate. Furthermore, strong diffusion coupling, comprising decane diffusion down a surfactant gradient and surfactant diffusion up a decane gradient, was also observed with cross diffusivities that were on the order of or larger than the main diffusivities. Measurements of the micelle aggregation number, hydration index, and the hydrodynamic radius, obtained using both static and dynamic light scattering methods, indicate that decane-containing micelles interacted as hard spheres and had radii and aggregation numbers that increased linearly with the molar ratio of solute to surfactant. A theoretical model, developed using Batchelor's theory for gradient diffusion in a polydisperse system of interacting hard spheres, was effectively used to predict [**D**] with no adjustable parameters. A comparison with the theory indicates that decane diffused down its own gradient by micelle *self*-diffusion while surfactant diffused down a surfactant gradient by micelle *gradient* diffusion. It is also shown that intermicellar interactions drove decane diffusion down a $C_{12}E_{10}$ gradient by a volume exclusion effect while an increase in the micelle aggregation number and hydrodynamic radius with decane was necessary to drive surfactant diffusion up a decane gradient.

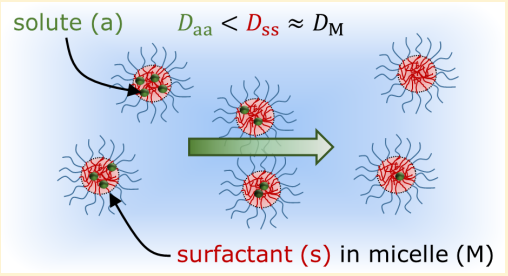

INTRODUCTION

Recently, diffusion in "crowded systems" and complex fluids has attracted increasing attention, as new results have challenged our understanding of diffusion at a very fundamental level. Recent studies of multicomponent diffusion in aqueous micellar solutions, for example, have shown that the partitioning of hydrophobic solute, such as a drug or nutrient, into the oily interior of the micelles strongly affects the rate of diffusion of both the solute and the surfactant.[1−7] In this work, we examine the surprisingly strong and nonintuitive effects of multicomponent interactions in ternary systems comprised of water, nonionic surfactant, and hydrophobic solutes that are nearly insoluble in water in the absence of micelle-forming surfactants.

Interestingly, the diffusion of a hydrophobic solute in an aqueous micellar solution occurs naturally in the human body within the lumen of the small intestine. In that region, hydrophobic solutes such as fats, drugs, and nutrients solubilize within bile-salt micelles that diffuse through an aqueous boundary layer, often described as an unstirred water layer (UWL), to the membrane of the enterocytes (cells) that constitute the lining of the intestinal wall. Research suggests that, at least in vitro, the micelle-mediated diffusion of hydrophobic solute across the UWL can be rate-limiting and may control the rate of hydrophobic solute absorption during digestion.[8,9] Hence, a detailed understanding of multicomponent diffusion in aqueous surfactant solutions may be necessary to predict oral drug delivery rates and nutrient bioavailability, especially if the drug or nutrient is very hydrophobic.[9]

The hydrophobic core of micelles enables them to solubilize (and thus transport) hydrophobic material and, in this way, act as mobile nanocontainers for solute. Micelles generally raise the effective solubility of hydrophobic solute in water and may enable one to establish relatively large solute concentration gradients that have the potential to enhance the rate of hydrophobic solute diffusion. A simple theoretical model for the diffusion of solute in a micellar solution would predict that the effective solute gradient diffusion coefficient (D_{eff}) is a weighted average of the free molecular solute gradient diffusion coefficient (D_a) and the micelle gradient diffusion coefficient (D_M).[10−12] According to this model, either solute molecules can diffuse in water as free solute molecules or they can be carried by solute-containing micelles. When the solute is very hydrophilic, D_{eff} is predicted to be that of the free solute (D_a); that is, a hydrophilic solute is predicted to diffuse in a micellar solution as if the micelles were not there. If the solute is very hydrophobic and the solute transports exclusively within

Received: June 14, 2019
Revised: September 14, 2019
Published: September 25, 2019

DOI: 10.1021/acs.langmuir.9b01823
Langmuir 2019, 35, 13595−13606

solute-containing micelles, then D_{eff} would be predicted to be equivalent to the micelle gradient diffusion coefficient D_M, where the effect of solute on D_M has been neglected. Hence, this framework, known as the pseudobinary model for diffusion, predicts that the effective solute gradient diffusion coefficient is bounded by the gradient diffusion coefficients of the micelle and the free molecular solute:

$$D_M \leq D_{eff} \leq D_a \quad (1)$$

However, in contrast to this prediction, our group has previously measured effective solute gradient diffusion coefficients in aqueous micellar solutions that fall outside of these bounds.[2] The pseudobinary model, evidently, was inadequate to describe diffusion in those multicomponent systems.

Generally, multicomponent gradient diffusion in a ternary solution can be described with either the Maxwell-Stefan equations or the generalized form of Fick's law, the latter being given by the matrix equation

$$-\begin{bmatrix} J_a \\ J_s \end{bmatrix} = \begin{bmatrix} D_{aa} & D_{as} \\ D_{sa} & D_{ss} \end{bmatrix} \begin{bmatrix} \partial C_a/\partial x \\ \partial C_s/\partial x \end{bmatrix} \quad (2)$$

Equation 2 describes diffusion in one dimension (x) and accommodates diffusion coupling between two components denoted by the subscripts "a" and "s". The third component, typically the solvent, is excluded from eq 2 because the fluxes of the three components are not independent.[13] The main terms in the diffusivity matrix (D_{aa} and D_{ss}) relate the flux response of each component to its own concentration gradient, while the cross terms (D_{as} and D_{sa}) relate the flux of one component to a gradient in the other. The magnitude of the cross terms reflect the strength of diffusion coupling; they can be greater in magnitude than the main terms and are sometimes negative.

Although the off-diagonal diffusivities D_{as} and D_{sa} are often negligible in liquid solutions with weakly interacting components,[14] it has become increasingly clear that, in other mixtures with strongly interacting components, they can be significant. Non-negligible cross diffusivities have been measured in a variety of aqueous surfactant solutions, including systems with ionic surfactant and solute,[1,2,5,6] nonionic or zwitterionic surfactant and solute,[2−4,7] and aqueous solutions with mixed surfactants.[15−21]

Multicomponent gradient diffusion in aqueous surfactant solutions with ionic components, where multicomponent effects were driven largely by electrostatic coupling, have received the most attention to date. Surprisingly, there have been relatively few similar studies with nonionic or zwitterionic components, and nearly all of those studies were confined to dilute solutions, in which the surfactant and/or the solute were abundantly present as dissolved molecular species.[2−4,15,20] Those nonionic or zwitterionic studies have shown that diffusion coupling may occur in solutions with large quantities of free molecular solute and/or surfactant monomer by two independent mechanisms: (1) the solubilization of free solute molecules into micelles can generate a large gradient in free molecular solute, which can drive solute diffusion up the surfactant gradient, and (2) the effect of solute on the micellization free energy of a surfactant with a high critical micelle concentration (CMC) can cause a large surfactant monomer gradient, which can drive surfactant diffusion up (or down) the solute gradient.

These mechanistic descriptions raise a set of interesting questions. What if the solute is very hydrophobic (and strongly partitions into the micelles) and the surfactant CMC is very low, so that the concentrations of the molecular species are negligible? Are diffusion coupling effects present? Is diffusion pseudobinary in these strongly partitioning micellar solutions? Indeed, only weak multicomponent effects have been observed and mechanistically explained in dilute solutions of mixed nonionic or zwitterionic surfactants with negligible molecular species.[15] However, a limited amount of existing data shows strong multicomponent effects in crowded aqueous nonionic surfactant solutions with very hydrophobic solutes,[2] caused by mechanisms that remain unclear.

In the present study, we obtained new data on multicomponent diffusion in crowded aqueous nonionic surfactant solutions with a very hydrophobic solute. The nonionic surfactant was decaethylene glycol monododecyl ether ($C_{12}E_{10}$), and the hydrophobic solute was decane. The Taylor dispersion method was used to measure the ternary diffusivity matrix [**D**],[22] and dynamic light scattering (DLS) was used to measure the solute-containing micelle gradient diffusivities D_{DLS}. The theory developed by Batchelor[23,24] for diffusion in a polydisperse system of interacting spheres allowed us to predict the diffusivity matrix [**D**] from measured values of the surfactant aggregation number m, the hydration index n_H, and the decane-free infinite dilution diffusivity D^0. The parameters (m, n_H, and D^0) were acquired using both static and dynamic light scattering techniques.

MATERIALS AND METHODS

Materials. The surfactant decaethylene glycol monododecyl ether ($C_{12}E_{10}$, lot #SLBT1187 with a hydroxyl value equal to 92.0 mg/g), the solute decane, and HPLC grade toluene, used as a reference standard for static light scattering measurements, were all purchased from Sigma-Aldrich and used without modification. All micellar solutions destined for the Taylor dispersion apparatus were prepared with unfiltered deionized water, while micellar solutions prepared for either static or dynamic light scattering measurements were mixed using "Molecular Biology Reagent" water from Sigma-Aldrich that was filtered through 0.1 μm filters by the manufacturer. All solutions, regardless of the measurement technique, were prepared by volume with aliquots from 100 mL stock solutions and were allowed to equilibrate overnight at room temperature. Nonideal changes in volume upon mixing were neglected.

Light Scattering. Dynamic (DLS) and static (SLS) light scattering measurements were performed with a Malvern Zetasizer Nano ZS90 at a 90° scattering angle. The light source was a solid state 4 mW He−Ne laser that emitted vertically polarized light with a wavelength of 633 nm. In order to ensure the removal of dust particles, all surfactant solutions prepared for light scattering measurements were filtered through 0.1 μm Whatman polycarbonate filters (model WHA800309), using an Avanti mini-extruder (model 610000), directly into quartz cuvettes topped with Teflon stoppers by Starna (model 23-Q-10). Each 1 mL sample was then allowed to equilibrate at 25 °C within the instrument for 10 min prior to measurement. All DLS measurements generated intensity-weighted size distributions with a single, narrow peak. Assuming a Gaussian micelle size distribution, the method of cumulants was then used to fit the DLS intensity autocorrelation functions. The cumulants analysis yielded Z-average diffusion coefficients (D_{DLS}) and polydispersity indices (defined in this context as the square of the ratio of the standard deviation over the mean of the Gaussian size distribution curve), with the latter determined to be <0.1 for all samples.

SLS measurements yielded reduced scattering intensities $K_s c_s/R_{90}$, where K_s is the optical contrast constant, c_s is the surfactant mass concentration, and $R_{90} = (I_A/I_T)(n_s/n_T)^2 R_T$ is the excess Rayleigh

DOI: 10.1021/acs.langmuir.9b01823
Langmuir 2019, 35, 13595−13606

ratio, calibrated with a pure toluene standard. The Rayleigh ratio for pure toluene is given by $R_T = 1.3522 \times 10^{-5}$ cm^{-1} at 25 °C. I_A is the residual scattering intensity, defined as the difference between the scattering intensity of the solution and that of the pure solvent I_0. I_T is the scattering intensity of the toluene standard. n_s is the solution refractive index, and n_T (equal to 1.496) is the refractive index of pure toluene at 25 °C. K_s for vertically polarized light is given by $4\pi n_s^2(N_A\lambda^4)^{-1}(dn_s/dc_s)^2$, where N_A is Avogadro's number, λ is the wavelength of incident light, and dn_s/dc_s is the independently determined refractive index derivative of the solution with respect to the surfactant mass concentration. (Note that the precise value of n_s^2 is not needed since the quantity n_s^2 in R_{90} cancels with that in K_s.) The diameters of the micelles in our solutions were 2 orders of magnitude smaller than the wavelength of incident light, thus satisfying the Rayleigh criteria, so that the scattered light intensity was independent of the scattering angle with a form factor equal to one.

Except where noted, all reported error bars for our scattering measurements represent two standard deviations.

Taylor Dispersion. The ternary diffusivity matrices [**D**] were measured using the Taylor dispersion method.[25,26] Briefly, a peristaltic metering pump (Gilson model Minipuls 3) delivered carrier solution, which contained a specified concentration of solute and/or surfactant, to a differential refractometer (Waters model 2414) through Teflon capillary tubing (length L = 1990.8 cm, inner radius r = 0.0144 cm) wound into a helical coil with radius R_c = 11.3 cm. A 20 μL pulse with either excess solute (ΔC_a = 5 mM) or excess surfactant (ΔC_s = 5 mM) was rapidly injected into the laminar carrier stream upstream of the coil, using a Rheodyne injection valve (model 7725). The dispersion of solute and surfactant then broadened the pulse as it moved downstream to generate a refractive index profile, which was measured at the detector. The pulse residence times t_R, set by the pump flow rate, were chosen to be t_R > 8000 s in order to minimize distortion of the refractive index profiles caused by "secondary" flows, introduced by the presence of the helical coil, and to reduce continued broadening of the pulse as it slowly passed through the measurement chamber of the refractometer.[27−29] All of the refractive index profiles appeared symmetric, indicating that the error from those effects was negligible. Measurements were made at room temperature, which had day-to-day variation within 22−24 °C. Temperatures during each dispersion experiment were monitored and were always constant within ±0.2 °C. Measurements on the binary $C_{12}E_{10}$/water system with the Taylor dispersion device gave a Gaussian profile exhibiting a single mode, yielding a binary micelle diffusion coefficient that was in good agreement with our dynamic light scattering result.

The refractive index profiles were fit with the following ternary Taylor dispersion model equation[30,31]

$$V(t) = V_0 + V_1 t + V_{max}\sqrt{\frac{t_R}{t}}\left\{W \exp\left[-\frac{12D_-(t-t_R)^2}{r^2 t}\right] + (1-W)\exp\left[-\frac{12D_+(t-t_R)^2}{r^2 t}\right]\right\} \quad (3)$$

Here, V_0 is the baseline voltage of the detector, V_{max} is the signal voltage when $t = t_R$, and $V_1 t$ captures linear drift in the signal voltage. D_- and D_+ are the eigenvalues of [**D**].

$$D_+ = \frac{(D_{aa}+D_{ss})}{2} + \frac{\sqrt{(D_{aa}-D_{ss})^2 + 4D_{as}D_{sa}}}{2} \quad (4)$$

$$D_- = \frac{(D_{aa}+D_{ss})}{2} - \frac{\sqrt{(D_{aa}-D_{ss})^2 + 4D_{as}D_{sa}}}{2} \quad (5)$$

In eq 3, W is a weighting factor, given by

$$W = \frac{(a+b\alpha_1)\sqrt{D_-}}{(a+b\alpha_1)\sqrt{D_-} + (1-a-b\alpha_1)\sqrt{D_+}} \quad (6)$$

and

$$\alpha_1 = \frac{R_a\Delta C_a}{R_a\Delta C_a + R_s\Delta C_s} \quad (7)$$

$$a = \frac{D_+ - D_{ss} - \frac{R_a}{R_s}D_{as}}{D_+ - D_-} \quad (8)$$

$$b = \frac{D_{ss} + \frac{R_a}{R_s}D_{as} - D_{aa} - \frac{R_s}{R_a}D_{sa}}{D_+ - D_-} \quad (9)$$

where $R_a = (\partial n_s/\partial C_a)_{Cs}$ and $R_s = (\partial n_s/\partial C_s)_{Ca}$ are the respective refractive index increments with either C_s or C_a held constant.

In order to acquire the four nonlinear fit parameters a, b, D_-, and D_+ of eq 3, two refractive index profiles with two different values of α_1 were fit simultaneously, using nonlinear least-squares regression performed with Matlab's "patternsearch" algorithm.[32] One profile was generated from a pulse with excess solute ($\alpha_1 \approx 1$) and another from a pulse with excess surfactant ($\alpha_1 \approx 0$). The fit parameters were then used to evaluate [**D**] via

$$D_{aa} = D_- + \frac{a(1-a-b)}{b}(D_- - D_+) \quad (10)$$

$$D_{as} = \frac{R_s}{R_a}\frac{a(1-a)}{b}(D_- - D_+) \quad (11)$$

$$D_{sa} = \frac{R_a}{R_s}\frac{(a+b)(1-a-b)}{b}(D_+ - D_-) \quad (12)$$

$$D_{ss} = D_+ + \frac{a(1-a-b)}{b}(D_+ - D_-) \quad (13)$$

Error bars for the resulting elements of [**D**] represent two standard deviations.

Refractive Index Increments. All refractive index measurements were performed with a differential refractometer at room temperature (22−24 °C). In order to determine the refractive index derivatives dn_s/dc_s that were used to evaluate SLS optical contrast constants, the difference between the refractive index of the surfactant solutions n_s and that of the solvent n_0 were measured from a dilution series comprised of six different surfactant concentrations that ranged from 1 to 6 mM in increments of 1 mM, with the solute to surfactant molar ratio held constant. The dn_s/dc_s derivatives were subsequently determined from the slopes of the plots of $n_s - n_0$ versus c_s for the following molar ratios: C_a/C_s = 0, 0.1, 0.2, and 0.3. Each plot was reproduced in triplicate and was well fit with a linear function with an intercept through zero. From this procedure, dn_s/dc_s values equal to 0.1314 ± 0.0006, 0.133 ± 0.004, 0.135 ± 0.001, and 0.139 ± 0.002 mL/g, respectively, were obtained.

The refractive index increments R_a and R_s used to evaluate the Taylor dispersion cross diffusivities (D_{as} and D_{sa}) were determined using finite difference approximations where $R_a \approx (\Delta n_s/\Delta C_a)_{Cs}$ and $R_s \approx (\Delta n_s/\Delta C_s)_{Ca}$. Here, Δn_s is the difference in the refractive index between a reference surfactant solution with composition (C_a, C_s) and another solution with a composition equal to either ($C_a + \Delta C_a$, C_s) or (C_a, $C_s + \Delta C_s$). The respective solute and surfactant concentration differences were ΔC_a = 5 mM and ΔC_s = 4 mM. The R_a/R_s ratios obtained for solutions with C_s = 200, 150, 100, or 50 mM, with C_a/C_s = 0.1, were 0.19 ± 0.05, 0.18 ± 0.04, 0.16 ± 0.04, and 0.150 ± 0.003, respectively. The error limits for these ratios, as well as for the derivatives provided above, represent two standard deviations.

R_a and R_s were also determined by integrating the Taylor dispersion refractive index profiles using $R_a = (A_a\pi r^2 L)/(G_a\Delta C_a V_p t_R)$ and $R_s = (A_s\pi r^2 L)/(G_s\Delta C_s V_p t_R)$. Here, A_a and A_s are the areas under the respective Taylor dispersion profiles that were generated using an injection pulse with either excess solute or excess surfactant. G_a and G_s are the corresponding detector gains, also known as detector sensitivity settings, expressed in units of volt per μRIU (10^{-6}

DOI: 10.1021/acs.langmuir.9b01823
Langmuir 2019, 35, 13595−13606

refractive index units), and V_p is the injection pulse volume. Both methods used to measure R_a and R_s produced results that agreed within error. However, the refractive index increments determined by the finite difference method were more precise and thus were used to calculate the cross diffusivities (D_{as} and D_{sa}).

RESULTS

Ternary Diffusivities. The ternary diffusivity matrix [**D**] was measured at room temperature (22−24 °C) with the Taylor dispersion method, using aqueous solutions of 200 mM $C_{12}E_{10}$ with various decane concentrations (Figure 1). [**D**] was

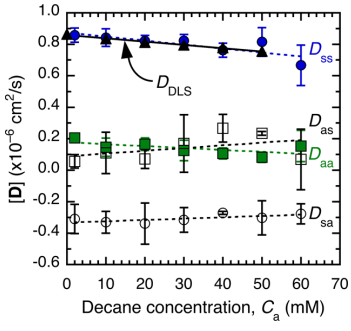

Figure 1. Ternary diffusion coefficients for aqueous 200 mM $C_{12}E_{10}$ (s) + decane (a).

also measured in solutions with a constant molar ratio of solute to surfactant equal to C_a/C_s = 0.1 for several surfactant concentrations (Figure 2). Here, C_a and C_s are the molar concentrations of solute and surfactant, respectively.

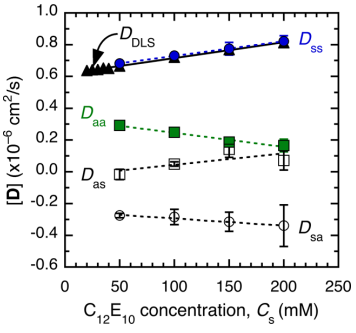

Figure 2. Ternary diffusion coefficients for aqueous $C_{12}E_{10}$ (s) + decane (a) with C_a/C_s = 0.1.

The measured diffusivities correspond to a volume-fixed reference frame. Generally, gradient diffusion measurements yield diffusivities relative to a fixed-laboratory reference frame, which becomes identical to the volume-fixed reference frame when nonideal changes in the volume of the solution are negligible upon mixing.[33] That condition is satisfied when either the component molar volumes are constant with composition or when the initial concentration differences, established during the measurement, are made sufficiently small.[33] In this work, we have established small initial concentration differences (5 mM) in either the solute or the surfactant. Larger initial concentration differences (10 mM) yielded the same results within error, indicating that the measured diffusivities were constant in both time and space during each experiment and corresponded to the volume-fixed reference frame.

Ternary diffusion coefficients can be evaluated unambiguously from Taylor dispersion refractive index profiles and eq 3 when the diffusivity matrix eigenvalues are distinct and differ by more than 10−20%. However, when ternary diffusion is pseudobinary and the eigenvalues are nearly equal, then numerical ill-conditioning makes it difficult, if not impossible, to evaluate the diffusivities from the Taylor dispersion refractive index profiles.[15,34] In this study, eigenvalues for the $C_{12}E_{10}$/decane/water diffusivity matrix were found to be distinct with a relative difference of 65−75% over the entire decane concentration range. Hence, the elements of [**D**] for this system could be unambiguously determined from refractive index profiles using eqs 3−13.

Dynamic Light Scattering (DLS). Gradient diffusion coefficients D_{DLS} that relate micelle fluxes to micelle concentration gradients were measured for binary and ternary solutions of solute-containing micelles at 25 °C. The data were obtained with dynamic light scattering in crowded aqueous solutions of 200 mM $C_{12}E_{10}$ surfactant with decane at concentrations that ranged from 0 to 50 mM in increments of 10 mM (Figure 1). D_{DLS} was also measured in $C_{12}E_{10}$/decane/water solutions with constant molar ratios C_a/C_s (0, 0.05, 0.10, 0.15, 0.20, 0.25, or 0.30) with surfactant concentrations that ranged from 20 to 200 mM (Figure 3). The binary DLS diffusivities agreed with previous values acquired by our group[2] via holographic interferometry.

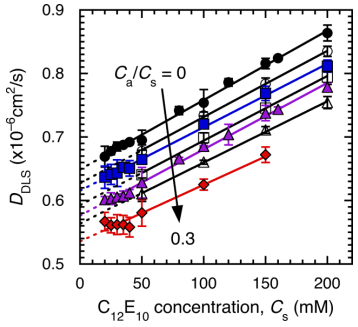

Figure 3. DLS diffusivities with respect to $C_{12}E_{10}$ concentration with C_a/C_s = 0, 0.05, 0.10, 0.15, 0.20, 0.25, and 0.30 from DLS data.

Earlier research by other groups[1,35,36] suggested that diffusivity matrix eigenvalues were the only diffusivities that could be acquired with a DLS apparatus, unless the cross terms of the matrix were negligible. In those studies, independent salt concentration fluctuations that dissipated by diffusion drove coupled flows in either lysozyme[35] or SDS micelles[1] during their respective DLS measurements. The resulting DLS diffusivities from those measurements were influenced by coupling phenomena and consequently produced a diffusivity matrix eigenvalue that was significantly different from the expected gradient diffusion coefficient.

In the current work, both $C_{12}E_{10}$ surfactant and the decane solute were bound exclusively within micelles. Hence, independent surfactant or solute concentration fluctuations were negligible relative to the dominant solute-containing micelle concentration fluctuations, and thus did not drive

DOI: 10.1021/acs.langmuir.9b01823
Langmuir 2019, 35, 13595−13606

substantial coupled flows that could have contributed to the DLS measurements. Only solute-containing micelle concentration fluctuations that dissipated by diffusion in accordance with the solute-containing micelle gradient diffusion coefficient contributed to our light scattering results, as evidenced by the excellent agreement between the DLS diffusivities and the main surfactant diffusivities shown in Figures 1 and 2 for the $C_{12}E_{10}$/decane/water system.

Static Light Scattering (SLS). The Debye equation, usually expressed as a function of the *particle* mass concentration, enables one to determine the second osmotic virial coefficient and the weight-averaged particle molecular weight from measurements of the reduced scattering intensity. However, in order to extract the aggregation number (m) from a ternary $C_{12}E_{10}$/decane/water solution (modeled here as a multicomponent solution of polydisperse decane-containing micelles in water), it is helpful to recast the Debye equation as a function of the surfactant mass concentration c_s:[37−39]

$$\frac{K_s c_s}{R_{90}} = \frac{1}{MW_s} + 2B_s c_s \tag{14}$$

Here, $K_s c_s/R_{90}$ is the reduced scattering intensity, where K_s is the optical contrast constant now defined using the refractive index derivative of the solution with respect to *surfactant* mass concentration dn_s/dc_s rather than with respect to the particle mass concentration. Thus, MW_s in this equation is the weight-averaged molecular weight of surfactant per micelle, and B_s is the second osmotic virial coefficient defined by a virial expansion of osmotic pressure in powers of the surfactant mass concentration. B_s is related to a more familiar form of the second virial coefficient B^*, defined by a virial expansion in powers of the micelle number density via $B_s = (N_A B^*/MW_s^2)$, where N_A is Avogadro's number.

The Debye plots for the $C_{12}E_{10}$/decane/water system in Figure 4 show that $K_s c_s/R_{90}$ increased linearly over the entire surfactant concentration range for each molar ratio. This behavior indicates that, with C_a/C_s held constant, the micelles did not grow or change shape with increasing surfactant concentration, thus validating our use of eq 14 to determine MW_s.

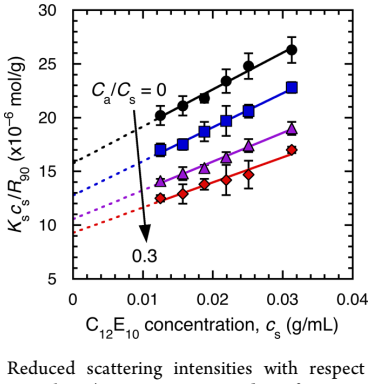

Figure 4. Reduced scattering intensities with respect to $C_{12}E_{10}$ concentration with C_a/C_s = 0, 0.1, 0.2, and 0.3 from SLS data.

Micelle Structure at Infinite Dilution and Intermicellar Interactions. Extrapolation of the DLS diffusion coefficients in Figure 3 to zero surfactant concentration yielded the diffusion coefficient D^0 of a micellar solution in the infinite dilution limit for each molar ratio. Assuming the micelles were spherical, the micelle hydrodynamic radius R_{DLS} for each C_a/C_s was then calculated with the Stokes−Einstein equation,

$$R_{DLS} = \frac{kT}{6\pi\eta D^0} \tag{15}$$

Here, k is Boltzmann's constant, T is temperature, and η is the solvent viscosity (0.89 mPa·s). In Figure 5, R_{DLS} is seen to increase with increasing C_a/C_s, indicating that $C_{12}E_{10}$ micelles grew with an increase in the average number of solubilized decane molecules per micelle. We note that our solute-free hydrodynamic radius (R_{DLS} = 3.78 ± 0.02 nm) is in reasonable agreement with previously reported results for binary aqueous $C_{12}E_{10}$ solutions acquired by DLS (3.92 nm)[40] and holographic interferometry (3.1 nm).[41]

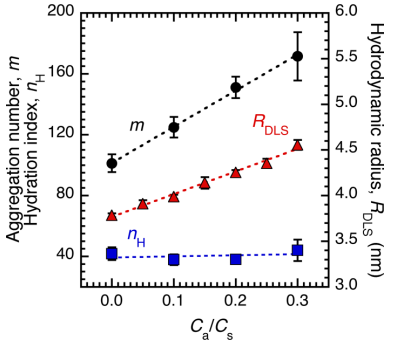

Figure 5. Aggregation numbers m from SLS data and eq 14, hydrodynamic radii R_{DLS} from DLS data and eq 15, and hydration indices n_H from eq 16 with respect to molar ratio C_a/C_s at infinite dilution. Error bars indicate 95% confidence intervals.

Following a similar procedure, extrapolation of the reduced scattering intensity in Figure 4 provided the molecular weight of surfactant per micelle MW_s at infinite dilution. The micelle aggregation number m was calculated by dividing MW_s by the $C_{12}E_{10}$ molecular weight (626.86 g/mol). As shown in Figure 5, m increased with increasing C_a/C_s, indicating that an increase in the micelle radius R_{DLS} resulted from an increase in both the number of decane molecules and the number of $C_{12}E_{10}$ molecules per micelle. Similar trends acquired using membrane osmometry were reported by Atwood et al.[42] for aqueous solutions of Cetomacrogol 1000 ($C_{16}E_n$) with decane. Furthermore, our solute-free aggregation number (m = 101 ± 6) agrees reasonably well with the result from Nolan et al.[43] (122 ± 10) for 1 wt % solutions of aqueous $C_{12}E_{10}$, determined using a frequency domain fluorescence quenching method.

The micelle hydration index n_H, defined as the average number of water molecules bound to each surfactant molecule within the micelle, was estimated by calculating the difference between the measured hydrated volume of a decane-containing micelle $\left(\frac{4}{3}\pi R_{DLS}^3\right)$ and its empirically determined dry volume $(mV_s + \langle i\rangle V_a)$:

$$n_H = \frac{\frac{4}{3}\pi R_{DLS}^3 - mV_s - \langle i\rangle V_a}{mV_w} \tag{16}$$

DOI: 10.1021/acs.langmuir.9b01823
Langmuir 2019, 35, 13595−13606

Here, V_s, V_a, and V_w are the respective molecular volumes of a dry molecule of $C_{12}E_{10}$ (0.99 nm^3), decane (0.32 nm^3), and water (0.03 nm^3); m is the average micelle aggregation number, and $\langle i \rangle = mC_a/C_s$ is the average number of solute molecules per micelle. V_a and V_w were calculated from the pure liquid densities of decane and water, respectively, at 25 °C, and V_s was interpolated from density data acquired for a homologous series of aqueous $C_{12}E_m$ surfactant solutions.[44]

Our results for n_H are plotted in Figure 5 and show that n_H remained constant with increasing C_a/C_s, indicating that decane, which is expected to solubilize within the hydrophobic core of the micelle, did not alter the amount of hydration water bound primarily within the micelle palisade layer. Our solute-free value ($n_H = 42 \pm 4$) agrees with Nilsson and Lindman[45] who estimated the number of bound water molecules per EO group to be 4.3, on the basis of NMR water self-diffusion measurements with 10 wt % $C_{12}E_8$ at $T = 25$ °C.

To characterize the interactions between micelles, we evaluated the slopes D_2 of the lines fit to plots of D_{DLS}/D^0 versus the total micelle volume fraction ϕ, calculated using $\phi = C_a\bar{V}_a + C_s\bar{V}_s + n_H\bar{V}_wC_s$. Here, $\bar{V}_a$, $\bar{V}_s$, and $\bar{V}_w$ are the respective molar volumes of the solute, surfactant, and water, which were assumed to remain constant with composition. According to theory by Batchelor,[46] the gradient diffusivity of a dilute, monodisperse system of hard spheres is predicted to increase with ϕ via $D = D^0(1 + 1.45\phi)$.

In Figure 6, the normalized diffusion coefficients D_{DLS}/D^0 are plotted as a function of ϕ, superimposed with Batchelor's theoretical result (solid line). Additionally, the diffusivity slopes D_2 are presented in the inset of Figure 6 with respect to C_a/C_s. As shown, the D_{DLS}/D^0 results for each molar ratio collapsed onto a line with a diffusivity slope D_2 that agreed reasonably well with Batchelor's theoretical prediction of 1.45, indicating that decane-containing micelles behaved as hard spheres regardless of the amount of decane solubilized within micelles. Our solute-free diffusivity slope is consistent with previously reported results for aqueous solutions of $C_{12}E_8$ by Corti et al.[47] and Buck et al.[48] when the results of the latter are corrected to account for micelle hydration water.

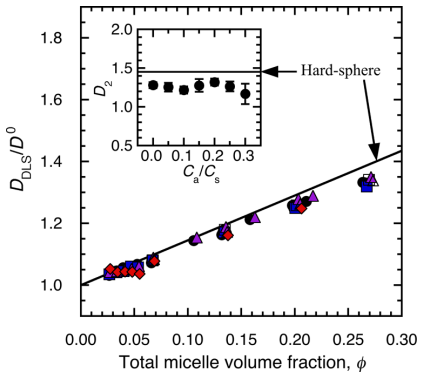

Figure 6. Normalized diffusion coefficients and diffusivity slopes (inset) plotted as a function of micelle volume fraction and molar ratio, respectively. Solid lines indicate theoretical predictions for a monodisperse solution of hard spheres. Error bars indicate 95% confidence intervals.

DISCUSSION

Diffusion Behavior in Decane/$C_{12}E_{10}$/Water Mixtures. Given the low solubility of decane (3.2×10^{-4} mM)[49] and the low cmc of $C_{12}E_{10}$ (0.09 mM),[50] these two compounds diffuse together exclusively as solute-containing micelles, and so one might expect the main terms in the diffusivity matrix, D_{aa} and D_{ss}, to be identical and equal to the micelle gradient diffusivity D_M. Indeed, this result is predicted if the solution is monodisperse and if one imposes the constraint that decane and surfactant concentration gradients are proportional throughout the diffusion process and cannot occur independently. In this special case, one has effectively removed a degree of freedom from the system, thereby reducing the ternary system to a binary system. As a result, the pseudobinary model for diffusion (satisfying the lower limit of eq 1) applies.[51] Generally, however, independent gradients in C_a and C_s can occur within $C_{12}E_{10}$/decane/water mixtures, generating strong multicomponent effects.

According to our data, the main $C_{12}E_{10}$ diffusivities D_{ss} and D_{DLS} were very similar over the entire decane concentration range (Figure 1) and over the entire surfactant concentration range (Figure 2) investigated in this study. Both D_{ss} and D_{DLS} decreased linearly with increasing decane concentration and increased linearly with increasing $C_{12}E_{10}$ concentration. Those trends provide strong evidence that $C_{12}E_{10}$ diffused down its own concentration gradient in a ternary micellar solution with the micelle gradient diffusion coefficient.

In contrast, decane was observed to diffuse with a main diffusivity D_{aa} that fell outside of the bounds indicated by eq 1 and had a value that was four times lower than the expected micelle gradient diffusion coefficient. Thus, compared with the pseudobinary prediction, decane transport down its own gradient was dramatically reduced, a phenomenon that has not been observed in recent studies of diffusion in aqueous micellar solutions with more hydrophilic solutes.[3,20] Furthermore, $C_{12}E_{10}$ diffused up the decane gradient, so that $D_{sa} < 0$, and decane diffused down the $C_{12}E_{10}$ gradient, so that $D_{as} > 0$. The magnitudes of both of the cross diffusivities were significant: the decane cross diffusivity exceeded the decane main diffusivity ($D_{as} > D_{aa}$) above a decane concentration of 30 mM, and the surfactant cross diffusivity exceeded the main decane diffusivity in magnitude ($|D_{sa}| > D_{aa}$) over the entire decane concentration range. Those results agree qualitatively with results acquired previously by our group[2] via holographic interferometry for aqueous micellar solutions with 200 mM $C_{12}E_{10}$ and 30 mM heptane. Interestingly, Figure 1 shows that those strong multicomponent coupling effects were found to persist at low decane concentrations ($C_a = 2$ mM), when there was only ≈1 decane molecule per micelle.

For the results shown in Figure 2, we held the solute to surfactant molar ratio constant at $C_a/C_s = 0.1$ and varied the mixture composition by dilution with water, to investigate the influence of intermicellar interactions on the diffusivity matrix and to see if coupling effects were still present in dilute solutions. Indeed, the multicomponent effects appear to weaken with decreasing surfactant concentration. However, these effects did not vanish but instead remained important in solutions that were considered dilute ($C_s < 50$ mM); extrapolation back to infinite dilution suggests they may persist at even lower concentrations. Those results indicate that intermicellar interactions contributed substantially but may not have been solely responsible for the strong

DOI: 10.1021/acs.langmuir.9b01823
Langmuir 2019, 35, 13595−13606

multicomponent behavior observed in the $C_{12}E_{10}$/decane/water system. In addition, we note that, at a fixed value of the molar ratio, both the component concentration gradients are driven to zero in the infinite dilution limit. Hence, $J_s \rightarrow 0$ as $C_s \rightarrow 0$ without requiring that $D_{sa} \rightarrow 0$. This argument is analogous to the explanation for why, in a binary solution at infinite dilution, the flux goes to zero even though the mutual diffusion coefficient remains nonzero.

Diffusion Predictions for Polydisperse Colloidal Mixtures. *Development of Theory.* In order to interpret the results in Figures 1 and 2, we use theory from Batchelor[23,24] to model transport in our ternary $C_{12}E_{10}$/decane/water solutions as gradient diffusion in a polydisperse system of interacting spheres. The system contains N different sphere types that comprise various numbers of decane and surfactant molecules. The flux of micelle species *i*, containing *m* surfactant molecules and *i* solute molecules, is given by the generalized form of Fick's law, which accommodates micelle−micelle diffusion coupling

$$-J_i = D_{ii}\nabla C_i + \sum_{\substack{j=0 \\ j\neq i}}^{N-1} D_{ij}\nabla C_j \tag{17}$$

The main micelle diffusivities D_{ii} relate the flux of micelle species *i* to its own concentration gradient while the micelle cross diffusivities D_{ij} relate the flux of micelle species *i* to a concentration gradient in a different micelle species *j*. The total flux of solute J_a and the total flux of surfactant J_s are related to the micelle species fluxes via

$$J_a = \sum_{i=0}^{N-1} iJ_i \tag{18}$$

$$J_s = \sum_{i=0}^{N-1} m_iJ_i \tag{19}$$

where the fluxes of molecular solute and surfactant monomer have been neglected. In eq 19, m_i represents the aggregation number for micelles with *i* solutes. Substituting eq 17 into eqs 18 and 19 and applying the chain rule generates the following expressions:

$$-J_a = \sum_{i=0}^{N-1} i\left(D_{ii}\frac{\partial C_i}{\partial C_a} + \sum_{\substack{j=0 \\ j\neq i}}^{N-1} D_{ij}\frac{\partial C_j}{\partial C_a}\right)\nabla C_a + \sum_{i=0}^{N-1} i\left(D_{ii}\frac{\partial C_i}{\partial C_s} + \sum_{\substack{j=0 \\ j\neq i}}^{N-1} D_{ij}\frac{\partial C_j}{\partial C_s}\right)\nabla C_s \tag{20}$$

and

$$-J_s = \sum_{i=0}^{N-1} m_i\left(D_{ii}\frac{\partial C_i}{\partial C_a} + \sum_{\substack{j=0 \\ j\neq i}}^{N-1} D_{ij}\frac{\partial C_j}{\partial C_a}\right)\nabla C_a + \sum_{i=0}^{N-1} m_i\left(D_{ii}\frac{\partial C_i}{\partial C_s} + \sum_{\substack{j=0 \\ j\neq i}}^{N-1} D_{ij}\frac{\partial C_j}{\partial C_s}\right)\nabla C_s \tag{21}$$

Equations 20 and 21 are then compared with eq 2 to yield the ternary diffusivities

$$D_{aa} = \sum_{i=0}^{N-1} i\left(D_{ii}\frac{\partial C_i}{\partial C_a} + \sum_{\substack{j=0 \\ j\neq i}}^{N-1} D_{ij}\frac{\partial C_j}{\partial C_a}\right) \tag{22}$$

$$D_{as} = \sum_{i=0}^{N-1} i\left(D_{ii}\frac{\partial C_i}{\partial C_s} + \sum_{\substack{j=0 \\ j\neq i}}^{N-1} D_{ij}\frac{\partial C_j}{\partial C_s}\right) \tag{23}$$

$$D_{sa} = \sum_{i=0}^{N-1} m_i\left(D_{ii}\frac{\partial C_i}{\partial C_a} + \sum_{\substack{j=0 \\ j\neq i}}^{N-1} D_{ij}\frac{\partial C_j}{\partial C_a}\right) \tag{24}$$

$$D_{ss} = \sum_{i=0}^{N-1} m_i\left(D_{ii}\frac{\partial C_i}{\partial C_s} + \sum_{\substack{j=0 \\ j\neq i}}^{N-1} D_{ij}\frac{\partial C_j}{\partial C_s}\right) \tag{25}$$

The multicomponent micelle diffusivities (D_{ii} and D_{ij}) in eqs 22−25 are evaluated using theory developed previously by Batchelor[23,24] for gradient diffusion in a dilute, polydisperse system of spheres:

$$D_{ii} = D_i^0\left(1 + 1.45\phi_i - \sum_{\substack{k=0 \\ k\neq i}}^{N-1} \frac{2.5\phi_k}{1 + 0.16\lambda_{ik}}\right) \tag{26}$$

$$D_{ij\ (i\neq j)} = D_i^0\phi_i\left(\lambda_{ij}^3 + 2\lambda_{ij}^2 + \frac{\lambda_{ij}^2}{1 + \lambda_{ij}^3}\right) \tag{27}$$

Here, D_i^0 and ϕ_i are the infinite dilution diffusivity and volume fraction of micelle species *i*. $\lambda_{ij} = R_j/R_i$ is the micelle size ratio, where R_j is the radius of a type *j* micelle and R_i the radius for a type *i*. Using eqs 22−27, one finds

$$D_{aa} = \sum_{i=0}^{N-1} iD_i^0\left\{\left(1 + 0.105\phi_i - \sum_{k=0}^{N-1} \frac{2.5\phi_k}{1 + 0.16\lambda_{ik}}\right)\frac{\partial C_i}{\partial C_a} + \phi_i\sum_{j=0}^{N-1}\left(\lambda_{ij}^3 + 2\lambda_{ij}^2 + \frac{\lambda_{ij}^2}{1 + \lambda_{ij}^3}\right)\frac{\partial C_j}{\partial C_a}\right\} \tag{28}$$

DOI: 10.1021/acs.langmuir.9b01823
Langmuir 2019, 35, 13595−13606

$$D_{as} = \sum_{i=0}^{N-1} iD_i^0 \left\{ \left(1 + 0.105\phi_i - \sum_{k=0}^{N-1} \frac{2.5\phi_k}{1 + 0.16\lambda_{ik}} \right) \frac{\partial C_i}{\partial C_s} + \phi_i \sum_{j=0}^{N-1} \left(\lambda_{ij}^3 + 2\lambda_{ij}^2 + \frac{\lambda_{ij}^2}{1 + \lambda_{ij}^3} \right) \frac{\partial C_j}{\partial C_s} \right\} \quad (29)$$

$$D_{sa} = \sum_{i=0}^{N-1} m_i D_i^0 \left\{ \left(1 + 0.105\phi_i - \sum_{k=0}^{N-1} \frac{2.5\phi_k}{1 + 0.16\lambda_{ik}} \right) \frac{\partial C_i}{\partial C_a} + \phi_i \sum_{j=0}^{N-1} \left(\lambda_{ij}^3 + 2\lambda_{ij}^2 + \frac{\lambda_{ij}^2}{1 + \lambda_{ij}^3} \right) \frac{\partial C_j}{\partial C_a} \right\} \quad (30)$$

$$D_{ss} = \sum_{i=0}^{N-1} m_i D_i^0 \left\{ \left(1 + 0.105\phi_i - \sum_{k=0}^{N-1} \frac{2.5\phi_k}{1 + 0.16\lambda_{ik}} \right) \frac{\partial C_i}{\partial C_s} + \phi_i \sum_{j=0}^{N-1} \left(\lambda_{ij}^3 + 2\lambda_{ij}^2 + \frac{\lambda_{ij}^2}{1 + \lambda_{ij}^3} \right) \frac{\partial C_j}{\partial C_s} \right\} \quad (31)$$

D_i^0 can be evaluated from the solute-free infinite dilution diffusivity D^0 using

$$D_i^0 = D^0 \left\{ \frac{m_0(\bar{V}_s + n_H\bar{V}_w)}{i\bar{V}_a + m_i(\bar{V}_s + n_H\bar{V}_w)} \right\}^{1/3} \quad (32)$$

The ratio λ_{ij} is determined as

$$\lambda_{ij} = \left\{ \frac{j\bar{V}_a + m_j(\bar{V}_s + n_H\bar{V}_w)}{i\bar{V}_a + m_i(\bar{V}_s + n_H\bar{V}_w)} \right\}^{1/3} \quad (33)$$

and the volume fraction ϕ_i can be calculated from

$$\phi_i = C_i\{i\bar{V}_a + m_i(\bar{V}_s + n_H\bar{V}_w)\} \quad (34)$$

Here, ϕ_i includes contributions from solubilized solute, micellized surfactant, and hydration water.

According to Figure 5, the weight-averaged aggregation number, determined via SLS, varied linearly with C_a/C_s. This result suggests that the aggregation number of an individual micelle within the mixture depends on the number of solutes within the aggregate. Consequently, m_i in eqs 28−34 was set to vary linearly with i within the distribution according to $m_i = i\alpha + m_0$. Here, m_0 is the solute-free aggregation number and α is a constant interpreted as the sensitivity of the aggregation number to solubilizate. In order to determine the local micelle species concentrations C_i, the distribution of solubilized decane within $C_{12}E_{10}$ micelles is assumed to obey a Poisson distribution,[3,4] modified to accommodate the linear increase in aggregation number with solubilized decane:

$$C_i = \frac{C_s}{\alpha\langle i\rangle + m_0} \left(\frac{\langle i\rangle^i}{i!} \right) e^{-\langle i\rangle} \quad (35)$$

with

$$\langle i\rangle = \frac{C_a m_0}{C_s - \alpha C_a} \quad (36)$$

From eqs 35 and 36, micelle growth alters the Poisson distribution by reducing the total number of micelles, thereby increasing the distribution average number $\langle i\rangle$ of solute molecules per micelle, relative to the average without growth. This solubilization-induced shift in the Poisson distribution toward larger aggregates not only modifies the micelle concentration gradients that drive the diffusion of both the solute and the surfactant, via the derivatives in the eqs 28−31, but also affects the complex network of pairwise intermicellar interactions (hydrodynamic and thermodynamic) between the various micellar species through its effect on ϕ_i and ϕ_k. Growth further affects [**D**] through D_i^0 by increasing the Stokes resistance to the Brownian motion of each micelle species.

Comparison with Experimental Data. The ternary diffusivities for the $C_{12}E_{10}$/decane/water system were theoretically determined using eqs 28−36 with $N = 200$, $\bar{V}_a = 1.949 \times 10^{-4}$ mM^{-1}, $\bar{V}_s = 5.968 \times 10^{-4}$ mM^{-1}, $\bar{V}_w = 1.802 \times 10^{-5}$ mM^{-1}, $m_0 = 105$, $\alpha = 1.3$, $n_H = 40$, and $D^0 = 0.648 \times 10^{-6}$ cm^2/s, in accordance with our light scattering results. Here, n_H is an average of the hydration indices presented in Figure 5, while m_0 and α are intercept and slope values, respectively, acquired from a fit of a plot of m versus $\langle i\rangle$. Setting N to values larger than 200 had no effect on the results. The theoretically predicted ternary diffusivities are shown superimposed over our Taylor results in Figure 7A,B. Overall, the theoretical calculations are in good agreement with the experimental values, which is remarkable when one considers that this theory is based on interacting hard spheres and contains no adjustable parameters. The model captures the surprising reduction in decane transport down its own gradient, and correctly predicts large cross diffusivities—on the order of the main terms—which indicate decane diffusion down a $C_{12}E_{10}$

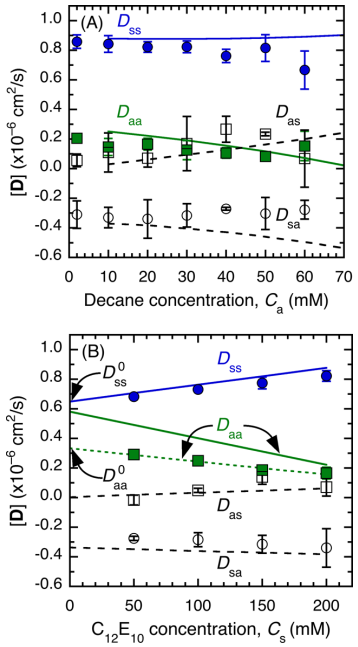

Figure 7. Ternary diffusion coefficients for (A) aqueous 200 mM $C_{12}E_{10}$ (s) + decane (a) and (B) aqueous $C_{12}E_{10}$ (s) + decane (a) with $C_a/C_s = 0.1$. Solid and dashed lines indicate theoretically determined main and cross diffusivities, respectively, calculated using eqs 28−36.

DOI: 10.1021/acs.langmuir.9b01823
Langmuir 2019, 35, 13595−13606

gradient ($D_{as} > 0$) and $C_{12}E_{10}$ diffusion up a decane gradient ($D_{sa} < 0$), in agreement with the experimental data. In Figure 7A, D_{as} is accurately predicted to increase with increasing decane concentration with a magnitude that eventually surpasses D_{aa}, while D_{sa} is predicted to exceed D_{aa} in magnitude over the entire decane concentration range. In Figure 7B, the theoretical results for both D_{as} and D_{ss} increase with increasing surfactant concentration in excellent agreement with the experimental values.

The theory moderately overpredicts the magnitude of D_{aa}, and the discrepancy appears to worsen as the system becomes more dilute (Figure 7B). In the limit of infinite dilution, the experimentally determined main decane diffusivity D^0_{aa} appears to fall significantly below the theoretically predicted value, indicating the presence of a significant nonideal effect that persists when the solution is very dilute. This effect is not captured by the model. On the other hand, excellent agreement between the theoretical and experimentally determined main terms is achieved when D_{aa} and D_{ss} are normalized by their respective values at infinite dilution (D^0_{aa} and D^0_{ss}) and plotted as a function of the total micelle volume fraction. These results, shown in Figure 8, indicate that our diffusion model accurately captures the influence of intermicellar interactions on both D_{aa} and D_{ss}.

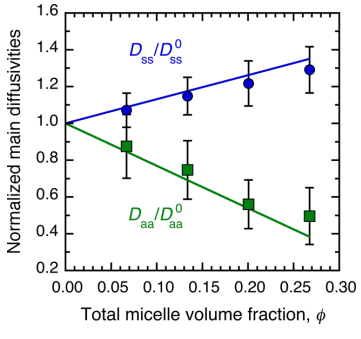

Figure 8. Main solute D_{aa} and main surfactant D_{ss} diffusivities, normalized with their respective values at infinite dilution, for aqueous $C_{12}E_{10}$ (s) + decane (a) with $C_a/C_s = 0.1$. Solid lines indicate normalized theoretical values calculated using eqs 28 and 31−36.

One possible explanation for the discrepancy between the theoretical prediction and experimental values for D_{aa} in Figure 7B is that nonideal mixing of decane and surfactant molecules within micelles may cause the micelle distribution to deviate significantly from a Poisson distribution, especially when the micelles are heavily loaded with decane. The Poisson distribution, derived assuming ideal mixing between solute and surfactant within micelles, is considered valid when $\langle i \rangle \ll m$.[3,52] This condition may be expressed equivalently as $C_a/C_s \ll 1$, a constraint we may not have satisfied in the theoretical predictions plotted in Figure 7B where $C_a/C_s = 0.1$. Since micelles remain loaded with solute at infinite dilution when C_a/C_s is held constant, this nonideal effect may be expected to persist even in very dilute micellar solutions. In support of this hypothesis, we note that data from Smith et al.[53] indicate that intramicellar activity coefficients for hexane in aqueous solutions of the alkylphenol ethoxylated surfactant $NP(EO)_{10}$ are significantly less than unity and decrease with increasing hexane concentration. However, further investigation will be required to verify this nonideality in aqueous solutions of $C_{12}E_{10}$ with decane, and to quantify its effect on the ternary diffusivity matrix.

Exploring Effects of Micelle Growth and Intermicellar Interactions. To gain further insight into the coupled nature of this diffusion process, we vary the micelle sensitivity parameter α in order to investigate the influence of micelle growth (in m_i and R_i) with solute on [**D**]. In Figure 9, theoretical calculations

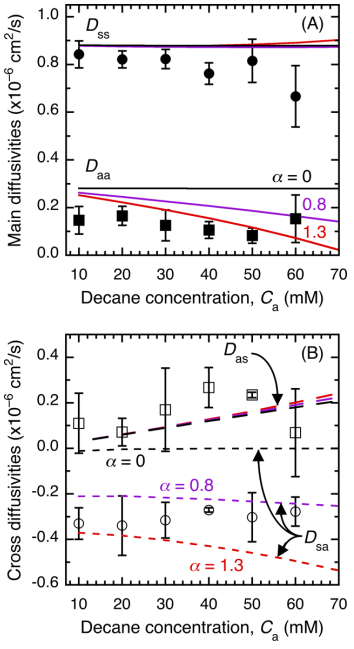

Figure 9. (A) Main diffusivities and (B) cross diffusivities for aqueous 200 mM $C_{12}E_{10}$ (s) + decane (a). Theoretically determined main (solid curves) and cross diffusivities (dashed curves) were calculated using eqs 28−36 with the micelle growth sensitivity set to either α = 0.8 or 1.3 or using eqs 37−40 with $\alpha = 0$.

for [**D**] with α = 0, 0.8, and 1.3 are plotted with our Taylor dispersion data. As shown in Figure 9A, the theory predicts a moderate decrease in D_{aa} with increasing α, indicating that growth modestly supplements the already large reduction in D_{aa} that is predicted in the absence of growth when $\alpha = 0$. Furthermore, the theoretical values for both D_{ss} (Figure 9A) and D_{as} (Figure 9B) are negligibly affected by changes in α. The results indicate that growth is relatively unimportant when estimating D_{aa}, D_{ss}, and D_{as}.

However, D_{sa} (Figure 9B) decreases sharply in magnitude with decreasing α and nearly vanishes when $\alpha = 0$, indicating that surfactant diffusion up a solute gradient ($D_{sa} < 0$) is almost entirely regulated by mechanisms that involve a solubilization-induced increase in the micelle aggregation number, m. An increase in m significantly affects D_{sa} in three ways. (1) It increases the micelle size via added volume of surfactant and hydration water (the added volume of decane provides a relatively small contribution) and thereby reduces the Brownian motion of micelles in the region of high decane concentration. As a result, relatively small, mobile micelles diffuse toward the region of high decane concentration faster than the larger, slower micelles diffuse away from this region,

DOI: 10.1021/acs.langmuir.9b01823
Langmuir 2019, 35, 13595−13606

generating a net surfactant flux up the decane gradient.[54] (2) An increase in m reduces the total micelle concentration in the region of high decane concentration, generating a micelle gradient that further drives surfactant up the decane gradient. (3) An increase in m more heavily weights the flux contributions of larger micelle species in the total net surfactant flux, since each of these micelles contain and thus transport more surfactant molecules. Effects 2 and 3 somewhat offset each other, but they do not entirely cancel and seem to provide a significant contribution to making D_{sa} more negative than effect 1 alone.

In order to reveal the underlying causes of the multicomponent effects that govern the diffusivities D_{ss}, D_{aa}, and D_{as}, which are either negligibly or weakly influenced by micelle growth, we use our model to take a closer look at diffusion in a system of interacting micelles with the growth mechanisms deactivated. Here, it is not enough to set $\alpha = 0$ so that $m_i = m_0$. One must also set $V_a = 0$ to completely remove the effect of solute on the micelle radius, necessitating $\lambda_{ij} = \lambda_{ik} = 1$, $D_i^0 = D^0$, and $\phi_i = C_i\{m_0(\bar{V}_s + n_H\bar{V}_w)\}$ per eqs 32−34. In this case, the solute effectively becomes a volume-less label in a solution of monodisperse micelles, and eqs 28−31 are simplified:

$$D_{aa} = D^0(1 - 2.2\phi) + 0.105D^0\sum_{i=0}^{N-1} i\phi_i\frac{\partial C_i}{\partial C_a} \tag{37}$$

$$D_{as} = 3.5D^0\phi\frac{C_a}{C_s} + 0.105D^0\sum_{i=0}^{N-1} i\phi_i\frac{\partial C_i}{\partial C_s} \tag{38}$$

$$D_{sa} = 0.105D^0m_0\sum_{i=0}^{N-1} \phi_i\frac{\partial C_i}{\partial C_a} \tag{39}$$

$$D_{ss} = D^0(1 + 1.34\phi) + 0.105D^0m_0\sum_{i=0}^{N-1} \phi_i\frac{\partial C_i}{\partial C_s} \tag{40}$$

The summation terms in eqs 37−40 are relatively small, of order $0.1D^0\phi$ or less, indicating that, under this scenario, solute primarily diffuses down its own gradient by micelle self-diffusion, according to $D_{aa} \approx D^0(1-2.2\phi)$. Surfactant, in turn, diffuses down its own gradient by micelle gradient diffusion, governed by $D_{ss} \approx D^0(1 + 1.34\phi)$. These two results differ only slightly from Batchelor's[23,24,46] predictions for the long-time self- and gradient diffusion coefficients, respectively, for a monomodal suspension of colloidal hard spheres. These trends are still observed when growth effects are included in the model. Micelle gradient diffusion also generates a coupled flux in solute down the surfactant gradient, according to $D_{as} \approx D^03.5\phi(C_a/C_s)$, via a volume-exclusion mechanism involving both thermodynamic and hydrodynamic interactions between pairs of micelles with different numbers of solute molecules.

We have also investigated effects of polydispersity on [**D**] by sampling Gaussian distributions in lieu of the Poisson, which enabled us to independently vary the standard deviation in the micelle size distribution. Variations in polydispersity had negligible effects on [**D**]. We believe that differential shifts in average micelle properties between populations along the concentration gradient of either solute or surfactant,[54] together with intermicellar interactions, mainly drive the multicomponent effects in [**D**], rather than the extent of polydispersity within the local micelle population.

Role of Molecular Species. In this study, intermicellar interactions greatly contributed to the striking multicomponent effects observed in aqueous $C_{12}E_{10}$/decane mixtures and may be expected to influence diffusion in a large variety of crowded micellar solutions. However, in aqueous solutions of micelles and hydrophilic solutes, diffusion coupling phenomena have been successfully predicted while neglecting intermicellar interactions, even when the infinite dilution assumption is severely tested.

In an effort to understand how infinite dilution theories can quantitatively predict coupling phenomena in solutions with dilute but finite concentrations, or in crowded systems, we examine the limiting case where ϕ_i and $\phi_k \to 0$, so that the effects of intermicellar interactions are neglected. Under these conditions, eqs 28−31 become equivalent to those derived by Leaist.[54] These equations were extended in later work by the same group,[3] to accommodate the diffusion of surfactant monomer and free molecular solute:

$$D_{aa} = D_D\frac{\partial C_D}{\partial C_a} + \sum_{i=0}^{N-1} iD_i^0\frac{\partial C_i}{\partial C_a} \tag{41}$$

$$D_{as} = D_D\frac{\partial C_D}{\partial C_s} + \sum_{i=0}^{N-1} iD_i^0\frac{\partial C_i}{\partial C_s} \tag{42}$$

$$D_{sa} = D_{mon}\frac{\partial C_{mon}}{\partial C_a} + \sum_{i=0}^{N-1} m_iD_i^0\frac{\partial C_i}{\partial C_a} \tag{43}$$

$$D_{ss} = D_{mon}\frac{\partial C_{mon}}{\partial C_s} + \sum_{i=0}^{N-1} m_iD_i^0\frac{\partial C_i}{\partial C_s} \tag{44}$$

Here, D_D, D_{mon}, C_D, and C_{mon} are the molecular diffusivities and concentrations of molecular solute and surfactant monomer, respectively. This theory was shown to be effective in capturing multicomponent diffusion effects in dilute mixtures with abundant molecular solute and/or surfactant, such as 10−20 mM SB12 zwitterionic solutions with butanol, pentanol, or hexanol solute.[3]

The summation terms in eqs 41−44 indicate contributions to [**D**], stemming from micelle diffusion, that are on the order of the D_i^0 or less. The terms involving molecular species, on the other hand, can be much larger. In aqueous mixtures with hydrophilic components, solubilization shifts the concentration of molecules dissolved outside of micelles. This shift can drive large free molecular gradients that are weighted by molecular diffusivities, which themselves are usually an order of magnitude larger than D_i^0. For this reason, ternary diffusivities are sometimes well predicted using eqs 41−44 because the summation terms are negligible, allowing one to ignore intermicellar interactions when estimating [**D**]. As a result, the cross terms are often small relative to the main terms, and D_{aa} satisfies eq 1.[3,4]

However, infinite dilution theories are likely insufficient in solutions with negligible molecular species, even in dilute solutions, when complex hydrodynamic and thermodynamic colloidal interactions may significantly contribute to the coupling phenomena. In this work, the diffusion of solute down a surfactant gradient ($D_{as} > 0$) and the widening divide between the solute and surfactant main diffusivities (Figure 8) with increasing micelle volume fraction exemplify the importance of intermicellar interactions on multicomponent effects.

DOI: 10.1021/acs.langmuir.9b01823
Langmuir 2019, 35, 13595−13606

CONCLUSIONS

A theoretical model for gradient diffusion in nonionic surfactant solutions with very hydrophobic solutes and negligible molecular species has been developed, using the theory of Batchelor[23,24] that describes gradient diffusion in a dilute polydisperse system of interacting spheres. For aqueous solutions of $C_{12}E_{10}$ with decane, we have shown that solute diffuses down its own gradient by micelle *self*-diffusion while surfactant diffuses down a surfactant gradient by micelle *gradient* diffusion. This result indicates that intermicellar hydrodynamic interactions are largely responsible for dramatically reducing the transport of solute down its own gradient. However, there appears to be an additional contribution lowering D_{aa}, perhaps from intramicellar nonideal mixing, which is currently unexplained and requires further investigation.

Measured cross-term diffusivities in this hydrophobic solute/surfactant mixture were found to be comparable in magnitude to the main terms. The comparison with theory allows us to find that, in the absence of molecular species, surfactant diffuses up a decane gradient via a micelle growth mechanism whose magnitude depends on the sensitivity of the micelle size and aggregation number to solute. Solute, on the other hand, diffuses down a surfactant gradient by a volume exclusion effect.

AUTHOR INFORMATION

Corresponding Author

*E-mail: srdungan@ucdavis.edu.

ORCID

Stephanie R. Dungan: 0000-0001-8420-987X

Notes

The authors declare no competing financial interest.

ACKNOWLEDGMENTS

The authors acknowledge funding from the National Science Foundation (CBET1506474) and from Hatch project 1010420 from the USDA National Institute of Food and Agriculture.

REFERENCES

(1) Leaist, D. G.; Hao, L. Comparison of Diffusion Coefficients of Multicomponent Solutions from Light Scattering and Macroscopic Gradient Techniques. Sodium Dodecyl Sulfate Micelles in Aqueous Salt Solutions. *J. Phys. Chem.* **1993**, *97*, 7763−7768.

(2) Musnicki, W. J.; Dungan, S. R.; Phillips, R. J. Multicomponent Diffusion in Solute-Containing Micelle and Microemulsion Solutions. *Langmuir* **2014**, *30*, 11019−11030.

(3) Everist, M.; MacNeil, J. A.; Moulins, J. R.; Leaist, D. G. Coupled Mutual Diffusion in Solutions of Micelles and Solubilizates. *Phys. Chem. Chem. Phys.* **2009**, *11*, 8173−8182.

(4) Zhang, H.; Annunziata, O. Modulation of Drug Transport Properties by Multicomponent Diffusion in Surfactant Aqueous Solutions. *Langmuir* **2008**, *24*, 10680−10687.

(5) Leaist, D. G. Coupled Diffusion of Butanol Solubilized in Aqueous Sodium Dodecylsulfate Micelles. *Can. J. Chem.* **1990**, *68*, 33−35.

(6) Leaist, D. G.; Hao, L. Model for Chemical Interdiffusion of Solubilizates and Ionic Micelles Aqueous Solutions of n-Alcohols and Sodium Dodecylsulfate. *J. Chem. Soc., Faraday Trans.* **1995**, *91*, 2837−2842.

(7) Zhang, H.; Annunziata, O. Diffusion of an Ionic Drug in Micellar Aqueous Solutions. *Langmuir* **2009**, *25*, 3425−3434.

(8) Naruhashi, K.; Tamai, I.; Li, Q.; Sai, Y.; Tsuji, A. Experimental Demonstration of the Unstirred Water Layer Effect on Drug Transport in Caco-2 Cells. *J. Pharm. Sci.* **2003**, *92*, 1502−1508.

(9) Stewart, A. M.; Grass, M. E.; Mudie, D. M.; Morgen, M. M.; Friesen, D. T.; Vodak, D. T. Development of a Biorelevant, Material-Sparing Membrane Flux Test for Rapid Screening of Bioavailability-Enhancing Drug Product Formulations. *Mol. Pharmaceutics* **2017**, *14*, 2032−2046.

(10) Burkey, T. J.; Griller, D.; Lindsay, D. A.; Scaiano, J. C. Simple Method for Quantifying the Distribution of Organic Substrates between the Micellar and Aqueous Phases of Sodium Dodecyl Sulfate Solution. *J. Am. Chem. Soc.* **1984**, *106*, 1983−1985.

(11) Armstrong, D. W.; Ward, T. J.; Berthod, A. Micellar Effects on Molecular Diffusion: Theoretical and Chromatographic Considerations. *Anal. Chem.* **1986**, *58*, 579−582.

(12) Armstrong, D. W.; Menges, R. A.; Han, S. M. Evaluation of Dye-Micelle Binding Constants Using Diffusion Sensitive Band Broadening Effects. *J. Colloid Interface Sci.* **1988**, *126*, 239−242.

(13) Bird, R. B.; Stewart, W. E.; Lightfoot, E. N. *Transport Phenomena*, 2nd ed.; Wiley: New York, 2007.

(14) Barros, C. F.; Ribeiro, A. C. F.; Verissimo, L. M. P.; Leaist, D. G.; Esteso, M. A. Diffusion in Ternary Aqueous {L-dopa + $(NaSO_3)_n$-β-cyclodextrin} Solutions Using the Pseudo-Binary Approximation. *J. Chem. Thermodyn.* **2018**, *123*, 17−21.

(15) Wygnal, E.; MacNeil, J. A.; Bowles, J.; Leaist, D. G. Mutual Diffusion with Equal Eigenvalues in Solutions of Strongly Associated Surfactants. A New Kind of Multicomponent Diffusion. *J. Mol. Liq.* **2010**, *156*, 95−102.

(16) Castaldi, M.; Costantino, L.; Ortona, O.; Paduano, L.; Vitagliano, V. Mutual Diffusion Measurements in a Ternary System: Ionic Surfactant-Nonionic Surfactant-Water at 25 °C. *Langmuir* **1998**, *14*, 5994−5998.

(17) Leaist, D. G.; MacEwan, K. Coupled Diffusion of Mixed Ionic Micelles in Aqueous Sodium Dodecyl Sulfate + Sodium Octanoate Solutions. *J. Phys. Chem. B* **2001**, *105*, 690−695.

(18) Leaist, D. G.; Abdu, S. M. Ternary Mutual Diffusion Coefficients and Critical Micelle Concentrations of Aqueous Sodium Dodecyl Sulfate + Lithium Dodecyl Sulfate Solutions at 25 °C. *J. Chem. Eng. Data* **2001**, *46*, 922−926.

(19) MacEwan, K.; Leaist, D. G. Incongruent Diffusion (Negative Main Mutual Diffusion Coefficient) for a Ternary Mixed Surfactant System. *J. Phys. Chem. B* **2002**, *106*, 10296−10300.

(20) Das, B.; Maitra, B.; Mercer, S. M.; Everist, M.; Leaist, D. G. A Comparison of Diffusion Coefficients for Ternary Mixed Micelle Solutions Measured by Macroscopic Gradient and Dynamic Light Scattering Techniques. *Phys. Chem. Chem. Phys.* **2008**, *10*, 3083−3092.

(21) Mangiapia, G.; Paduano, L.; Ortona, O.; Sartorio, R.; D'Errico, G. Analysis of Main- and Cross-Term Diffusion Coefficients in Bile Salt Mixtures. *J. Phys. Chem. B* **2013**, *117*, 741−749.

(22) Leaist, D. G. Determination of Ternary Diffusion Coefficients by the Taylor Dispersion Method. *J. Phys. Chem.* **1990**, *94*, 5180−5183.

(23) Batchelor, G. K. Diffusion in a Dilute Polydisperse System of Interacting Spheres. *J. Fluid Mech.* **1983**, *131*, 155−175.

(24) Batchelor, G. K. Corrigendum. *J. Fluid Mech.* **1983**, *137*, 467−469.

(25) Taylor, G. I. Dispersion of Soluble Matter in Solvent Flowing Slowly through a Tube. *Proc. R. Soc. London, Ser. A* **1953**, *219*, 186−203.

(26) Aris, R. On the Dispersion of a Solute in a Fluid Flowing through a Tube. *Proc. R. Soc. London, Ser. A* **1956**, *235*, 67−77.

(27) Alizadeh, A.; Nieto de Castro, C. A.; Wakeham, W. A. The Theory of the Taylor Dispersion Technique for Liquid Diffusivity Measurements. *Int. J. Thermophys.* **1980**, *1*, 243−284.

(28) Johnson, M.; Kamm, R. D. Numerical Studies of Steady Flow Dispersion at Low Dean Number in a Gently Curving Tube. *J. Fluid Mech.* **1986**, *172*, 329−345.

DOI: 10.1021/acs.langmuir.9b01823
Langmuir 2019, 35, 13595−13606

(29) Wakeham, W. A.; Nagashima, A.; Sengers, J. V. *Measurement of the Transport Properties of Fluids*; Blackwell Scientific Publications: Boca Raton, 1991.
(30) Price, W. E. Theory of the Taylor Dispersion Technique for Three-component-system Diffusion Measurements. *J. Chem. Soc., Faraday Trans. 1* **1988**, *84*, 2431−2439.
(31) Deng, Z.; Leaist, D. G. Ternary Mutual Diffusion Coefficients of $MgCl_2$ + $MgSO_4$ + H_2O and Na_2SO_4 + $MgSO_4$ + H_2O from Taylor Dispersion Profiles. *Can. J. Chem.* **1991**, *69*, 1548−1553.
(32) Russo, V.; Ortona, O.; Tesser, R.; Paduano, L.; Di Serio, M. On the Importance of Choosing the Best Minimization Algorithm for Determination of Ternary Diffusion Coefficients by the Taylor Dispersion Method. *ACS Omega* **2017**, *2*, 2945−2952.
(33) Kirkwood, J. G.; Baldwin, R. L.; Dunlop, P. J.; Gosting, L. J.; Kegeles, G. Flow Equations and Frames of Reference for Isothermal Diffusion in Liquids. *J. Chem. Phys.* **1960**, *33*, 1505−1513.
(34) Ray, G. B.; Leaist, D. G. Measurement of Ternary Mutual Diffusion Coefficients from Ill-Conditioned Taylor Dispersion Profiles in Cases of Identical or Nearly Identical Eigenvalues of the Diffusion Coefficient Matrix. *J. Chem. Eng. Data* **2010**, *55*, 1814−1820.
(35) Annunziata, O.; Buzatu, D.; Albright, J. G. Protein Diffusion Coefficients Determined by Macroscopic-Gradient Rayleigh Interferometry and Dynamic Light Scattering. *Langmuir* **2005**, *21*, 12085−12089.
(36) Sutherland, E.; Mercer, S. M.; Everist, M.; Leaist, D. G. Diffusion in Solutions of Micelles. What Does Dynamic Light Scattering Measure? *J. Chem. Eng. Data* **2009**, *54*, 272−278.
(37) Gimel, J. C.; Brown, W. A. Light Scattering Investigation of the Sodium Dodecyl Sulfate-Lysozyme System. *J. Chem. Phys.* **1996**, *104*, 8112−8117.
(38) Tanford, C. *Physical Chemistry of Macromolecules*; John Wiley & Sons: New York, 1961.
(39) Chevalier, Y.; Kamenka, N.; Chorro, M.; Zana, R. Aqueous Solutions of Zwitterionic Surfactants with Varying Carbon Number of the Intercharge Group. 3. Intermicellar Interactions. *Langmuir* **1996**, *12*, 3225−3232.
(40) Vierros, S.; Sammalkorpi, M. Effects of 1-Hexanol on $C_{12}E_{10}$ Micelles: A Molecular Simulations and Light Scattering Study. *Phys. Chem. Chem. Phys.* **2018**, *20*, 6287−6298.
(41) Kong, D. D.; Kosar, T. F.; Dungan, S. R.; Phillips, R. J. Diffusion of Proteins and Nonionic Micelles in Agarose Gels by Holographic Interferometry. *AIChE J.* **1997**, *43*, 25−32.
(42) Attwood, D.; Elworthy, P. H.; Kayne, S. B. Membrane Osmometry of Solubilized Systems. *J. Pharm. Pharmacol.* **1971**, *23*, 77S−84S.
(43) Nolan, S.; Phillips, R. J.; Dungan, S. R. Frequency Domain Fluorescence Measurements of the Aggregation Properties of C_nE_m Surfactants in Agarose Gels. *Langmuir* **2000**, *16*, 911−921.
(44) Kaneshina, S.; Yoshimoto, M.; Kobayashi, H.; Nishikido, N.; Sugihara, G.; Tanaka, M. Effect of Pressure on Apparent Molal Volumes of Nonionic Surfactants in Aqueous Solutions. *J. Colloid Interface Sci.* **1980**, *73*, 124−129.
(45) Nilsson, G.; Lindman, B. Water Self-Diffusion in Nonionic Surfactant Solutions. Hydration and Obstruction Effects. *J. Phys. Chem.* **1983**, *87*, 4756−4761.
(46) Batchelor, G. K. Brownian Diffusion of Particles with Hydrodynamic Interaction. *J. Fluid Mech.* **1976**, *74*, 1−29.
(47) Corti, M.; Degiorgio, V.; Hayter, J. B.; Zulauf, M. Micelle Structure in Isotropic $C_{12}E_8$ Amphiphile Solutions. *Chem. Phys. Lett.* **1984**, *109*, 579−583.
(48) Buck, K. K. S.; Dungan, S. R.; Phillips, R. J. The Effect of Solute Concentration on Hindered Gradient Diffusion in Polymeric Gels. *J. Fluid Mech.* **1999**, *396*, 287−317.
(49) Tolls, J.; van Dijk, J.; Verbruggen, E. J. M.; Hermens, J. L. M.; Loeprecht, B.; Schüürmann, G. Aqueous Solubility-Molecular Size Relationships: a Mechanistic Case Study Using C_{10^-} to C_{19^-}Alkanes. *J. Phys. Chem. A* **2002**, *106*, 2760−2765.
(50) Berthod, A.; Tomer, S.; Dorsey, J. G. Polyoxyethylene Alkyl Ether Nonionic Surfactants: Physicochemical Properties and Use for Cholesterol Determination in Food. *Talanta* **2001**, *55*, 69−83.
(51) Costantino, L.; Volpe, C. D.; Ortona, O.; Vitagliano, V. Diffusion in Microemulsion Systems. *J. Colloid Interface Sci.* **1992**, *148*, 72−79.
(52) Tachiya, M. Kinetics of Quenching of Luminescent Probes in Micellar Systems. II. *J. Chem. Phys.* **1982**, *76*, 340−348.
(53) Smith, G. A.; Christian, S. D.; Tucker, E. E.; Scamehorn, J. F. Solubilization of Hydrocarbons by Surfactant Micelles and Mixed Micelles. *J. Colloid Interface Sci.* **1989**, *130*, 254−265.
(54) Leaist, D. G. Relating Multicomponent Mutual Diffusion and Intradiffusion for Associating Solutes. Application to Coupled Diffusion in Water-in-oil Microemulsions. *Phys. Chem. Chem. Phys.* **2002**, *4*, 4732−4739.

DOI: 10.1021/acs.langmuir.9b01823
Langmuir 2019, 35, 13595−13606

Chapter 2

Multicomponent diffusion of interacting, nonionic micelles with hydrophobic solutes

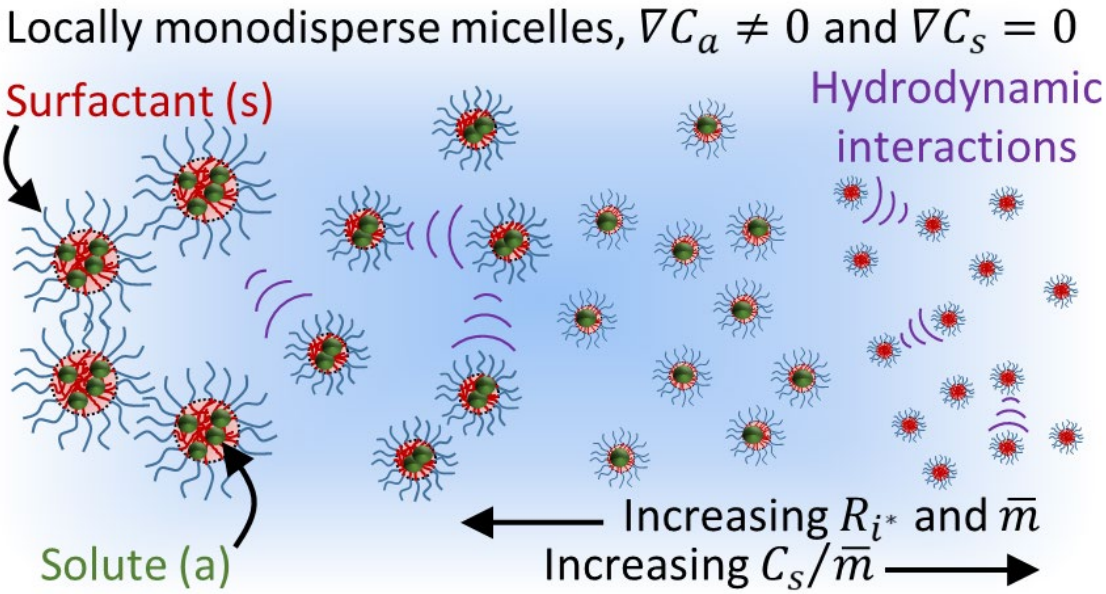

Reproduced from N. P. Alexander, R. J. Phillips, S. R. Dungan, Multicomponent diffusion of interacting, nonionic micelles with hydrophobic solutes, Soft Matter, 2021, 17, 531–542, with permission from the Royal Society of Chemistry.

Soft Matter

PAPER

View Article Online
View Journal | View Issue

Cite this: *Soft Matter*, 2021, **17**, 531

Multicomponent diffusion of interacting, nonionic micelles with hydrophobic solutes

Nathan P. Alexander,[a] Ronald J. Phillips[a] and Stephanie R. Dungan *[ab]

Received 1st August 2020,
Accepted 4th October 2020

DOI: 10.1039/d0sm01406k

rsc.li/soft-matter-journal

Ternary diffusion coefficient matrices [**D**] were measured using the Taylor dispersion method, for crowded aqueous solutions of decaethylene glycol monododecyl ether ($C_{12}E_{10}$) with either decane or limonene solute. The matrix [**D**], for both systems, was found to be highly non-diagonal, and concentration dependent, over a broad domain of solute to surfactant molar ratios and micelle volume fractions. A recently developed theoretical model, based on Batchelor's theory for gradient diffusion in dilute, polydisperse mixtures of interacting spheres, was simplified by neglecting local polydispersity, and effectively used to predict [**D**] with no adjustable parameters. Even though the model originates from dilute theory, the theoretical results were in surprisingly good agreement with experimental data for concentrated mixtures, with volume fractions up to $\phi \approx 0.47$. In addition, the theory predicts eigenvalues D_- and D_+ that correspond to long-time self and gradient diffusion coefficients, respectively, for monodisperse spheres, in reasonable agreement with experimental data.

1 Introduction

Solute-containing micelle and microemulsion solutions diffuse in response to gradients in chemical potential of either solute or surfactant. Since strong molecular interactions drive self-assembly in these mixtures, the resulting fluxes of solute and surfactant occur in the form of many different species, including free molecular solute, surfactant monomer, dimers, trimers, *etc.*, as well as a distribution of interacting colloidal aggregates with various sizes and shapes. When viewed broadly as a ternary mixture of solute (a), surfactant (s), and solvent, gradient diffusion can be described using the ternary form of Fick's law,

$$-\begin{bmatrix} J_a \\ J_s \end{bmatrix} = \begin{bmatrix} D_{aa} & D_{as} \\ D_{sa} & D_{ss} \end{bmatrix} \begin{bmatrix} \nabla C_a \\ \nabla C_s \end{bmatrix}. \quad (1)$$

Here, the main diffusivities (D_{aa} and D_{ss}) relate the molar flux of solute J_a and surfactant J_s to their own concentration gradients, while the off-diagonal diffusivities (D_{as} and D_{sa}) relate the flux of one component to a concentration gradient of the other. The solvent is excluded from eqn (1) because fluxes of three components in a ternary solution are not independent.[1]

Recent studies on multicomponent diffusion in nonionic micellar solutions[2,3] and water-in-oil microemulsions[4,5] indicate strong multicomponent effects, including enhanced surfactant and suppressed solute diffusion down their respective gradients, surfactant diffusion up a solute gradient ($D_{sa} < 0$), and solute diffusion down a surfactant gradient ($D_{as} > 0$). Both cross diffusion effects ($D_{sa} < 0$ and $D_{as} > 0$) were shown capable of establishing buoyancy driven convection (known more generally as double diffusive convection) at the interface between two initially stable ternary microemulsions.[5] Furthermore, suppressed solute diffusion may play a role in limiting the oral absorption rates of hydrophobic drugs, nutrients, and fats when delivered using surfactants to enhance their aqueous solubility.[6,7]

Significant progress has been made toward understanding multicomponent effects in mixtures with nonionic surfactants and solutes.[2–4,8,9] Leaist *et al.*[4,9] developed a theoretical model for multicomponent diffusion in very dilute solutions with negligible intermicellar interactions. According to this theory, multicomponent effects are driven by solubilization-induced gradients in free molecular solute and surfactant monomer and by counter diffusion of non-interacting micelles with size-dependent Stokes–Einstein mobilities.[4,9] This model was shown to be effective in predicting [**D**] in dilute zwitterionic solutions with relatively hydrophilic alcohols.[9] However, at higher concentrations and in dilute solutions with negligible molecular species, micellar and microemulsion solutions resemble colloidal dispersions, and the influence of particle interactions on [**D**] is expected to play a larger role.

In a series of influential papers,[10–15] Batchelor developed a theory for gradient diffusion in dilute colloidal hard-sphere suspensions, which rigorously accounts for the influence of two-sphere thermodynamic and hydrodynamic interactions (HI). The latter, which are characterized by velocity disturbances transmitted through the viscous liquid between Brownian particles, decay so

[a] *Department of Chemical Engineering, University of California at Davis, Davis, CA 95616, USA. E-mail: srdungan@ucdavis.edu*
[b] *Department of Food Science and Technology, University of California at Davis, Davis, CA 95616, USA*

slowly with interparticle separation distance that they are rarely negligible in colloidal dispersions.[16] However, until recently,[2] HI have been neglected in models that describe multicomponent diffusion in surfactant solutions.

The exception is a recent theoretical model by Alexander *et al.*,[2] developed for nonionic surfactant solutions with negligible molecular species, based on the theory of Batchelor for gradient diffusion in dilute, polydisperse hard-sphere suspensions.[14,15] Hence, this model rigorously accounts for pairwise hydrodynamic and thermodynamic intermicellar interactions, and it successfully predicted [**D**] in $C_{12}E_{10}$/decane/water mixtures with no adjustable parameters, up to volume fractions near $\phi = 0.25$.[2]

In the present study, we further test the model of Alexander *et al.*[2] with new experimental data for aqueous solutions with $C_{12}E_{10}$ micelles and either limonene or decane solutes, at concentrations that approach a micellar solution phase boundary, marking the emergence of a liquid crystalline phase. In addition, we simplify our theoretical equations by neglecting local size polydispersity in an effort to make the theory more tractable, and thereby gain physical insight.

2 Materials and methods

2.1 Materials

Nonionic surfactant decaethylene glycol monododecyl ether ($C_{12}E_{10}$, lot #SLBT1187 or #0000057654, each with a hydroxyl value equal to 92.0 mg g^{-1}), and hydrophobic solutes decane and limonene, were all purchased from Sigma-Aldrich and used without modification. Unfiltered, de-ionized water was used to prepare all stock micellar solutions. All mixtures were prepared by volume with aliquots from 100 mL stock solutions, and were allowed to equilibrate overnight at room temperature. Non-ideal changes in volume upon mixing were neglected.

2.2 Taylor dispersion

Ternary diffusion coefficient matrices [**D**] were acquired by the Taylor dispersion method,[17,18] using an apparatus and experimental procedure described previously.[2] Data analysis was performed by fitting measured refractive index profiles with the following Taylor dispersion model equation:[19,20]

$$V(t) = V_0 + V_1 t + V_{\max}\sqrt{\frac{t_R}{t}}\left\{ W\exp\left[-\frac{12D_-(t-t_R)^2}{r^2 t}\right] + (1-W)\exp\left[-\frac{12D_+(t-t_R)^2}{r^2 t}\right]\right\}. \quad (2)$$

Here, V_0 is the baseline voltage of the detector, $V_{\max}$ is the signal voltage when $t = t_R$, and $V_1 t$ captures linear drift in the signal voltage. D_- and D_+ are the eigenvalues of [**D**]:

$$D_- = \frac{(D_{aa}+D_{ss})}{2} - \frac{\sqrt{(D_{aa}-D_{ss})^2 + 4D_{as}D_{sa}}}{2} \quad (3)$$

$$D_+ = \frac{(D_{aa}+D_{ss})}{2} + \frac{\sqrt{(D_{aa}-D_{ss})^2 + 4D_{as}D_{sa}}}{2}. \quad (4)$$

In eqn (2), W is a weighting factor, given by

$$W = \frac{(a+b\alpha_1)\sqrt{D_-}}{(a+b\alpha_1)\sqrt{D_-} + (1-a-b\alpha_1)\sqrt{D_+}} \quad (5)$$

and

$$\alpha_1 = \frac{R_a\Delta C_a}{R_a\Delta C_a + R_s\Delta C_s} \quad (6)$$

$$a = \frac{D_+ - D_{ss} - \frac{R_a}{R_s}D_{as}}{D_+ - D_-} \quad (7)$$

$$b = \frac{D_{ss} + \frac{R_a}{R_s}D_{as} - D_{aa} - \frac{R_s}{R_a}D_{sa}}{D_+ - D_-}. \quad (8)$$

The parameters $R_a = (\partial n/\partial C_a)_{C_s}$ and $R_s = (\partial n/\partial C_s)_{C_a}$ are the refractive index increments with either C_s or C_a held constant, respectively.

In order to acquire the four non-linear fit parameters a, b, D_-, and D_+ of eqn (2), two refractive index profiles with two different values for α_1 were fit simultaneously, using non-linear least squares regression performed with Matlab's "pattern-search" algorithm.[21] One profile was generated from a pulse with excess solute ($\alpha_1 \approx 1$) and another from a pulse with excess surfactant ($\alpha_1 \approx 0$). The fit parameters were then used to evaluate [**D**] *via*

$$D_{aa} = D_- + \frac{a(1-a-b)}{b}(D_- - D_+) \quad (9)$$

$$D_{as} = \frac{R_s}{R_a}\frac{a(1-a)}{b}(D_- - D_+) \quad (10)$$

$$D_{sa} = \frac{R_a}{R_s}\frac{(a+b)(1-a-b)}{b}(D_+ - D_-) \quad (11)$$

$$D_{ss} = D_+ + \frac{a(1-a-b)}{b}(D_+ - D_-). \quad (12)$$

The ratios R_a/R_s in eqn (10) and (11) were evaluated by integrating the refractive index profiles according to $R_a/R_s \approx A_aG_s/A_sG_a$. Here, A_a and A_s are the areas under the dispersion profiles with $\alpha_1 \approx 1$ and $\alpha_1 \approx 0$, respectively, and G_a and G_s are the corresponding detector gain settings. Error bars for the resulting elements of [**D**] represent two standard deviations.

3 Results

3.1 Ternary diffusivities and eigenvalues

The Taylor dispersion method was used to measure the ternary diffusion coefficient matrix [**D**] at constant temperature T = 23.0 ± 0.3 °C and pressure for aqueous $C_{12}E_{10}$/limonene and $C_{12}E_{10}$/decane mixtures. In Fig. 1, [**D**] and eigenvalues D_- and D_+ are shown for aqueous solutions of 200 mM $C_{12}E_{10}$ with limonene concentrations C_a in the range $0 \le C_a \le 100$ mM. The coefficients that comprise [**D**] were also measured in $C_{12}E_{10}$/limonene (Fig. 2) and $C_{12}E_{10}$/decane (Fig. 3) solutions

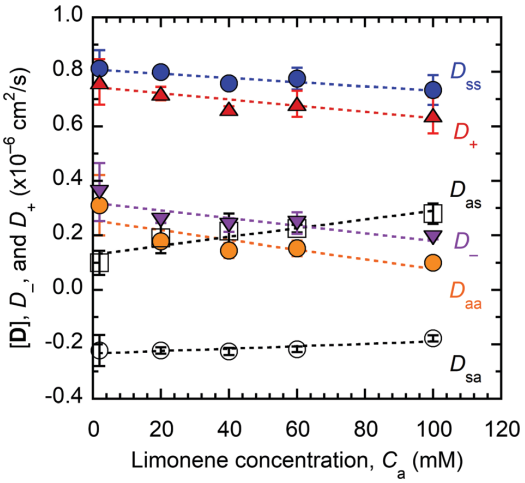

Fig. 1 Ternary diffusion coefficients and eigenvalues for aqueous 200 mM $C_{12}E_{10}$ (s) + limonene (a) for C_a/C_s = 0.01, 0.1, 0.2, 0.3, and 0.5.

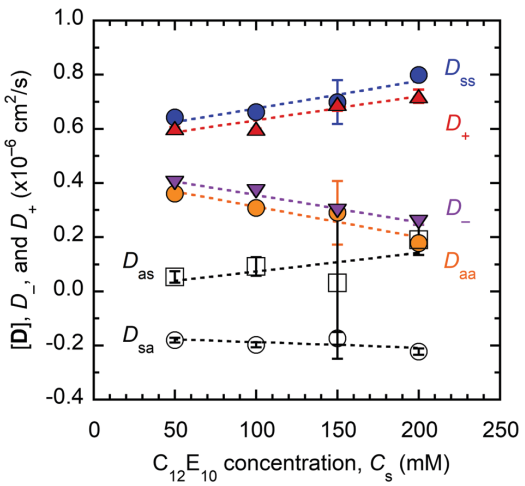

Fig. 2 Ternary diffusion coefficients and eigenvalues for aqueous $C_{12}E_{10}$ (s) + limonene (a) with C_a/C_s = 0.1.

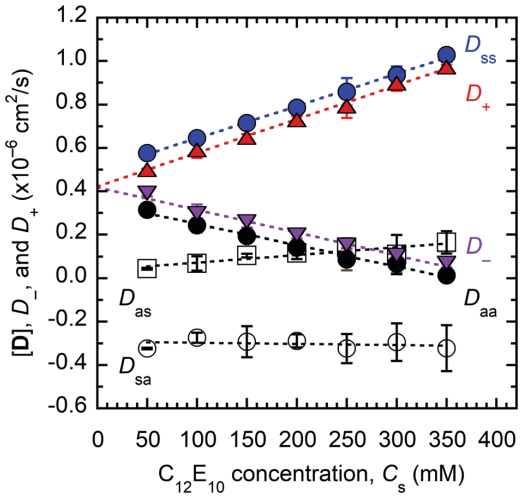

Fig. 3 Ternary diffusion coefficients and eigenvalues for aqueous $C_{12}E_{10}$ (s) + decane (a) with C_a/C_s = 0.1.

that were diluted with water while maintaining a constant molar ratio of solute to surfactant equal to C_a/C_s = 0.1.

The critical micelle concentration of $C_{12}E_{10}$ (0.09 mM)[22] and the aqueous solubilities of limonene (0.10 mM)[23] and decane (3.2×10^{-4} mM)[24] are small compared with the surfactant ($C_s \geq 20$ mM) and solute ($C_a \geq 2$ mM) concentrations used in this study. Hence, aqueous $C_{12}E_{10}$/limonene and $C_{12}E_{10}$/decane mixtures diffused almost exclusively as solute-containing micelles while surfactant monomer and molecular solute fluxes contributed negligibly to [**D**].

Theoretical results for gradient diffusion of colloidal hard spheres by Batchelor[13–15] were derived relative to a volume-fixed reference frame, defined such that the net flux of material volume is zero. Diffusion measurements are generally performed relative to a fixed-laboratory reference frame. However, the lab frame approximates the volume-fixed frame when non-ideal changes in the volume of the solution are negligible upon mixing.[25] That condition is satisfied when either the component molar volumes are constant with composition or when the initial concentration differences, established during the measurement, are made sufficiently small.[25] In this work, we have established small initial concentration differences (5 mM) in either the solute or the surfactant in an effort to minimize non-ideal changes in volume upon mixing. As a result, [**D**] correspond to the volume-fixed reference frame.

4 Discussion

4.1 Ternary diffusion in $C_{12}E_{10}$/solute/water mixtures

As shown in Fig. 1–3, the diffusion coefficient matrices [**D**], measured *via* the Taylor dispersion method for both $C_{12}E_{10}$/limonene/water and $C_{12}E_{10}$/decane/water mixtures, are qualitatively similar. Both systems exhibit strong diffusion coupling, including solute diffusion down a surfactant gradient ($D_{as} > 0$) and surfactant diffusion up a solute gradient ($D_{sa} < 0$). Interestingly, the cross diffusivity D_{sa} for both limonene (Fig. 2) and decane (Fig. 3) is insensitive to surfactant concentration and extrapolates to a nonzero value in the limit as $C_s \to 0$, indicating that this strong coupling effect is weakly influenced by intermicellar interactions. In contrast, the main solute D_{aa} and surfactant D_{ss} diffusivities (Fig. 2 and 3), strongly diverge with increasing C_s and are similar to the slow D_- and fast D_+ eigenvalues, respectively, with ($D_{aa} < D_-$) and ($D_{ss} > D_+$) for all mixtures. In Fig. 3, D_{aa} (and D_-) fall to near zero with increasing C_s, indicating solute diffusion down its own gradient

is nearly arrested at the highest surfactant concentration, C_s = 350 mM.

4.2 Development of theory

In this section, we further develop a theoretical model introduced in our earlier work,[2] which is based on Batchelor's[14,15] theory for gradient diffusion in polydisperse colloidal mixtures, to describe gradient diffusion in solutions of solute-containing micelles with negligible molecular species. Here, micellar solutions are modeled as polydisperse, colloidal dispersions containing N different particle types, self-assembled from various numbers of solute and surfactant molecules. The molar flux J_i of micelle type i containing n_i solutes and m_i surfactants is defined relative to a volume-fixed reference frame and given by the generalized form of Fick's law,

$$-J_i = \sum_{j=1}^{N} D_{ij} \nabla C_j. \tag{13}$$

The main micelle diffusivities D_{ii} relate the flux of each micelle species i to its own molar concentration gradient ∇C_i, whereas the micelle cross diffusivities $D_{ij}(j \neq i)$, which accommodate micelle–micelle diffusion coupling, relate the flux of a micelle species i to a concentration gradient in a different micelle species j.

The diffusivities D_{ij} are evaluated using Batchelor's theory for gradient diffusion of polydisperse colloidal particle mixtures,[14]

$$D_{ij} = \frac{D_i^0}{k_B T} \sum_{k=1}^{N} B_{ik} \phi_i \left\{ {\lambda_{ij}}^3 \left(\frac{\partial \mu_k}{\partial \phi_j} \right)_{p,T} + \frac{{\lambda_{ik}}^3}{1-\phi} \sum_{l=1}^{N} {\lambda_{lj}}^3 \phi_l \left(\frac{\partial \mu_l}{\partial \phi_j} \right)_{p,T} \right\}. \tag{14}$$

Here, as applied to our system, D_i^0, B_{ik}, and ϕ_i are the infinite dilution diffusivity, bulk mobility coefficient, and volume fraction of micelle species i. $\phi = \sum_{i=1}^{N} \phi_i$ is the total micelle volume fraction, μ_k is the chemical potential of micelle species k, and $\lambda_{ij} = \left(\frac{V_j}{V_i} \right)^{1/3}$ is a ratio of characteristic lengths, where V_j and V_i are the volumes for a type j and i micelle, respectively.

Neglecting flux contributions from singly dissolved solute and surfactant molecules, the net flux of solute J_a and surfactant J_s are calculated *via* weighted sums of the micelle species fluxes

$$J_a = \sum_{i=1}^{N} n_i J_i \tag{15}$$

$$J_s = \sum_{i=1}^{N} m_i J_i. \tag{16}$$

To derive the diffusivity matrix [**D**], one can expand eqn (13) with the chain rule and combine the result with eqn (1) and (14)–(16),

$$D_{aa} = \sum_{i=1}^{N} \frac{n_i D_i^0}{k_B T} \sum_{j=1}^{N} \sum_{k=1}^{N} B_{ik} \phi_i \left\{ {\lambda_{ij}}^3 \left(\frac{\partial \mu_k}{\partial \phi_j} \right)_{p,T} + \frac{{\lambda_{ik}}^3}{1-\phi} \sum_{l=1}^{N} {\lambda_{lj}}^3 \phi_l \left(\frac{\partial \mu_l}{\partial \phi_j} \right)_{p,T} \right\} \frac{\partial C_j}{\partial C_a} \tag{17}$$

$$D_{as} = \sum_{i=1}^{N} \frac{n_i D_i^0}{k_B T} \sum_{j=1}^{N} \sum_{k=1}^{N} B_{ik} \phi_i \left\{ {\lambda_{ij}}^3 \left(\frac{\partial \mu_k}{\partial \phi_j} \right)_{p,T} + \frac{{\lambda_{ik}}^3}{1-\phi} \sum_{l=1}^{N} {\lambda_{lj}}^3 \phi_l \left(\frac{\partial \mu_l}{\partial \phi_j} \right)_{p,T} \right\} \frac{\partial C_j}{\partial C_s} \tag{18}$$

$$D_{sa} = \sum_{i=1}^{N} \frac{m_i D_i^0}{k_B T} \sum_{j=1}^{N} \sum_{k=1}^{N} B_{ik} \phi_i \left\{ {\lambda_{ij}}^3 \left(\frac{\partial \mu_k}{\partial \phi_j} \right)_{p,T} + \frac{{\lambda_{ik}}^3}{1-\phi} \sum_{l=1}^{N} {\lambda_{lj}}^3 \phi_l \left(\frac{\partial \mu_l}{\partial \phi_j} \right)_{p,T} \right\} \frac{\partial C_j}{\partial C_a} \tag{19}$$

$$D_{ss} = \sum_{i=1}^{N} \frac{m_i D_i^0}{k_B T} \sum_{j=1}^{N} \sum_{k=1}^{N} B_{ik} \phi_i \left\{ {\lambda_{ij}}^3 \left(\frac{\partial \mu_k}{\partial \phi_j} \right)_{p,T} + \frac{{\lambda_{ik}}^3}{1-\phi} \sum_{l=1}^{N} {\lambda_{lj}}^3 \phi_l \left(\frac{\partial \mu_l}{\partial \phi_j} \right)_{p,T} \right\} \frac{\partial C_j}{\partial C_s}. \tag{20}$$

Eqn (17)–(20) define [**D**] for a polydisperse solution of micelles with arbitrary shapes, sizes, interaction potentials, and volume fractions. However, for suspensions of arbitrary concentration, the task of evaluating [**D**] using this result is formidable.

For dilute mixtures ($\phi \ll 1$), B_{ik} and $(\partial \mu_k / \partial \phi_j)_{p,T}$, which are generally functions of the species volume fractions (ϕ_1, ϕ_2,..., ϕ_N) and size ratios λ_{ik}, may each be approximated with a series truncated to $O(\phi)$. The series approximations combine with eqn (14) to yield,[14]

$$D_{ii} = D_i^0 \left\{ 1 + (\beta + S)\phi_i + \sum_{\substack{k=1 \\ k \neq i}}^{N} K'_{ik} \phi_k \right\} \tag{21}$$

$$D_{\substack{ij \\ (j \neq i)}} = D_i^0 \phi_i \left\{ \beta_{ij} \left(\frac{1+\lambda_{ij}}{2} \right)^3 + K''_{ij} \right\}. \tag{22}$$

Here, the second osmotic virial coefficients β_{ij} and bulk mobility coefficients K_{ik}' and K_{ij}'' depend on the interaction potential between pairs of particles and provide corrections to infinitely dilute particle thermodynamic driving forces and mobilities, respectively. The coefficients $\beta = \beta_{ii}$ and $S = K_{ii}' + K_{ii}''$ account for interactions between identical particles of the same species. Using eqn (21) and (22) in lieu of eqn (14), one may derive a

theoretical result for [**D**] for dilute mixtures of polydisperse micelles with arbitrary shapes, sizes, and pair interactions:

$$D_{aa} = \sum_{i=1}^{N} n_i D_i^0 \left\{ \left(1 + \sum_{k=1}^{N} K'_{ik}\phi_k \right) \frac{\partial C_i}{\partial C_a} + \phi_i \sum_{j=1}^{N} \left(\beta_{ij} \left(\frac{1+\lambda_{ij}}{2} \right)^3 + K''_{ij} \right) \frac{\partial C_j}{\partial C_a} \right\} \quad (23)$$

$$D_{as} = \sum_{i=1}^{N} n_i D_i^0 \left\{ \left(1 + \sum_{k=1}^{N} K'_{ik}\phi_k \right) \frac{\partial C_i}{\partial C_s} + \phi_i \sum_{j=1}^{N} \left(\beta_{ij} \left(\frac{1+\lambda_{ij}}{2} \right)^3 + K''_{ij} \right) \frac{\partial C_j}{\partial C_s} \right\} \quad (24)$$

$$D_{sa} = \sum_{i=1}^{N} m_i D_i^0 \left\{ \left(1 + \sum_{k=1}^{N} K'_{ik}\phi_k \right) \frac{\partial C_i}{\partial C_a} + \phi_i \sum_{j=1}^{N} \left(\beta_{ij} \left(\frac{1+\lambda_{ij}}{2} \right)^3 + K''_{ij} \right) \frac{\partial C_j}{\partial C_a} \right\} \quad (25)$$

$$D_{ss} = \sum_{i=1}^{N} m_i D_i^0 \left\{ \left(1 + \sum_{k=1}^{N} K'_{ik}\phi_k \right) \frac{\partial C_i}{\partial C_s} + \phi_i \sum_{j=1}^{N} \left(\beta_{ij} \left(\frac{1+\lambda_{ij}}{2} \right)^3 + K''_{ij} \right) \frac{\partial C_j}{\partial C_s} \right\}. \quad (26)$$

In order to calculate [**D**] using eqn (23)–(26), the coefficients β_{ij}, K_{ik}', and K_{ij}'', as well as the micelle distribution function, must be known. For mixtures of particles that interact as hard spheres, the virial coefficients are given by,[26]

$$\beta_{ij} = 8. \quad (27)$$

Relations from Batchelor[15] provide estimates for the bulk mobility coefficients,

$$K'_{ik} = \frac{-2.5}{1 + 0.16\lambda_{ik}}, \quad (28)$$

and

$$K''_{ij} = \frac{{\lambda_{ij}}^2}{1+{\lambda_{ij}}^3} - \left({\lambda_{ij}}^2 + 3\lambda_{ij} + 1 \right), \quad (29)$$

which are accurate to within 5% of numerical calculations for $\frac{1}{8} \leq \lambda_{ij} \leq 8$.

Previously,[2] eqn (21)–(29) were successfully used to predict [**D**] for $C_{12}E_{10}$/decane/water mixtures. In that study, the distribution of micelle species was assumed to obey a Poisson distribution with a mean, variance, and higher moments dependent on the average number of solubilizate molecules per micelle $\bar{n} = C_a/C_s\bar{m}$, where $\bar{m}$ is the average micelle aggregation number and the overbar indicates local number averages. As a result, the moments of the Poisson varied locally with composition along solute and/or surfactant concentration gradients.

However, our previous dynamic light scattering results indicate that decane-containing $C_{12}E_{10}$ micelles in water are narrowly polydisperse with a small relative standard deviation $\sigma_R < 0.1$.[2] Hence, in this work, local polydispersity and the higher moments are neglected, and the micelle distribution is defined using a Kronecker delta with a composition dependent mean:

$$C_i = \frac{C_s}{\bar{m}}\delta_{ii^*} = \left\{ \begin{array}{ll} \frac{C_s}{\bar{m}} & \text{when } i = i^* \\ 0 & \text{when } i \neq i^* \end{array} \right\}. \quad (30)$$

Here, i^* designates a micelle type with $\bar{n}$ solutes, $\bar{m}$ surfactants, radius R_{i^*}, and a local concentration equal to $C_s/\bar{m}$. Using the delta distribution $C_i = C_s/\bar{m}\delta_{ii^*}$, eqn (23)–(26) may be simplified to (see Appendix A)

$$\frac{D_{aa}}{D_{i^*}^0} = 1 + K'\phi - M\left(\phi, \frac{C_a}{C_s}\right) \quad (31)$$

$$\frac{D_{as}}{D_{i^*}^0} = \frac{C_a}{C_s}\left\{ (\beta + K'')\phi + M\left(\phi, \frac{C_a}{C_s}\right) \right\} \quad (32)$$

$$\frac{D_{sa}}{D_{i^*}^0} = -\frac{C_s}{C_a} M\left(\phi, \frac{C_a}{C_s}\right) \quad (33)$$

$$\frac{D_{ss}}{D_{i^*}^0} = 1 + (\beta + S)\phi + M\left(\phi, \frac{C_a}{C_s}\right). \quad (34)$$

The function $M\left(\phi, \frac{C_a}{C_s}\right)$ is given by

$$M\left(\phi, \frac{C_a}{C_s}\right) = \frac{\partial \ln R_{i^*}}{\partial \ln C_a}(1 + \chi\phi) - (\beta + K'')\phi_a, \quad (35)$$

where $\phi_a = C_a N_A V_a$ is the solute volume fraction, N_A is Avogadro's number, V_a is the molecular volume of the solute, and the parameter χ is evaluated according to

$$\chi = \left(\frac{3}{2}\beta + K' + 3K'' \right) - \left\{ \frac{d(K'' - K')}{d\lambda} \right\}_{\lambda=1}. \quad (36)$$

$D_{i^*}^0$ is calculated using the Stokes–Einstein equation

$$D_{i^*}^0 = \frac{k_B T}{6\pi\eta R_{i^*}}, \quad (37)$$

the volume fraction ϕ is determined using

$$\phi = N_A \frac{C_s}{\bar{m}} \frac{4}{3}\pi {R_{i^*}}^3, \quad (38)$$

and the aggregation number can be evaluated using a micelle volume balance with $\bar{n} = C_a/C_s\bar{m}$,

$$\bar{m} = \frac{\frac{4}{3}\pi {R_{i^*}}^3}{\frac{C_a}{C_s}V_a + V_s + n_H V_w}. \quad (39)$$

Here, V_s, V_a, and V_w are the respective molecular volumes of a dry molecule of $C_{12}E_{10}$, solute, and water, and the hydration index n_H is the number of bound water molecules per surfactant molecule.

Note, according to eqn (B.1) in Appendix B, the derivative $\frac{\partial \ln R_{i^*}}{\partial \ln C_a}$ is a univariate function of C_a/C_s. Furthermore, the solute volume fraction ϕ_a can be rewritten using eqn (38) and (39) to yield $\phi_a = \frac{C_a}{C_s}\left(\frac{V_a}{\frac{C_a}{C_s}V_a + V_s + n_H V_w}\right)\phi$. Thus, the function $M\left(\phi, \frac{C_a}{C_s}\right)$, defined by eqn (35), is dependent on C_a/C_s and ϕ.

The parameters n_H and R_{i^*} are experimentally accessible as functions of C_a/C_s *via* light scattering measurements extrapolated to infinite dilution, while data at higher concentrations indicates the particle interaction potential. For solutions of micelles that interact as hard spheres, $\beta = 8$ and exact calculations by Batchelor[12,15] provide $K' = -2.10$, $K'' = -4.45$, $S = K' + K'' = -6.55$, and $\chi = 1.25$ (see Appendix A). The remaining parameters are determined using eqn (37)–(39). As a result, the model defined by eqn (31)–(39) has no adjustable parameters.

Theoretical predictions for the eigenvalues of [**D**] may be determined using eqn (3), (4), and (31)–(34),

$$\frac{D_-}{D^0_{i^*}} = 1 + K'\phi \tag{40}$$

$$\frac{D_+}{D^0_{i^*}} = 1 + (\beta + S)\phi. \tag{41}$$

Remarkably, eqn (40) and (41) indicate that D_- and D_+ correspond to self and gradient diffusion coefficients, respectively, for colloidal suspensions of monodisperse spheres, even though strong multicomponent diffusion effects may cause [**D**] to be highly non-diagonal.

4.3 Label and tracer limits for [D]

It is insightful to examine [**D**] for the special case in which a solute behaves as a volume-less label in a solution of equally sized micelles with $\phi_a = 0$, $\bar{m} = m_0$, $R_{i^*} = R_0$, and $D^0_{i^*} = D^0$ where m_0, R_0, and D^0 are the solute-free micelle aggregation number, radius, and infinite dilution diffusivity, respectively. Here, micelles containing various numbers of solute labels diffuse with an average size and aggregation number that do not vary along solute or surfactant gradients. As a result, $M\left(\phi, \frac{C_a}{C_s}\right) = 0$, and eqn (31)–(34) simplify to

$$\frac{D_{aa}}{D^0} = 1 + K'\phi \tag{42}$$

$$\frac{D_{as}}{D^0} = \frac{C_a}{C_s}(\beta + K'')\phi \tag{43}$$

$$D_{sa} = 0 \tag{44}$$

$$\frac{D_{ss}}{D^0} = 1 + (\beta + S)\phi. \tag{45}$$

In this case, solute diffuses down its own gradient at a rate determined by the micelle self diffusion coefficient, according to eqn (42), and surfactant diffuses down a surfactant gradient according to the micelle gradient diffusion coefficient, given by eqn (45). Furthermore, solute is carried within micelles down a surfactant gradient according to eqn (43), while D_{sa} is predicted to equal zero. Eqn (42)–(45) describe 'baseline' multicomponent effects, common to ternary mixtures with any hydrophobic solute. Comparison of eqn (31)–(34) with eqn (42)–(45) indicate that the unique properties of a particular solute (*i.e.* its size, polarity, *etc.*) may affect [**D**] through the function $M\left(\phi, \frac{C_a}{C_s}\right)$ and the Stokes–Einstein diffusivity $D^0_{i^*}$. Per eqn (35)–(37), solubilizate alters the microstructure of a solution through $M\left(\phi, \frac{C_a}{C_s}\right)$ and $D^0_{i^*}$ by shifting the average micelle size R_{i^*}, which it may accomplish by occupying volume and by changing the average micelle aggregation number.

Some appreciation for the implications of eqn (42)–(45) can be gained by considering their predictions in different physical conditions. In the limit of infinite dilution, there are no off-diagonal elements of [**D**], and both of the diagonal terms D_{aa} and D_{ss} equal the solute-free Stokes–Einstein diffusivity D^0. Hence, in the absence of micelle–micelle interactions, solute and surfactant fluxes are both proportional to gradients in their own concentrations, and independent of the other. Next, consider a case where there is no gradient in surfactant concentration, but there is a gradient in solute concentration. The role of solute is only to label the micelles. The solute flux, therefore, must be governed by the self diffusion coefficient that describes the random walk of identical micelles in the absence of any imposed gradient in micelle concentration. That coefficient is given by eqn (42). By contrast, if solute and surfactant gradients are imposed with the molar ratio C_a/C_s held fixed, so that every micelle along the gradient has the same amount of solute with the same radius and aggregation number, then clearly the solute (and surfactant) flux is governed by the gradient diffusion coefficient of the micelles. Indeed, using eqn (1) and (42)–(45) (or, more generally, using eqn (31)–(34)), and the constraint $\nabla(C_a/C_s) = 0$, one can show that [**D**] degenerates to the micelle gradient diffusion coefficient according to $[\mathbf{D}] = D^0\{1 + (\beta + S)\phi\}[\mathbf{I}]$, where [**I**] is the identity matrix. Absent any such constraints, even in a solution with no gradient in solute concentration, micelle–micelle interactions can yield a gradient in solute chemical potential that drives a solute flux.

We now examine [**D**] for a different special case in which solute retains its identity but is present in trace amounts, corresponding to the limit $C_a/C_s \to 0$. In this limit, $M\left(\phi, \frac{C_a}{C_s}\right) \to 0$ and $D^0_{i^*} \to D^0$, so that eqn (31)–(34) become (see Appendix B)

$$\frac{D_{aa}}{D^0} = 1 + K'\phi \tag{46}$$

$$D_{as} = 0 \tag{47}$$

$$\frac{D_{sa}}{D^0} = -\frac{a_1}{R_0}(1 + \chi\phi) + (\beta + K'')\left(\frac{V_a}{V_s + n_H V_w}\right)\phi \tag{48}$$

$$\frac{D_{ss}}{D^0} = 1 + (\beta + S)\phi. \tag{49}$$

Here, a_1 may be interpreted as a micelle growth rate, indicating how strongly the average micelle radius varies with the molar ratio C_a/C_s (see eqn (A.21)). Eqn (46) and (49) indicate that solute and surfactant diffuse down their respective gradients according to self and gradient diffusion coefficients of monodisperse spheres, which is the same behaviour predicted by eqn (42) and (45) when solute was assumed to behave as a label. Furthermore, solutes with larger growth rates a_1 drive stronger uphill surfactant fluxes ($D_{sa} < 0$) per eqn (48) and surfactant gradients do not drive solute fluxes per eqn (47) when micelles carry only trace amounts of solute.

4.4 Comparison with experimental data

Theoretical predictions for [**D**] for aqueous $C_{12}E_{10}$/decane and $C_{12}E_{10}$/limonene mixtures were calculated using eqn (31)–(39) with V_a = 0.32 nm^{-3} (decane) or 0.26 nm^{-3} (limonene), V_s = 0.99 nm^{-3}, V_w = 0.03 nm^{-3}, β = 8, K' = −2.10, K'' = −4.45, $S = K' + K''$ = −6.55, and χ = 1.25. The remaining parameters, n_H and R_{i^*}, were evaluated in accordance with our light scattering results,[2] which indicate n_H = 40 and $R_{i^*} = a_1\frac{C_a}{C_s} + R_0$ with a solute-free micelle radius R_0 = 3.78 nm and growth rate a_1 = 2.42 nm (decane) or 1.56 nm (limonene). The growth rate for limonene was determined from currently unpublished dynamic light scattering data, following the same procedure used to acquire the decane value.[2] In Fig. 4A and B, theoretical results and experimental data for [**D**] are plotted as a function of C_a/C_s and ϕ for concentrated solutions of $C_{12}E_{10}$ micelles with either limonene (Fig. 4A) or decane (Fig. 4B), respectively.

Overall, the theoretical results are in good agreement with the experimental values over the entire volume fraction and molar ratio domains, which is surprising given that the model is based on Batchelor's theory for dilute particle mixtures, and has no adjustable parameters. As shown, the model captures cross diffusion coupling, including solute diffusion down a surfactant gradient ($D_{as} > 0$) and surfactant diffusion up a solute gradient ($D_{sa} < 0$). Furthermore, in Fig. 4B, enhanced surfactant (D_{ss}) and suppressed solute (D_{aa}) diffusion down their respective gradients with increasing ϕ are also accurately predicted.

As noted by others,[27,28] Batchelor's dilute theory for gradient diffusion in monodisperse hard sphere dispersions agrees well with numerical results[28,29] for concentrated particle mixtures up to $\phi \approx 0.4$, suggesting a near cancellation of higher order, many-body hydrodynamic and thermodynamic virial contributions. Similarly, as shown in Fig. 4B, linear variation in the measured values for [**D**] with respect to ϕ may also suggest a significant cancellation of these higher order terms, thereby extending the domain over which our dilute multicomponent theory, defined by eqn (31)–(39), provides accurate results.

Eqn (31)–(34) were derived assuming locally monodisperse, spherical micelles that may vary in R_{i^*} and $\bar{m}$ with C_a/C_s but not with ϕ (see Appendix A, eqn (A.21) and (A.22)). Hence, good agreement between our theoretical and experimental values for [**D**] for mixtures comprising $C_{12}E_{10}$ micelles with either decane or limonene solute provides evidence that, to a good approximation, these micelles behave as hard spheres that do not significantly change in size or shape with respect to surfactant concentration, while holding the molar ratio constant, over the entire volume fraction and molar ratio domain explored in this study. This result is consistent with literature[2,30–37] on the morphological behaviour of micelles formed with $C_{12}E_{10}$ or related $C_{12}E_n$ surfactants, at least over a portion of the micellar solution region of their respective phase diagrams. Furthermore, the large size of $C_{12}E_{10}$'s headgroup suggests that it should form spherical micellar aggregates over a significant temperature-composition domain.[30,31]

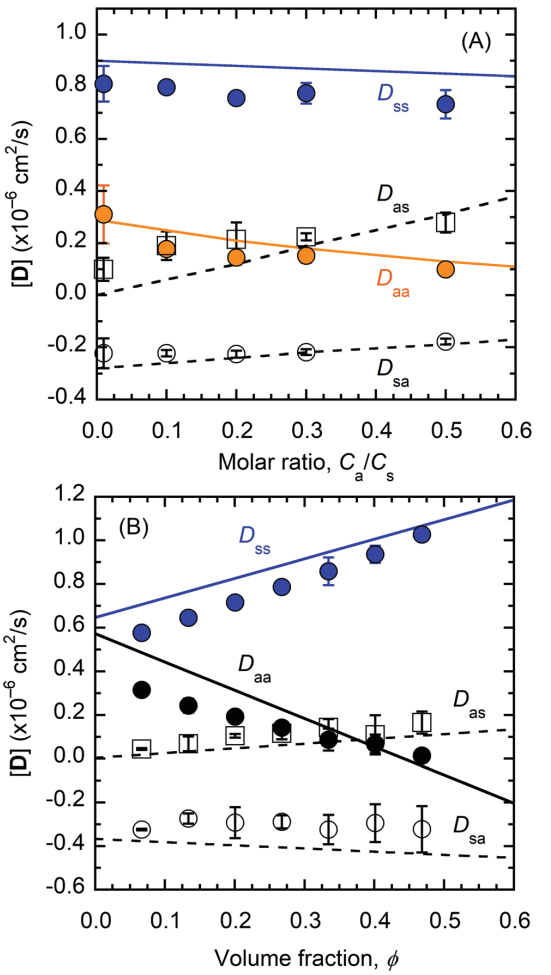

Fig. 4 Ternary diffusion coefficients for (A) aqueous 200 mM $C_{12}E_{10}$ (s) + limonene (a) and (B) aqueous $C_{12}E_{10}$ (s) + decane (a) with C_a/C_s = 0.1. Theoretical predictions for [**D**], shown as solid and dashed lines, were calculated using eqn (31)–(39).

At temperatures sufficiently far below the cloud point curve, hard-sphere behaviour and a weak dependence of micelle size with respect to surfactant concentration have been reported for mixtures of $C_{12}E_6$/water,[35] $C_{12}E_8$/water,[35,38] $C_{12}E_{10}$/water,[2] $C_{12}E_{10}$/decane/water,[2] and $C_{12}E_5$/decane/water.[36,37] The latter

system is particularly interesting, since light scattering and cryo-TEM data for $C_{12}E_5$/water indicate the presence of worm-like micelles that grow and form branched micellar networks with increasing surfactant concentration for dilute mixtures at temperatures as low as 8 °C.[39] However, when loaded to capacity with decane at significantly higher temperature (23.5 °C), decane-containing $C_{12}E_5$ micelles are reported to behave as nearly ϕ-independent, monodisperse hard spheres over a large volume fraction domain.[36,37] Hence, it is plausible that hard sphere theory could be applicable to ternary mixtures comprising a variety of nonionic surfactants and hydrophobic solutes, especially for nonionic surfactants with large head-groups relative to their hydrocarbon tails,[30,31] or when heavily loaded with solute.

Predictions for [**D**] in the solute tracer limit (eqn (46)–(49)) indicate that [**D**] varies with solute type mainly through D_{sa} at low molar ratios. Hence, in order to compare [**D**] for different solutes, experimental values for D_{sa} *versus* C_s for aqueous $C_{12}E_{10}$/decane and $C_{12}E_{10}$/limonene mixtures with C_a/C_s = 0.1 are presented in Fig. 5, superimposed over theoretical predictions (solid and dashed lines). As shown, D_{sa} values for $C_{12}E_{10}$ micelles with decane are greater in magnitude relative to those with limonene, suggesting that solutes with stronger growth rates a_1 drive stronger uphill surfactant fluxes.

According to solubilization theory,[40,41] micelle growth rates vary with the size and polarity of the solubilizate. Solubilization increases the interfacial area and alters the composition of the micelle core, both of which affect the core–shell interfacial energy of the micelle, driving changes in the aggregation number that affect micelle size. Small solubilizates with relatively high polarities, such as limonene, inflict a smaller interfacial energy penalty when solubilized, driving a smaller increase in the aggregation number, relative to larger, less polar solutes, such as decane. As a result, $C_{12}E_{10}$ micelles with limonene are expected to have a smaller growth rate and weaker cross diffusion coupling than those with decane, which is supported by the data shown in Fig. 5, and is consistent with predictions for D_{sa} in the tracer limit according to eqn (48).

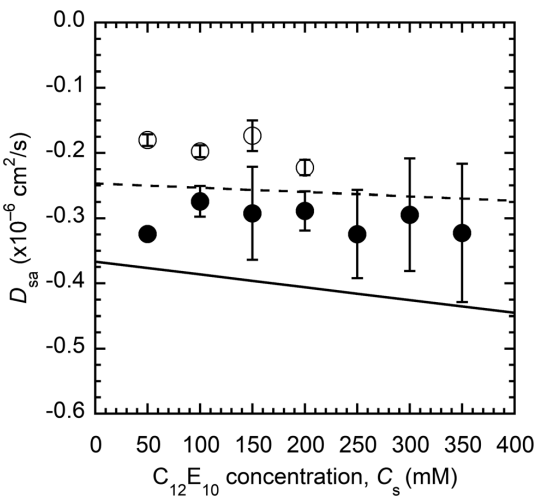

Fig. 5 Cross diffusion coefficients D_{sa} for aqueous $C_{12}E_{10}$/decane (closed circles) and $C_{12}E_{10}$/limonene (open circles) with C_a/C_s = 0.1. Theoretical predictions for D_{sa} were calculated using eqn (33) and (35)–(38) and are indicated by solid and dashed lines for mixtures with decane and limonene, respectively.

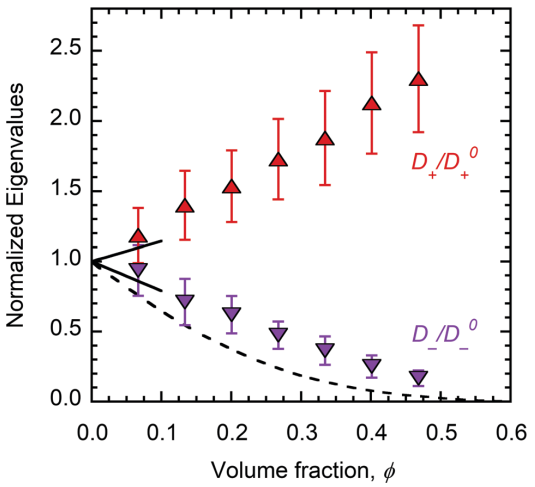

Fig. 6 Normalized eigenvalues for aqueous $C_{12}E_{10}$ (s) + decane (a) with C_a/C_s = 0.1. Monodisperse hard sphere theory by Batchelor[13–15] and Brady[42] are shown as solid and dashed lines, respectively. Error bars indicate 95% confidence intervals.

In Fig. 6, measurements for the eigenvalues D_- and D_+ for $C_{12}E_{10}$/decane/water mixtures with C_a/C_s = 0.1 are normalized with their respective values at infinite dilution (D_-^0 and D_+^0) and plotted as a function of ϕ. The experimental data are superimposed over dilute theory by Batchelor[13–15] (solid lines) for gradient and long-time self diffusion of monodisperse hard spheres. In addition, theory by Brady[42] (dashed line), for long-time self diffusion in concentrated monodisperse hard-sphere suspensions, is also shown. Here, Batchelor's dilute theory is expected to be more accurate for $\phi \ll 1$, while the theory by Brady provides an approximate result over the entire concentration domain up to the random close packing fraction for hard spheres ($\phi \approx 0.63$). As shown, the normalized eigenvalues D_-/D_-^0 and D_+/D_+^0 diverge with increasing ϕ, with slopes over the entire range of volume fractions equal to -1.9 ± 0.2 and 2.7 ± 0.1, respectively. These values are in reasonable agreement with predictions by Batchelor[13–15] for long-time self (-2.10) and gradient (1.45) diffusion of monodisperse hard spheres, supporting our theoretical predictions given by eqn (40) and (41).

5 Conclusions

Interactions between nonionic micelles in concentrated aqueous $C_{12}E_{10}$/decane and $C_{12}E_{10}$/limonene mixtures are shown to strongly affect the ternary diffusion coefficient matrices [**D**] for both systems.

Hence, theoretical predictions for [**D**] that do not account for both thermodynamic and hydrodynamic intermicellar interactions may be misleading. A theoretical model developed previously, based on the rigorous theory by Bachelor for dilute, polydisperse colloidal hard spheres, was simplified by neglecting local size polydispersity, and was effectively used to predict [**D**] for both micellar systems with no adjustable parameters. Furthermore, the theoretical predictions are surprisingly accurate far beyond the dilute regime, up to concentrations approaching a phase boundary. Lastly, despite strong multicomponent diffusion effects, the fast D_+ and slow D_- eigenvalues of [**D**] for aqueous $C_{12}E_{10}$/decane mixtures correspond to gradient and self diffusion coefficients for monodisperse hard sphere dispersions.

Conflicts of interest

There are no conflicts of interest to declare.

Appendix A: derivation of [D] for dilute mixtures of spherical micelles with negligible polydispersity

In this section, we provide a detailed derivation of D_{aa} in eqn (31), starting from eqn (23). Eqn (32)–(34) may be derived by an analogous approach, yielding the complete matrix [**D**]. We begin with eqn (23),

$$D_{aa} = \sum_{i=1}^{N} n_i D_i^0 \left\{ \left(1 + \sum_{k=1}^{N} K'_{ik}\phi_k\right)\frac{\partial C_i}{\partial C_a} + \phi_i \sum_{j=1}^{N} \left(\beta_{ij}\left(\frac{1+\lambda_{ij}}{2}\right)^3 + K''_{ij}\right)\frac{\partial C_j}{\partial C_a}\right\}. \quad (A.1)$$

In eqn (A.1), C_i and $\phi_i = C_i N_A V_i$ are the only functions of C_a and C_s, permitting rearrangement to the following amenable form,

$$D_{aa} = \sum_{i=1}^{N} \frac{\partial\left(n_i D_i^0 C_i\right)}{\partial C_a}\left(1 + \sum_{k=1}^{N} K'_{ik}\phi_k\right) + \sum_{i=1}^{N} n_i D_i^0 \phi_i \frac{\partial}{\partial C_a} \sum_{j=1}^{N} \left\{\beta_{ij}\left(\frac{1+\lambda_{ij}}{2}\right)^3 + K''_{ij}\right\} C_j. \quad (A.2)$$

For micelle distributions that are monomodal and narrow, reasonable approximations for the species concentrations C_i, and volume fractions ϕ_i, can be defined using a Kronecker delta distribution function (see eqn (30)), so that $C_i = C_s/\bar{m}\delta_{ii^*}$ and $\phi_i = C_s/\bar{m}N_A V_i \delta_{ii^*}$. According to this definition, C_i is nonzero only when the index $i = i^*$, which denotes a micelle type representative of the distribution mean and characterized as having $\bar{n}$ solutes, $\bar{m}$ surfactants, radius R_{i^*}, and concentration $C_s/\bar{m}$, all of which are functions of composition (C_a and C_s). Inserting the Kronecker distribution into eqn (A.2) yields,

$$D_{aa} = \sum_{i=1}^{N} \frac{\partial\left(n_i D_i^0 \frac{C_s}{\bar{m}}\delta_{ii^*}\right)}{\partial C_a}\left(1 + \sum_{k=1}^{N} K'_{ik}\frac{C_s}{\bar{m}}N_A V_k \delta_{ki^*}\right) + \sum_{i=1}^{N} n_i D_i^0 \frac{C_s}{\bar{m}} N_A V_i \delta_{ii^*} \frac{\partial}{\partial C_a} \times \left\{\sum_{j=1}^{N}\left\{\beta_{ij}\left(\frac{1+\lambda_{ij}}{2}\right)^3 + K''_{ij}\right\}\frac{C_s}{\bar{m}}\delta_{ji^*}\right\}. \quad (A.3)$$

Using the sifting property, which selects the micelle type i^* from a set of N different micelle types, with equations $\phi = C_s/\bar{m}N_A V_{i^*}$ and $C_a = \bar{n}/\bar{m}C_s$, the summations over k and j in eqn (A.3) are evaluated to give

$$D_{aa} = \sum_{i=1}^{N} \frac{\partial\left(n_i D_i^0 \frac{C_s}{\bar{m}}\delta_{ii^*}\right)}{\partial C_a}\left(1 + K'_{ii^*}\phi\right) + \sum_{i=1}^{N} n_i D_i^0 \frac{C_s}{\bar{m}} N_A V_i \delta_{ii^*} \frac{\partial}{\partial C_a}\left\{\left\{\beta_{ii^*}\left(\frac{1+\lambda_{ii^*}}{2}\right)^3 + K''_{ii^*}\right\}\frac{C_s}{\bar{m}}\right\}. \quad (A.4)$$

The product rule is used to rearrange the first summation in eqn (A.4),

$$\sum_{i=1}^{N} \frac{\partial\left(n_i D_i^0 \frac{C_s}{\bar{m}}\delta_{ii^*}\right)}{\partial C_a}\left(1 + K'_{ii^*}\phi\right) = \sum_{i=1}^{N}\left\{\frac{\partial}{\partial C_a}\left\{n_i D_i^0 \frac{C_s}{\bar{m}}\delta_{ii^*}\left(1 + K'_{ii^*}\phi\right)\right\} - n_i D_i^0 \frac{C_s}{\bar{m}}\delta_{ii^*}\frac{\partial\left(K'_{ii^*}\phi\right)}{\partial C_a}\right\}. \quad (A.5)$$

The i summation on the right side of eqn (A.5) is evaluated using the sifting property, $\phi = C_s/\bar{m}N_A V_{i^*}$, and $C_a = \bar{n}/\bar{m}C_s$,

$$\sum_{i=1}^{N} \frac{\partial\left(n_i D_i^0 \frac{C_s}{\bar{m}}\delta_{ii^*}\right)}{\partial C_a}\left(1 + K'_{ii^*}\phi\right) = \frac{\partial}{\partial C_a}\left\{C_a D_{i^*}^0\left(1 + K'_{i^*i^*}\phi\right)\right\} - C_a D_{i^*}^0\left\{\frac{\partial\left(K'_{ii^*}\phi\right)}{\partial C_a}\right\}_{i=i^*}. \quad (A.6)$$

Here, $K_{i^*i^*}{}'$ is a constant and the derivatives in eqn (A.6) are expanded to provide,

$$\sum_{i=1}^{N} \frac{\partial\left(n_i D_i^0 \frac{C_s}{\bar{m}}\delta_{ii^*}\right)}{\partial C_a}\left(1 + K'_{ii^*}\phi\right) = \frac{\partial\left(C_a D_{i^*}^0\right)}{\partial C_a}\left(1 + K'_{i^*i^*}\phi\right) - C_a D_{i^*}^0 \phi\left(\frac{\partial K'_{ii^*}}{\partial C_a}\right)_{i=i^*}. \quad (A.7)$$

Differentiating the Stokes–Einstein equation, $D^0_{i^*} = \frac{k_B T}{6\pi\eta R_{i^*}}$, one can show,

$$\frac{\partial\left(C_a D^0_{i^*}\right)}{\partial C_a} = D^0_{i^*}\left(1 - \frac{\partial \ln R_{i^*}}{\partial \ln C_a}\right). \tag{A.8}$$

Combining eqn (A.7) and (A.8) yields,

$$\sum_{i=1}^{N} \frac{\partial\left(n_i D^0_i \frac{C_s}{\bar{m}}\delta_{ii^*}\right)}{\partial C_a}\left(1 + K'_{ii^*}\phi\right) = D^0_{i^*}\left\{\left(1 - \frac{\partial \ln R_{i^*}}{\partial \ln C_a}\right)\left(1 + K'_{i^*i^*}\phi\right) - \phi\left(\frac{\partial K'_{ii^*}}{\partial \ln C_a}\right)_{i=i^*}\right\}. \tag{A.9}$$

Now, focusing on the second summation on the right side of eqn (A.4), the derivative can be evaluated,

$$\begin{aligned}\sum_{i=1}^{N} n_i D^0_i \frac{C_s}{\bar{m}} N_A V_i \delta_{ii^*} \frac{\partial}{\partial C_a}\left\{\left\{\beta_{ii^*}\left(\frac{1+\lambda_{ii^*}}{2}\right)^3 + K''_{ii^*}\right\}\frac{C_s}{\bar{m}}\right\} &= \sum_{i=1}^{N} n_i D^0_i \frac{C_s}{\bar{m}} N_A V_i \delta_{ii^*}\frac{C_s}{\bar{m}}\left\{\frac{3}{8}\beta_{ii^*}(1+\lambda_{ii^*})^2\left(\frac{\partial\lambda_{ii^*}}{\partial C_a}\right)\right.\\ &\left. + \left(\frac{1+\lambda_{ii^*}}{2}\right)^3\left(\frac{\partial\beta_{ii^*}}{\partial C_a}\right) + \left(\frac{\partial K''_{ii^*}}{\partial C_a}\right)\right\}\\ &+ \sum_{i=1}^{N} n_i D^0_i \frac{C_s}{\bar{m}} N_A V_i \delta_{ii^*}\left\{\beta_{ii^*}\left(\frac{1+\lambda_{ii^*}}{2}\right)^3 + K''_{ii^*}\right\}\frac{\partial}{\partial C_a}\left(\frac{C_s}{\bar{m}}\right),\end{aligned} \tag{A.10}$$

and the sum over i is performed using the sifting property, $\phi = C_s/\bar{m}N_A V_{i^*}$, and $C_a = \bar{n}/\bar{m}C_s$:

$$\begin{aligned}\sum_{i=1}^{N} n_i D^0_i \frac{C_s}{\bar{m}} N_A V_i \delta_{ii^*} \frac{\partial}{\partial C_a}\left\{\left\{\beta_{ii^*}\left(\frac{1+\lambda_{ii^*}}{2}\right)^3 + K''_{ii^*}\right\}\frac{C_s}{\bar{m}}\right\} &= C_a D^0_{i^*}\phi\left\{\frac{3}{2}\beta_{i^*i^*}\left(\frac{\partial\lambda_{ii^*}}{\partial C_a}\right)_{i=i^*} + \left\{\frac{\partial\left(\beta_{ii^*} + K''_{ii^*}\right)}{\partial C_a}\right\}_{i=i^*}\right.\\ &\left. + \left(\beta_{i^*i^*} + K''_{i^*i^*}\right)\frac{\bar{m}}{C_s}\frac{\partial}{\partial C_a}\left(\frac{C_s}{\bar{m}}\right)\right\}.\end{aligned} \tag{A.11}$$

The size ratio for spheres is defined as $\lambda_{ii^*} = \frac{R_{i^*}}{R_i}$. Hence,

$$\left(\frac{\partial\lambda_{ii^*}}{\partial C_a}\right)_{i=i^*} = \frac{\partial \ln R_{i^*}}{\partial C_a}. \tag{A.12}$$

Furthermore, since C_a and C_s are independent variables,

$$\frac{\bar{m}}{C_s}\frac{\partial}{\partial C_a}\left(\frac{C_s}{\bar{m}}\right) = -\frac{\partial \ln \bar{m}}{\partial C_a}. \tag{A.13}$$

Combining eqn (A.11)–(A.13), one finds,

$$\begin{aligned}\sum_{i=1}^{N} n_i D^0_i \frac{C_s}{\bar{m}} N_A V_i \delta_{ii^*} \frac{\partial}{\partial C_a}\left\{\left\{\beta_{ii^*}\left(\frac{1+\lambda_{ii^*}}{2}\right)^3 + K''_{ii^*}\right\}\frac{C_s}{\bar{m}}\right\} &= D^0_{i^*}\phi\left\{\frac{3}{2}\beta_{i^*i^*}\frac{\partial \ln R_{i^*}}{\partial \ln C_a} + \left\{\frac{\partial\left(\beta_{ii^*} + K''_{ii^*}\right)}{\partial \ln C_a}\right\}_{i=i^*}\right.\\ &\left. - \left(\beta_{i^*i^*} + K''_{i^*i^*}\right)\frac{\partial \ln \bar{m}}{\partial \ln C_a}\right\}.\end{aligned} \tag{A.14}$$

Eqn (A.4), (A.9), and (A.14) combine to yield

$$\begin{aligned}\frac{D_{aa}}{D^0_{i^*}} &= 1 + K'\phi - \left\{1 + \left(K' - \frac{3}{2}\beta\right)\phi\right\}\frac{\partial \ln R_{i^*}}{\partial \ln C_a}\\ &+ \phi\left\{\frac{\partial\left(\beta_{ii^*} + K''_{ii^*} - K'_{ii^*}\right)}{\partial \ln C_a}\right\}_{i=i^*} - (\beta + K'')\frac{\partial \ln \bar{m}}{\partial \ln C_a}\phi.\end{aligned} \tag{A.15}$$

In eqn (A.15), redundant subscripts on the interaction coefficients have been removed. If the hydration index n_H is constant with composition, differentiation of eqn (39) provides,

$$\frac{\partial \ln \bar{m}}{\partial \ln C_a} = 3\frac{\partial \ln R_{i^*}}{\partial \ln C_a} - \frac{\phi_a}{\phi}, \tag{A.16}$$

where $\phi_a = C_a N_A V_a$ is the solute volume fraction. Furthermore, if the interaction potential between pairs of micelles is, at most, a single variable function of the interparticle separation distance, then we may write,

$$\left\{\frac{\partial\left(\beta_{ii^*} + K''_{ii^*} - K'_{ii^*}\right)}{\partial \ln C_a}\right\}_{i=i^*} = \left\{\frac{d(K'' - K')}{d\lambda}\right\}_{\lambda=1}\left\{\frac{\partial\lambda_{ii^*}}{\partial \ln C_a}\right\}_{i=i^*}. \tag{A.17}$$

Finally, eqn (A.12) and (A.15)–(A.17) combine, after some rearrangement, to produce,

$$\frac{D_{aa}}{D^0_{i^*}} = 1 + K'\phi - M\left(\phi, \frac{C_a}{C_s}\right), \tag{A.18}$$

where the function $M\left(\phi, \frac{C_a}{C_s}\right)$ is given by,

$$M\left(\phi, \frac{C_a}{C_s}\right) = \frac{\partial \ln R_{i^*}}{\partial \ln C_a}(1 + \chi\phi) - (\beta + K'')\phi_a, \tag{A.19}$$

and

$$\chi = \left(\frac{3}{2}\beta + K' + 3K''\right) - \left\{\frac{d(K'' - K')}{d\lambda}\right\}_{\lambda=1}. \tag{A.20}$$

In order to determine the remaining elements of [**D**] in terms of $M\left(\phi, \frac{C_a}{C_s}\right)$, we note that R_{i^*} and $\bar{m}$ are thermodynamic state functions of a ternary solution. According to the Gibbs phase rule, these functions depend on four independent, intensive variables, which we choose to be T, p, C_a/C_s and ϕ. Our light scattering results[2] at constant T and p indicate R_{i^*} and $\bar{m}$ vary strongly with C_a/C_s but are weak functions of ϕ. Hence,

to a good approximation, we may write expressions for R_{i^*} and $\bar{m}$ at constant T and p as a power series in C_a/C_s,

$$R_{i^*} = R_0 + \sum_{k=1}^{\infty} a_k \left(\frac{C_a}{C_s}\right)^k \quad \text{(A.21)}$$

$$\bar{m} = m_0 + \sum_{k=1}^{\infty} b_k \left(\frac{C_a}{C_s}\right)^k. \quad \text{(A.22)}$$

Differentiating eqn (A.21) and (A.22) with respect to C_a and C_s, one finds,

$$\frac{\partial \ln R_{i^*}}{\partial \ln C_a} = -\frac{\partial \ln R_{i^*}}{\partial \ln C_s} \quad \text{(A.23)}$$

$$\frac{\partial \ln \bar{m}}{\partial \ln C_a} = -\frac{\partial \ln \bar{m}}{\partial \ln C_s}. \quad \text{(A.24)}$$

Eqn (A.23) and (A.24) may be used in derivations similar to that described above for D_{aa} to find

$$\frac{D_{as}}{D^0_{i^*}} = \frac{C_a}{C_s}\left\{(\beta + K'')\phi + M\left(\phi, \frac{C_a}{C_s}\right)\right\} \quad \text{(A.25)}$$

$$\frac{D_{sa}}{D^0_{i^*}} = -\frac{C_s}{C_a} M\left(\phi, \frac{C_a}{C_s}\right) \quad \text{(A.26)}$$

$$\frac{D_{ss}}{D^0_{i^*}} = 1 + (\beta + S)\phi + M\left(\phi, \frac{C_a}{C_s}\right). \quad \text{(A.27)}$$

In Table 1, exact numerical calculations by Batchelor[12,15] for the mobility coefficients K_{ij}' and K_{ij}'' are provided for λ_{ij} = 0.9, 1.0, and 1.1. These numerical results were used to calculate the central difference approximation for the derivative, $\left\{\frac{d(K'' - K')}{d\lambda}\right\}_{\lambda=1} = -4.70$, in eqn (A.20). Thus, for micelles that interact as identically sized (λ = 1) hard spheres, β = 8, K' = −2.10, K'' = −4.45, $S = K' + K''$ = −6.55, and χ = 1.25.

Appendix B: the solute tracer limit for [D]

Differentiation of eqn (A.21) provides

$$\frac{\partial \ln R_{i^*}}{\partial \ln C_a} = \frac{\sum_{k=1}^{\infty} k a_k \left(\frac{C_a}{C_s}\right)^k}{R_0 + \sum_{k=1}^{\infty} a_k \left(\frac{C_a}{C_s}\right)^k}. \quad \text{(B.1)}$$

Table 1 Mobility coefficients calculated by Batchelor[12,15]

λ_{ij}	K_{ij}'	K_{ij}''
0.9	−2.13	−4.02
1.0	−2.10	−4.45
1.1	−2.06	−4.89

Eqn (B.1) is divided by C_a/C_s to yield

$$\frac{C_s}{C_a}\frac{\partial \ln R_{i^*}}{\partial \ln C_a} = \frac{a_1 + \sum_{k=2}^{\infty} k a_k \left(\frac{C_a}{C_s}\right)^{k-1}}{R_0 + \sum_{k=1}^{\infty} a_k \left(\frac{C_a}{C_s}\right)^k}. \quad \text{(B.2)}$$

Furthermore, we note that

$$\frac{C_s}{C_a}\frac{\phi_a}{\phi} = \frac{V_a}{\frac{C_a}{C_s}V_a + V_s + n_H V_w}. \quad \text{(B.3)}$$

According to eqn (B.1)–(B.3), $\frac{\partial \ln R_{i^*}}{\partial \ln C_a} \to 0$, $\frac{C_s}{C_a}\frac{\partial \ln R_{i^*}}{\partial \ln C_a} \to \frac{a_1}{R_0}$, and $\frac{C_s}{C_a}\frac{\phi_a}{\phi} \to \frac{V_a}{V_s + n_H V_w}$ in the limit as $C_a/C_s \to 0$. Hence, eqn (31)–(35) and (B.1)–(B.3) combine to give

$$\frac{D_{aa}}{D^0} = 1 + K'\phi \quad \text{(B.4)}$$

$$D_{as} = 0 \quad \text{(B.5)}$$

$$\frac{D_{sa}}{D^0} = -\frac{a_1}{R_0}(1 + \chi\phi) + (\beta + K'')\left(\frac{V_a}{V_s + n_H V_w}\right)\phi \quad \text{(B.6)}$$

$$\frac{D_{ss}}{D^0} = 1 + (\beta + S)\phi. \quad \text{(B.7)}$$

Acknowledgements

This research was funded by the National Science Foundation (CBET1506474), and from Hatch project 1010420, from the USDA National Institute of Food and Agriculture. N. P. A. acknowledges a Jastro-Shields fellowship from the University of California at Davis.

References

1 R. B. Bird, W. E. Stewart and E. N. Lightfoot, *Transport Phenomena*, Wiley, New York, 2nd edn, 2007.
2 N. P. Alexander, R. J. Phillips and S. R. Dungan, Multicomponent Diffusion in Aqueous Solutions of Nonionic Micelles and Decane, *Langmuir*, 2019, **35**(42), 13595–13606.
3 W. J. Musnicki, S. R. Dungan and R. J. Phillips, Multicomponent Diffusion in Solute-Containing Micelle and Microemulsion Solutions, *Langmuir*, 2014, **30**, 11019–11030.
4 D. G. Leaist, Relating Multicomponent Mutual Diffusion and Intradiffusion for Associating Solutes. Application to Coupled Diffusion in Water-in-oil Microemulsions, *Phys. Chem. Chem. Phys.*, 2002, **4**, 4732–4739.
5 M. A. Budroni, J. Carballido-Landeira, A. Intiso, A. De Wit and F. Rossi, Interfacial Hydrodynamic Instabilities driven by Cross-Diffusion in Reverse Microemulsions, *Chaos*, 2015, **25**, 1–10.
6 D. Porat and A. Dahan, Active Intestinal Drug Absorption and the Solubility–Permeability Interplay, *Int. J. Pharm.*, 2018, **537**, 84–93.

7 J. M. Miller, A. Beig, B. J. Krieg, R. A. Carr, T. B. Borchardt, G. E. Amidon, G. L. Amidon and A. Dahan, The Solubility–Permeability Interplay: Mechanistic Modeling and Predictive Application of the Impact of Micellar Solubilization on Intestinal Permeation, *Mol. Pharmaceutics*, 2011, **8**, 1848–1856.
8 H. Zhang and O. Annunziata, Modulation of Drug Transport Properties by Multicomponent Diffusion in Surfactant Aqueous Solutions, *Langmuir*, 2008, **24**, 10680–10687.
9 M. Everist, J. A. MacNeil, J. R. Moulins and D. G. Leaist, Coupled Mutual Diffusion in Solutions of Micelles and Solubilizates, *Phys. Chem. Chem. Phys.*, 2009, **11**, 8173–8182.
10 G. K. Batchelor, Sedimentation in a dilute dispersion of spheres, *J. Fluid Mech.*, 1972, **52**, 245–268.
11 G. K. Batchelor, Sedimentation in a Dilute Polydisperse System of Interacting Spheres. Part 1. General Theory, *J. Fluid Mech.*, 1982, **119**, 379–408.
12 G. K. Batchelor and C. S. Wen, Sedimentation in a Dilute Polydisperse System of Interacting Spheres. Part 2. Numerical Results, *J. Fluid Mech.*, 1982, **124**, 495–528.
13 G. K. Batchelor, Brownian Diffusion of Particles with Hydrodynamic Interaction, *J. Fluid Mech.*, 1976, **74**, 1–29.
14 G. K. Batchelor, Diffusion in a Dilute Polydisperse System of Interacting Spheres, *J. Fluid Mech.*, 1983, **131**, 155–175.
15 G. K. Batchelor, Corrigendum, *J. Fluid Mech.*, 1983, **137**, 467–469.
16 W. B. Russel, D. A. Saville and W. R. Schowalter, *Colloidal Dispersions*, Cambridge University Press, New York, 1st edn, 1989, vol. 2, pp. 21–63.
17 G. I. Taylor, Dispersion of Soluble Matter in Solvent Flowing Slowly through a Tube, *Proc. R. Soc. London, Ser. A*, 1953, **219**, 186–203.
18 R. Aris, On the Dispersion of a Solute in a Fluid Flowing through a Tube, *Proc. R. Soc. London, Ser. A*, 1956, **235**, 67–77.
19 W. E. Price, Theory of the Taylor Dispersion Technique for Three-component-system Diffusion Measurements, *J. Chem. Soc., Faraday Trans. 1*, 1988, **84**, 2431–2439.
20 Z. Deng and D. G. Leaist, Ternary Mutual Diffusion Coefficients of $MgCl_2$ + $MgSO_4$ + H_2O and Na_2SO_4 + $MgSO_4$ + H_2O from Taylor Dispersion Profiles, *Can. J. Chem.*, 1991, **69**, 1548–1553.
21 V. Russo, O. Ortona, R. Tesser, L. Paduano and M. Di Serio, On the Importance of Choosing the Best Minimization Algorithm for Determination of Ternary Diffusion Coefficients by the Taylor Dispersion Method, *ACS Omega*, 2017, **2**, 2945–2952.
22 A. Berthod, S. Tomer and J. G. Dorsey, Polyoxyethylene Alkyl Ether Nonionic Surfactants: Physicochemical Properties and Use for Cholesterol Determination in Food, *Talanta*, 2001, **55**, 69–83.
23 H. A. Massaldi and C. Judson King, Simple Technique to Determine Solubilities of Sparingly Soluble Organics: Solubility and Activity Coefficients of d–Limonene, n–Butylbenzene, and 7–Hexyl Acetate in Water and Sucrose Solutions, *J. Chem. Eng. Data*, 1973, **18**, 393–397.
24 J. Tolls, J. V. Dijk, E. J. M. Verbruggen, J. L. M. Hermens, B. Loeprecht and G. Schüürmann, Aqueous Solubility–Molecular Size Relationships: a Mechanistic Case Study Using C_{10}- to C_{19}-Alkanes, *J. Phys. Chem. A*, 2002, **106**, 2760–2765.
25 J. G. Kirkwood, R. L. Baldwin, P. J. Dunlop, L. J. Gosting and G. Kegeles, Flow Equations and Frames of Reference for Isothermal Diffusion in Liquids, *J. Chem. Phys.*, 1960, **33**, 1505–1513.
26 T. Hill, *An Introduction to Statistical Thermodynamics*, Addison-Wesley Publishing Company, Inc., United States, 2nd edn, 1960, vol. 19, pp. 340–368.
27 A. J. Banchio and G. Nägele, Short-time Transport Properties in Dense Suspensions: From Neutral to Charge Stabilized Colloidal Spheres, *J. Chem. Phys.*, 2008, **128**, 104903.
28 P. N. Segre, O. P. Behrend and P. N. Pusey, Short-time Brownian motion in Colloidal Suspensions: Experiment and Simulation, *Phys. Rev. E: Stat. Phys., Plasmas, Fluids, Relat. Interdiscip. Top.*, 1995, **52**(5), 5070–5083.
29 A. J. C. Ladd, Hydrodynamic Transport Coefficients of Random Dispersions of Hard Spheres, *J. Chem. Phys.*, 1990, **93**, 3484–3494.
30 B. Lindman, B. Medronho and G. Karlström, Clouding of Nonionic Surfactants, *Curr. Opin. Colloid Interface Sci.*, 2016, **22**, 23–29.
31 N. Zoeller, L. Lue and D. Blankschtein, Statistical-Thermodynamic Framework to Model Nonionic Micellar Solutions, *Langmuir*, 1997, **13**, 5258–5275.
32 S. Vierros and M. Sammalkorpi, Effects of 1-Hexanol on $C_{12}E_{10}$ Micelles: A Molecular Simulations and Light Scattering Study, *Phys. Chem. Chem. Phys.*, 2018, **20**, 6287–6298.
33 O. Glatter, G. Fritz, H. Lindner, J. Brunner-Popela, R. Mittelbach, R. Strey and S. U. Egelhaaf, Nonionic Micelles near the Critical Point: Micellar Growth and Attractive Interaction, *Langmuir*, 2000, **16**, 8692–8701.
34 D. Danino, Y. Talmon and R. Zana, Aggregation and Microstructure in Aqueous Solutions of the Nonionic Surfactant $C_{12}E_8$, *J. Colloid Interface Sci.*, 1997, **186**, 170–179.
35 M. Zulauf, K. Weckstrom, J. B. Hayter, V. Degiorgio and M. Corti, Neutron Scattering Study of Micelle Structure In Isotropic Aqueous Solutions of Poly(oxyethylene) Amphiphiles, *J. Phys. Chem.*, 1985, **89**, 3411–3417.
36 U. Olsson and P. Schurtenberger, Structure, Interactions, and Diffusion in a Ternary Nonionic Microemulsion Near Emulsification Failure, *Langmuir*, 1993, **9**, 3389–3394.
37 U. Olsson and P. Schurtenberger, A Hard Sphere Microemulsion, *Prog. Colloid Polym. Sci.*, 1997, **104**, 157–159.
38 M. Imai, M. Kurimoto, F. Matsuura, Y. Sakuma and T. Kawakatsu, Diffusion of Surfactant Micelles in Fluid and Crystal Phases, *Soft Matter*, 2012, **8**, 9892–9905.
39 A. Bernheim-Groswasser, E. Wachtel and Y. Talmon, Micellar Growth, Network Formation, and Criticality in Aqueous Solutions of the Nonionic Surfactant $C_{12}E_5$, *Langmuir*, 2000, **16**, 4131–4140.
40 R. Nagarajan and E. Ruckenstein, Theory of Surfactant Self-Assembly: A Predictive Molecular Thermodynamic Approach, *Langmuir*, 1991, **7**, 2934–2969.
41 R. Nagarajan, Constructing a Molecular Theory of Self-Assembly: Interplay of Ideas from Surfactants and Block Copolymers, *Adv. Colloid Interface Sci.*, 2017, **244**, 113–123.
42 J. F. Brady, The Long-time Self-diffusivity in Concentrated Colloidal Dispersions, *J. Fluid Mech.*, 1994, **212**, 109–133.

Chapter 3

Light Scattering Correlation Functions for Mixtures of Interacting, Nonionic Micelles with Hydrophobic Solutes using Thermodynamic Fluctuation Theory

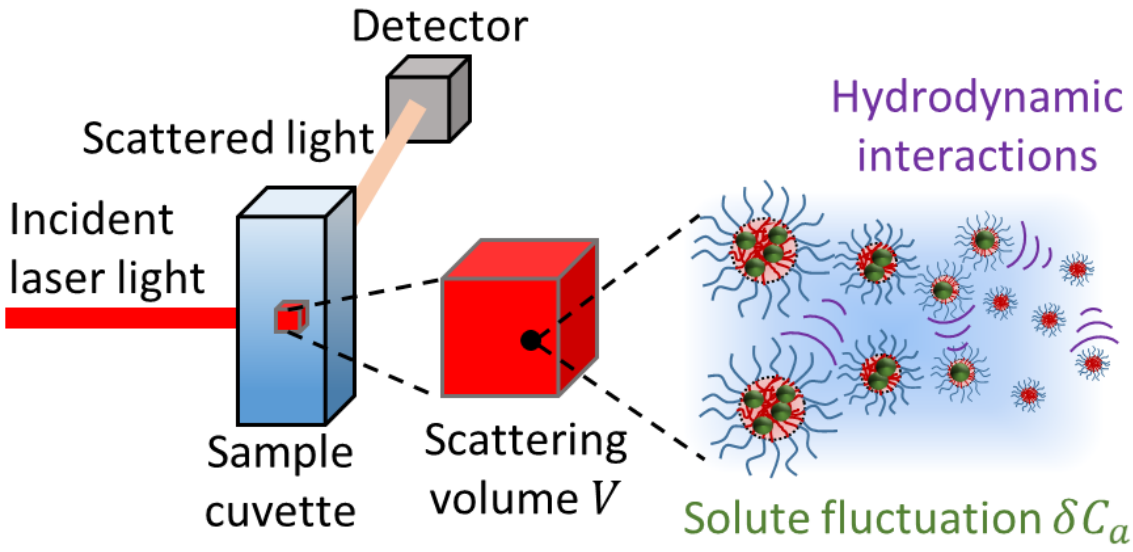

ARTICLE

Light Scattering Correlation Functions for Mixtures of Interacting, Nonionic Micelles with Hydrophobic Solutes using Thermodynamic Fluctuation Theory

Nathan P. Alexander,[a] Ronald J. Phillips,[a] and Stephanie R. Dungan*[,a,b]

Model equations for the Rayleigh ratio and the mode amplitudes of the normalized time correlation function for the scattered electric field are derived using thermodynamic fluctuation theory for crowded solute-containing micellar solutions and microemulsions with negligible molecular species and polydispersity. This theory invokes nonequilibrium thermodynamics and enforces local equilibrium between molecular solute, surfactant, and the various micellar species, in order to elucidate the influence of self-assembly on the light scattering functions for the first time. We find that micelle growth effects along the diffusion path in these mixtures, which were previously shown to drive strong multicomponent diffusion effects, expressed via the ternary diffusivity matrix $[\mathbf{D}]$, do not affect the scattering functions in the limit of zero local polydispersity. Hence, theoretical predictions for the Rayleigh ratio and the field correlation function for ternary mixtures of solute-containing, locally monodisperse micellar solutions are identical to those developed for binary mixtures of monodisperse, colloidal hard spheres. However, micelle growth effects are predicted to influence the thermodynamic driving forces and eigenmodes for diffusion. In support of our theoretical results, measurements for the Rayleigh ratio and the field correlation function for ternary aqueous solutions of decaethylene glycol monododecyl ether ($C_{12}E_{10}$) with either decane or limonene solute were performed for several molar ratios and volume fractions up to $\phi \approx 0.25$, and for binary mixtures of $C_{12}E_{10}$/water up to $\phi \approx 0.5$. Excellent agreement between our light scattering theory and experimental data is achieved for low to moderate volume fractions ($\phi < 0.3$), and at higher concentration when our volume fraction calculations are corrected to account for micelle dehydration.

1 Introduction

According to the Onsager regression hypothesis,[1] microscopic fluctuations in the thermodynamic variables of a multicomponent fluid, such as temperature, pressure, and the species concentrations, relax by the same transport equations that govern the relaxation of macroscopic gradients. For small departures from equilibrium, the independent diffusive fluxes for $n-1$ components in an n-component liquid mixture, at constant temperature and pressure, may be described by the generalized form of Fick's law:

$$\boldsymbol{J}_i = -D_{ij}\boldsymbol{\nabla}C_j \qquad for\ i,j\ =\ 1,2,\ldots,n-1. \tag{1}$$

Here, D_{ij} is an element of the diffusivity matrix $[\mathbf{D}]$ that relates the flux $\boldsymbol{J}_i$ of component i to a concentration gradient $\boldsymbol{\nabla}C_j$ in component j. Since concentration fluctuations also cause an irradiated mixture to scatter light, the same multicomponent diffusion phenomena observed during a macro gradient experiment, such as the Taylor dispersion[2–4] or interferometric methods,[5,6] are expected to influence the correlation functions used to model light scattering data acquired via photon correlation and time averaged spectroscopy.

Recent studies on multicomponent diffusion in nonionic micellar solutions[5,7,8] and water-in-oil microemulsions[9,10] indicate strong multicomponent effects, including strong uphill diffusion, driven by solubilization-induced micelle growth that drives surfactant up a solute gradient. However, these effects appear to be absent in measurements of the field autocorrelation function and the Rayleigh ratio, which, surprisingly, conform to theory for binary mixtures of colloidal hard spheres.[7,11,12] The main goal of this article is to present a rigorous derivation for the field correlation function and the Rayleigh ratio for ternary surfactants solutions with hydrophobic solutes in the limit of local monodispersity. This derivation supports the observation that multicomponent diffusion phenomena, which strongly affect the diffusivity matrix, negligibly affect the light scattering functions for aqueous mixtures of nonionic micelles and hydrophobic solutes.

Theoretical results[13–17] for the field correlation function and the Rayleigh ratio for polydisperse mixtures of rigid, colloidal hard spheres have been derived, mainly to examine the influence of optical and size polydispersity on the intensity of scattered light. Some of these models were later extended to apply to ternary mixtures of solute-containing micelles,

[a] Department of Chemical Engineering, University of California at Davis, Davis, CA 95616 USA. Email: srdungan@ucdavis.edu
[b] Department of Food Science and Technology, University of California at Davis, Davis, CA 95616 USA

modelled as immutable, colloidal spheres with a core-shell morphology.[18,19] However, self-assembled surfactant solutions differ fundamentally from dispersions comprised of discrete, rigid particles, since micelles may grow and change shape as they diffuse, re-equilibrating locally to variations in temperature, pressure, and composition along the diffusion path. Hence, one may wonder if light scattering theory developed for distributions of discrete colloidal scatterers with fixed shapes and sizes, which does not account for the effects of self-assembly during light scattering measurements, is applicable to multicomponent surfactant solutions.

In order to capture the influence of self-assembly on light scattered from solute-containing micelles, thermodynamic fluctuation theory[20–24] is used here to derive the field correlation function and the Rayleigh ratio for aqueous mixtures of nonionic surfactants and hydrophobic solutes. Per this framework, surfactant solutions are modelled as a continuous medium comprised of solute (a), surfactant (s), and solvent (w) that self-assemble on a time scale much faster than that of diffusion, thereby satisfying the local equilibrium assumption of irreversible thermodynamics.[25] Here, local equilibrium is enforced by the Gibbs-Duhem equation, which provides equilibrium relations between the chemical potentials of free solute, surfactant monomer, and various micelle species. Thus, chemical potential gradients in solute and surfactant are related to gradients in the micelle species chemical potentials, which drive diffusive transport governed by rigorous theory by Batchelor[26–28] for polydisperse colloidal hard sphere dispersions. At the continuum level, the resulting diffusion of solute and surfactant relax fluctuations in the composition-dependent, local dielectric constant of the solution, which determines the intensity of scattered light.

In the following sections we introduce equilibrium data that establishes strong micellar growth with respect to composition for aqueous, mixtures of $C_{12}E_{10}$ micelles with limonene. Next, thermodynamic fluctuation theory is reviewed and applied to derive both the Rayleigh ratio and the field correlation function for ternary mixtures. Thermodynamic derivatives for the solute and surfactant are then derived for ternary micellar solutions, followed by derivations for the scattering functions for a variety of limiting special cases. This work concludes with a comparison and validation of our locally monodisperse theory, in which local polydispersity is neglected but micelle growth effects are retained, with our experimental data.

2 Materials and Methods

2.1 Materials

Nonionic surfactant decaethylene glycol monododecyl ether ($C_{12}E_{10}$, lot #SLBT1187 or #0000057654 each with a hydroxyl value equal to 92.0 mg/g), the hydrophobic solutes decane and limonene, and HPLC grade toluene (used as a reference standard for static light scattering measurements), were all purchased from Sigma-Aldrich and used without modification. “Molecular Biology Reagent” water from Sigma-Aldrich (filtered through 0.1 µm filters by the manufacturer) was used to mix solutions for light scattering measurements. All mixtures were prepared by volume with aliquots from 100 mL stock solutions and were allowed to equilibrate overnight at room temperature. Non-ideal changes in volume upon mixing were neglected.

2.2 Light Scattering

Dynamic (DLS) and static (SLS) light scattering measurements were performed using either a Malvern Zetasizer Nano ZS90 or Malvern Ultra at a 90° scattering angle. The light source was a solid state 4 mW He-Ne laser that emitted vertically polarized light with a wavelength of 633 nm. To ensure the removal of dust particles, all surfactant solutions prepared for light scattering measurements were filtered through 0.1 µm Whatman polycarbonate filters (model WHA800309), using an Avanti mini-extruder (model 610000), directly into quartz cuvettes topped with Teflon stoppers by Starna (model 23-Q-10). Each 1mL sample was then allowed to equilibrate at 25 °C within the instrument for several minutes prior to measurement. For each DLS measurement, monomodal or nearly monomodal decay of the field autocorrelation function was observed for all samples. Hence, the method of cumulants was used to acquire diffusion coefficients (D_{DLS}) and polydispersity indices.

SLS measurements yielded excess Rayleigh ratios R_θ, at scattering angle θ, calculated using[29]

$$R_\theta = \left(\frac{n}{n_T}\right)^2 R_T \frac{\langle I_a(0)\rangle}{\langle I_T(0)\rangle} \ . \qquad (2)$$

Here, $n_T(= 1.496)$, $R_T(= 1.3522 \times 10^{-5} cm^{-1})$, and $\langle I_T(0)\rangle$ are the refractive index, Rayleigh ratio, and time averaged scattering intensity, respectively, of the reference standard toluene at 25 °C. $\langle I_a(0)\rangle$ is the residual scattering intensity, defined as the difference between the scattering intensity of the solution and that of the pure solvent, and n is the solution refractive index, which was assumed to vary linearly according to $n = (dn/dc_s)c_s + n_0$. The refractive index derivatives dn/dc_s were independently measured using a differential refractometer (Waters model 2414) at room temperature (23.0 ± 0.3 °C) by varying the surfactant mass concentration c_s, and $n_0 = 1.33$ is the refractive index of pure water at 25 °C.

To evaluate the derivatives dn/dc_s, the solution refractive index n was measured relative to the solvent n_0 from a dilution series of six different surfactant concentrations that ranged from 1–6 mM in increments of 1 mM, with the solute to surfactant molar ratio C_a/C_s held constant. For the limonene system, dn/dc_s values were then determined from the slopes of the plots of $(n - n_0)$ versus c_s for the following molar ratios: C_a/C_s = 0, 0.1, 0.2, 0.3, and 0.5. Each plot was reproduced in triplicate and was well fit with a linear function with an intercept through zero. This procedure yielded values for dn/dc_s equal to 0.1314 ± 0.0006, 0.133 ± 0.001, 0.1372 ± 0.0007, 0.140 ± 0.001 and 0.1491 ± 0.0005 mL/g, respectively. Derivatives dn/dc_s used for the decane system were obtained from an earlier study.[7]

Except where noted, all reported error bars for our scattering measurements represent two standard deviations.

3 Results

3.1 Dynamic light scattering (DLS)

Diffusion coefficients D_{DLS} for ternary $C_{12}E_{10}$/limonene/water mixtures are shown in Fig. 1 with constant molar ratios $C_a/C_s = 0, 0.10, 0.20, 0.30,$ or 0.50, and surfactant concentrations that ranged from 20 mM to 400 mM. The D_{DLS} values reported here, and in previous work for $C_{12}E_{10}$/decane/water mixtures,[7] were acquired using the method of cumulants. The latter were shown consistent with the theory of Batchelor for gradient diffusion of monodisperse hard spheres.[26]

3.2 Static light scattering (SLS)

In Fig. 2A, reduced scattering intensities $K_s c_s/R_{90}$ for dilute, aqueous $C_{12}E_{10}$(s)/limonene(a) mixtures are plotted versus surfactant mass concentration c_s with constant molar ratios $C_a/C_s = 0, 0.1, 0.2, 0.3,$ and 0.5. As shown, $K_s c_s/R_{90}$ increased linearly for each molar ratio. This behavior indicates that, with constant C_a/C_s, the micelles did not grow or change shape with increasing surfactant concentration, thus validating extrapolation of the data to determine MW_s as presented below. In Fig. 2B, R_{90} values for concentrated $C_{12}E_{10}$/water, and for $C_{12}E_{10}$/limonene/water and $C_{12}E_{10}$/decane/water solutions with constant molar ratios equal to $C_a/C_s = 0.2$, are plotted against the molar surfactant concentration C_s. The R_{90} values were calculated using eqn (2), for which no assumptions were made regarding the shape, size distribution, hydration, or interparticle interactions.

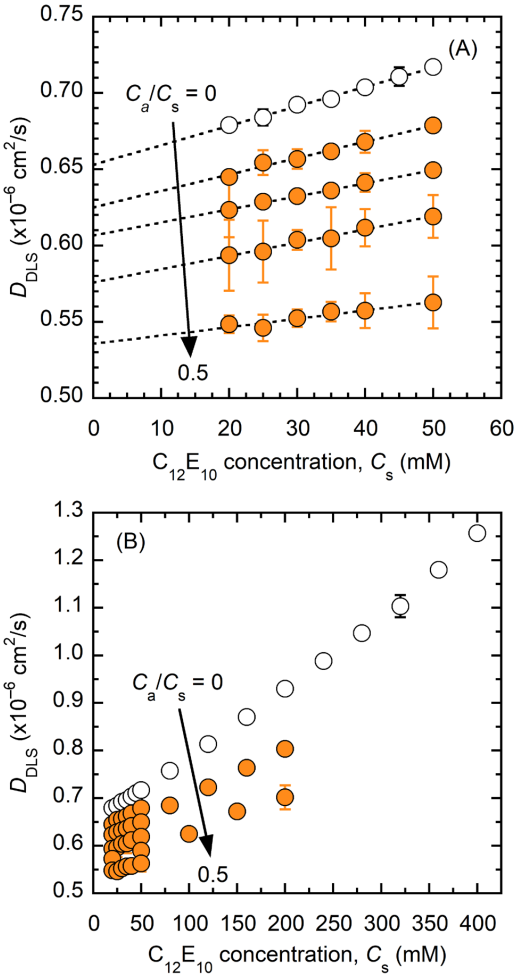

Fig. 1 DLS diffusion coefficients for aqueous $C_{12}E_{10}$ (s) + limonene (a) for $C_a/C_s = 0, 0.10, 0.20, 0.30,$ and 0.50 plotted versus surfactant concentration over $0\ mM \leq C_s \leq 50\ mM$ (A) and for concentrated mixtures with $C_a/C_s = 0, 0.10, 0.20, 0.30, 0.36,$ and 0.50 up to $C_s = 400\ mM$ (B).

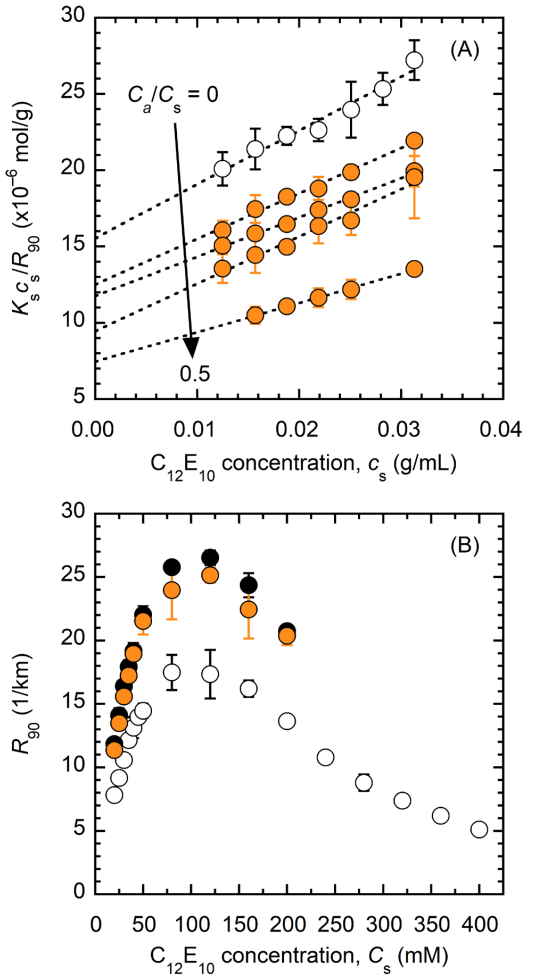

Fig. 2 (A) Reduced scattering intensities with respect to $C_{12}E_{10}$ (s) concentration with $C_a/C_s = 0, 0.10, 0.20, 0.30,$ and 0.50 for dilute $C_{12}E_{10}$/limonene/water mixtures and (B) Rayleigh ratios for concentrated $C_{12}E_{10}$/water (white), and $C_{12}E_{10}$/decane/water (black) and $C_{12}E_{10}$/limonene/water (orange) mixtures with $C_a/C_s = 0.2$.

3.3 Micelle structure at infinite dilution

DLS diffusion coefficients (Fig. 1) and reduced scattering intensities (Fig. 2A) were extrapolated to zero surfactant concentration to determine the diffusion coefficient D^0_{DLS} and the molecular weight of surfactant per micelle MW_s at infinite dilution for each molar ratio C_a/C_s. Assuming the micelles were spherical, the micelle hydrodynamic radius R_{DLS} for each C_a/C_s was calculated using the Stokes-Einstein equation,

$$R_{DLS} = \frac{k_B T}{6\pi\eta D^0_{DLS}} \quad . \tag{3}$$

Here, k_B is Boltzmann's constant, T is temperature, and η is the solvent viscosity (0.89 mPa·s at 25 °C). The micelle aggregation number $\bar{m}$ was calculated by dividing MW_s by the molecular weight of $C_{12}E_{10}$ (626.86 g/mol). Using the experimentally determined values for R_{DLS} and $\bar{m}$, the micelle hydration indices n_H, defined as the average number of water molecules bound to each surfactant molecule within the micelle, were estimated by calculating the difference between the measured hydrated volume of a solute-containing micelle $\left(4/3\,\pi {R_{DLS}}^3\right)$ and its empirically determined dry volume ($\bar{m}V_s + \bar{n}V_a$):

$$n_H = \frac{4/3\,\pi {R_{DLS}}^3 - \bar{m}V_s - \bar{n}V_a}{\bar{m}V_w} \quad . \tag{4}$$

Here, V_s, V_a, and V_w are the respective molecular volumes of a dry molecule of $C_{12}E_{10}$ (0.99 nm³), limonene (0.27 nm³), and water (0.03 nm³), and $\bar{n} = \bar{m}\,C_a/C_s$ is the average number of solute molecules per micelle. V_a and V_w were calculated from the pure liquid densities of limonene and water, respectively, at 25 °C and V_s was interpolated from density data acquired for a homologous series of aqueous $C_{12}E_m$ surfactant solutions.[30]

In Fig. 3, R_{DLS}, $\bar{m}$, and n_H for aqueous $C_{12}E_{10}$/limonene solutions are plotted versus C_a/C_s. As shown, R_{DLS} and $\bar{m}$ both increased with increasing C_a/C_s, indicating that $C_{12}E_{10}$ micelles grew via the added volume of both limonene and hydrated $C_{12}E_{10}$ surfactant. The trend in R_{DLS} with limonene concentration is consistent with results by others for aqueous solutions of $C_{16}E_{10}$/limonene via DLS.[31] Furthermore, n_H remained approximately constant, indicating that limonene, which is expected to solubilize within the hydrophobic core of the micelles, had little effect on the PEG/water composition within the micelle shell. Similar results were observed previously by us for aqueous $C_{12}E_{10}$/decane mixtures.[7] Furthermore, our solute-free aggregation number ($m_0 = 103 \pm 7$), hydrodynamic radius ($R_{DLS} = 3.76 \pm 0.02\ nm$), and hydration index ($n_H = 41 \pm 5$), agree with our previous results.[7] Using $n_H = 40$ in accordance with Fig. 3, one finds that the volume $\bar{m}n_H V_w$ occupied by hydration water within each $C_{12}E_{10}$ micelle is significant, accounting for roughly half of the total volume per micelle. Furthermore, the micelle growth rate $a_1 = 1.56\,nm$ for limonene-containing micelles was determined from the slope of the plot of R_{DLS} versus C_a/C_s.

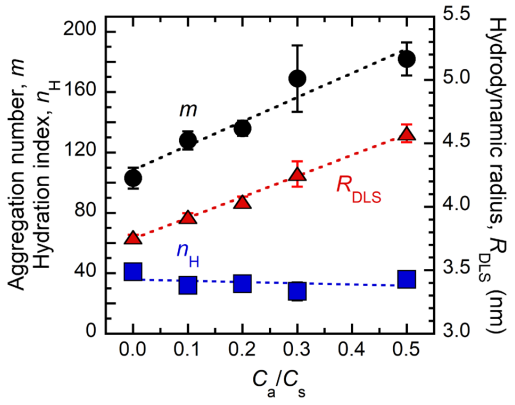

Fig. 3 Aggregation numbers $\bar{m}$ from SLS data, hydrodynamic radii R_{DLS} from DLS data, and hydration indices n_H with respect to molar ratio C_a/C_s for aqueous $C_{12}E_{10}$(s) + limonene (a) at infinite dilution. Error bars indicate 95% confidence intervals.

4 Theory

4.1 Development of light scattering correlation functions for ternary mixtures

4.1.1 Thermodynamic fluctuation theory

Following Berne and Pecora,[20] a liquid mixture within the sample cuvette of a light scattering apparatus is modelled as a composite thermodynamic system, where a subsystem A, representing the illuminated region of the solution with scattering volume V, exists within a much larger bath B, representing the remaining liquid of the sample. Mass and energy may exchange between subsystems A and B, but the total composite system is assumed isolated overall. The probability for a particular fluctuation in A is given by the master formula for thermodynamic fluctuation theory

$$P(\delta \boldsymbol{x}) = {\Omega_0}^{-1} exp\left(\frac{\delta S_T}{k_B}\right) \quad . \tag{5}$$

Here, Ω_0 is a normalization constant, $\delta \boldsymbol{x}$ is a fluctuation in a vector of thermodynamic variables, and $P(\delta \boldsymbol{x})$ is the fluctuation probability.

The total entropy fluctuation δS_T of a ternary mixture comprising the composite thermodynamic system is given by

$$\delta S_T = -\frac{1}{2T}\left(\delta T \delta S - \delta p \delta V + \sum_{i=1}^{3} \delta\mu_i \delta N_i\right) \quad . \tag{6}$$

In eqn (6), S is entropy, μ_i are the species chemical potentials, and N_i is the number of moles of species i in subsystem A. During a typical light scattering experiment, the scattering volume is fixed ($\delta V = 0$). Furthermore, temperature fluctuations, and thereby thermo-diffusion coupling effects, are neglected in this study, so that $\delta T = 0$ and eqn (6) becomes

$$\delta S_T = -\frac{1}{2T}\left(\sum_{i=1}^{3} \delta\mu_i \delta N_i\right) \quad . \tag{7}$$

It is desirable to re-express eqn (7) in terms of concentration fluctuations, and to eliminate the contributions from the solvent. Using the constant volume constraint and the Gibbs-Duhem equation, one can show (see Appendix A)

$$\sum_{i=1}^{3} \delta\mu_i \delta N_i = V \sum_{i=1}^{2}\sum_{k=1}^{2} G_{ik}\delta C_i \delta C_k = V\delta\boldsymbol{C}^T \cdot [\boldsymbol{G}] \cdot \delta\boldsymbol{C} \ , \qquad (8)$$

where the superscript T indicates the transpose of the molar concentration vector $\boldsymbol{C}$. The elements of the matrix $[\mathbf{G}]$ are given by

$$G_{ik} = \left(\frac{\partial \mu_i}{\partial C_k}\right)_{T,\mu_n,V,C_{i\neq k}} = \left(\frac{\partial \mu_i}{\partial C_k}\right)_{p,T,C_{i\neq k}} + \frac{\bar{V}_i}{1-\phi}\sum_{j=1}^{2} C_j \left(\frac{\partial \mu_j}{\partial C_k}\right)_{p,T,C_{i\neq k}}$$
$$for\ i,k = 1{,}2 \ , \qquad (9)$$

and the chemical potentials are defined as

$$\mu_i = \left(\frac{\partial \tilde{F}}{\partial N_i}\right)_{T,\mu_n,V,N_{k\neq i}} = \left(\frac{\partial g}{\partial N_i}\right)_{p,T,N_{k\neq i}} \quad for\ i,k = 1{,}2, \qquad (10)$$

where $\tilde{F}$ and g are the extensive McMillan-Mayer and Gibbs free energies, respectively. For the remainder of this article, we will abbreviate the subscripts $T,\mu_n,V,N_{k\neq i}$ and $p,T,N_{k\neq i}$ as T,μ_n and p,T, respectively.

In order to decouple the concentration fluctuations in eqn (8), a modal matrix $[\mathbf{P}]$ for the diffusion coefficient matrix $[\mathbf{D}]$, which is constructed with column vectors equal to the eigenvectors for $[\mathbf{D}]$, is used to diagonalize $[\mathbf{G}]$ via (see Appendix B)

$$\left[\hat{\mathbf{G}}\right] = [\mathbf{P}]^{\mathrm{T}}[\mathbf{G}][\mathbf{P}] \ , \qquad (11)$$

satisfying the Onsager symmetry relation,[1] where the matrix $[\mathbf{P}]$ is given by

$$\begin{bmatrix} P_{11} & P_{12} \\ P_{21} & P_{22} \end{bmatrix} = \begin{bmatrix} 1 & \left(\frac{D_{12}}{D_+ - D_{11}}\right) \\ \left(\frac{D_- - D_{11}}{D_{12}}\right) & 1 \end{bmatrix} , \qquad (12)$$

and the eigenvalues of the diffusivity matrix are

$$D_- = \frac{(D_{11}+D_{22})}{2} - \frac{\sqrt{(D_{11}-D_{22})^2 + 4D_{12}D_{21}}}{2} \qquad (13)$$

and

$$D_+ = \frac{(D_{11}+D_{22})}{2} + \frac{\sqrt{(D_{11}-D_{22})^2 + 4D_{12}D_{21}}}{2} \ . \qquad (14)$$

Eqn (5), and (7)–(11) yield

$$P(\delta\boldsymbol{x}) = \Omega_0^{-1} exp\left\{-\frac{V}{2k_BT}\left(\sum_{i=1}^{2} \hat{G}_i \delta\hat{C}_i^{\,2}\right)\right\} \ . \qquad (15)$$

Here, $\hat{G}_i$ are the diagonal elements of $\left[\hat{\mathbf{G}}\right]$ and $\hat{C}_i$ are elements of the transformed concentration vector $\left[\hat{\mathbf{C}}\right]$, defined via $[\mathbf{C}] = [\mathbf{P}]\cdot\left[\hat{\mathbf{C}}\right]$. Using eqn (15), ensemble averages of the square of the local, decoupled concentration fluctuations are determined to be (see Appendix C)

$$\langle \delta\hat{C}_i^{\,2} \rangle = \frac{k_BT}{V\hat{G}_i} \ , \qquad (16)$$

Eqn (16) is used to derive both the field correlation function and the Rayleigh ratio for ternary micellar solutions in the following sections.

4.1.2 Normalized time correlation function $g^{(1)}(\boldsymbol{q},t)$ for the scattered electric field

The intensity of scattered light measured at the detector of a light scattering apparatus at time t and scattering vector $\boldsymbol{q}$ is given by a time correlation function of the scattered electric field[20]

$$I(\boldsymbol{q},t) = \langle E^*(\boldsymbol{q},0)E(\boldsymbol{q},t)\rangle = \frac{I_0V^2{k_f}^4}{16\pi^2L^2\varepsilon^2}\langle \delta\varepsilon^*(\boldsymbol{q},0)\delta\varepsilon(\boldsymbol{q},t)\rangle \ . \qquad (17)$$

Here, I_0 is the incident light intensity, k_f is the magnitude of the propagation vector of scattered light, L is the distance from the scattering volume to the detector, $E(\boldsymbol{q},t)$ is the magnitude of the scattered electric field in reciprocal space, the asterisk indicates a complex conjugate, and $\varepsilon(\boldsymbol{q},t)$ is a spatial Fourier transform of the local dielectric constant, averaged over the scattering volume,

$$\varepsilon(\boldsymbol{q},t) = \frac{1}{V}\int d^3\boldsymbol{z}\, e^{i\boldsymbol{q}\cdot\boldsymbol{z}}\varepsilon(\boldsymbol{z},t) \ , \qquad (18)$$

where $\boldsymbol{z}$ is a position vector. Eqn (17) for the scattered light intensity is normalized to define the field correlation function

$$g^{(1)}(\boldsymbol{q},t) = \frac{\langle E^*(\boldsymbol{q},0)E(\boldsymbol{q},t)\rangle}{\langle |E(\boldsymbol{q},0)|^2\rangle} = \frac{\langle \delta\varepsilon^*(\boldsymbol{q},0)\delta\varepsilon(\boldsymbol{q},t)\rangle}{\langle |\delta\varepsilon(\boldsymbol{q},0)|^2\rangle} \ , \qquad (19)$$

For a non-magnetic, non-absorbing liquid, the dielectric constant is related to the solution refractive index via $n = \sqrt{\varepsilon}$ and the fluctuation $\delta\varepsilon(\boldsymbol{q},t)$ is expanded using the chain rule at constant temperature and pressure,

$$\delta\varepsilon(\boldsymbol{q},t) = 2n\sum_{i=1}^{2}\left(\frac{\partial n}{\partial \hat{C}_i}\right)_{p,T}\delta\hat{C}_i(\boldsymbol{q},t) \ . \qquad (20)$$

According to the Onsager regression hypothesis,[1] the concentration fluctuations $\delta\hat{C}_i$ in eqn (20) decay by the same equations that govern the relaxation of macroscopic concentration gradients. Hence, the diagonalized, Fourier transformed version of Fick's law governs the relaxation of $\delta\hat{C}_i$ via

$$\frac{\partial\delta\hat{C}_i(\boldsymbol{q},t)}{\partial t} = -q^2\hat{D}_i\delta\hat{C}_i(\boldsymbol{q},t) \ , \qquad (21)$$

where $\hat{D}_i$ are elements of the diagonalized diffusivity matrix given by $\left[\hat{\mathbf{D}}\right] = [\mathbf{P}]^{-1}[\mathbf{D}][\mathbf{P}]$, and are equal to the eigenvalues of $[\mathbf{D}]$. Eqn (21) is solved to acquire the transformed concentration fluctuations in reciprocal space

$$\delta\hat{C}_i(\boldsymbol{q},t) = \delta\hat{C}_i(\boldsymbol{q},0)exp\left(-q^2\hat{D}_it\right) \ . \qquad (22)$$

Combining eqn (16), (19), (20), and (22), and designating components 1 and 2 as solute (a) and hydrated surfactant (s), respectively, one finds (see Appendix C)

$$g^{(1)}(q,t) = \left(\frac{B}{1+B}\right) exp(-q^2 D_- t) + \left(\frac{1}{1+B}\right) exp(-q^2 D_+ t), \quad (23)$$

where the mode amplitude ratio B equals

$$B = \left(\frac{\hat{R}_a}{\hat{R}_s}\right)^2 \left(\frac{\hat{G}_s}{\hat{G}_a}\right) . \quad (24)$$

Eqn (23) indicates that concentration fluctuations in a ternary mixture at constant temperature and pressure decay via two diffusional relaxation modes, governed by the eigenvalues of the diffusivity matrix (*cf*. eqn (13) and (14)),

$$D_- = \frac{(D_{aa} + D_{ss})}{2} - \frac{\sqrt{(D_{aa} - D_{ss})^2 + 4D_{as}D_{sa}}}{2} \quad (25)$$

and

$$D_+ = \frac{(D_{aa} + D_{ss})}{2} + \frac{\sqrt{(D_{aa} - D_{ss})^2 + 4D_{as}D_{sa}}}{2} . \quad (26)$$

In eqn (24), the transformed refractive index derivatives $\hat{R}_i = \left(\partial n/\partial \hat{C}_i\right)_{p,T\hat{C}_{j\neq i}}$ are

$$\hat{R}_a = P_{aa}R_a + P_{sa}R_s \quad (27)$$

and

$$\hat{R}_s = P_{as}R_a + P_{ss}R_s , \quad (28)$$

where the measurable refractive index increments $R_i = (\partial n/\partial C_i)_{p,T,C_{j\neq i}}$ are given by (see Appendix D)

$$R_a = \bar{V}_a \left(\frac{\partial n}{\partial \phi}\right)_{p,T,C_a/C_s} + \frac{1}{C_s}\left\{\frac{\partial n}{\partial (C_a/C_s)}\right\}_{p,T,\phi} \quad (29)$$

and

$$R_s = \bar{V}_{hs}\left(\frac{\partial n}{\partial \phi}\right)_{p,T,C_a/C_s} - \frac{\bar{V}_{hs}\, C_a/C_s}{(\phi - \phi_a)}\left\{\frac{\partial n}{\partial (C_a/C_s)}\right\}_{p,T,\phi} . \quad (30)$$

Here, $\bar{V}_{hs} = \bar{V}_s + n_H \bar{V}_w$ is the hydrated surfactant molar volume, ϕ is the micelle volume fraction, and $\phi_a = C_a \bar{V}_a$ is the solute volume fraction. The matrix $[\mathbf{P}]$ is given by eqn (12),

$$\begin{bmatrix} P_{aa} & P_{as} \\ P_{sa} & P_{ss} \end{bmatrix} = \begin{bmatrix} 1 & \left(\frac{D_{as}}{D_+ - D_{aa}}\right) \\ \left(\frac{D_- - D_{aa}}{D_{as}}\right) & 1 \end{bmatrix} , \quad (31)$$

and the elements of $[\hat{\mathbf{G}}]$ are determined using

$$\hat{G}_a = G_{aa}{P_{aa}}^2 + 2G_{as}P_{aa}P_{sa} + G_{ss}{P_{sa}}^2 \quad (32)$$

and

$$\hat{G}_s = G_{aa}{P_{as}}^2 + 2G_{as}P_{as}P_{ss} + G_{ss}{P_{ss}}^2 , \quad (33)$$

where G_{aa}, G_{as}, and G_{ss} are calculated via eqn (9) and P_{aa}, P_{as}, P_{sa}, and P_{ss} are given in eqn (31).

4.1.3 Rayleigh ratio

Assuming ergodicity, the time-average scattered light intensity recorded during a static light scattering (SLS) measurement is approximately equal to the static correlation function of the scattered electric field, which is given by eqn (17) with $t = 0$:

$$I(\boldsymbol{q}) = \langle E^*(\boldsymbol{q},0)E(\boldsymbol{q},0)\rangle = \frac{I_0 V^2 {k_f}^4}{16\pi^2 L^2 \varepsilon^2}\langle \delta\varepsilon^*(\boldsymbol{q},0)\delta\varepsilon(\boldsymbol{q},0)\rangle . \quad (34)$$

Combining eqn (16), (20), and (34), and setting $\varepsilon^2 = n^4$ and $k_f \approx 2\pi n/\lambda_0$, where λ_0 is the wavelength of incident light, one can write (see Appendix C)

$$I(\boldsymbol{q}) = \frac{I_0 V}{L^2}\frac{4\pi^2 n^2}{{\lambda_0}^4}{\hat{R}_s}^2\left(\frac{k_B T}{\hat{G}_s}\right)(1+B) . \quad (35)$$

The Rayleigh ratio is defined as $R_{90} = I(\boldsymbol{q})L^2/(I_0 V)$. Hence,

$$R_{90} = \frac{4\pi^2 n^2}{{\lambda_0}^4}{\hat{R}_s}^2\left(\frac{k_B T}{\hat{G}_s}\right)(1+B) . \quad (36)$$

Evaluation of R_{90} thus requires knowledge of the chemical potential derivatives, refractive index increments, and the ternary diffusion coefficient matrix.

4.2 Chemical potential derivatives for nonionic micellar solutions with hydrophobic solutes

Thermodynamic equilibrium relations for an n-component micellar solution with N different micelles types, comprised of solute (a), hydrated surfactant (s), and solvent (n), are given by (see Appendix E)

$$n_k\mu_a + m_k\mu_s = \mu_k$$
$$for\ k = 0,1,\ldots,N-1 . \quad (37)$$

In eqn (37), m_k is the micelle aggregation number for the micelle type k, n_k is the corresponding number of solutes per micelle, and μ_a, μ_s, and μ_k are chemical potentials for the solute, surfactant, and micelle species k, respectively, and are defined per eqn (10). Differentiation of eqn (37) with respect to either C_a or C_s at constant V, T and μ_n, followed by expansion of the micelle chemical potential derivatives using the chain rule, yields

$$n_k\left(\frac{\partial \mu_a}{\partial C_a}\right)_{T,\mu_n} + m_k\left(\frac{\partial \mu_s}{\partial C_a}\right)_{T,\mu_n} = \sum_{j=0}^{N-1}\left(\frac{\partial \mu_k}{\partial C_j}\right)_{T,\mu_n}\left(\frac{\partial C_j}{\partial C_a}\right) \quad (38)$$

and

$$n_k\left(\frac{\partial \mu_a}{\partial C_s}\right)_{T,\mu_n} + m_k\left(\frac{\partial \mu_s}{\partial C_s}\right)_{T,\mu_n} = \sum_{j=0}^{N-1}\left(\frac{\partial \mu_k}{\partial C_j}\right)_{T,\mu_n}\left(\frac{\partial C_j}{\partial C_s}\right) . \quad (39)$$

Here, contributions from free molecular solute and surfactant monomer to the thermodynamic derivatives, and thereby on the driving forces for the diffusion of solute and surfactant, have

been neglected. Hence, the summations in eqn (38) and (39) index over N micelle species, rather than $n-1$ mixture components. In addition, we assume a 1:1 correspondence between the number of solute and surfactant molecules for each micelle type. Thus, $k=0$ corresponds to the only solute-free micelle species considered in this model, comprised of $n_0=0$ solute molecules and m_0 surfactant monomers. Hence, for $k=0$, eqn (38) and (39) become

$$m_0\left(\frac{\partial \mu_s}{\partial C_a}\right)_{T,\mu_n}=\sum_{j=0}^{N-1}\left(\frac{\partial \mu_0}{\partial C_j}\right)_{T,\mu_n}\left(\frac{\partial C_j}{\partial C_a}\right) \tag{40}$$

and

$$m_0\left(\frac{\partial \mu_s}{\partial C_s}\right)_{T,\mu_n}=\sum_{j=0}^{N-1}\left(\frac{\partial \mu_0}{\partial C_j}\right)_{T,\mu_n}\left(\frac{\partial C_j}{\partial C_s}\right). \tag{41}$$

Furthermore, multiplication by C_k of eqn (38) and (39) and summation over all micelle types provides the result

$$C_a\left(\frac{\partial \mu_a}{\partial C_a}\right)_{T,\mu_n}+C_s\left(\frac{\partial \mu_s}{\partial C_a}\right)_{T,\mu_n}=\left(\frac{\partial \Pi}{\partial C_a}\right)_{T,\mu_n} \tag{42}$$

and

$$C_a\left(\frac{\partial \mu_a}{\partial C_s}\right)_{T,\mu_n}+C_s\left(\frac{\partial \mu_s}{\partial C_s}\right)_{T,\mu_n}=\left(\frac{\partial \Pi}{\partial C_s}\right)_{T,\mu_n}, \tag{43}$$

where the osmotic pressure derivatives are given by (see Appendix F)

$$\left(\frac{\partial \Pi}{\partial C_a}\right)_{T,\mu_n}=\sum_{k=0}^{N-1}\sum_{j=0}^{N-1}C_k\left(\frac{\partial \mu_k}{\partial C_j}\right)_{T,\mu_n}\left(\frac{\partial C_j}{\partial C_a}\right) \tag{44}$$

and

$$\left(\frac{\partial \Pi}{\partial C_s}\right)_{T,\mu_n}=\sum_{k=0}^{N-1}\sum_{j=0}^{N-1}C_k\left(\frac{\partial \mu_k}{\partial C_j}\right)_{T,\mu_n}\left(\frac{\partial C_j}{\partial C_s}\right). \tag{45}$$

The micelle chemical potential derivatives at constant T and μ_n are generally written as a sum of ideal and nonideal terms,[13,27]

$$\frac{1}{N_A k_B T}\left(\frac{\partial \mu_k}{\partial C_j}\right)_{T,\mu_n}=\frac{\delta_{kj}}{\left(C_k C_j\right)^{1/2}}+A_{kj}, \tag{46}$$

where the non-ideal mixing contribution A_{kj} captures the influence of interparticle interactions between micelles of various types. The following symmetry relation for $[\mathbf{G}]$ (see Appendix A)

$$\left(\frac{\partial \mu_a}{\partial C_s}\right)_{T,\mu_n}=\left(\frac{\partial \mu_s}{\partial C_a}\right)_{T,\mu_n}, \tag{47}$$

enforces equality between mixed partial derivatives of the total McMillan-Mayer free energy of the mixture with respect to solute and surfactant concentration.[32] Eqn (40)–(43), (46), and (47) combine to provide the elements $G_{ik}=(\partial \mu_i/\partial C_k)_{T,\mu_n}$ of the chemical potential derivative matrix $[\mathbf{G}]$

$$C_a G_{aa}=\left(\frac{\partial \Pi}{\partial C_a}\right)_{T,\mu_n}-C_s G_{sa}, \tag{48}$$

$$G_{as}=G_{sa}=\left(\frac{N_A k_B T}{m_0}\right)\left\{\frac{1}{C_a}\frac{\partial lnC_0}{\partial lnC_a}+\sum_{j=0}^{N-1}A_{0j}\left(\frac{\partial C_j}{\partial C_a}\right)\right\}, \tag{49}$$

and

$$C_s G_{ss}=\left(\frac{\partial \Pi}{\partial C_s}\right)_{T,\mu_n}-C_a G_{sa}. \tag{50}$$

Eqn (48)–(50) define chemical potential derivatives for polydisperse mixtures of spherical particles with arbitrary interaction potentials and concentrations. In eqn (49), the solute-free micelle concentration derivative $\partial lnC_0/\partial lnC_a$ accounts for variations in the solute-free micelle mixing entropy with respect to the local solute concentration C_a. For instance, as C_a increases, the micelle distribution shifts toward micelles that contain more solutes, causing C_0, and thereby the solute-free micelle mixing entropy, to decrease. In addition, A_{0j} captures the influence of inter-micellar interactions between solute-free and various type j micelles.

4.3 Scattering functions $g^{(1)}(q,\tau)$ and R_{90} and the Onsager matrix $[\mathbf{L}]$ for locally monodisperse, nonionic micellar solutions with hydrophobic solutes

We now examine the scattering functions described by eqn (23) and (36) for the special case in which local micelle polydispersity is neglected. In this scenario, the micelle distribution is modelled using a Kronecker delta function with a composition dependent mean

$$C_i=\frac{C_s}{\overline{m}}\delta_{ii^*}=\left\{\begin{matrix}\frac{C_s}{\overline{m}}\ when\ i=i^*\\ 0\ when\ i\neq i^*\end{matrix}\right\}, \tag{51}$$

where i^* designates a micelle type with $\overline{n}$ solutes, $\overline{m}$ surfactants, radius R_{i^*}, and a local concentration equal to $C_s/\overline{m}$. Such a delta distribution is consistent with thermodynamic theory for self-assembly of surfactant and hydrophobic solutes.[33] As shown in our previous work,[8] the corresponding ternary diffusion coefficient matrix $[\mathbf{D}]$ for locally monodisperse micellar solutions comprising nonionic surfactants and hydrophobic solutes was determined to be

$$\frac{D_{aa}}{D_{i^*}^0}=1+K'\phi-M\left(\phi,\frac{C_a}{C_s}\right), \tag{52}$$

$$\frac{D_{as}}{D_{i^*}^0}=\frac{C_a}{C_s}\left\{(\beta+K'')\phi+M\left(\phi,\frac{C_a}{C_s}\right)\right\}, \tag{53}$$

$$\frac{D_{sa}}{D_{i^*}^0}=-\frac{C_s}{C_a}M\left(\phi,\frac{C_a}{C_s}\right), \tag{54}$$

and

$$\frac{D_{ss}}{D_{i^*}^0}=1+(\beta+S)\phi+M\left(\phi,\frac{C_a}{C_s}\right), \tag{55}$$

where the function $M(\phi,C_a/C_s)$ is given by

$$M\left(\phi,\frac{C_a}{C_s}\right)=\frac{\partial lnR_{i^*}}{\partial lnC_a}(1+\chi\phi)-(\beta+K'')\phi_a \qquad (56)$$

and the parameter χ is evaluated according to

$$\chi=\left(\frac{3}{2}\beta+K'+3K''\right)-\left\{\frac{d(K''-K')}{d\lambda}\right\}_{\lambda=1} . \qquad (57)$$

Here, $D_{i^*}^0$ is the solute-containing micelle diffusivity at infinite dilution, β is the 2nd osmotic virial coefficient, and K', K'', and $S=K'+K''$ are bulk mobility coefficients. Eqn (52)–(67) were derived using dilute theory by Batchelor for polydisperse hard sphere suspensions.[26–28]

In our earlier work,[8] dilute multicomponent theory was shown to be effective at predicting $[\mathbf{D}]$ for concentrated mixtures of nonionic micelles and hydrophobic solutes. Hence, eqn (52)–(55) are used here to estimate the scattering functions for concentrated mixtures. The corresponding eigenvalues of $[\mathbf{D}]$ are given by

$$\frac{D_-}{D_{i^*}^0}=1+K'\phi \qquad (58)$$

and

$$\frac{D_+}{D_{i^*}^0}=1+(\beta+S)\phi \ , \qquad (59)$$

indicating that the (−) and (+) eigenmodes for diffusion correspond to long-time self and gradient diffusion of monodisperse hard spheres, respectively. We note that this result is exact and supports arguments by Pusey for bimodal decay of the field correlation function, corresponding to self and gradient diffusion in narrowly polydisperse particle dispersions.[14] Eqn (31), (52)–(55), (58) and (59) combine to produce the following modal matrix for $[\mathbf{D}]$,

$$[\mathbf{P}]=\begin{bmatrix}P_{aa} & P_{as}\\ P_{sa} & P_{ss}\end{bmatrix}=\begin{bmatrix}1 & C_a/C_s\\ \dfrac{C_s/C_aM(\phi,C_a/C_s)}{(\beta+K'')\phi+M(\phi,C_a/C_s)} & 1\end{bmatrix} . \qquad (60)$$

In order to determine the elements of the matrix $[\boldsymbol{G}]$ in the limit of zero local polydispersity, we start by evaluating the solute-free micelle concentration derivative $\partial lnC_0/\partial lnC_a$, shown in eqn (49). Consider a Gaussian micelle distribution function given by

$$C_i=\frac{C_s}{\bar{m}}\frac{exp\left\{-\frac{1}{2}\left(\frac{n_i-\bar{n}}{\sigma}\right)^2\right\}}{\sigma\sqrt{2\pi}}, \qquad (61)$$

where σ^2 is the distribution variance. Differentiating eqn (61) with respect to solute concentration C_a for $i=0$ yields

$$\frac{\partial lnC_0}{\partial lnC_a}=-\left(\frac{\bar{n}}{\sigma}\right)^2\left(1+\frac{\partial ln\bar{m}}{\partial lnC_a}\right)+\frac{\partial lnC_{tot}}{\partial lnC_a}, \qquad (62)$$

where we have used $\bar{n}=\bar{m}\,C_a/C_s$ and $C_{tot}=C_s/\bar{m}$ is the total micelle concentration. In the limit as the variance approaches zero, eqn (61) becomes

$$\lim_{\sigma^2\to 0}\frac{C_s}{\bar{m}}\frac{exp\left\{-\frac{1}{2}\left(\frac{n_i-\bar{n}}{\sigma}\right)^2\right\}}{\sigma\sqrt{2\pi}}=\frac{C_s}{\bar{m}}\delta_{ii^*}, \qquad (63)$$

and eqn (62) yields

$$\lim_{\sigma^2\to 0}\frac{\partial lnC_0}{\partial lnC_a}\to-\infty \ . \qquad (64)$$

Hence, per eqn (49) and (64),

$$\lim_{\sigma^2\to 0}G_{sa}\to-\infty \ , \qquad (65)$$

and, per eqn (48)–(50) and (65), the elements $[\mathbf{G}]$ are infinite. However, as shown in Appendix G, the scattering functions in this limit are finite.

Using eqn (23), (24), (27)–(30), (36), (48)–(50), and (60) one may determine the mode amplitude ratio (see Appendix G),

$$B=0 \ , \qquad (66)$$

and thereby the field correlation function

$$g^{(1)}(q,t)=exp\{-q^2D_{i^*}^0[1+(\beta+S)\phi]t\} \ , \qquad (67)$$

which indicates monomodal decay via gradient diffusion. In addition, the Rayleigh ratio is determined to be (see Appendix G)

$$R_{90}=\frac{4\pi^2n^2}{{\lambda_0}^4}\left(\frac{\partial n}{\partial\phi}\right)^2_{p,T,C_a/C_s}V_{i^*}\phi\left\{\frac{d[\phi Z(\phi)]}{d\phi}\right\}^{-1} , \qquad (68)$$

where, V_{i^*} is the volume of a type i^* micelle and $Z(\phi)$ is the compressibility factor. The latter is given accurately by the Carnahan–Starling equation[34]

$$Z(\phi)=\frac{\Pi}{C_{tot}N_Ak_BT}=\frac{1+\phi+\phi^2-\phi^3}{(1-\phi)^3} \ . \qquad (69)$$

Remarkably, eqn (67) and (68) correspond to theoretical predictions for binary mixtures of monodisperse hard spheres. These results indicate that multicomponent diffusion effects, such as uphill diffusion ($D_{sa}<0$), which strongly affect the diffusivity matrix $[\mathbf{D}]$ per eqn (52)–(55) via the function $M(\phi,C_a/C_s)$, have no effect on the scattering functions $g^{(1)}(q,t)$ and R_{90} in the limit of negligible local polydispersity. These results provide theoretical support for earlier investigations by others,[11,12,29] who have used eqn (67)–(69) without *a priori* justification, to successfully model light scattering data from $C_{12}E_5$/decane/water solutions.

The Onsager coefficient matrix $[\mathbf{L}]$ is related to $[\mathbf{D}]$ and $[\mathbf{G}]$ via $[\mathbf{D}]=[\mathbf{L}][\mathbf{G}]$. Hence, the matrix $[\mathbf{G}]$ can be inverted to yield expressions for the Onsager coefficients

$$L_{aa}=(D_{aa}G_{ss}-D_{as}G_{sa})/|\boldsymbol{G}| \ , \qquad (70)$$

$$L_{as}=(D_{as}G_{aa}-D_{aa}G_{as})/|\mathbf{G}| \ , \qquad (71)$$

$$L_{sa}=(D_{sa}G_{ss}-D_{ss}G_{sa})/|\mathbf{G}| \ , \qquad (72)$$

and

$$L_{ss}=(D_{ss}G_{aa}-D_{sa}G_{as})/|\mathbf{G}| \ , \qquad (73)$$

where $|\mathbf{G}|$ is the determinant of the chemical potential derivative matrix $[\mathbf{G}]$. Using eqn (48)–(50), (52)–(55), and (70)–(73), one can derive the Onsager coefficients for dilute ($\phi \ll 1$) mixtures of nonionic micelles with hydrophobic solutes (see Appendix H) to find

$$L_{aa} = \bar{n}^2 C_{tot}\left(\frac{D_{i^*}^0}{N_A k_B T}\right)(1+S\phi) \ , \tag{74}$$

$$L_{as} = L_{sa} = \bar{n}\bar{m} C_{tot}\left(\frac{D_{i^*}^0}{N_A k_B T}\right)(1+S\phi) \ , \tag{75}$$

and

$$L_{ss} = \bar{m}^2 C_{tot}\left(\frac{D_{i^*}^0}{N_A k_B T}\right)(1+S\phi) \ . \tag{76}$$

Per eqn (75), the Onsager reciprocal relations are satisfied. Furthermore, the determinant $|\mathbf{L}| = L_{aa}L_{ss} - L_{as}L_{sa} = 0$, which indicates that the Onsager matrix $[\mathbf{L}]$ is singular, and thus not invertible, in the locally monodisperse limit as the micelle distribution variance approaches zero ($\sigma^2 \to 0$). This result is consistent with the $[\mathbf{G}]$ matrix given by eqn (48)–(50) and (65), whose elements approach infinity in this limit.

4.4 Limiting results for $\phi \to 0$, $C_a \to 0$, and in the label limit

4.4.1 $g^{(1)}(q,t)$ and R_{90} for locally monodisperse micelles at infinite dilution $\phi \to 0$

In the limit of infinite dilution, $\phi \to 0$ and the diffusivity matrix $[\mathbf{D}]$ for locally monodisperse micellar solutions, given by eqn (52)–(57), reduces to

$$\frac{D_{\mathrm{aa}}}{D_{i^*}^0} = 1 - \frac{\partial ln R_{i^*}}{\partial ln C_a} \ , \tag{77}$$

$$\frac{D_{\mathrm{as}}}{D_{i^*}^0} = \frac{C_a}{C_s}\frac{\partial ln R_{i^*}}{\partial ln C_a} \ , \tag{78}$$

$$\frac{D_{\mathrm{sa}}}{D_{i^*}^0} = -\frac{C_s}{C_a}\frac{\partial ln R_{i^*}}{\partial ln C_a} \ , \tag{79}$$

and

$$\frac{D_{\mathrm{ss}}}{D_{i^*}^0} = 1 + \frac{\partial ln R_{i^*}}{\partial ln C_a} \ . \tag{80}$$

Per eqn (58) and (59), the corresponding eigenvalues become identical and equal to the Stokes-Einstein diffusivity

$$D_- = D_+ = D_{i^*}^0 \ . \tag{81}$$

Eqn (23) and (81) combine to yield the expected result for the field correlation function at infinite dilution

$$g^{(1)}(q,t) = exp\left(-q^2 D_{i^*}^0 t\right) \ , \tag{82}$$

which indicates monomodal decay according to the solute-containing micelle Stokes-Einstein diffusivity. Furthermore, using eqn (68) with the relation $\phi = V_{i^*} c_s (N_A/MW_s)$ in the limit as $\phi \to 0$, for which $Z(\phi) \to 1$, one finds

$$\frac{K_s c_s}{R_{90}} = \frac{1}{MW_s} \ , \tag{83}$$

where c_s is the surfactant mass concentration, MW_s is the molecular weight of surfactant per micelle, N_A is Avogadro's number, and $K_s = 4\pi^2 n^2 / \left(N_A {\lambda_0}^4\right)(\partial n/\partial c_s)^2_{p,T,C_a/C_s}$ is the optical contrast constant. The results given by eqn (82) and (83) indicate that micelle growth effects, which are responsible for significant multicomponent diffusion effects per eqn (77)–(80), do not affect the scattering functions at infinite dilution, enabling one to acquire estimates for average morphological parameters for solute-containing micelles, such as hydrodynamic radii R_{i^*} and aggregations numbers $\bar{m}$ with respect to composition C_a/C_s.

4.4.2 Tracer limit $C_a \to 0$ for $[\mathbf{G}]$, $g^{(1)}(q,t)$, and R_{90}

In this section, we evaluate the scattering functions and the chemical potential derivative matrix for the special case in which solute is present in vanishingly small amounts, corresponding to the tracer limit, $C_a \to 0$. In this scenario, the derivative G_{sa} , given by eqn (49), is finite. Hence, the matrix $[\mathbf{G}]$ can be evaluated given expressions for the osmotic pressure and the micelle chemical potential derivatives. Here, we use theoretical results by Vrij[13,35] for polydisperse hard sphere mixtures in the Percus-Yevick approximation for the osmotic pressure

$$\frac{\Pi}{N_A k_B T} = \frac{6}{\pi}\left\{\frac{\xi_0}{(1-\xi_3)} + \frac{3\xi_1\xi_2}{(1-\xi_3)^2} + \frac{3{\xi_2}^3}{(1-\xi_3)^3}\right\} \tag{84}$$

and the particle chemical potential derivatives

$$\begin{aligned}\frac{1}{N_A k_B T}\left(\frac{\partial \mu_k}{\partial C_j}\right)_{T,\mu_n} = &\frac{\delta_{kj}}{\left(C_k C_j\right)^{1/2}} \\ &+ \frac{\pi/6}{(1-\phi)}\{{d_k}^3 + {d_j}^3 + {d_k}^3 {d_j}^3 \eta_0 \\ &+ 3 d_k d_j [d_k(1+d_k\eta_2)(1+{d_j}^2\eta_1) \\ &+ d_j(1+d_j\eta_2)(1+{d_k}^2\eta_1)] \\ &+ 9{d_k}^2{d_j}^2\eta_2(1+d_k\eta_2)(1+d_j\eta_2)\}\end{aligned} \tag{85}$$

where d_k is the diameter of a type k particle,

$$\eta_\nu = \frac{\xi_\nu}{1-\phi} \ , \tag{86}$$

and

$$\xi_\nu = \frac{\pi}{6}\sum_{i=0}^{N-1}\frac{\phi_i}{V_i}{d_i}^\nu = \sum_{i=0}^{N-1}\phi_i\,{d_i}^{\nu-3} \ . \tag{87}$$

Using eqn (48)–(50) and (84)–(87), the chemical potential derivatives $[\mathbf{G}]$ for locally monodisperse micelles in the tracer limit are given by (see Appendix I)

$$\frac{C_a G_{aa}}{N_A k_B T} = 1 \ , \tag{88}$$

$$\frac{C_s G_{as}}{N_A k_B T} = \frac{C_s G_{sa}}{N_A k_B T} = -1 - \frac{3a_1}{m_0 R_0}\frac{(1+\phi+\phi^2)}{(1-\phi)^3} + \frac{V_a}{m_0 V_{hs}}\frac{(1+2\phi)^2}{(1-\phi)^4} \quad , \tag{89}$$

and

$$\frac{C_s G_{ss}}{N_A k_B T} = \frac{1}{m_0}\frac{(1+2\phi)^2}{(1-\phi)^4} \quad . \tag{90}$$

Here, a_1 is the micelle growth rate, which indicates how strongly the average micelle radius varies with the solute to surfactant molar ratio C_a/C_s, V_a is the molecular volume of the solute, and $V_{hs} = V_s + n_H V_w$ is the molecular volume of a hydrated surfactant monomer, where n_H is the hydration index, and V_w and V_s are the molecular volumes for the solvent and a dry surfactant molecule, respectively. Per eqn (88), when only trace amounts of solute are present, the chemical potential of the solute varies with respect to solute concentration via ideal mixing within the micellar solution. Eqn (90), on the other hand, describes variations in the surfactant chemical potential with respect to surfactant concentration resulting from the non-ideal mixing of interacting, monodisperse, solute-free micelles. Interestingly, the cross terms, given by eqn (89), describe variations in chemical potential that are affected by a term proportional to the micelle growth rate a_1 and the molecular volume of the solute V_a. These non-ideal contributions capture the influence of self-assembly on micellar solution thermodynamics and are not included in thermodynamic models derived for rigid particle dispersions.

In order to view the relative importance of the micellar growth contributions on the cross terms of the [**G**] matrix, theoretical predictions for [**G**] in the tracer limit for aqueous $C_{12}E_{10}$/decane mixtures were calculated using eqn (88)–(90) with $V_a = 0.32$ nm³, $V_s = 0.99$ nm³, $V_w = 0.03$ nm³, $m_0 = 103$, $n_H = 40$, $a_1 = 2.4226$ nm, and $R_0 = 3.76$ nm, consistent with our light scattering data shown in Fig. 3. The results are plotted versus volume fraction ϕ in Fig. 4. As shown, the main solute chemical potential derivative G_{aa} is independent of volume fraction, indicating that trace amounts of solute mix ideally within micelles, even in crowded mixtures. In contrast, the surfactant main term G_{ss} increases strongly with increasing volume fraction, resulting from the interactions between monodisperse solute-free micelles. Interestingly, the cross terms G_{as} and G_{sa} are shown to become more negative with increasing volume fraction, illustrating the influence of micelle growth effects on the matrix [**G**].

The tracer limit described in this section is a special case of the locally monodisperse limit discussed in section 4.5. Hence, the scattering functions are determined via eqn (67) and (68), in the limit as $C_a \to 0$, to yield the field correlation function

$$g^{(1)}(q,t) = exp\{-q^2 D^0[1 + (\beta + S)\phi]t\} \quad , \tag{91}$$

and the Rayleigh ratio

$$R_{90} = \frac{4\pi^2 n^2}{{\lambda_0}^4}\left(\frac{\partial n}{\partial \phi}\right)^2_{p,T,C_a/C_s} V_0 \phi \left\{\frac{d[\phi Z(\phi)]}{d\phi}\right\}^{-1} , \tag{92}$$

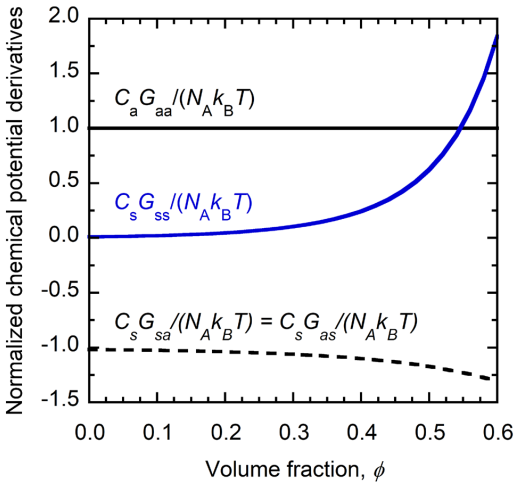

Fig. 4 Theoretical predictions for the normalized chemical potential derivatives [**G**], calculated using eqn (88)–(90) and plotted with respect to volume fraction for aqueous $C_{12}E_{10}$(s) + decane (a) in the tracer limit as $C_a \to 0$.

which is not restricted to the Percus-Yevick result for interacting hard spheres.

4.4.3 Label limit for [**G**], $g^{(1)}(q,t)$, R_{90}, and [**L**]

We now examine the scattering functions described by eqn (23) and (36) for various finite solute concentrations, for the special case in which the solute behaves as a volume-less label. In this scenario, solute-containing micelles are identically sized ($d_k = d_0 = d$), but optically polydisperse. Hence, eqn (85) simplifies to

$$\frac{1}{N_A k_B T}\left(\frac{\partial \mu_k}{\partial C_j}\right)_{T,\mu_n} = \frac{\delta_{kj}}{(C_k C_j)^{1/2}} + \frac{\phi}{V_0}\left\{\frac{(1+2\phi)^2}{(1-\phi)^4} - 1\right\} \quad , \tag{93}$$

where V_0 is the solute-free micelle volume. Using eqn (48)–(50), (84), (87), and (93), the solute and surfactant chemical potential derivatives reduce to (see Appendix J)

$$G_{aa} = -\frac{N_A k_B T}{\bar{n} C_a}\frac{\partial ln C_0}{\partial ln C_a} \quad , \tag{94}$$

$$G_{as} = G_{sa} = \frac{N_A k_B T}{\bar{n} C_s}\frac{\partial ln C_0}{\partial ln C_a} \quad , \tag{95}$$

and

$$G_{ss} = \frac{N_A k_B T}{m_0 C_s}\left\{\frac{(1+2\phi)^2}{(1-\phi)^4} - \frac{\partial ln C_0}{\partial ln C_a}\right\} \quad . \tag{96}$$

where C_0 is the solute-free micelle concentration. Note, in this development it was not necessary to specify a particular micelle distribution function C_i, and, unlike our results presented in sections 4.3 and 4.4.2 for locally monodisperse micelles or in the tracer limit, respectively, the derivatives $\partial ln C_0/\partial ln C_a$ for the label limit are finite.

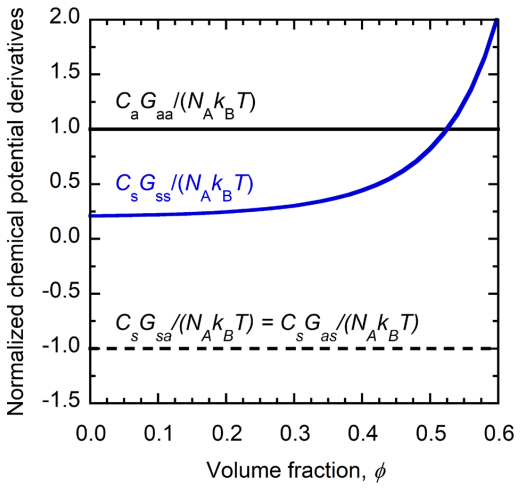

Fig. 5 Theoretical predictions in the label limit for the normalized chemical potential derivatives [**G**], calculated using eqn (94)–(96) and plotted with respect to volume fraction for aqueous $C_{12}E_{10}$(s) micelles with Poisson distributed solute labels and molar ratio $C_a/C_s = 0.2$.

Theoretical predictions for [**G**] in the label limit for aqueous mixtures of label-containing $C_{12}E_{10}$ micelles were calculated using eqn (94)–(96) with $V_a = 0$ nm³, $V_s = 0.99$ nm³, $V_w = 0.03$ nm³, $m_0 = 103$, and $n_H = 40$, consistent with Fig. 3, with $C_a/C_s = 0.2$. In addition, a Poisson distribution was assumed, so that $\partial lnC_0/\partial lnC_a = -\overline{n}$, and the results are plotted versus volume fraction ϕ in Fig. 5.

For the Poisson distribution considered here, G_{aa} in the label limit is identical to that of the tracer limit, consistent with ideal mixing of solute labels within this hypothetical micellar solution. However, as shown in Fig. 5, the normalized cross terms of [**G**] are absent any effects from micelle growth, as expected, and thus do not vary with respect to volume fraction, as they do for the tracer limit.

In previous work by our group,[7,8] the ternary diffusion coefficient matrix [**D**] for the label case was determined to be

$$\frac{D_{\mathrm{aa}}}{D^0} = 1 + K'\phi \ , \tag{97}$$

$$\frac{D_{\mathrm{as}}}{D^0} = \frac{C_{\mathrm{a}}}{C_{\mathrm{s}}}(\beta + K'')\phi \ , \tag{98}$$

$$D_{\mathrm{sa}} = 0 \ , \tag{99}$$

and

$$\frac{D_{\mathrm{ss}}}{D^0} = 1 + (\beta + S)\phi \ . \tag{100}$$

Here, D^0 is the solute-free micelle infinite dilution diffusivity, β is the 2nd osmotic virial coefficient, and K', K'', and $S = K' + K''$ are bulk mobility coefficients. The corresponding eigenvalues of [**D**] are given by

$$\frac{D_-}{D^0} = 1 + K'\phi \tag{101}$$

and

$$\frac{D_+}{D^0} = 1 + (\beta + S)\phi \ . \tag{102}$$

Eqn (31) and (97)–(102) combine to produce the modal matrix for the label case,

$$[\mathbf{P}] = \begin{bmatrix} 1 & C_a/C_s \\ 0 & 1 \end{bmatrix} \ . \tag{103}$$

Eqn (24), (27)–(30), (36), (94)–(96), and (103), are then used to determine the Rayleigh ratio for the label limit (see Appendix J):

$$R_{90} = \frac{4\pi^2 n^2}{{\lambda_0}^4}\left(\frac{\partial n}{\partial \phi}\right)^2_{p,T,C_a/C_s} V_0\phi\frac{(1-\phi)^4}{(1+2\phi)^2}(1 + B_{LL}) \ , \tag{104}$$

where the mode amplitude ratio B_{LL} for the label limit is given by

$$B_{LL} = \left\{\frac{[\partial n/\partial(C_a/C_s)]_{p,T,\phi}}{\phi(\partial n/\partial\phi)_{p,T,C_a/C_s}}\right\}^2 \frac{(C_a/C_s)^2}{(-\partial lnC_0/\partial lnC_a)}\frac{(1+2\phi)^2}{(1-\phi)^4} . \tag{105}$$

Per eqn (105), the mode amplitude ratio for the label limit is generally nonzero. Hence, decay of the field correlation function, given by eqn (23), is bimodal, corresponding to the eigenvalue diffusivities given by eqn (101) and (102).

Furthermore, since micelle growth effects are deactivated in the label limit, so that micelles with different numbers of solute molecules are uniform in size, one can compare B_{LL} in eqn (105) with theory by Pusey et al.[14,15] for colloidal dispersions comprised of rigid spheres that are equal in size but optically polydisperse. In their theory, optical polydispersity is captured via variations in scattering power f_i between the different particle species and the solvent. In the following discussion, we relate this approach to our own, for which optical polydispersity is captured using measurable derivatives for the refractive index of the solution, given by $[\partial n/\partial(C_a/C_s)]_{p,T,\phi}$ and $(\partial n/\partial\phi)_{p,T,C_a/C_s}$.

Theory by Pusey et al.[14,15] for the mode amplitude ratio in the Percus-Yevick approximation is given by

$$B_P = \left(\frac{\overline{f^2} - \bar{f}^2}{\bar{f}^2}\right)\frac{(1+2\phi)^2}{(1-\phi)^4} , \tag{106}$$

where

$$\bar{f} = \sum_{i=0}^{N-1} C_i f_i \Big/ \sum_{i=0}^{N-1} C_i \ , \tag{107}$$

and

$$\overline{f^2} = \sum_{i=0}^{N-1} C_i {f_i}^2 \Big/ \sum_{i=0}^{N-1} C_i \ , \tag{108}$$

are number averages of the particle scattering power f_i. Unlike eqn (105), which captures the influence of particle scattering power via measurable refractive index derivatives of the mixture, eqn (106)–(108) require additional information pertaining to the particle microstructure. Yan and Clarke[18] suggested the following core-shell model for the scattering amplitude f_i of water-in-oil microemulsion droplets of volume V_i

$$f_i \propto (n_{p,i} - n_{solv})V_i \,. \tag{109}$$

where n_{solv} is the refractive index of the solvent and $n_{p,i}$ is the volume-average refractive index for an i-type particle, given by

$$n_{p,i} = \frac{n_{core}V_{core,i} + n_{shell}V_{shell,i}}{V_i} \,. \tag{110}$$

Here, n_{core} and n_{shell} are the refractive indices of the particle core and shell, respectively, and $V_{core,i}$ and $V_{shell,i}$ are the corresponding volumes.

Eqn (110) can be modified to apply to mixtures of solute-containing micelles by replacing the constant n_{core} with a core refractive index $n_{core,i}$ that varies with the number of solutes per micelle. In the label limit, $V_i = V_0$ for all i and eqn (107) and (109) combine to provide

$$\bar{f} \propto (\bar{n}_p - n_{solv})V_0 \,, \tag{111}$$

where $\bar{n}_p$ is the number average particle refractive index. At the optical matching point, the average particle refractive index equals that of the solvent $\bar{n}_p = n_{solv}$, so that $\bar{f} = 0$ per eqn (111). Furthermore, fluctuations in the total micelle concentration (volume fraction) at constant solute to surfactant molar ratio at the optical matching point do not generate variations in the overall refractive index of the solution, so that $(\partial n/\partial\phi)_{p,T,C_a/C_s} = 0$. Hence, eqn (105) and eqn (106)–(108) yield

$$B_{LL} \to \infty \;\; and \;\; B_P \to \infty \,, \tag{112}$$

and eqn (23), (101), and (112) give

$$g^{(1)}(q,t) = exp[-q^2D^0(1 + K'\phi)t] \,. \tag{113}$$

Eqn (113) indicates that both theories for the mode amplitude ratio predict decay of $g^{(1)}(q,t)$ corresponding to long-time self diffusion of monodisperse hard spheres at the optical matching point. In this case, the number average refractive index of the particles is equal to that of the solvent, so that fluctuations in the overall particle concentration do not scatter light. However, variations in scattering power may still exist between the different particle species. Hence, particle exchange events may still weakly scatter light at the optical matching point via self diffusion. On the other hand, one can remove the self mode for light scattering via particle exchange by assuming a delta distribution, corresponding to a single particle type i^*, for which $-\partial lnC_0/\partial lnC_a \to \infty$, $\bar{f} = f_{i^*}$, $\overline{f^2} = {f_{i^*}}^2$, and $(\overline{f^2} - \bar{f}^2)/\bar{f}^2 = 0$, so that eqn (105)–(108) provide

$$B_{LL} = B_P = 0 \,. \tag{114}$$

Per eqn (23), (102), and (114), the field correlation function is then given by

$$g^{(1)}(q,t) = exp\{-q^2D^0[1 + (\beta + S)\phi]t\} \,. \tag{115}$$

This result indicates that decay of $g^{(1)}(q,t)$ occurs via gradient diffusion of monodisperse hard spheres in the limit of negligible local polydispersity. Thus, in these two limits, the predictions of Yan and Clark and eqn (105) agree.

The Onsager matrix for the dilute, label limit is acquired using eqn (70)–(73) and (94)–(100) (see Appendix J)

$$L_{aa} = \bar{n}^2C_{tot}\left(\frac{D^0}{N_Ak_BT}\right)\left[1 + S\phi + \frac{1 + K'\phi}{(-\partial lnC_0/\partial lnC_a)}\right] \,, \tag{116}$$

$$L_{as} = L_{sa} = \bar{n}m_0C_{tot}\left(\frac{D^0}{N_Ak_BT}\right)(1 + S\phi) \,, \tag{117}$$

and

$$L_{ss} = {m_0}^2C_{tot}\left(\frac{D^0}{N_Ak_BT}\right)(1 + S\phi) \,. \tag{118}$$

Per eqn (116), the main Onsager coefficient L_{aa}, which is related to the mobility of the solute when it is acted on a by a steady thermodynamic driving force, depends on the micelle distribution function through the derivative $\partial lnC_0/\partial lnC_a$, and, per eqn (117), the Onsager reciprocal relations are satisfied.

4.5 Method of cumulants

The method of cumulants, which is often used to analyze dynamic light scattering data, is based on a general description of $g^{(1)}(q,\tau)$ for polydisperse solutions, expressed as a sum or integral of exponentials:[36]

$$g^{(1)}(q,\tau) = \int_0^\infty G(\Gamma)\, e^{-\Gamma\tau} d\Gamma \,, \tag{119}$$

where τ is a measurement time interval or time delay. Here, the integral defines a raw moment-generating function for the decay rate distribution $G(\Gamma)$, where Γ is a continuous decay rate variable. The logarithm of the integral in eqn (119) defines a cumulant generating function, which can be shown via a Taylor expansion of $e^{-\Gamma\tau}$ around $\Gamma\tau = 0$ to yield the following:

$$ln\{g^{(1)}(q,\tau)\} = -\bar{\Gamma}\tau + \frac{\kappa_2}{2}\tau^2 + \cdots \,. \tag{120}$$

In eqn (120), $\bar{\Gamma}$ and κ_2 are the first and second cumulants of $G(\Gamma)$, respectively. At infinite dilution, $G(\Gamma)$ for narrowly disperse hard sphere mixtures is monomodal with a mean $\bar{\Gamma} = q^2D_z$ and variance $\kappa_2 = \overline{\Gamma^2} - \bar{\Gamma}^2$, defined via $\overline{\Gamma^m} = \int_0^\infty G(\Gamma)\,\Gamma^m d\Gamma$. The parameter D_z is the z-average diffusion coefficient, and the normalized second cumulant $\kappa_2/\bar{\Gamma}^2$ is used to provide an estimate for particle size polydispersity. However, at finite concentrations, $G(\Gamma)$ does not closely approximate the particle size distribution in general. This can be seen by merging eqn (23) with eqn (119). The resulting decay rate distribution for concentrated hard sphere dispersions,

$$G(\Gamma) = \left(\frac{1}{1+B}\right)\delta(\Gamma-\Gamma_+) + \left(\frac{B}{1+B}\right)\delta(\Gamma-\Gamma_-)\,, \qquad (121)$$

is bimodal even if the particle size distribution is monomodal. In eqn (121), $\Gamma_+ = q^2 D_+$ and $\Gamma_- = q^2 D_-$ are the respective fast and slow mode decay rates. For concentrated solutions, the corresponding first and second cumulants of $G(\Gamma)$ can be directly related to parameters D_{DLS}, and $\kappa_2/\bar{\Gamma}^2$ that are routinely obtained when the method of cumulants analysis is applied to DLS measurements:

$$D_{DLS} = \frac{\bar{\Gamma}}{q^2} = \left(\frac{D_+ + BD_-}{1+B}\right)\,, \qquad (122)$$

and

$$\frac{\kappa_2}{\bar{\Gamma}^2} = B\left(\frac{D_+ - D_-}{D_+ + BD_-}\right)^2\,. \qquad (123)$$

Per eqn (122), the cumulant diffusivity D_{DLS} is a mode amplitude weighted average of eigenvalue diffusivities. Hence, D_+ is acquired via the cumulants analysis only when the slow mode amplitude is small relative to that of the fast mode, *i.e.*, when $B \ll 1$. Furthermore, the normalized second cumulant $\kappa_2/\bar{\Gamma}^2$ depends strongly on the difference $D_+ - D_-$, which increases with increasing ϕ for hard-sphere dispersions. Thus, $\kappa_2/\bar{\Gamma}^2$ for concentrated solutions does not solely depend on the variance of the particle size and refractive index distributions, in contrast to the case at infinite dilution.

5 Discussion

5.1 Eigenmodes for diffusion

As discussed in previous sections, the field correlation function for a ternary mixture at constant temperature and pressure is bimodal, and decays according to the eigenvalues of the ternary diffusivity matrix. In this section, we identify the underlying transport processes (diffusional modes) corresponding to the eigenvalues, and the independent, linear combinations of solute and surfactant concentration fluctuations that activate them during a typical dynamic light scattering measurement. Here, transport equations governing the light scattering diffusional modes are derived in terms of macroscopic concentration gradients. However, invoking the Onsager regression hypothesis,[1] the results presented here also govern the relaxation of local, microscopic concentration fluctuations. Following the analysis of Toor,[37] and invoking the Onsager regression hypothesis,[1] the modal matrix, given by eqn (31), is used to diagonalize $[\mathbf{D}]$

$$[\mathbf{P}]^{-1}[\mathbf{D}][\mathbf{P}] = \begin{bmatrix} D_- & 0 \\ 0 & D_+ \end{bmatrix}\,, \qquad (124)$$

and decouple the ternary form of Fick's law, to provide

$$-\begin{bmatrix} \hat{J}_- \\ \hat{J}_+ \end{bmatrix} = \begin{bmatrix} D_- & 0 \\ 0 & D_+ \end{bmatrix}\begin{bmatrix} \nabla\hat{C}_- \\ \nabla\hat{C}_+ \end{bmatrix}\,. \qquad (125)$$

Eqn (125) describes two independent, uncoupled fluctuation modes of diffusion corresponding to the eigenvalues D_- and D_+. The mode fluxes $\hat{J}_-$ and $\hat{J}_+$ are related to the fluxes of solute J_a and surfactant J_s via

$$\begin{bmatrix} \hat{J}_- \\ \hat{J}_+ \end{bmatrix} = [\mathbf{P}]^{-1}\begin{bmatrix} J_a \\ J_s \end{bmatrix}\,, \qquad (126)$$

and the corresponding gradients $\nabla\hat{C}_-$ and $\nabla\hat{C}_+$ are linear combinations of solute and surfactant concentration gradients, given by

$$\begin{bmatrix} \nabla\hat{C}_- \\ \nabla\hat{C}_+ \end{bmatrix} = [\mathbf{P}]^{-1}\begin{bmatrix} \nabla C_a \\ \nabla C_s \end{bmatrix}\,. \qquad (127)$$

Eqn (52)–(55), (60), and (124)–(137) combine to provide expressions for $\hat{J}_-$ and $\hat{J}_+$ for locally monodisperse micellar solutions (see Appendix K) given by

$$-\frac{\hat{J}_-}{C_a D_-} = -\left\{1 + \frac{M\left(\phi, \frac{C_a}{C_s}\right)}{(\beta + K'')\phi}\right\}\left(\frac{J_a}{C_a D_-} - \frac{J_s}{C_s D_-}\right)$$

$$= \frac{\nabla\hat{C}_-}{C_a} = \left\{1 + \frac{M\left(\phi, \frac{C_a}{C_s}\right)}{(\beta + K'')\phi}\right\}\nabla ln\left(\frac{C_a}{C_s}\right)\,, \qquad (128)$$

and

$$-\frac{\hat{J}_+}{C_s D_+} = -\frac{J_s}{C_s D_+} + \left\{\frac{M\left(\phi, \frac{C_a}{C_s}\right)}{(\beta + K'')\phi}\right\}\left(\frac{J_a}{C_a D_+} - \frac{J_s}{C_s D_+}\right)$$

$$= \frac{\nabla\hat{C}_+}{C_s} = \nabla ln\left(\frac{C_s}{\bar{m}}\right) + \left\{\frac{\partial ln\bar{m}}{\partial lnC_a} - \frac{M\left(\phi, \frac{C_a}{C_s}\right)}{(\beta + K'')\phi}\right\}\nabla ln\left(\frac{C_a}{C_s}\right)\,. \qquad (129)$$

These fluxes are given in terms of gradients in composition, $\nabla ln(C_a/C_s) = \nabla C_a/C_a - \nabla C_s/C_s$, and in the total micelle concentration $\nabla ln(C_s/\bar{m})$, corresponding to exchange $(-)$ and collective, compression-dilation $(+)$ fluctuation modes similar to those described by others[14,15,18,22] for polydisperse colloidal mixtures.

According to eqn (128), the $(-)$ mode is activated by gradients in composition and describes the relative flux of solute and surfactant via interdiffusion.[38] The $(+)$ mode, on the other hand, is driven by gradients in both composition and in the total micelle concentration per eqn (129), the former perhaps accounting for the growth-induced generation of total micelle concentration and mobility gradients that occur via changes in the aggregation and average micelle radius, respectively, with variations in the molar ratio along the diffusion path. In general, it seems that neither of the diffusional modes, described by eqn (128) and (129), can be identified as binary gradient or long-time self diffusion of rigid monodisperse spheres, as both modes are influenced by micelle growth effects via the functions $M(\phi, C_a/C_s)$ and $\partial ln\bar{m}/\partial lnC_a$. This is the case, even though these modes relax according to eigenvalues that are identical to binary self and gradient diffusivities according to eqn (58) and (59).

There are, however, special cases for which these diffusional modes have a relatively clear interpretation. For instance, when the (−) mode is deactivated by restricting gradients in composition, via the constraint $\nabla(C_a/C_s)=0$, then only gradients in the total micelle concentration are allowed. As a result, eqn (59), (128), and (129) reduce to the following

$$-\frac{\hat{J}_+}{\bar{m}}=-\frac{J_s}{\bar{m}}=-\frac{J_a}{\bar{n}}=D_i^0\{1+(\beta+S)\phi\}\nabla\left(\frac{C_s}{\bar{m}}\right)\ . \qquad (130)$$

Eqn (130) describes monomodal diffusion of solute and surfactant via the (+) mode, occurring by gradient diffusion in a binary mixture of monodisperse, solute-containing micelles.

In the tracer limit as $C_a\to 0$, eqn (128) and (129) reduce to (see Appendix K)

$$-\hat{J}_-=-J_a=D_-\nabla C_a \qquad (131)$$

and

$$-\frac{\hat{J}_+}{m_0}=-\frac{J_s}{m_0}+\left\{\frac{a_1}{R_0}\frac{(1+\chi\phi)}{(\beta+K'')\phi}-\frac{V_a}{V_{hs}}\right\}\frac{J_a}{m_0}$$
$$=D_+\nabla\left(\frac{C_s}{m_0}\right)+D_+\frac{a_1}{R_0}\left\{\frac{3(\beta+K'')\phi-(1+\chi\phi)}{(\beta+K'')\phi}\right\}\nabla C_a\,. \qquad (132)$$

As indicated by eqn (131), the (−) mode in the tracer limit is activated only by gradients in the solute concentration, which relax according to the micelle self diffusion coefficient D_-. Notably, this mode is independent of the identity (i. e., physical properties) of the solute. However, the (+) mode, given by eqn (132), is affected by the solute identity and describes micelle gradient diffusion according to the term $D_+\nabla(C_s/m_0)$, modified with a contribution from solubilization-induced micelle growth, driven by gradients in solute concentration, via the term proportional to the micelle growth rate a_1.

Finally, consider the locally monodisperse label scenario. In this case, the effects of micelle growth are removed, so that $M(\phi,C_a/C_s)=\partial ln\bar{m}/\partial lnC_a=0$, and eqn (128) and (129) become

$$-\frac{\hat{J}_-}{C_a}=-\left(\frac{J_a}{C_a}-\frac{J_s}{C_s}\right)=D_-\nabla ln\left(\frac{C_a}{C_s}\right) \qquad (133)$$

and

$$-\frac{\hat{J}_+}{m_0}=-\frac{J_s}{m_0}=D_+\nabla\left(\frac{C_s}{m_0}\right). \qquad (134)$$

Here, in the label limit, the (−) and (+) modes describe pure interdiffusion[38] and micelle gradient diffusion, respectively, which are absent any micelle growth effects. Similar diffusional modes have been derived for systems of bidisperse colloidal spheres that are identical in size and differ only in labelling.[14,38]

5.2 Driving forces for diffusion in the tracer and label limits

Within the framework of nonequilibrium thermodynamics,[35] the fluxes of solute (a) and surfactant (s) in a ternary mixture are linearly related to thermodynamic driving forces through a matrix of Onsager coefficients

$$\begin{bmatrix}\boldsymbol{J}_a\\ \boldsymbol{J}_s\end{bmatrix}=\begin{bmatrix}L_{aa} & L_{as}\\ L_{sa} & L_{ss}\end{bmatrix}\begin{bmatrix}\boldsymbol{X}_a\\ \boldsymbol{X}_s\end{bmatrix}\ . \qquad (135)$$

If $\boldsymbol{J}_a$ and $\boldsymbol{J}_s$ are molar diffusive fluxes defined relative to a volume-fixed reference frame, then the conjugate, independent driving forces for diffusion can be expanded in terms of concentration gradients (see Appendix L)

$$-\begin{bmatrix}(\boldsymbol{X}_a)_{T,\mu_n}\\ (\boldsymbol{X}_s)_{T,\mu_n}\end{bmatrix}=\begin{bmatrix}(\boldsymbol{\nabla}\mu_a)_{T,\mu_n}\\ (\boldsymbol{\nabla}\mu_s)_{T,\mu_n}\end{bmatrix}=\begin{bmatrix}G_{aa} & G_{as}\\ G_{sa} & G_{ss}\end{bmatrix}\begin{bmatrix}\boldsymbol{\nabla}C_a\\ \boldsymbol{\nabla}C_s\end{bmatrix}. \qquad (136)$$

Here, $(\boldsymbol{X}_a)_{T,\mu_n}$ and $(\boldsymbol{X}_s)_{T,\mu_n}$ are the driving forces for diffusion of the solute and surfactant, respectively, relative to a volume-fixed reference frame and the solvent is force-free according to $(\boldsymbol{X}_n)_{T,\mu_n}=-(\boldsymbol{\nabla}\mu_n)_{T,\mu_n}=0$.

In the tracer limit, eqn (88)–(90) combine with eqn (136) to provide

$$\frac{C_a(\boldsymbol{X}_a)_{T,\mu_n}}{N_Ak_BT}=-\nabla C_a\ , \qquad (137)$$

and

$$\frac{C_s(\boldsymbol{X}_s)_{T,\mu_n}}{N_Ak_BT}=\left[1+\frac{3a_1}{m_0R_0}\frac{(1+\phi+\phi^2)}{(1-\phi)^3}-\frac{V_a}{m_0V_{hs}}\frac{(1+2\phi)^2}{(1-\phi)^4}\right]\nabla C_a$$
$$-\frac{(1+2\phi)^2}{(1-\phi)^4}\nabla C_{tot} \qquad (138)$$

Eqn (137) describes a purely entropic thermodynamic driving force for the diffusion of solute in the tracer limit, identical to that predicted for solute diffusion in a dilute, binary mixture of solute and solvent. Furthermore, per eqn (137), surfactant gradients do not impose a driving force on the solute in the tracer limit, consistent with our previous results[8] for $[\mathbf{D}]$ in the tracer limit, which indicates that surfactant gradients do not drive coupled solute fluxes in the tracer limit ($D_{as}=0$). However, the driving force acting on the surfactant in the tracer limit, given by eqn (138), is more complicated. The second term on the right-hand side of eqn (138) is an expected contribution to the surfactant thermodynamic force, indicating surfactant diffusion driven by gradients in the total micelle concentration, enhanced by a factor that accounts for the influence of intermicellar interactions. The second term on the right-hand side of eqn (138) indicates that solute gradients also impose a driving force on the surfactant in a direction that points up the solute gradient. This contribution is enhanced by a term proportional to the micelle growth rate a_1 and is reduced by a term proportional to the molecular volume of the solute V_a. Again, this result is consistent with our previous predictions[8] for $[\mathbf{D}]$ in the tracer limit, which indicate uphill surfactant diffusion in response to a solute gradient in the tracer limit.

For the label case, eqn (94)–(96), and (136) combine to yield

$$\frac{\bar{n}(\boldsymbol{X}_a)_{T,\mu_n}}{N_Ak_BT}=\frac{\partial lnC_0}{\partial lnC_a}\nabla ln\left(\frac{C_a}{C_s}\right) \qquad (139)$$

and

$$\frac{m_0(\boldsymbol{X}_s)_{T,\mu_n}}{N_Ak_BT}=-\frac{\partial lnC_0}{\partial lnC_a}\nabla ln\left(\frac{C_a}{C_s}\right)-\frac{(1+2\phi)^2}{(1-\phi)^4}\nabla lnC_{tot}\ . \qquad (140)$$

Per eqn (139), solute label diffusion is driven exclusively by gradients in composition, per the so-called "exchange" or "self" or "interdiffusion" mode, which is purely entropic and depends on the distribution of solute within micelles via $\partial lnC_0/\partial lnC_a$. On the other hand, both gradients in composition and total micelle concentration contribute to the driving force on the surfactant within micelles according to eqn (140). The former contribution is interesting because, according to eqn (99), solute gradients do not drive coupled fluxes of surfactant in the label limit corresponding to $D_{sa} = 0$. However, per eqn (140), solute gradients do impose a driving force contribution on the surfactant, via the composition gradient.

In order to understand this paradox, one may calculate the surfactant flux, $J_s = L_{sa}X_a + L_{ss}X_s$, by combining eqn (117), (118), (135), (139), and (140) to find

$$J_s = m_0 C_{tot}\left(\frac{D^0}{N_A k_B T}\right)(1+S\phi)\left[\bar{n}(\boldsymbol{X}_a)_{T,\mu_n} + m_0(\boldsymbol{X}_s)_{T,\mu_n}\right]. \quad (141)$$

Now, consider a solute gradient in the absence of a surfactant gradient, so that $\nabla C_s = 0$. Due to its label nature, a solute gradient has no ability to generate a total micelle concentration gradient in this scenario, since $\nabla lnC_{tot} = \nabla lnC_S = 0$. Hence, eqn (139) and (140) reduce to

$$\bar{n}(\boldsymbol{X}_a)_{T,\mu_n} = -m_0(\boldsymbol{X}_s)_{T,\mu_n}, \quad (142)$$

and, per eqn (141) and (142), $J_s = 0$. Physically, in the label limit, solute gradients (which entail composition gradients at uniform surfactant concentration) impose entropic forces on both the surfactant and the solute within micelles that are equal and opposite, producing a net zero force on micelles. Hence, composition gradients $\nabla ln(C_a/C_s)$ do not generate a net surfactant flux in the label limit, and act only to mix solute via the random motion of identically sized micelles in the absence of an overall micelle concentration gradient.

5.3 Multimodal analysis of $g^{(1)}(\boldsymbol{q},\tau)$

In Fig. 6, the logarithm of the field autocorrelation function $ln\{g^{(1)}(q,\tau)\}$ is plotted as a function of the time delay τ for $C_{12}E_{10}$/water binary mixtures, and ternary mixtures of either $C_{12}E_{10}$/decane/water or $C_{12}E_{10}$/limonene/water with $C_s = 200$mM and $C_a/C_s = 0.2$. Similarly, in Fig. 7, plots of $ln\{g^{(1)}(q,\tau)\}$ versus τ are provided for binary $C_{12}E_{10}$/water mixtures with $C_s = 20, 200,$ and 400 mM. As shown in Fig. 6A and 7A, the data for dilute to moderately concentrated micellar solutions are linear with respect to time, indicating nearly monomodal decay of $g^{(1)}(q,\tau)$ up to $\phi = 0.25$. However, as shown in Fig. 7A, the profile is nonlinear when $C_s = 400$mM, corresponding to $\phi = 0.53$. Similar results have been observed by others in concentrated ternary $C_{12}E_5$/decane/water[11] and binary $C_{12}E_8$/water systems.[39]

The nonlinearity in $ln\{g^{(1)}(\boldsymbol{q},\tau)\}$ versus τ in Fig. 7A for concentrated mixtures of solute-free micelles could indicate the emergence of the self mode, resulting from optical and size polydispersity between micelles with various aggregation numbers. As discussed by Pusey et al.,[14] N decay modes for $g^{(1)}(\boldsymbol{q},\tau)$ are predicted for narrowly polydisperse colloidal mixtures with N different particle species, corresponding the eigenvalues of the $N \times N$ particle diffusivity matrix. However, since the various exchange modes between different particle species cannot be resolved experimentally when the particle distribution is narrow, only two decay modes for $g^{(1)}(\boldsymbol{q},\tau)$, corresponding to long-time self and gradient diffusion, are prominent. As a result, the working model equation for DLS in a narrowly polydisperse colloidal mixture is identical to eqn (23), (58), and (59). Since D_+ is enhanced with increasing ϕ, the gradient term $1/(1+B)\,exp(-q^2D_+\tau)$ in eqn (23) at high ϕ decays quickly, revealing the slowly decaying self term $B/(1+B)\,exp(-q^2D_-\tau)$ when $\tau \gg 1/(q^2D_+)$. For some

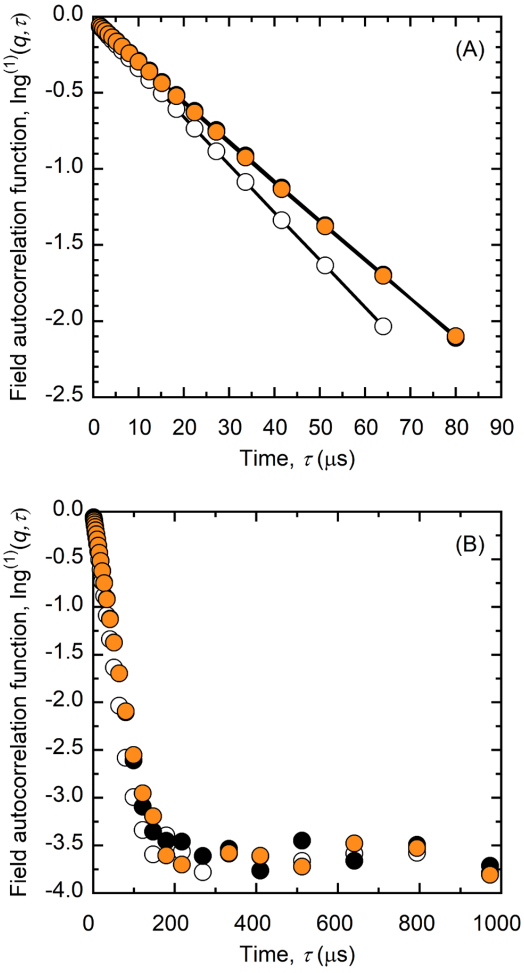

Fig. 6. Logarithm of the normalized field autocorrelation function $g^{(1)}(q,\tau)$ plotted as a function of time delay τ over 80 μs (A) and 1000 μs (B) for $C_{12}E_{10}$/water (open), $C_{12}E_{10}$/decane/water (black), and $C_{12}E_{10}$/limonene/water (orange) mixtures with $C_s = 200$mM, and $C_a/C_s = 0.2$ for ternary mixtures. The solid lines in (A) provide a guide for the eye, and error bars have been omitted for clarity.

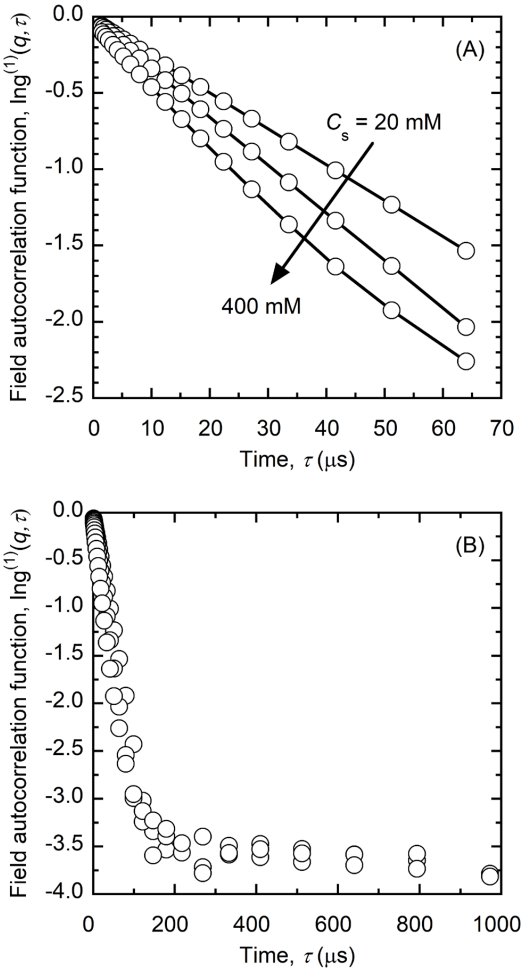

Fig. 7. The logarithm of the normalized field autocorrelation function $g^{(1)}(q,\tau)$ is plotted as a function of the time delay τ over 65 μs (A) and 1000 μs (B) for binary $C_{12}E_{10}$ (s)/water mixtures with $C_s = 20,\ 200$, and 400 mM. The solid lines in (A) provide a guide for the eye, and error bars have been omitted for clarity.

systems, such as ternary water–in–oil microemulsions of AOT/water/octane,[40] two decay modes (slopes) are distinct in a plot of $ln\{g^{(1)}(q,\tau)\}$ versus τ, which enables a robust fit using eqn (23). However, as shown in Fig. 6B and 7B, two modes are not evident for the $C_{12}E_{10}$/water system, even when $\phi = 0.53$. Measurement noise appears to overtake the signal before the self mode can establish itself, preventing access to the long–time self diffusivity predicted by eqn (58). Hence, in this study, we found our data could be more robustly analyzed using the method of cumulants (eqn (120)), in lieu of a multiexponential fit, even at high concentrations.

5.4 Diffusion coefficients measured by DLS for $C_{12}E_{10}$/solute/water mixtures

In this section, DLS diffusivities, acquired using the method of cumulants for ternary, nonionic micellar solutions with hydrophobic solutes, are compared with theory for gradient diffusion in dilute and concentrated monodisperse colloidal dispersions. As discussed in section 4.5, the mode amplitude ratio $B = 0$ for locally monodisperse micellar solutions, so that eqn (59), (66), and (122) combine to provide the following

$$D_{DLS} = D_t^0\{1 + (\beta + S)\phi\}\,. \qquad (143)$$

Eqn (143) indicates that DLS measurements, analyzed via the method of cumulants, are predicted to yield micelle gradient diffusion coefficients. For concentrated hard sphere dispersions, the gradient diffusion coefficient D_c can be expressed via the following form of the generalized Stokes-Einstein equation,[26,41,42]

$$\frac{D_c}{D^0} = \frac{K(\phi)}{S^I(0,\phi)} = K(\phi)\phi\left(\frac{\partial\mu}{\partial\phi}\right)_{T,\mu_n}\,. \qquad (144)$$

Here, $S^I(0,\phi)$ is the ideal static structure factor in the low wavevector limit and $K(\phi) = \langle U\rangle/U^0$ is the sedimentation coefficient for randomly dispersed particles. $K(\phi)$ is defined as the ratio of the ensemble averaged sedimentation velocity $\langle U\rangle$ of a particle dispersion, moving in response to a uniform force field, divided by the velocity U^0 of a single, isolated particle. Rigorous theoretical results for $K(\phi)$, applicable to dilute mixtures of colloidal hard spheres, have been derived accounting for pairwise[43] and three-body[44] hydrodynamic interactions. For concentrated hard sphere dispersions, numerical simulations that include many-body hydrodynamic interactions have also been performed to determine $K(\phi)$ using either Stokesian dynamics[45] or the lattice Boltzmann method.[46]

In Fig. 8A, normalized gradient diffusion coefficients D_{DLS}/D^0_{DLS} are plotted versus ϕ for $C_{12}E_{10}$/water, and for $C_{12}E_{10}$/limonene/water, and $C_{12}E_{10}$/limonene/decane[7] mixtures with $C_a/C_s = 0.2$. The experimental values are compared with dilute theory by Batchelor[26] (solid line), *i.e.*, using eqn (59), (66), and (122) with $\beta + S = 1.45$, for monodisperse hard sphere dispersions. In addition, D_{DLS}/D^0_{DLS} values are plotted as a function of ϕ in Fig. 8B for binary $C_{12}E_{10}$/water mixtures up to $\phi = 0.53$, superimposed with numerical results for concentrated monodisperse hard sphere suspensions. Micelle volume fractions were calculated using

$$\phi = C_a\bar{V}_a + C_s(\bar{V}_s + n_H\bar{V}_w)\,, \qquad (145)$$

where the molar volumes for the solute (a) and water (w) are given by $\bar{V}_a = MW_a/\rho_a$ and $\bar{V}_w = MW_w/\rho_w$, respectively, with MW_a, MW_w, ρ_a, and ρ_w indicating the respective molecular weights and pure component densities. The dry $C_{12}E_{10}$ surfactant molar volume was interpolated from density data for

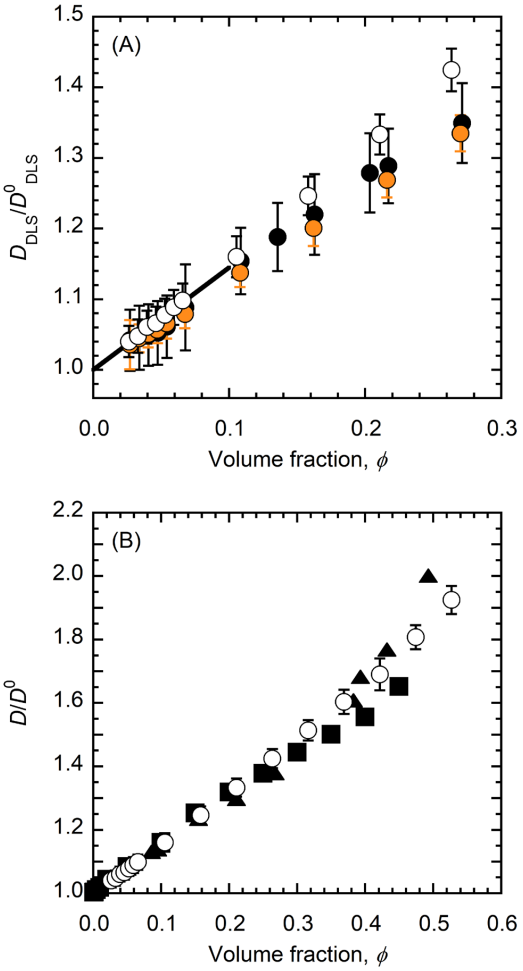

Fig. 8. (A) Normalized diffusion coefficients for $C_{12}E_{10}$/water (open circles), $C_{12}E_{10}$/decane/water[7] (black circles), and $C_{12}E_{10}$/limonene/water (orange circles) with $C_a/C_s = 0.2$ as a function of volume fraction, superimposed with theoretical predictions by Bachelor[26] for dilute, monodisperse hard-sphere dispersions (solid line). (B) Normalized diffusion coefficients for concentrated $C_{12}E_{10}$/water mixtures (open circles) with numerical simulation results for crowded hard sphere dispersions calculated using Stokesian Dynamics[45] (squares) and the Lattice Boltzmann method[46] (triangles). Error bars indicate 95% confidence intervals.

a homologous series of $C_{12}E_m$ surfactants.[30] Molar volume calculations for decane, limonene, dry $C_{12}E_{10}$ surfactant, and water yield $\overline{V}_a = 1.949 \times 10^{-4}\ mM^{-1}$, $\overline{V}_a = 1.622 \times 10^{-4}\ mM^{-1}$, $\overline{V}_s = 5.968 \times 10^{-4}\ mM^{-1}$, and $\overline{V}_w = 1.802 \times 10^{-5}\ mM^{-1}$, respectively. In addition, the conversion factor $6.022 \times 10^{-4}\ (nm^3/molecule)/mM$ was used in this work to convert between molecular and molar volume.

Numerical calculations were performed using the Carnahan-Starling equation[34] for the ideal static structure factor in eqn (144), and results for $K(\phi)$ were determined from numerical simulations via either Stokesian dynamics[45] (squares) or the lattice Boltzmann method method[46] (triangles). As shown in Fig. 8, solute-free, decane-containing, and limonene-containing $C_{12}E_{10}$ micelles diffused as hard spheres in accordance with the most rigorous theoretical results available for gradient diffusion in dilute and concentrated colloidal hard sphere dispersions. Furthermore, as noted by others,[46,47] Batchelor's dilute theory[26] provides an excellent approximation for D_c/D^0 for concentrated monodisperse hard sphere dispersions up to $\phi \approx 0.4$, indicating a near cancellation of higher order, many body hydrodynamic and thermodynamic virial contributions.

5.5 Rayleigh ratios for $C_{12}E_{10}$/solute/water mixtures

Neglecting local micelle polydispersity, theoretical predictions for the Rayleigh ratio for binary $C_{12}E_{10}$/water and ternary $C_{12}E_{10}$/solute/water mixtures were calculated using eqn (68) and (69) with $V_{hs} = 2.19\text{nm}^{-3}$, $V_a = 0.32\text{nm}^{-3}$ (decane) or 0.26nm^{-3} (limonene), and $\lambda_0 = 633\text{nm}$. The refractive indices were determined via $n = (\partial n/\partial\phi)_{p,T,C_a/C_s}\phi + n_0$ with $n_0 = 1.33$ and $(\partial n/\partial\phi)_{p,T,C_a/C_s} = 0.063,\ 0.064$, and 0.065 for solute-free, decane and limonene containing micelles, respectively. Average micelle volumes were calculated from DLS data using $V_{i^*} = 4/3\,\pi R_{DLS}{}^3$, where hydrodynamic radii for solute-free, decane, and limonene-containing micelles are given by $R_{DLS} = 3.75$ nm, 4.25 nm, and 4.04 nm, respectively.

In Fig. 9, R_{90} results for $C_{12}E_{10}$/water (open circles), $C_{12}E_{10}$/decane/water (black), and $C_{12}E_{10}$/limonene/water (orange) mixtures are compared with these theoretical

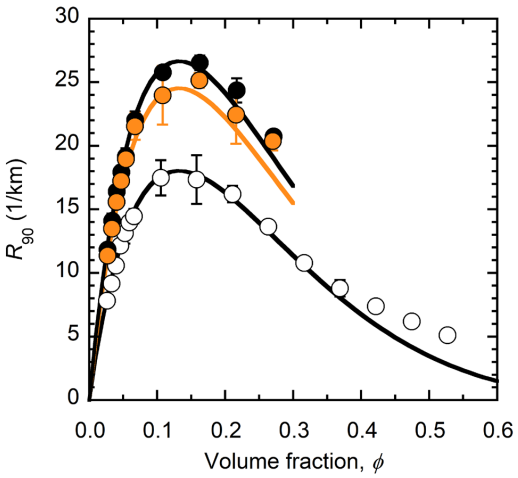

Fig. 9. Rayleigh ratios plotted versus ϕ for $C_{12}E_{10}$/water (open circles) and $C_{12}E_{10}$/decane/water (black) and $C_{12}E_{10}$/limonene/water (orange) mixtures with $C_a/C_s = 0.2$. Theoretical predictions calculated using eqn (68) and (69) for binary and ternary solutions are shown as solid curves. Error bars indicate two standard deviations.

predictions derived using thermodynamic fluctuation theory (solid lines) as a function of ϕ. As shown, the experimental data for both binary and ternary mixtures is in excellent agreement with theoretical predictions up to $\phi = 0.3$, indicating that $C_{12}E_{10}$ micelles interacted as hard spheres, regardless of the presence of decane or limonene solubilizate. These results are consistent with those reported for similar systems, including $C_{12}E_8$/water[48] and $C_{12}E_5$/decane/water.[11]

5.6 Effect of crowding on micelle hydration

As shown in Fig. 10, eqn (68) and (69) appear to underestimate R_{90} for binary aqueous $C_{12}E_{10}$ mixtures when $\phi > 0.3$, to an extent that increases with increasing ϕ. To explain this effect, we note that micelle dehydration has been observed in aqueous $C_{12}E_8$ solutions at high concentrations $\phi > 0.3$ using NMR,[49] and in dilute aqueous C_8E_5 solutions at high pressures up to 310 MPa via SANS.[50] These results indicate that, unlike hard spheres, hydrated micelles tend to relax the system free energy by reducing their size, and thus the volume fraction of the mixture, via dehydration. In order to capture the influence of dehydration on our theoretical predictions for the Rayleigh ratio, we use thermodynamic fluctuation theory to derive R_{90} for a binary mixture of hydrated surfactant (s) and water with a concentration dependent hydration index $n_H = n_H(T, p, C_s)$ (see Appendix M)

$$R_{90} = \frac{4\pi^2 n^2}{{\lambda_0}^4} \frac{\left(\frac{\partial n}{\partial C_s}\right)_{p,T}^2}{\left[1 + {C_s}^2 \bar{V}_w \left(\frac{\partial n_H}{\partial C_s}\right)_{p,T}\right]} \frac{C_s m_0}{N_A} \left\{\frac{d[C_s Z(\phi)]}{dC_s}\right\}^{-1} . \quad (146)$$

In eqn (146), the refractive index increment is given by

$$\left(\frac{\partial n}{\partial C_s}\right)_{T,p} = \left(\frac{\partial n}{\partial C_s}\right)_{p,T,n_H} + \left(\frac{\partial n}{\partial n_H}\right)_{p,T,C_s} \left(\frac{\partial n_H}{\partial C_s}\right)_{p,T} , \quad (147)$$

and, using eqn (69) for the Carnahan-Starling compressibility factor, we have

$$\frac{d[C_s Z(\phi)]}{dC_s} = \frac{(1+2\phi)^2 - \phi^3(4-\phi)}{(1-\phi)^4} - {C_s}^2 \bar{V}_w \left(\frac{\partial n_H}{\partial C_s}\right)_{p,T} \frac{(4+4\phi-2\phi^2)}{(1-\phi)^4} , \quad (148)$$

Per eqn (145)–(148), micelle dehydration affects the Rayleigh ratio in several ways via terms involving the hydration index derivative $(\partial n_H/\partial C_s)_{T,p}$. According to Nilsson et al.[49] the hydration index for $C_{12}E_8$ micelles decreases linearly with surfactant concentration with a slope approximately equal to $(\partial n_H/\partial C_s)_{T,p} = -1/20\, mM^{-1}$ when $\phi > 0.3$. Furthermore, n_H is expected to remain unchanged with ϕ at lower concentrations, suggesting one may use eqn (68) and (69) with constant n_H to predict R_{90} for $\phi \leq 0.3$.

Using eqn (145)–(148) with $\bar{V}_s = 5.968 \times 10^{-4}\, mM^{-1}$, $\bar{V}_w = 1.802 \times 10^{-5}\, mM^{-1}$, $(\partial n/\partial C_s)_{T,p} \approx (\partial n/\partial C_s)_{T,p,n_H} = 8.24 \times 10^{-5}\, mM^{-1}$, $(\partial n_H/\partial C_s)_{T,p} = -1/20\, mM^{-1}$, $m_0 = 103$, and $n_H = 50 - C_s/20$, in accordance with refractive index data by us and NMR data by Nilsson et al.,[49] theoretical predictions for Rayleigh ratios and volume fractions for binary aqueous $C_{12}E_{10}$ solutions were re-calculated and plotted against the new values for $\phi > 0.3$ in Fig. 10. As shown, good agreement is achieved, indicating dehydration is a likely explanation for the discrepancy in R_{90} between our data for binary $C_{12}E_{10}$/water mixtures and monodisperse hard sphere theory. In addition, we note that dehydration does not significantly affect the slope of the normalized solute-free DLS diffusivities shown in Fig. 8B, since values for ϕ and D^0 corrected for dehydration are reduced and enhanced, respectively, causing the DLS data points above $\phi > 0.3$ in Fig. 8A to shift left and down.

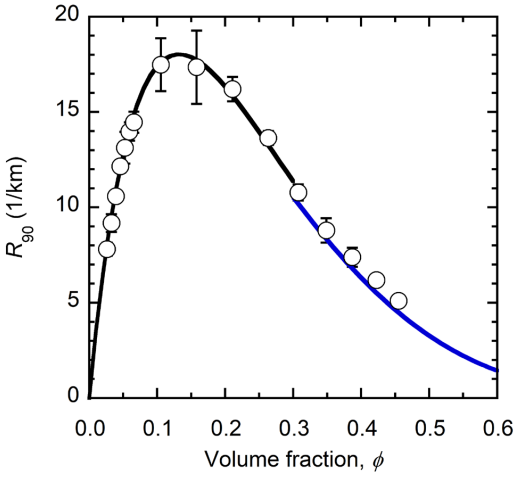

Fig. 10. Rayleigh ratios for binary, aqueous $C_{12}E_{10}$ solutions plotted versus the micelle volume fraction. Values for $\phi > 0.3$ were calculated assuming linear dehydration according to $n_H = 50 - C_s/20$, where C_s has (mM) units. Theoretical predictions indicated by the solid curves were calculated using either eqn (68) and (69) (black curve) or eqn (145)–(148) (blue curve).

6 Conclusions

The self-assembled nature of aqueous micellar solutions comprised of nonionic surfactants and hydrophobic solutes may drive strong micelle growth as these molecules reassemble in response to variations in composition, thereby distinguishing these mixtures from rigid particle dispersions. These effects were previously demonstrated to have a strong effect on the ternary diffusivity matrix $[\mathbf{D}]$, via the microstructure function $M(\phi, C_a/C_s)$. In this work, however, micelle growth effects are shown to have no influence on the either the Rayleigh ratio or the field correlation function in the limit of zero local micelle polydispersity. These results suggest that light scattering theory, developed for monodisperse, colloidal hard sphere dispersions, applies to narrowly polydisperse, ternary solutions comprised of solute-containing micelles. Furthermore, rigorous

theoretical results in the tracer limit for the thermodynamic derivatives, eigenmodes, and the driving forces for diffusion, display the influence of micelle growth/self-assembly effects and show that the diffusional transport processes, which occur during light scattering measurements, are different from those of binary, monodisperse colloidal dispersions comprised of rigid spheres.

Conflicts of interest

There are no conflicts of interest to declare.

Appendix A: Derivation for the total entropy fluctuation δS_T and symmetry relation for $[\mathbf{G}]$

In this section the total entropy fluctuation δS_T, given by eqn (7)–(9), is derived for an n-component mixture at constant temperature and volume using either the Gibbs thermodynamic framework at constant pressure, corresponding to typical experimental conditions, or, equivalently, the McMillan-Mayer framework at constant solvent chemical potential, which defines the chemical potential fluctuations of a mixture with a force-free solvent. We begin with eqn (7)

$$-2T\delta S_T = \sum_{i=1}^{n} \delta\mu_i \delta N_i = \sum_{i=1}^{n-1} \delta\mu_i \delta N_i + \delta\mu_n \delta N_n \ . \qquad (A.1)$$

According to the Gibbs framework, the total fluctuation differential of the extensive Gibbs free energy is given by

$$\delta g = -S\delta T + V\delta p + \sum_{i=1}^{n-1} \mu_i \delta N_i + \mu_n \delta N_n \ , \qquad (A.2)$$

and the chemical potentials are defined as

$$\mu_i = \left(\frac{\partial g}{\partial N_i}\right)_{p,T,N_{k\neq i}} \quad for\ i = 1,2,\dots,n. \qquad (A.3)$$

and N_i is the number of moles of component i. Furthermore, using the constant volume constraint, we have

$$\delta V = \sum_{i=1}^{n} \bar{V}_i \delta N_i = \sum_{i=1}^{n-1} \bar{V}_i \delta N_i + \bar{V}_n \delta N_n = 0 \ , \qquad (A.6)$$

where $\bar{V}_i$ is the molar volume of species i, which is assumed to be constant. Solving for the fluctuation δN_n in eqn (A.6) provides

$$\delta N_n = -\sum_{i=1}^{n-1} \frac{\bar{V}_i}{\bar{V}_n} \delta N_i \ . \qquad (A.7)$$

Eqn (A.1), (A.5), and (A.7), combine to yield

$$\sum_{i=1}^{n} \delta\mu_i \delta N_i = \sum_{i=1}^{n-1} \left(\delta\mu_i - \frac{\bar{V}_i}{\bar{V}_n}\delta\mu_n\right) \delta N_i \ . \qquad (A.8)$$

Now, using the Gibbs-Duhem relation at constant temperature, pressure, and volume, we have

$$\sum_{j=1}^{n} N_j \delta\mu_j = \sum_{j=1}^{n-1} N_j \delta\mu_j + N_n \delta\mu_n = 0 \ . \qquad (A.9)$$

Solving for the solvent fluctuation $\delta\mu_n$ in eqn (A.9) provides

$$\delta\mu_n = -\sum_{j=1}^{n-1} \frac{V}{V}\frac{N_j}{N_n}\delta\mu_j = -\sum_{j=1}^{n-1} \frac{C_j}{C_n}\delta\mu_j \ . \qquad (A.10)$$

Eqn (A.8) and (A.10) combine with the solvent volume fraction $C_n\bar{V}_n = 1 - \phi$ to provide

$$\sum_{i=1}^{n} \delta\mu_i \delta N_i = \sum_{i=1}^{n-1} \left(\delta\mu_i + \frac{\bar{V}_i}{1-\phi}\sum_{j=1}^{n-1} C_j \delta\mu_j\right) \delta N_i \ . \qquad (A.11)$$

At constant temperature and pressure, the species chemical potentials $\mu_i = \mu_i(T, p, C_k, \dots, C_{n-1})$ are expanded via the chain rule

$$\delta\mu_i = -\sum_{k=1}^{n-1} \left(\frac{\partial\mu_i}{\partial C_k}\right)_{p,T,N_{i\neq k}} \delta C_k \ , \qquad (A.12)$$

and eqn (A.11) and (A.12) combine to give

$$-2T\delta S_T = V \sum_{i=1}^{n-1}\sum_{k=1}^{n-1} G_{ik}\delta C_i \delta C_k \ , \qquad (A.13)$$

where

$$G_{ik} = \left(\frac{\partial\mu_i}{\partial C_k}\right)_{p,T,C_{i\neq k}} + \frac{\bar{V}_i}{1-\phi}\sum_{j=1}^{n-1} C_j \left(\frac{\partial\mu_j}{\partial C_k}\right)_{p,T,C_{i\neq k}}$$
$$for\ i,k = 1,2,\dots,n-1 \ . \qquad (A.14)$$

Now, using the McMillan-Mayer framework, we will first show that $[\mathbf{G}]$ is symmetric, followed by a derivation for the total entropy fluctuation δS_T. The extensive McMillan-Mayer free energy for an n-component mixture is given by a Legendre transform of the Helmholtz free energy $A(V, T, N_1, \dots, N_n)$.[51,52]

$$\tilde{F}(V, T, N_1, \dots, N_{n-1}, \bar{\mu}_n) = A(V, T, N_1, \dots, N_n) - N_n\bar{\mu}_n \ , \qquad (A.15)$$

and the total fluctuation differential of $\tilde{F}$ is given by

$$\delta\tilde{F} = -S\delta T - p\delta V + \sum_{i=1}^{n-1} \mu_i \delta N_i - N_n \delta\mu_n \ , \qquad (A.16)$$

where the chemical potential of component i at constant volume is defined according to

$$\mu_i = \left(\frac{\partial\tilde{F}}{\partial N_i}\right)_{T,\mu_n,V,N_{k\neq i}} \quad for\ i = 1,2,\dots,n-1. \qquad (A.17)$$

At constant volume, temperature, and solvent chemical potential, mixed partial derivatives of the McMillan-Mayer free energy are given by

$$\left(\frac{\partial^2 \tilde{F}}{\partial N_k \partial N_i}\right)_{T,\mu_n,V,C_{k\neq i}} = \left(\frac{\partial^2 \tilde{F}}{\partial N_i \partial N_k}\right)_{T,\mu_n,V,C_{k\neq i}}$$
$$for\ i,k = 1,2,\dots,n-1\ . \qquad (A.18)$$

Multiplying eqn (A.18) through and by constant volume V yields

$$\left(\frac{\partial^2 \tilde{F}}{\partial C_k \partial N_i}\right)_{T,\mu_n,V,C_{k\neq i}} = \left(\frac{\partial^2 \tilde{F}}{\partial C_i \partial N_k}\right)_{T,\mu_n,V,C_{k\neq i}}$$
$$for\ i,k = 1,2,\dots,n-1\ , \qquad (A.19)$$

and eqn (A.17) and (A.19) combine to provide

$$\left(\frac{\partial \mu_i}{\partial C_k}\right)_{T,\mu_n,V,C_{k\neq i}} = \left(\frac{\partial \mu_k}{\partial C_i}\right)_{T,\mu_n,V,C_{k\neq i}}$$
$$for\ i,k = 1,2,\dots,n-1\ . \qquad (A.20)$$

Furthermore, at constant V, T, and μ_n, eqn (A.1) reduces to

$$-2T\delta S_T = \sum_{i=1}^{n-1} \delta\mu_i \delta N_i\ . \qquad (A.21)$$

and the species chemical potentials $\mu_i = \mu_i(T,\mu_n,C_k,\dots,C_{n-1})$ are expanded via the chain rule

$$\delta\mu_i = \sum_{k=1}^{n-1} \left(\frac{\partial \mu_i}{\partial C_k}\right)_{T,\mu_n,V,C_{k\neq i}} \delta C_k\ . \qquad (A.22)$$

Eqn (A.21) and (A.22) combine to give

$$-2T\delta S_T = V \sum_{i=1}^{n-1}\sum_{k=1}^{n-1} \left(\frac{\partial \mu_i}{\partial C_k}\right)_{T,\mu_n,V,C_{k\neq i}} \delta C_k\, \delta C_i\ . \qquad (A.23)$$

Finally, combination of eqn (A.13), (A.14), and (A.23) yield

$$G_{ik} = \left(\frac{\partial \mu_i}{\partial C_k}\right)_{T,\mu_n,V,C_{k\neq i}} = \left(\frac{\partial \mu_i}{\partial C_k}\right)_{p,T,C_{i\neq k}} + \frac{\bar{V}_i}{1-\phi}\sum_{j=1}^{n-1} C_j \left(\frac{\partial \mu_j}{\partial C_k}\right)_{p,T,C_{i\neq k}}$$
$$for\ i,k = 1,2,\dots,n-1\ . \qquad (A.25)$$

Appendix B: Diagonalization of $[\mathbf{G}]$

In this section, the modal matrix $[\mathbf{P}]$ for the diffusivity matrix $[\mathbf{D}]$ is shown to diagonalize the chemical potential derivative matrix $[\mathbf{G}]$ via

$$\left[\hat{\boldsymbol{G}}\right] = [\boldsymbol{P}]^T[\boldsymbol{G}][\boldsymbol{P}]\ . \qquad (B.1)$$

To begin, note that for a ternary mixture, the matrix $\left[\hat{\mathbf{G}}\right]$ is diagonal if

$$\hat{G}_{as} = \hat{G}_{sa} = 0. \qquad (B.2)$$

Furthermore, $[\mathbf{G}]$ is symmetric,[32] so that

$$G_{as} = G_{sa}\ . \qquad (B.3)$$

Combining eqn (B.1)–(B.3) provides

$$G_{aa}P_{aa}P_{as} + G_{as}(P_{aa}P_{ss} + P_{as}P_{sa}) + G_{ss}P_{sa}P_{ss} = 0\ . \qquad (B.4)$$

Eqn (B.4) and (31) combine to yield

$$G_{aa}{D_{as}}^2 + G_{as}(D_+ + D_- - 2D_{aa})D_{as} + G_{ss}\{D_+D_- - D_{aa}(D_+ + D_-) + {D_{aa}}^2\} = 0\ . \qquad (B.5)$$

The following relations for the trace

$$D_+ + D_- = D_{aa} + D_{ss}\ . \qquad (B.6)$$

and the determinant

$$D_+D_- = D_{ss}D_{aa} - D_{as}D_{sa}. \qquad (B.7)$$

of $[\mathbf{D}]$ are then combined with eqn (B.5) to give

$$D_{aa}G_{as} + D_{sa}G_{ss} = G_{aa}D_{as} + G_{as}D_{ss}\ , \qquad (B.8)$$

which is the Onsager Reciprocal relation.[32] Hence, eqn (B.2) is satisfied and $\left[\hat{\mathbf{G}}\right]$ is diagonal.

Appendix C: Derivation for B and R_{90} for a multicomponent mixture at constant temperature and pressure

In this section, we begin with eqn (15), generalized for an n-component mixture at constant temperature and pressure

$$P(\delta\boldsymbol{x}) = {\Omega_0}^{-1} exp\left\{-\frac{V}{2k_BT}\left(\sum_{i=1}^{n-1}\hat{G}_i{\delta\hat{C}_i}^2\right)\right\}\ . \qquad (C.1)$$

Using the product rule for exponents, we can write

$$P(\delta\boldsymbol{x}) = P_1(\delta\hat{C}_1)P_2(\delta\hat{C}_2)\cdots P_{n-1}(\delta\hat{C}_{n-1})\ , \qquad (C.2)$$

where,

$$P_i(\delta\hat{C}_i) = {\Omega_i}^{-1} e^{\left(-\frac{V}{2k_BT}\hat{G}_i{\delta\hat{C}_i}^2\right)}\ . \qquad (C.3)$$

Eqn (C.2) and (C.3) indicate that the decoupled concentration fluctuations $\delta\hat{C}_i$ are statistically uncorrelated with a fluctuation probability $P_i(\delta\hat{C}_i)$ that obeys a Gaussian distribution. The constants Ω_i are determined via integration of the fluctuation probability over all possible fluctuations,

$$\Omega_i = \langle\delta\hat{C}_i\rangle = \int_{-\infty}^{\infty} d\left(\delta\hat{C}_i\right) e^{\left(-\frac{V}{2k_BT}\hat{G}_i{\delta\hat{C}_i}^2\right)} = \left(\frac{2\pi k_BT}{V\hat{G}_i}\right)^{\frac{1}{2}}\ , \qquad (C.4)$$

Using eqn (C.3), the mean square fluctuation in concentration is given by

$$\langle \delta\hat{C}_i{}^2 \rangle = \int_{-\infty}^{\infty} d\left(\delta\hat{C}_i\right)\delta\hat{C}_i{}^2 P_i\left(\delta\hat{C}_i\right)$$
$$= \Omega_i{}^{-1} \int_{-\infty}^{\infty} d\left(\delta\hat{C}_i\right)\delta\hat{C}_i{}^2 e^{\left(-\frac{V}{2k_BT}\hat{G}_i\delta\hat{C}_i{}^2\right)}$$
$$= \Omega_i{}^{-1}\left(\frac{2\pi k_BT}{V\hat{G}_i}\right)^{\frac{1}{2}}\frac{k_BT}{V\hat{G}_i} \ , \qquad (C.5)$$

and eqn (C.4) and (C.5) combine to yield

$$\langle \delta\hat{C}_i{}^2 \rangle = \frac{k_BT}{V\hat{G}_i} \ . \qquad (C.6)$$

In order to determine the field correlation function, given by eqn (19), we expand the total fluctuation of the local dielectric constant $\varepsilon = \varepsilon\left(T, p, \hat{C}_1, \hat{C}_i, \ldots \hat{C}_{n-1}\right)$, expressed here as function of thermodynamic variables, using the chain rule

$$\delta\varepsilon(\boldsymbol{q}, t) = \sum_{i=1}^{n-1}\left(\frac{\partial\varepsilon}{\partial\hat{C}_i}\right)_{T,p}\delta\hat{C}_i(\boldsymbol{q}, t) \ , \qquad (C.7)$$

where, $\delta\hat{C}_i(\boldsymbol{q}, t)$ is the Fourier transform of the decoupled local concentration fluctuation $\delta\hat{C}_i(\boldsymbol{z}, t)$, given by

$$\delta\hat{C}_i(\boldsymbol{q}, t) = \frac{1}{V}\int d^3\boldsymbol{z}\, e^{i\boldsymbol{q}\cdot\boldsymbol{z}}\delta\hat{C}_i(\boldsymbol{z}, t) \ . \qquad (C.8)$$

The time correlation function for fluctuations in ε is given by

$$\langle\delta\varepsilon^*(\boldsymbol{q}, 0)\delta\varepsilon(\boldsymbol{q}, t)\rangle$$
$$= \sum_{i=1}^{n-1}\sum_{j=1}^{n-1}\left(\frac{\partial\varepsilon}{\partial\hat{C}_i}\right)_{T,p}\left(\frac{\partial\varepsilon}{\partial\hat{C}_j}\right)_{T,p}\langle\delta\hat{C}_i^*(\boldsymbol{q}, 0)\delta\hat{C}_j(\boldsymbol{q}, t)\rangle \ . \qquad (C.9)$$

per eqn (C.2), the concentration fluctuations $\delta\hat{C}_i(\boldsymbol{q}, t)$ are statistically uncorrelated, so that

$$\langle\delta\hat{C}_i^*(\boldsymbol{q}, 0)\delta\hat{C}_j(\boldsymbol{q}, t)\rangle = \langle\delta\hat{C}_i^*(\boldsymbol{q}, 0)\delta\hat{C}_j(\boldsymbol{q}, t)\rangle\delta_{ij} \ , \qquad (C.10)$$

where δ_{ij} is the Kronecker delta. Eqn (C.9), (C.10), and (22) combine to yield

$$\langle\delta\varepsilon^*(\boldsymbol{q}, 0)\delta\varepsilon(\boldsymbol{q}, t)\rangle$$
$$= \sum_{i=1}^{n-1}\left(\frac{\partial\varepsilon}{\partial\hat{C}_i}\right)_{T,p}^2\langle\delta\hat{C}_i^*(\boldsymbol{q}, 0)\delta\hat{C}_i(\boldsymbol{q}, 0)\rangle exp\left(-q^2\hat{D}_it\right) \ . \qquad (C.11)$$

Setting $t = 0$ and using eqn (C.8) with (C.11), we can write

$$\langle\delta\hat{C}_i^*(\boldsymbol{q}, 0)\delta\hat{C}_i(\boldsymbol{q}, 0)\rangle$$
$$= \langle\frac{1}{V}\int d^3\boldsymbol{z}\, e^{-i\boldsymbol{q}\cdot\boldsymbol{z}}\delta\hat{C}_i(\boldsymbol{z}, 0)\frac{1}{V}\int d^3\boldsymbol{z}\, e^{i\boldsymbol{q}\cdot\boldsymbol{z}}\delta\hat{C}_i(\boldsymbol{z}, 0)\rangle$$
$$= \langle\left(\frac{1}{V}\int d^3\boldsymbol{z}\,\delta\hat{C}_i(\boldsymbol{z}, 0)\right)^2\rangle$$
$$= \langle\delta\hat{C}_i{}^2\rangle \ , \qquad (C.12)$$

and eqn (C.6), (C.11), and (C.12) combine to provide

$$\langle\delta\varepsilon^*(\boldsymbol{q}, 0)\delta\varepsilon(\boldsymbol{q}, t)\rangle = \sum_{i=1}^{n-1}\left(\frac{\partial\varepsilon}{\partial\hat{C}_i}\right)_{T,p}^2\frac{k_BT}{V\hat{G}_i}exp\left(-q^2\hat{D}_it\right) \ . \qquad (C.13)$$

For a non-magnetic, non-absorbing material, the solution refractive index is related to the dielectric constant via $\varepsilon = n^2$, so that eqn (C.13) becomes

$$\langle\delta\varepsilon^*(\boldsymbol{q}, 0)\delta\varepsilon(\boldsymbol{q}, t)\rangle = 4n^2\sum_{i=1}^{n-1}\hat{R}_i{}^2\frac{k_BT}{V\hat{G}_i}exp\left(-q^2\hat{D}_it\right) \ , \qquad (C.14)$$

where the refractive index increments are given by $\hat{R}_i = \left(\partial n/\partial\hat{C}_i\right)_{T,\boldsymbol{p}}$. Eqn (19) and (C.14) combine to yield the field correlation function for a n-component mixture at constant temperature and pressure

$$g^{(1)}(\boldsymbol{q}, t) = \frac{\langle\delta\varepsilon^*(\boldsymbol{q}, 0)\delta\varepsilon(\boldsymbol{q}, t)\rangle}{\langle|\delta\varepsilon(\boldsymbol{q}, 0)|^2\rangle} = \sum_{i=1}^{n-1}\left\{\frac{exp\left(-q^2\hat{D}_it\right)}{\sum_{j=1}^{n-1}\left(\frac{\hat{R}_j}{\hat{R}_i}\right)^2\frac{G_i}{\hat{G}_j}}\right\} . \qquad (C.15)$$

For a ternary mixture ($n = 3$), eqn (C.15) reduces to

$$g^{(1)}(q, t) = \left(\frac{B}{1+B}\right)exp\left(-q^2\hat{D}_1t\right) + \left(\frac{1}{1+B}\right)exp\left(-q^2\hat{D}_2t\right), \qquad (C.16)$$

where the mode amplitude ratio equals

$$B = \left(\frac{\hat{R}_1}{\hat{R}_2}\right)^2\left(\frac{\hat{G}_2}{\hat{G}_1}\right) \ . \qquad (C.17)$$

In order determine the Rayleigh ratio R_{90} for an n-component mixture at constant temperature and pressure, we combine eqn (34) and (C.14) and set $t = 0$, $\varepsilon^2 = n^4$, and $k_f \approx 2\pi n/\lambda_0$ to provide

$$R_{90} = \frac{I(\boldsymbol{q})L^2}{I_0V} = \frac{4\pi^2n^2}{\lambda_0{}^4}\sum_{i=1}^{n-1}\hat{R}_i{}^2\frac{k_BT}{V\hat{G}_i} \ . \qquad (C.18)$$

For a ternary mixture ($n = 3$), we have

$$R_{90} = \frac{4\pi^2n^2}{\lambda_0{}^4}\hat{R}_2{}^2\left(\frac{k_BT}{\hat{G}_2}\right)(1+B) \ . \qquad (C.19)$$

Appendix D: Refractive index increments

The solution refractive index for a ternary, single phase mixture can be defined as a function of four independent, intensive variables $n = n(T, p, C_a, C_s) = n(T, p, C_a/C_s, \phi)$.[53] Thus, at constant temperature T and pressure p, which are the typical conditions under which measurements are performed, the total differential of the solution refractive index is given by

$$dn = \left(\frac{\partial n}{\partial C_a}\right)_{p,T,C_s}dC_a + \left(\frac{\partial n}{\partial C_s}\right)_{p,T,C_a}dC_s$$
$$= \left\{\frac{\partial n}{\partial(C_a/C_s)}\right\}_{p,T,\phi}d\left(\frac{C_a}{C_s}\right) + \left(\frac{\partial n}{\partial\phi}\right)_{p,T,C_a/C_s}d\phi \ . \qquad (D.1)$$

Total differentials for the solute to surfactant molar ratio and the volume fraction are given by

$$d\left(\frac{C_a}{C_s}\right) = \frac{1}{C_s}dC_a - \frac{C_a}{{C_s}^2}dC_s \qquad (D.2)$$

and

$$d\phi = \bar{V}_a dC_a + \bar{V}_{hs} dC_s \ . \qquad (D.3)$$

Combining eqn (D.1)–(D.3) yields,

$$R_a = \bar{V}_a \left(\frac{\partial n}{\partial \phi}\right)_{p,T,C_a/C_s} + \frac{1}{C_s}\left\{\frac{\partial n}{\partial (C_a/C_s)}\right\}_{p,T,\phi} \qquad (D.4)$$

and

$$R_s = \bar{V}_{hs} \left(\frac{\partial n}{\partial \phi}\right)_{p,T,C_a/C_s} - \frac{\bar{V}_{hs}\, C_a/C_s}{(\phi - \phi_a)}\left\{\frac{\partial n}{\partial (C_a/C_s)}\right\}_{p,T,\phi} \ . \qquad (D.5)$$

Appendix E: Local equilibrium relations for multicomponent micellar solutions

Consider an n-component mixture comprised of free water, free molecular solute, hydrated surfactant monomer, and a distribution of N different micelle types, comprised of various numbers of solute and hydrated surfactant molecules. During a typical light scattering measurement, fluctuations in the concentrations of the mixture components occur and then relax by diffusion. As diffusion occurs, it is assumed the local equilibrium is achieved on a time scale much faster than that of diffusion. Hence, one may define the total free energy minimum for a mixture within a fixed, local control volume (sometimes described as material point) at constant temperature T and pressure p. The re-equilibration process via self-assembly occurs very quickly, therefore, the system may be considered isolated (no mass or energy transfer into or out of the material point) on the time scale of equilibration. Hence, the total molar Gibbs free energy differential at constant volume, temperature and pressure, is given by

$$dg = \mu_a dC_{a,free} + \mu_s dC_{mon} + \mu_n dC_n + \sum_{k=0}^{N-1} \mu_k dC_k = 0 \ , \quad (E.1)$$

where $C_{a,free}$, C_{mon}, C_n, and C_k are molar concentrations for free solute, hydrated surfactant, solvent, and micelles of type k, respectively.

For an incompressible fluid at constant volume, we have

$$\bar{V}_a dC_{a,free} + \bar{V}_{hs} dC_{mon} + \bar{V}_n dC_n + \sum_{k=0}^{N-1} \bar{V}_k dC_k = 0 \ . \qquad (E.2)$$

Here, $\bar{V}_n$ is the partial molar volume of the solvent. Solving eqn (E.2) for dC_n yields,

$$dC_n = -\frac{\bar{V}_a}{\bar{V}_n} dC_{a,free} - \frac{\bar{V}_{hs}}{\bar{V}_n} dC_{mon} - \sum_{k=0}^{N-1} \frac{\bar{V}_k}{\bar{V}_n} dC_k = 0 \ . \qquad (E.3)$$

The total concentrations of solute (a) and surfactant (s) are conserved, so that

$$dC_a = dC_{a,free} + \sum_{k=0}^{N-1} n_k dC_k = 0 \qquad (E.4)$$

and

$$dC_s = dC_{mon} + \sum_{k=0}^{N-1} m_k dC_k = 0 \ . \qquad (E.5)$$

Combining eqn (E.1) and (E.3)–(E.5) yields

$$\mu_k - n_k \mu_a - m_k \mu_s = \bar{V}_k - n_k \bar{V}_a - m_k \bar{V}_{hs} \ . \qquad (E.6)$$

Since the molar volume of a micelle type k is given by $\bar{V}_k = n_k \bar{V}_a + m_k \bar{V}_{hs}$, eqn (E.6) yields

$$\mu_k = n_k \mu_a + m_k \mu_s$$
$$for\ k = 0,1,\dots,N-1 \ . \qquad (E.7)$$

In eqn (E.7) the chemical potentials are not uniquely defined, and may be expressed, for instance, according to

$$\mu_k = \left(\frac{\partial g}{\partial C_k}\right)_{p,T,C_{i\neq k}} = \left(\frac{\partial \tilde{F}}{\partial C_k}\right)_{T,\mu_n,V,C_{i\neq k}} = \left(\frac{\partial A}{\partial C_k}\right)_{T,V,C_{i\neq k}} \ , \quad (E.8)$$

where $\tilde{F}$ and A are the extensive McMillan-Mayer and Helmholtz free energies, respectively.

Appendix F: Osmotic pressure derivatives

Mixtures of nonionic surfactants and hydrophobic solutes can be modelled as either ternary, single phase mixtures comprised of solute, surfactant, and solvent, or as n-component mixtures of free molecular solute, monomer surfactant, and a distribution of aggregates, containing various numbers of solute and surfactant molecules. Hence, the osmotic pressure of these mixtures can be defined as a function of either four or $n+1$ independent, intensive variables according to $\Pi = \Pi(T, \mu_n, C_a, C_s) = \Pi(T, \mu_n, C_1, C_2, \dots, C_{n-1})$. Using the chain rule, the gradient in the osmotic pressure can be expanded at constant T, μ_n

$$(\boldsymbol{\nabla}\Pi)_{T,\mu_n} = \left(\frac{\partial \Pi}{\partial C_a}\right)_{T,\mu_n} \boldsymbol{\nabla} C_a + \left(\frac{\partial \Pi}{\partial C_s}\right)_{T,\mu_n} \boldsymbol{\nabla} C_s \ . \qquad (F.1)$$

Eqn (F.1) and the Gibbs-Duhem equation at constant T, μ_n (*cf.* eqn (L.8)) combine to yield

$$\left(\frac{\partial \Pi}{\partial C_a}\right)_{T,\mu_n} \boldsymbol{\nabla} C_a + \left(\frac{\partial \Pi}{\partial C_s}\right)_{T,\mu_n} \boldsymbol{\nabla} C_s = \sum_{j=1}^{n-1} C_j \left(\boldsymbol{\nabla}\mu_j\right)_{T,\mu_n} \ . \qquad (F.2)$$

Similarly, the micelle species chemical potentials can also be expressed as a function of either four or $n+1$ independent, intensive variables, according to $\mu_j = \mu_j(T, \mu_n, C_a, C_s) = \mu_j(T, \mu_n, C_1, C_2, \dots, C_{n-1})$ and the gradients in μ_j can also be expanded using the chain rule at constant T, μ_n

$$\left(\boldsymbol{\nabla}\mu_j\right)_{T,\mu_n} = \left(\frac{\partial \mu_j}{\partial C_a}\right)_{T,\mu_n} \boldsymbol{\nabla} C_a + \left(\frac{\partial \mu_j}{\partial C_s}\right)_{T,\mu_n} \boldsymbol{\nabla} C_s \ . \qquad (F.3)$$

Combination of eqn (F.1)–(F.3) and expansion using the chain rule provides

$$\left(\frac{\partial \Pi}{\partial C_a}\right)_{T,\mu_n} = \sum_{k=1}^{n-1}\sum_{j=1}^{n-1} C_k \left(\frac{\partial \mu_k}{\partial C_j}\right)_{T,\mu_n}\left(\frac{\partial C_j}{\partial C_a}\right) \qquad (F.4)$$

and

$$\left(\frac{\partial \Pi}{\partial C_s}\right)_{T,\mu_n} = \sum_{k=1}^{n-1}\sum_{j=1}^{n-1} C_k \left(\frac{\partial \mu_k}{\partial C_j}\right)_{T,\mu_n}\left(\frac{\partial C_j}{\partial C_s}\right) \qquad (F.5)$$

In this work, the concentrations of free molecular solute and surfactant monomer are vanishingly small, so that eqn (F.4) and (F.5) reduce to summations over N micellar species

$$\left(\frac{\partial \Pi}{\partial C_a}\right)_{T,\mu_n} = \sum_{k=0}^{N-1}\sum_{j=0}^{N-1} C_k \left(\frac{\partial \mu_k}{\partial C_j}\right)_{T,\mu_n}\left(\frac{\partial C_j}{\partial C_a}\right) \qquad (F.6)$$

and

$$\left(\frac{\partial \Pi}{\partial C_s}\right)_{T,\mu_n} = \sum_{k=0}^{N-1}\sum_{j=0}^{N-1} C_k \left(\frac{\partial \mu_k}{\partial C_j}\right)_{T,\mu_n}\left(\frac{\partial C_j}{\partial C_s}\right) \qquad (F.7)$$

Appendix G: Derivation of B and R_{90} for locally monodisperse micelles

In this section, the mode amplitude ratio B, and the Rayleigh ratio R_{90} are derived in the limit as the local micelle polydispersity approaches zero. First, eqn (31)–(33) and (48)–(50) combine to produce the elements of the diagonalized chemical potential derivative matrix $[\widehat{\mathbf{G}}]$

$$C_a\hat{G}_a = \left(\frac{\partial \Pi}{\partial C_a}\right)_{T,\mu_n} + \frac{C_a}{C_s}{P_{sa}}^2\left(\frac{\partial \Pi}{\partial C_s}\right)_{T,\mu_n} - C_s G_{sa}\left(\frac{C_a}{C_s}P_{sa} - 1\right)^2 \qquad (G.1)$$

and

$$C_s\hat{G}_s = \left(\frac{\partial \Pi}{\partial C_s}\right)_{T,\mu_n} + \frac{C_s}{C_a}{P_{as}}^2\left(\frac{\partial \Pi}{\partial C_a}\right)_{T,\mu_n} - C_a G_{sa}\left(\frac{C_s}{C_a}P_{as} - 1\right)^2 \qquad (G.2)$$

In the limit as the local micelle polydispersity approaches zero, $G_{sa} \to -\infty$, so that eqn (24), (60), (65), (G.1) and (G.2) combine to yield the ratio

$$B = 0\ , \qquad (G.3)$$

and eqn (23), (59), and (G.3) provide the field correlation function

$$g^{(1)}(q,\tau) = exp\{-q^2 D_i^0[1 + (\beta + S)\phi]\tau\}\ . \qquad (G.4)$$

Now, turning our focus toward the Rayleigh ratio, a general form for the osmotic pressure in a mixture of monodisperse micelles is given by

$$\frac{\Pi}{N_A k_B T} = C_{tot} Z(\phi)\ , \qquad (G.5)$$

Differentiating eqn (G.5) with respect to either C_a or C_s and combining the results with eqn (60) and (G.2) yields

$$\begin{aligned} {C_s}^2\hat{G}_s = C_a\left(\frac{\partial \Pi}{\partial C_a}\right)_{T,\mu_n} + C_s\left(\frac{\partial \Pi}{\partial C_s}\right)_{T,\mu_n} \\ = C_{tot}N_A k_B T\left\{\left[\frac{\partial Z(\phi)}{\partial lnC_a} + \frac{\partial Z(\phi)}{\partial lnC_s}\right]\right. \\ \left. + Z(\phi)\left(\frac{\partial lnC_{tot}}{\partial lnC_a} + \frac{\partial lnC_{tot}}{\partial lnC_s}\right)\right\} \end{aligned} \qquad (G.6)$$

Differentiation of the total micelle concentration $C_{tot} = C_s/\overline{m}$ provides

$$\frac{\partial lnC_{tot}}{\partial lnC_a} = -\frac{\partial ln\overline{m}}{\partial lnC_a} \qquad (G.7)$$

and

$$\frac{\partial lnC_{tot}}{\partial lnC_s} = 1 - \frac{\partial ln\overline{m}}{\partial lnC_s}\ . \qquad (G.8)$$

As argued in our previous work,[8] if the aggregation number is a univariate function of the solute to surfactant molar ratio C_a/C_s at constant temperature and pressure, then the aggregation number derivatives are related via

$$\frac{\partial ln\overline{m}}{\partial lnC_s} = -\frac{\partial ln\overline{m}}{\partial lnC_a}\ . \qquad (G.9)$$

Hence, eqn (G.7)–(G.9) combine to give

$$\frac{\partial lnC_{tot}}{\partial lnC_a} + \frac{\partial lnC_{tot}}{\partial lnC_s} = 1\ . \qquad (G.10)$$

Furthermore, the compressibility factor derivatives in eqn (G.6) can be expanded using the chain rule, so that

$$\frac{\partial Z(\phi)}{\partial lnC_a} + \frac{\partial Z(\phi)}{\partial lnC_s} = \phi\frac{dZ(\phi)}{d\phi}\left(\frac{\partial ln\phi}{\partial lnC_a} + \frac{\partial ln\phi}{\partial lnC_s}\right)\ . \qquad (G.11)$$

Differentiation of the volume fraction $\phi = C_a\overline{V}_a + C_s\overline{V}_{hs}$ with respect to C_a gives

$$\frac{\partial ln\phi}{\partial lnC_a} = \frac{\phi_a}{\phi}\ . \qquad (G.12)$$

Now, differentiating with respect to C_s and using $C_s\overline{V}_{hs} = \phi - \phi_a$, we have

$$\frac{\partial ln\phi}{\partial lnC_s} = 1 - \frac{\phi_a}{\phi}\ . \qquad (G.13)$$

Hence, eqn (G.12) and (G.13) combine to provide

$$\frac{\partial ln\phi}{\partial lnC_a} + \frac{\partial ln\phi}{\partial lnC_s} = 1\ . \qquad (G.14)$$

Eqn (G.6), (G.10), and (G.14) combine to produce

$$\frac{{C_s}^2\hat{G}_s}{C_{tot}N_A k_B T} = \phi\frac{dZ(\phi)}{d\phi} + Z(\phi) = \frac{d[\phi Z(\phi)]}{d\phi}\ . \qquad (G.15)$$

The diagonalized refractive index increment $\widehat{R}_s$ is evaluated using eqn (28)–(30) and (60)

$$\widehat{R}_s = \frac{\phi}{C_s}\left(\frac{\partial n}{\partial \phi}\right)_{p,T,C_a/C_s} . \qquad (G.16)$$

Finally, eqn (36), (G.3), (G.15), (G.16), and $\phi = N_A\, C_s/m_0\, V_{i^*}$ yield

$$R_{90} = \frac{4\pi^2 n^2}{{\lambda_0}^4}\left(\frac{\partial n}{\partial \phi}\right)^2_{p,T,C_a/C_s} V_{i^*}\phi\left\{\frac{d[\phi Z(\phi)]}{d\phi}\right\}^{-1} . \qquad (G.17)$$

Appendix H: Derivation of the Onsager matrix $[\mathbf{L}]$ for locally monodisperse micelles

The main Onsager coefficient L_{aa} in eqn (74) is derived in this appendix. Eqn (75) and (76) can be derived using a similar approach to provide the complete Onsager matrix $[\mathbf{L}]$. We begin by evaluating the determinant of the chemical potential derivative matrix $[\mathbf{G}]$ using eqn (48)–(50)

$$C_a C_s|\boldsymbol{G}| = \left(\frac{\partial \Pi}{\partial C_a}\right)_{T,\mu_n}\left(\frac{\partial \Pi}{\partial C_s}\right)_{T,\mu_n} - G_{sa}\left\{C_a\left(\frac{\partial \Pi}{\partial C_a}\right)_{T,\mu_n} + C_s\left(\frac{\partial \Pi}{\partial C_s}\right)_{T,\mu_n}\right\} . \qquad (H.1)$$

Eqn (48)–(50), (72) and (G.1) combine in the limit as the local micelle polydispersity approaches zero, so that $G_{sa} \to -\infty$, to produce

$$L_{aa} = \frac{{C_a}^2 D_{aa} + C_a C_s D_{as}}{C_a\left(\frac{\partial \Pi}{\partial C_a}\right)_{T,\mu_n} + C_s\left(\frac{\partial \Pi}{\partial C_s}\right)_{T,\mu_n}} . \qquad (H.2)$$

Per eqn (G.6) and (G.15)

$$C_a\left(\frac{\partial \Pi}{\partial C_a}\right)_{T,\mu_n} + C_s\left(\frac{\partial \Pi}{\partial C_s}\right)_{T,\mu_n} = C_{tot} N_A k_B T\left\{\frac{d[\phi Z(\phi)]}{d\phi}\right\} . \qquad (H.3)$$

Eqn (H.2) and (H.3) combine with $C_a = \bar{n} C_{tot}$ to give

$$L_{aa} = \frac{\bar{n}^2 C_{tot}}{N_A k_B T}\left(D_{aa} + \frac{C_s}{C_a} D_{as}\right)\left\{\frac{d[\phi Z(\phi)]}{d\phi}\right\}^{-1} . \qquad (H.4)$$

For dilute mixtures ($\phi \ll 1$), the compressibility factor derivative for monodisperse hard spheres reduces to

$$\left\{\frac{d[\phi Z(\phi)]}{d\phi}\right\}^{-1} \approx 1 - \beta\phi \qquad (H.5)$$

Where β is the 2nd osmotic virial coefficient. Using eqn (52)–(55), (H.4), and (H.5) we have

$$L_{aa} = \bar{n}^2 C_{tot}\left(\frac{D^0_{i^*}}{N_A k_B T}\right)(1 + S\phi) . \qquad (H.6)$$

This approach may be used to derive the remaining Onsager coefficients, applicable to dilute mixtures:

$$L_{as} = L_{sa} = \bar{n}\bar{m} C_{tot}\left(\frac{D^0_{i^*}}{N_A k_B T}\right)(1 + S\phi) \qquad (H.7)$$

and

$$L_{ss} = \bar{m}^2 C_{tot}\left(\frac{D^0_{i^*}}{N_A k_B T}\right)(1 + S\phi) . \qquad (H.8)$$

Appendix I: Derivation for $[\mathbf{G}]$ in the tracer limit

In this section, we provide a detailed derivation for $[\mathbf{G}]$ in the tracer limit, given by eqn (88)–(90). We begin with eqn (49)

$$G_{sa} = \left(\frac{N_A k_B T}{m_0}\right)\left\{\frac{1}{C_a}\frac{\partial ln C_0}{\partial ln C_a} + \sum_{j=0}^{N-1} A_{0j}\left(\frac{\partial C_j}{\partial C_a}\right)\right\} . \qquad (I.1)$$

The derivation in this section is simplified by introducing the following function

$$\tilde{A}_{0j} = (1-\phi)A_{0j} , \qquad (I.2)$$

so that eqn (I.1) can be rewritten as

$$\frac{m_0(1-\phi)G_{sa}}{N_A k_B T} = \frac{(1-\phi)}{C_a}\frac{\partial ln C_0}{\partial ln C_a} + \sum_{j=0}^{N-1}\tilde{A}_{0j}\left(\frac{\partial C_j}{\partial C_a}\right) . \qquad (I.3)$$

The summation in eqn (I.3) is then rearranged, using the product rule, to the following more amenable form:

$$\sum_{j=0}^{N-1}\tilde{A}_{0j}\left(\frac{\partial C_j}{\partial C_a}\right) = \frac{\partial}{\partial C_a}\left(\sum_{j=0}^{N-1} C_j\tilde{A}_{0j}\right) - \sum_{j=0}^{N-1} C_j\left(\frac{\partial \tilde{A}_{0j}}{\partial C_a}\right) . \qquad (I.4)$$

For micelle distributions that are monomodal and narrow, the micelle distribution function can be reasonable approximated using a Kronecker delta distribution function $C_j = C_{tot}\delta_{jj^*}$. According to this definition, C_j is nonzero only when the index $j = j^*$, which denotes a micelle type representative of the distribution mean and characterized as having $\bar{n}$ solutes, $\bar{m}$ surfactants, radius R_{j^*}, and concentration C_{tot}, all of which are functions of composition (C_a/C_s). Inserting the Kronecker distribution into eqn (I.4) yields,

$$\sum_{j=0}^{N-1}\tilde{A}_{0j}\left(\frac{\partial C_j}{\partial C_a}\right) = \frac{\partial}{\partial C_a}\left(\sum_{j=0}^{N-1} C_{tot}\delta_{jj^*}\tilde{A}_{0j}\right) - \sum_{j=0}^{N-1} C_{tot}\delta_{jj^*}\left(\frac{\partial \tilde{A}_{0j}}{\partial C_a}\right) . \qquad (I.5)$$

Using the sifting property, which selects a micelle type j^* from a set of N different micelle types, the summations on the right-hand side of eqn (I.5) are evaluated to give

$$\sum_{j=0}^{N-1}\tilde{A}_{0j}\left(\frac{\partial C_j}{\partial C_a}\right) = \frac{\partial}{\partial C_a}\left(C_{tot}\tilde{A}_{0j^*}\right) - C_{tot}\left(\frac{\partial \tilde{A}_{0j}}{\partial C_a}\right)_{j=j^*} . \qquad (I.6)$$

The derivative $\partial\left(C_{tot}\tilde{A}_{0j^*}\right)/\partial C_a$ in eqn (I.6) can be expanded with the product rule to provide

$$\sum_{j=0}^{N-1} \tilde{A}_{0j}\left(\frac{\partial C_j}{\partial C_a}\right) = \tilde{A}_{0j^*}\frac{\partial C_{tot}}{\partial C_a} + C_{tot}\left\{\frac{\partial \tilde{A}_{0j^*}}{\partial C_a} - \left(\frac{\partial \tilde{A}_{0j}}{\partial C_a}\right)_{j=j^*}\right\} \ . \quad (I.7)$$

In order to determine the first term on the right-hand side of eqn (I.7) we start by combining eqn (46), (85), and (I.2) with $k = 0$ to give

$$\begin{aligned}\tilde{A}_{0j} = \frac{\pi}{6}\{ & {d_0}^3 + {d_j}^3 + {d_0}^3{d_j}^3\eta_0 \\ & + 3d_0d_j\left[d_0(1+d_0\eta_2)\left(1+{d_j}^2\eta_1\right)\right. \\ & \left. + d_j\left(1+d_j\eta_2\right)\left(1+{d_0}^2\eta_1\right)\right] \\ & + 9{d_0}^2{d_j}^2\eta_2(1+d_0\eta_2)(1 \\ & + d_j\eta_2)\} \ . \end{aligned} \quad (I.8)$$

where d_0 and d_j are the respective diameters of a solute-free and a type j particle,

$$\eta_v = \frac{\xi_v}{1-\phi} \ , \quad (I.9)$$

and

$$\xi_v = \sum_{i=0}^{N-1} \phi_i \, {d_i}^{v-3} \ . \quad (I.10)$$

Using the Kronecker distribution, so that $C_j = C_{tot}\delta_{jj^*}$ and $\phi_i = C_{tot}N_AV_i\delta_{ii^*}$, eqn (I.8)–(I.10) combine to yield

$$\begin{aligned}\frac{\tilde{A}_{0j}}{\frac{\pi}{6}{d_0}^3} = & \left(\frac{d_j}{d_0}\right)^3 + \frac{\left\{1+\left[\left(\frac{d_j}{d_{j^*}}\right)^3-1\right]\phi\right\}}{(1-\phi)} \\ & + 3\left(\frac{d_j}{d_0}\right)\frac{\left[1+\left(\frac{d_0}{d_{j^*}}-1\right)\phi\right]\left\{1+\left[\left(\frac{d_j}{d_{j^*}}\right)^2-1\right]\phi\right\}}{(1-\phi)^2} \\ & + 3\left(\frac{d_j}{d_0}\right)^2\frac{\left[1+\left(\frac{d_j}{d_{j^*}}-1\right)\phi\right]\left\{1+\left[\left(\frac{d_0}{d_{j^*}}\right)^2-1\right]\phi\right\}}{(1-\phi)^2} \\ & + 9\phi\left(\frac{{d_j}^2}{d_0d_{j^*}}\right)\frac{\left[1+\left(\frac{d_0}{d_{j^*}}-1\right)\phi\right]\left[1+\left(\frac{d_j}{d_{j^*}}-1\right)\phi\right]}{(1-\phi)^3} \ . \end{aligned} \quad (I.11)$$

Imposing $j = j^*$ onto eqn (I.11) provides

$$\begin{aligned}\frac{\tilde{A}_{0j^*}}{\frac{\pi}{6}{d_0}^3} = & \left(\frac{d_{j^*}}{d_0}\right)^3 + \frac{1}{(1-\phi)} + 3\left(\frac{d_{j^*}}{d_0}\right)\frac{\left[1+\left(\frac{d_0}{d_{j^*}}-1\right)\phi\right]}{(1-\phi)^2} \\ & + 3\left(\frac{d_{j^*}}{d_0}\right)^2\frac{\left\{1+\left[\left(\frac{d_0}{d_{j^*}}\right)^2-1\right]\phi\right\}}{(1-\phi)^2} \\ & + 9\phi\left(\frac{d_{j^*}}{d_0}\right)\frac{\left[1+\left(\frac{d_0}{d_{j^*}}-1\right)\phi\right]}{(1-\phi)^3} \ . \end{aligned} \quad (I.12)$$

With the aid of Mathematica (see Supplementary Information section A), eqn (I.12) simplifies to

$$\frac{\tilde{A}_{0j^*}}{\frac{\pi}{6}{d_0}^3} = \lambda^3 + \frac{3\lambda^2}{(1-\phi)} + \frac{3\lambda(1+\phi-2\phi^2)}{(1-\phi)^3} + \frac{(1+2\phi)^2}{(1-\phi)^3} \ , \quad (I.13)$$

where $\lambda = d_{j^*}/d_0$ is a micelle size ratio. Multiplying eqn (I.13) by λ^{-3} provides

$$\frac{\tilde{A}_{0j^*}}{\frac{\pi}{6}{d_{j^*}}^3} = 1 + \frac{3\lambda^{-1}}{(1-\phi)} + \frac{3\lambda^{-2}(1+\phi-2\phi^2)}{(1-\phi)^3} + \frac{\lambda^{-3}(1+2\phi)^2}{(1-\phi)^3} \quad (I.14)$$

Furthermore, using eqn (G.7) from Appendix G and eqn (A.16) from Appendix A in our previous work,[8] we find

$$\frac{\partial lnC_{tot}}{\partial lnC_a} = \frac{\phi_a}{\phi} - 3\frac{\partial lnR_{j^*}}{\partial lnC_a} \ . \quad (I.15)$$

Eqn (I.14), (I.15), and $\phi = C_{tot}N_A\,\pi/6\,{d_{j^*}}^3$ combine to provide the first term on the right-hand side of eqn (I.7),

$$\begin{aligned}\tilde{A}_{0j^*}\frac{\partial C_{tot}}{\partial C_a} = & \ \frac{1}{C_a}\left\{1+\frac{3\lambda^{-1}}{(1-\phi)}+\frac{3\lambda^{-2}(1+\phi-2\phi^2)}{(1-\phi)^3}\right. \\ & \left. + \frac{\lambda^{-3}(1+2\phi)^2}{(1-\phi)^3}\right\}\left(\phi_a - 3\phi\frac{\partial lnR_{j^*}}{\partial lnC_a}\right). \end{aligned} \quad (I.16)$$

Now, focusing on the second term of eqn (I.7), differentiation of eqn (I.11) and (I.13) with respect to solute concentration C_a is accomplished via symbolic computation performed using Mathematica (see Supplementary Information, section B) to provide

$$\begin{aligned} C_{tot}\left\{\frac{\partial \tilde{A}_{0j^*}}{\partial C_a} - \left(\frac{\partial \tilde{A}_{0j}}{\partial C_a}\right)_{j=j^*}\right\} = & \\ & \frac{1}{C_a}\left\{1+\frac{\lambda^{-1}(2-3\phi+\phi^3)}{(1-\phi)^3}\right. \\ & + \frac{\lambda^{-2}(1+6\phi-6\phi^2-\phi^3)}{(1-\phi)^3} \\ & \left. + \frac{\lambda^{-3}\phi(2+\phi)^2}{(1-\phi)^3}\right\}3\phi\frac{\partial lnR_{j^*}}{\partial lnC_a} \ , \end{aligned} \quad (I.17)$$

where we have used $\partial lnR_{j^*}/\partial lnC_a = \partial ln d_{j^*}/\partial lnC_a$. Combination of eqn (I.3), (I.7), (I.16), and (I.17), again via symbolic computation using Mathematica (see Supplementary Information, section C), yield

$$\begin{aligned}\frac{m_0(1-\phi)G_{sa}}{N_Ak_BT} = & \ (1-\phi)\frac{1}{C_a}\frac{\partial lnC_0}{\partial lnC_a} + \tilde{A}(\lambda,\phi)\frac{\phi_a}{C_a} \\ & - \tilde{B}(\lambda,\phi)\frac{1}{C_a}\frac{\partial lnR_{j^*}}{\partial lnC_a} \end{aligned} \quad (I.18)$$

where

$$\tilde{A}(\lambda,\phi) = 1 + \frac{3\lambda^{-1}}{(1-\phi)} + \frac{3\lambda^{-2}(1+\phi-2\phi^2)}{(1-\phi)^3} + \frac{\lambda^{-3}(1+2\phi)^2}{(1-\phi)^3} \quad (I.19)$$

and

$$\tilde{B}(\lambda,\phi) = 3\phi\left\{\lambda^{-1} + \frac{\lambda^{-2}(2+\phi)}{(1-\phi)} + \frac{\lambda^{-3}(1+\phi+\phi^2)}{(1-\phi)^2}\right\}. \quad (I.20)$$

To evaluate the solute-free micelle derivative in eqn (I.18), consider the Poisson distribution, given by

$$C_i = \frac{C_s}{\bar{m}}\frac{\bar{n}^{n_i}}{n_i!}exp(-\bar{n}) \ . \quad (I.21)$$

where $\bar{n}$, the average number of solutes per micelle, is equal to the distribution variance. The Poisson distribution, which is derived assuming ideal mixing between solute and surfactant within micelles, and is considered valid when $\bar{n} \ll \bar{m}$,[54,55] is useful here because the Poisson variance approaches zero $\bar{n} \to 0$ in the tracer limit as $C_a \to 0$, causing eqn (I.21) to approach a Kronecker delta function

$$\lim_{C_a \to 0} \frac{C_s}{\bar{m}}\frac{\bar{n}^{n_i}}{n_i!}exp(-\bar{n}) = \frac{C_s}{m_0}\delta_{i0} \ . \quad (I.22)$$

Hence, in the tracer limit, the Poisson distribution becomes consistent with the delta distribution applied earlier in this derivation to evaluate the summation given by eqn (I.4). Differentiation of eqn (I.22) for $i = 0$ yields

$$\frac{\partial lnC_0}{\partial lnC_a} = 1 - (\bar{n}+1)\left(1 + \frac{\partial ln\bar{m}}{\partial lnC_a}\right). \quad (I.23)$$

Combining eqn (I.23) with eqn (A.16) from Appendix A in our previous work,[8] we have

$$\frac{\partial lnC_0}{\partial lnC_a} = 1 - (\bar{n}+1)\left(1 + 3\frac{\partial lnR_{j^*}}{\partial lnC_a} - \frac{\phi_a}{\phi}\right). \quad (I.24)$$

Eqn (I.18) and (I.24) combine to provide

$$\frac{m_0(1-\phi)G_{sa}}{N_A k_B T} = -(1-\phi)\frac{\bar{n}}{C_a} + \left[\tilde{A}(\lambda,\phi) + \frac{(1-\phi)(\bar{n}+1)}{\phi}\right]\frac{\phi_a}{C_a} - [\tilde{B}(\lambda,\phi) + 3(1-\phi)(\bar{n}+1)]\frac{1}{C_a}\frac{\partial lnR_{j^*}}{\partial lnC_a} \quad (I.25)$$

In the limit as $C_a \to 0$, for which $\lambda \to 1$, $\bar{n} \to 0$, $\bar{n}/C_a \to m_0/C_s$, $1/C_a\left(\partial lnR_{j^*}/\partial lnC_a\right) \to a_1/(R_0 C_s)$, $\phi \to C_s\bar{V}_{hs}$, and $\phi_a/C_a \to \bar{V}_a$, with the aid of Mathematica (see Supplemental Information, section D), eqn (I.19), (I.20), and (I.25) simplify to

$$\frac{C_s G_{sa}}{N_A k_B T} = -1 + \frac{\bar{V}_a}{m_0\bar{V}_{hs}}\frac{(1+2\phi)^2}{(1-\phi)^4} - \frac{3a_1}{m_0 R_0}\frac{(1+\phi+\phi^2)}{(1-\phi)^3} \quad (I.26)$$

In order to determine the remaining elements of the matrix $[\mathbf{G}]$, defined by eqn (48) and (50), one must evaluate the osmotic pressure derivatives $(\partial\Pi/\partial C_a)_{T,\mu_n}$ and $(\partial\Pi/\partial C_s)_{T,\mu_n}$. Imposing the delta distribution $C_j = C_{tot}\delta_{jj^*}$ on eqn (84) provides the Percus-Yevick result for monodisperse hard spheres

$$\frac{\Pi}{N_A k_B T} = C_{tot}\frac{(1+\phi+\phi^2)}{(1-\phi)^3} \ . \quad (I.27)$$

Differentiation of eqn (I.27) with respect to C_a provides (see Supplementary Information, section E)

$$\frac{(\partial\Pi/\partial C_a)_{T,\mu_n}}{N_A k_B T} = \frac{C_{tot}}{C_a}\left\{\frac{(1-\phi^3)}{(1-\phi)^4}\frac{\partial lnC_{tot}}{\partial lnC_a} + \frac{(2+\phi)^2}{(1-\phi)^4}\phi\frac{\partial ln\phi}{\partial lnC_a}\right\} \quad (I.28)$$

Using eqn (I.28), (G.12), and (I.15) with $C_{tot} = C_s/\bar{m}$, we have

$$\frac{(\partial\Pi/\partial C_a)_{T,\mu_n}}{N_A k_B T} = \frac{C_s/C_a}{\bar{m}\phi(1-\phi)^4}\left\{(1+2\phi)^2\phi_a - 3\phi(1-\phi^3)\frac{\partial lnR_{j^*}}{\partial lnC_a}\right\} \ . \quad (I.29)$$

The osmotic pressure derivative with respect to surfactant concentration C_s is similarly derived, using eqn (G.10) and (G.14),

$$\frac{(\partial\Pi/\partial C_s)_{T,\mu_n}}{N_A k_B T} = \frac{1}{\bar{m}\phi(1-\phi)^4}\left\{(1+2\phi)^2(\phi-\phi_a) + 3\phi(1-\phi^3)\frac{\partial lnR_{j^*}}{\partial lnC_a}\right\} \ . \quad (I.30)$$

In the tracer limit, as $\left(\partial lnR_{j^*}/\partial lnC_a\right) \to 0$, $1/C_a\left(\partial lnR_{j^*}/\partial lnC_a\right) \to a_1/(R_0 C_s)$, $\phi_a \to 0$, $\phi_a/C_a \to \bar{V}_a$, and $\phi \to C_s\bar{V}_{hs}$, eqn (I.29) and (I.30) reduce to

$$\frac{(\partial\Pi/\partial C_a)_{T,\mu_n}}{N_A k_B T} = \frac{\bar{V}_a}{m_0\bar{V}_{hs}}\frac{(1+2\phi)^2}{(1-\phi)^4} - \frac{3a_1}{m_0 R_0}\frac{(1-\phi^3)}{(1-\phi)^4}. \quad (I.31)$$

and

$$\frac{(\partial\Pi/\partial C_s)_{T,\mu_n}}{N_A k_B T} = \frac{(1+2\phi)^2}{m_0(1-\phi)^4}. \quad (I.32)$$

Finally, eqn (48), (50), (I.26), (I.31), and (I.32) yield $[\mathbf{G}]$ in the tracer limit, with elements given by

$$\frac{C_a G_{as}}{N_A k_B T} = 1 \ , \quad (I.33)$$

$$\frac{C_s G_{as}}{N_A k_B T} = \frac{C_s G_{sa}}{N_A k_B T} = -1 - \frac{3a_1}{m_0 R_0}\frac{(1+\phi+\phi^2)}{(1-\phi)^3} + \frac{\bar{V}_a}{m_0\bar{V}_{hs}}\frac{(1+2\phi)^2}{(1-\phi)^4} \ , \quad (I.35)$$

and

$$\frac{C_s G_{ss}}{N_A k_B T} = \frac{1}{m_0}\frac{(1+2\phi)^2}{(1-\phi)^4} \ . \quad (I.36)$$

Appendix J: Derivation of $[\mathbf{G}]$, $\boldsymbol{R_{90}}$, $\boldsymbol{B_{LL}}$, and $[\mathbf{L}]$ for the label limit

In this section, the micelle potential derivative matrix $[\mathbf{G}]$, the Rayleigh ratio $\boldsymbol{R_{90}}$, and the mode amplitude ratioo $\boldsymbol{B_{LL}}$ are derived for the label limit, where solute behaves as a volume-

less label in a mixture of equally sized micelles with $\phi_a = 0$, $\bar{m} = m_0$, and $R_{j^*} = R_0$, where m_0 and R_0 are the solute-free micelle aggregation number and radius, respectively. Starting with our derivation for $[\mathbf{G}]$, we begin with eqn (49)

$$\frac{m_0 G_{as}}{N_A k_B T} = \frac{m_0 G_{sa}}{N_A k_B T} = \frac{1}{C_a}\frac{\partial lnC_0}{\partial lnC_a} + \sum_{j=0}^{N-1} A_{0j}\left(\frac{\partial C_j}{\partial C_a}\right) \ . \qquad (J.1)$$

Eqn (J.1) is combined with eqn (93) and $\partial C_{tot}/\partial C_a = 0$ to provide,

$$\frac{m_0 G_{sa}}{N_A k_B T} = \frac{1}{C_a}\frac{\partial lnC_0}{\partial lnC_a} \ . \qquad (J.2)$$

The osmotic pressure derivatives are determined using eqn (44), (45), (93), and $\partial C_{tot}/\partial C_a = 0$, yielding

$$\left(\frac{\partial \Pi}{\partial C_a}\right)_{T,\mu_n} = 0 \qquad (J.3)$$

and

$$\frac{(\partial \Pi/\partial C_s)_{T,\mu_n}}{N_A k_B T} = \frac{(1+2\phi)^2}{m_0(1-\phi)^4} \ . \qquad (J.4)$$

Eqn (48)–(50), (J.2)–(J.4), and $\phi_a = 0$ combine to generate $[\mathbf{G}]$ in the label limit, equal to

$$G_{aa} = -\frac{N_A k_B T}{\bar{n} C_a}\frac{\partial lnC_0}{\partial lnC_a} \ , \qquad (J.5)$$

$$G_{as} = G_{sa} = \frac{N_A k_B T}{\bar{n} C_s}\frac{\partial lnC_0}{\partial lnC_a} \ , \qquad (J.6)$$

and

$$G_{ss} = \frac{N_A k_B T}{m_0 C_s}\left\{\frac{(1+2\phi)^2}{(1-\phi)^4} - \frac{\partial lnC_0}{\partial lnC_a}\right\} \ , \qquad (J.7)$$

Derivations for R_{90} and B_{LL} for labelled micelles are similar that those in Appendix G. We begin by combining eqn (G.1) and (G.2) with (103), (I.2)–(I.4), and $\phi_a = 0$, to yield the diagonalized elements of $[\mathbf{G}]$ in the label limit

$$\frac{C_a \hat{G}_a}{N_A k_B T} = -\frac{C_s}{C_a}\frac{\partial lnC_0}{\partial lnC_a} \qquad (J.8)$$

and

$$\frac{C_s \hat{G}_s}{N_A k_B T} = \frac{(1+2\phi)^2}{m_0(1-\phi)^4} \ . \qquad (J.9)$$

The diagonalized refractive index increments are evaluated using eqn (27)–(30), (103), and $\overline{V}_a = 0$ to give

$$\hat{R}_a = \frac{1}{C_s}\left\{\frac{\partial n}{\partial (C_a/C_s)}\right\}_{p,T,\phi} \qquad (J.10)$$

and

$$\hat{R}_s = \frac{\phi}{C_s}\left(\frac{\partial n}{\partial \phi}\right)_{p,T,C_a/C_s} \ . \qquad (J.11)$$

Eqn (24), (36), (J.8)–(J.11), and $\phi = N_A C_s/m_0 V_0$ combine to yield the Rayleigh ratio

$$R_{90} = \frac{4\pi^2 n^2}{{\lambda_0}^4}\left(\frac{\partial n}{\partial \phi}\right)^2_{p,T,C_a/C_s} V_0 \phi \frac{(1-\phi)^4}{(1+2\phi)^2}(1+B_{LL}) \ , \qquad (J.12)$$

Where V_0 is the volume of a solute-free micelle and the mode amplitude ratio is given by

$$B_{LL} = \left\{\frac{[\partial n/\partial (C_a/C_s)]_{p,T,\phi}}{\phi(\partial n/\partial \phi)_{p,T,C_a/C_s}}\right\}^2 \frac{(C_a/C_s)^2}{(-\partial lnC_0/\partial lnC_a)}\frac{(1+2\phi)^2}{(1-\phi)^4} \ . \qquad (J.13)$$

In order to derive the Onsager coefficient matrix $[\mathbf{L}]$, we start by evaluating the determinant of $[\mathbf{G}]$ using eqn (H.1), (J.3), (J.4), (J.6), and $\bar{n} C_s = m_0 C_a$

$$|\boldsymbol{G}| = \left(\frac{N_A k_B T}{\bar{n} C_s}\right)^2 \left(-\frac{\partial lnC_0}{\partial lnC_a}\right)\frac{(1+2\phi)^2}{(1-\phi)^4} \ . \qquad (J.14)$$

Eqn (70) and (94)–(100) combine to provide

$$L_{aa} = \bar{n}^2 C_{tot}\left(\frac{D^0}{N_A k_B T}\right)\left\{[1+(\beta+S)\phi]\frac{(1-\phi)^4}{(1+2\phi)^2} + \frac{1+K'\phi}{(-\partial lnC_0/\partial lnC_a)}\right\} \ . \qquad (J.15)$$

For dilute mixtures ($\phi \ll 1$),

$$\frac{(1-\phi)^4}{(1+2\phi)^2} \approx 1-\beta\phi \qquad (J.16)$$

so that

$$[1+(\beta+S)\phi]\frac{(1-\phi)^4}{(1+2\phi)^2} \approx 1+S\phi \ . \qquad (J.17)$$

Eqn (J.15) and (J.17) combine to yeild

$$L_{aa} = \bar{n}^2 C_{tot}\left(\frac{D^0}{N_A k_B T}\right)\left[1+S\phi+\frac{1+K'\phi}{(-\partial lnC_0/\partial lnC_a)}\right] \qquad (J.19)$$

Similar arguments are mode to derive the remaining Onsager Coefficients:

$$L_{as} = L_{sa} = \bar{n} m_0 C_{tot}\left(\frac{D^0}{N_A k_B T}\right)(1+S\phi) \qquad (J.20)$$

and

$$L_{ss} = {m_0}^2 C_{tot}\left(\frac{D^0}{N_A k_B T}\right)(1+S\phi) \ . \qquad (J.21)$$

Appendix K: Derivation of eigenmode transport equations for locally monodisperse micellar solutions and in the tracer limit

We begin by evaluating the inverse of the modal matrix $[\mathbf{P}]$, using eqn (60)

$$[\mathbf{P}]^{-1} = \begin{bmatrix} 1 & -C_a/C_s \\ \dfrac{-C_s/C_a M(\phi, C_a/C_s)}{(\beta + K'')\phi + M(\phi, C_a/C_s)} & 1 \end{bmatrix} \frac{1}{|\mathbf{P}|} \ , \qquad (K.1)$$

where the determinant is given by

$$|\boldsymbol{P}| = \frac{(\beta + K'')\phi}{(\beta + K'')\phi + M(\phi, C_a/C_s)} \qquad (K.2)$$

The mode fluxes are determined using eqn (126), (K.1), and (K.2)

$$\begin{bmatrix} \hat{J}_- \\ \hat{J}_+ \end{bmatrix} = \begin{bmatrix} \left(1 + \dfrac{M(\phi, C_a/C_s)}{(\beta + K'')\phi}\right) & -\dfrac{C_a}{C_s}\left(1 + \dfrac{M(\phi, C_a/C_s)}{(\beta + K'')\phi}\right) \\ -\dfrac{C_s}{C_a}\dfrac{M(\phi, C_a/C_s)}{(\beta + K'')\phi} & \left(1 + \dfrac{M(\phi, C_a/C_s)}{(\beta + K'')\phi}\right) \end{bmatrix} \begin{bmatrix} J_a \\ J_s \end{bmatrix} , \qquad (K.3)$$

which provides

$$\frac{\hat{J}_-}{C_a} = \left[1 + \frac{M(\phi, C_a/C_s)}{(\beta + K'')\phi}\right]\left(\frac{J_a}{C_a} - \frac{J_s}{C_s}\right) \qquad (K.4)$$

and

$$\frac{\hat{J}_+}{C_s} = \frac{J_s}{C_s} - \left[\frac{M(\phi, C_a/C_s)}{(\beta + K'')\phi}\right]\left(\frac{J_a}{C_a} - \frac{J_s}{C_s}\right) . \qquad (K.5)$$

Combining eqn (127), (K.1), and (K.2) provides the mode gradients

$$\begin{bmatrix} \nabla\hat{C}_- \\ \nabla\hat{C}_+ \end{bmatrix} = \begin{bmatrix} \left(1 + \dfrac{M(\phi, C_a/C_s)}{(\beta + K'')\phi}\right) & -\dfrac{C_a}{C_s}\left(1 + \dfrac{M(\phi, C_a/C_s)}{(\beta + K'')\phi}\right) \\ -\dfrac{C_s}{C_a}\dfrac{M(\phi, C_a/C_s)}{(\beta + K'')\phi} & \left(1 + \dfrac{M(\phi, C_a/C_s)}{(\beta + K'')\phi}\right) \end{bmatrix} \begin{bmatrix} \nabla C_a \\ \nabla C_s \end{bmatrix} , \qquad (K.6)$$

Per eqn (K.6), the (−) mode gradient is given by

$$\frac{\nabla\hat{C}_-}{C_a} = \left[1 + \frac{M(\phi, C_a/C_s)}{(\beta + K'')\phi}\right]\left(\frac{\nabla C_a}{C_a} - \frac{\nabla C_s}{C_s}\right) , \qquad (K.7)$$

where

$$\left(\frac{\nabla C_a}{C_a} - \frac{\nabla C_s}{C_s}\right) = \nabla ln\left(\frac{C_a}{C_s}\right) . \qquad (K.8)$$

Eqn (K.7) and (K.8) combine

$$\frac{\nabla\hat{C}_-}{C_a} = \left[1 + \frac{M(\phi, C_a/C_s)}{(\beta + K'')\phi}\right]\nabla ln\left(\frac{C_a}{C_s}\right) . \qquad (K.9)$$

Similarly, per eqn (K.6) and (K.8), the (+) mode gradient is given by

$$\frac{\nabla\hat{C}_+}{C_s} = \nabla lnC_s - \left[\frac{M(\phi, C_a/C_s)}{(\beta + K'')\phi}\right]\nabla ln\left(\frac{C_a}{C_s}\right) . \qquad (K.10)$$

The surfactant concentration gradient can be recast in terms of total micelle and composition gradients. The natural logarithm of the total micelle concentration gradient is evaluated using the product rule

$$\nabla ln\left(\frac{C_s}{\bar{m}}\right) = \nabla lnC_s - \frac{\nabla\bar{m}}{\bar{m}} . \qquad (K.11)$$

Since $\bar{m} = \bar{m}(C_a, C_s)$, the aggregation number gradient can be expanded using the chain rule to provide

$$\frac{\nabla\bar{m}}{\bar{m}} = \frac{\partial ln\bar{m}}{\partial lnC_a}\frac{\nabla C_a}{C_a} + \frac{\partial ln\bar{m}}{\partial lnC_s}\frac{\nabla C_s}{C_s} . \qquad (K.12)$$

Eqn (A.24) from Appendix A of our previous work[8] provides the following relation between aggregation number partial derivatives

$$\frac{\partial ln\bar{m}}{\partial lnC_s} = -\frac{\partial ln\bar{m}}{\partial lnC_a} . \qquad (K.13)$$

Eqn (K.8) and (K.11)–(K.13) combine to yield

$$\nabla lnC_s = \nabla ln\left(\frac{C_s}{\bar{m}}\right) + \frac{\partial ln\bar{m}}{\partial lnC_a}\nabla ln\left(\frac{C_a}{C_s}\right) , \qquad (K.14)$$

and eqn (K.10) and (K.14) give

$$\frac{\nabla\hat{C}_+}{C_s} = \nabla ln\left(\frac{C_s}{\bar{m}}\right) + \left\{\frac{\partial ln\bar{m}}{\partial lnC_a} - \frac{M(\phi, C_a/C_s)}{(\beta + K'')\phi}\right\}\nabla ln\left(\frac{C_a}{C_s}\right) . \qquad (K.15)$$

Hence, eqn (125), (K.4), (K.5), (K.9), and (K.15) combine to yield the following diffusional mode transport equations for locally monodisperse micelles

$$-\frac{\hat{J}_-}{C_a D_-} = -\left\{1 + \frac{M\left(\phi, \frac{C_a}{C_s}\right)}{(\beta + K'')\phi}\right\}\left(\frac{J_a}{C_a D_-} - \frac{J_s}{C_s D_-}\right)$$

$$= \frac{\nabla\hat{C}_-}{C_a} = \left\{1 + \frac{M\left(\phi, \frac{C_a}{C_s}\right)}{(\beta + K'')\phi}\right\}\nabla ln\left(\frac{C_a}{C_s}\right) , \qquad (K.16)$$

and

$$-\frac{\hat{J}_+}{C_s D_+} = -\frac{J_s}{C_s D_+} + \left\{\frac{M\left(\phi, \frac{C_a}{C_s}\right)}{(\beta + K'')\phi}\right\}\left(\frac{J_a}{C_a D_+} - \frac{J_s}{C_s D_+}\right)$$

$$= \frac{\nabla\hat{C}_+}{C_s} = \nabla ln\left(\frac{C_s}{\bar{m}}\right) + \left\{\frac{\partial ln\bar{m}}{\partial lnC_a} - \frac{M\left(\phi, \frac{C_a}{C_s}\right)}{(\beta + K'')\phi}\right\}\nabla ln\left(\frac{C_a}{C_s}\right) . \qquad (K.17)$$

Now, multiply eqn (K.16) by C_a and take the limit as $C_a \to 0$, for which for which $M(\phi, C_a/C_s) \to 0$, to provide the transport equation that describes the (−) mode in the tracer limit

$$-\hat{J}_- = -J_a = D_-\nabla C_a \qquad (K.18)$$

In order to determine the (+) mode transport equation, we note that $1/C_a\left(\partial lnR_{j^*}/\partial lnC_a\right) \to a_1/(R_0 C_s)$, $\phi \to C_s\overline{V}_{hs}$, and $\phi_a/C_a \to \overline{V}_a$ in the tracer limit as $C_a \to 0$. Hence, using eqn (56), we have

$$\frac{1}{C_a}\frac{M(\phi,C_a/C_s)}{(\beta+K'')\phi}=\frac{1}{C_a}\frac{\partial lnR_{i^*}}{\partial lnC_a}\frac{(1+\chi\phi)}{(\beta+K'')\phi}-\frac{1}{C_a}\frac{\phi_a}{\phi}$$
$$\rightarrow\frac{a_1}{C_sR_0}\frac{(1+\chi\phi)}{(\beta+K'')\phi}-\frac{V_a}{C_sV_{hs}} \qquad (K.19)$$

and, per eqn (A.16) from Appendix A of previous work,[8]

$$\frac{1}{C_a}\frac{\partial ln\overline{m}}{\partial lnC_a}=\frac{3}{C_a}\frac{\partial lnR_{i^*}}{\partial lnC_a}-\frac{1}{C_a}\frac{\phi_a}{\phi}\rightarrow\frac{3a_1}{R_0C_s}-\frac{V_a}{C_sV_{hs}}\ . \qquad (K.20)$$

Therefore, eqn (K.17), (K.19), and (K.20) combine to produce

$$-\frac{\hat{J}_+}{m_0}=-\frac{J_s}{m_0}+\left\{\frac{a_1}{R_0}\frac{(1+\chi\phi)}{(\beta+K'')\phi}-\frac{V_a}{V_{hs}}\right\}\frac{J_a}{m_0}$$
$$=D_+\nabla\left(\frac{C_s}{m_0}\right)+D_+\frac{a_1}{R_0}\left\{\frac{3(\beta+K'')\phi-(1+\chi\phi)}{(\beta+K'')\phi}\right\}\nabla C_a\,. \qquad (K.21)$$

Appendix L: Chemical potential derivatives and driving forces for diffusion

The driving force for diffusion of component i in an n-component, single phase, incompressible mixture may be written as

$$\boldsymbol{X}_i=-\boldsymbol{\nabla}\mu_i\ , \qquad (L.1)$$

where the chemical potential μ_i of species i is a function of $n+1$ other independent, intensive variables $\mu_i=\mu_i(T,p,C_1,C_2,\dots,C_{n-1})=\mu_i(T,\mu_n,C_1,C_2,\dots,C_{n-1})$,[53] and μ_n is the chemical potential of the solvent. Using the chain rule, one can expand eqn (L.1) according to

$$\boldsymbol{X}_i=-\left(\frac{\partial\mu_i}{\partial T}\right)_{p,\boldsymbol{C}}\boldsymbol{\nabla}T-\left(\frac{\partial\mu_i}{\partial p}\right)_{T,\boldsymbol{C}}\boldsymbol{\nabla}p-(\boldsymbol{\nabla}\mu_i)_{p,T} \qquad (L.2)$$

or, equivalently,

$$\boldsymbol{X}_i=-\left(\frac{\partial\mu_i}{\partial T}\right)_{\mu_n,\boldsymbol{C}}\boldsymbol{\nabla}T-\left(\frac{\partial\mu_i}{\partial\mu_n}\right)_{T,\boldsymbol{C}}\boldsymbol{\nabla}\mu_n-(\boldsymbol{\nabla}\mu_i)_{T,\mu_n}\ . \qquad (L.3)$$

In eqn (L.2) and (L.3), the subscript $\boldsymbol{C}=[C_1,C_2,\dots,C_{n-1}]$ indicates the vector of component concentrations is held fixed. For an incompressible mixture, one can show

$$\left(\frac{\partial\mu_i}{\partial p}\right)_{T,\boldsymbol{C}}=\bar{V}_i \qquad (L.4)$$

and by using a chain rule expansion we have

$$\left(\frac{\partial\mu_i}{\partial\mu_n}\right)_{T,\boldsymbol{C}}=\frac{(\partial\mu_i/\partial p)_{T,\boldsymbol{C}}}{(\partial\mu_n/\partial p)_{T,\boldsymbol{C}}}=\frac{\bar{V}_i}{\bar{V}_n}\ . \qquad (L.5)$$

Eqn (L.2)–(L.5) combine to produce

$$\boldsymbol{X}_i=-\left(\frac{\partial\mu_i}{\partial T}\right)_{p,\boldsymbol{C}}\boldsymbol{\nabla}T-\bar{V}_i\boldsymbol{\nabla}p-(\boldsymbol{\nabla}\mu_i)_{p,T}$$
$$=-\left(\frac{\partial\mu_i}{\partial T}\right)_{\mu_n,\boldsymbol{C}}\boldsymbol{\nabla}T-\frac{\bar{V}_i}{\bar{V}_n}\boldsymbol{\nabla}\mu_n-(\boldsymbol{\nabla}\mu_i)_{T,\mu_n}\,. \qquad (L.6)$$

At constant T,μ_n, eqn (L.6) provides

$$(\boldsymbol{\nabla}\mu_i)_{p,T}=(\boldsymbol{\nabla}\mu_i)_{T,\mu_n}-\bar{V}_i(\boldsymbol{\nabla}p)_{T,\mu_n}\ , \qquad (L.7)$$

and according to the Gibbs-Duhem equation at constant T,μ_n, the total pressure gradient in the mixture is given by

$$(\boldsymbol{\nabla}p)_{T,\mu_n}=(\boldsymbol{\nabla}\Pi)_{T,\mu_n}=\sum_{j=1}^{n-1}C_j\left(\boldsymbol{\nabla}\mu_j\right)_{T,\mu_n}\ . \qquad (L.8)$$

Per McMillan-Mayer solution theory,[13,51] eqn (L.8) describes a total pressure gradient within a multicomponent mixture that is separated from pure solvent by a semi-permeable membrane, which is permeable to only the solvent. The total pressure p of the mixture is equal to the osmotic pressure Π, plus the pressure of the pure solvent p_w, which is held constant with μ_n. Hence $(\boldsymbol{\nabla}p)_{T,\mu_n}=[\boldsymbol{\nabla}(p_w+\Pi)]_{T,\mu_n}=(\boldsymbol{\nabla}\Pi)_{T,\mu_n}$. Eqn (L.7) and (L.8) combine to give

$$-(\boldsymbol{\nabla}\mu_i)_{p,T}=-(\boldsymbol{\nabla}\mu_i)_{T,\mu_n}+\bar{V}_i\sum_{j=1}^{n-1}C_j\left(\boldsymbol{\nabla}\mu_j\right)_{T,\mu_n}\ . \qquad (L.9)$$

Now, using eqn (L.6), hold T,p constant, so that

$$-(\boldsymbol{\nabla}\mu_i)_{T,\mu_n}=-(\boldsymbol{\nabla}\mu_i)_{p,T}+\frac{\bar{V}_i}{\bar{V}_n}(\boldsymbol{\nabla}\mu_n)_{p,T}\ . \qquad (L.10)$$

Per the Gibbs-Duhem eqn at constant T,p

$$(\boldsymbol{\nabla}\mu_n)_{p,T}=-\sum_{j=1}^{n-1}\frac{C_j}{C_n}\left(\boldsymbol{\nabla}\mu_j\right)_{p,T}\ . \qquad (L.11)$$

Combine eqn (L.10) and (L.11) with the solvent volume fraction $C_n\bar{V}_n=1-\phi$ to find

$$-(\boldsymbol{\nabla}\mu_i)_{T,\mu_n}=-(\boldsymbol{\nabla}\mu_i)_{p,T}-\frac{\bar{V}_i}{1-\phi}\sum_{j=1}^{n-1}C_j\left(\boldsymbol{\nabla}\mu_j\right)_{p,T}\ . \qquad (L.12)$$

According to the chain rule, we have

$$(\boldsymbol{\nabla}\mu_i)_{p,T}=\sum_{k=1}^{n-1}\left(\frac{\partial\mu_i}{\partial C_k}\right)_{p,T}\boldsymbol{\nabla}C_k \qquad (L.13)$$

and

$$(\boldsymbol{\nabla}\mu_i)_{T,\mu_n}=\sum_{k=1}^{n-1}\left(\frac{\partial\mu_i}{\partial C_k}\right)_{T,\mu_n}\boldsymbol{\nabla}C_k\ . \qquad (L.14)$$

Combine eqn (L.9), (L.13), and (L.14), so that

$$\left(\frac{\partial\mu_i}{\partial C_k}\right)_{p,T}=\left(\frac{\partial\mu_i}{\partial C_k}\right)_{T,\mu_n}-\bar{V}_i\sum_{j=1}^{n-1}C_j\left(\frac{\partial\mu_j}{\partial C_k}\right)_{T,\mu_n}\ . \qquad (L.15)$$

Now, combine eqn (L.12)–(L.14) to provide the elements of $[\mathbf{G}]$

$$G_{ik}=\left(\frac{\partial\mu_i}{\partial C_k}\right)_{T,\mu_n}=\left(\frac{\partial\mu_i}{\partial C_k}\right)_{p,T}+\frac{\bar{V}_i}{1-\phi}\sum_{j=1}^{n-1}C_j\left(\frac{\partial\mu_j}{\partial C_k}\right)_{p,T}$$
$$for\ i,k=1,2,\dots,n-1\ . \qquad (L.16)$$

Eqn (L.15) and (L.16) combine to yield

$$\left(\frac{\partial \mu_i}{\partial C_k}\right)_{p,T} = (1-\phi)\left(\frac{\partial \mu_i}{\partial C_k}\right)_{T,\mu_n}$$
$$for\ i,k = 1,2,\dots,n-1\ . \qquad (L.17)$$

Following DeGroot and Mazur,[56] the rate of entropy produced irreversibly by diffusion in an isothermal, non-reacting, multicomponent mixture with no externally applied forces is defined by

$$T\sigma = -\sum_{i=1}^{n} \boldsymbol{J}_i^a \cdot (\boldsymbol{\nabla}\mu_i)_{p,T} \geq 0\ . \qquad (L.18)$$

Here, the molar species flux of component i is given by

$$\boldsymbol{J}_i^a = C_i(\boldsymbol{v}_i - \boldsymbol{v}^a)\ , \qquad (L.19)$$

and is defined relative to an arbitrary reference velocity

$$\boldsymbol{v}^a = \sum_{i=1}^{n} a_i \boldsymbol{v}_i\ , \qquad (L.20)$$

where $\boldsymbol{v}_i$ and a_i are the respective velocity and normalized weighting factor for species i.

The forces $-(\boldsymbol{\nabla}\mu_i)_{p,T}$ and fluxes $\boldsymbol{J}_i^a$ in eqn (L.18) are not independent, since the flux and chemical potential gradient of the solvent, denoted by the subscript n, can be eliminated using the Gibbs-Duhem equation

$$(\boldsymbol{\nabla}\mu_n)_{p,T} = -\sum_{k=1}^{n-1} \frac{C_k}{C_n}(\boldsymbol{\nabla}\mu_k)_{p,T} \qquad (L.21)$$

and the following relation between the fluxes

$$\boldsymbol{J}_n^a = -\sum_{k=1}^{n-1} \frac{C_n}{C_i}\frac{a_i}{a_n}\boldsymbol{J}_i^a\ . \qquad (L.22)$$

Eqn (L.18), (L.21), and (L.22) combine to provide the rate of entropy production in terms of independent driving forces and fluxes

$$T\sigma = -\sum_{i=1}^{n-1} \boldsymbol{J}_i^a \cdot \boldsymbol{X}_i^a\ . \qquad (L.23)$$

where

$$\boldsymbol{X}_i^a = -\sum_{k=1}^{n-1} A_{ik}^a\,(\boldsymbol{\nabla}\mu_k)_{p,T}\ , \qquad (L.24)$$

and

$$A_{ik}^a = \delta_{ik} + \frac{a_i}{a_n}\frac{C_k}{C_i}\ . \qquad (L.25)$$

The independent fluxes and driving forces, described by eqn (L.19), (L.20), (L.24) and (L.25), are linked via the normalized reference velocity weighting factor a_i and are therefore often referred to as conjugate pairs.

By setting the weighing factor equal to the species volume fraction $a_i = \phi_i$, one can define the following mean volume reference velocity,

$$\boldsymbol{v} = \sum_{i=1}^{n} \phi_i \boldsymbol{v}_i\ , \qquad (L.26)$$

which is equal to zero for an incompressible mixture relative to a fixed-volume reference frame. Eqn (L.19), (L.24), and (L.25) combine with $a_i = \phi_i$ and $\boldsymbol{v}^a = \boldsymbol{v} = \boldsymbol{0}$ to provide the driving force,

$$\boldsymbol{X}_i = -\sum_{k=1}^{n-1}\left(\delta_{ik} + \frac{C_k\overline{V}_i}{C_n\overline{V}_n}\right)(\boldsymbol{\nabla}\mu_k)_{p,T}\ , \qquad (L.27)$$

and conjugate diffusive flux

$$\boldsymbol{J}_i = C_i\boldsymbol{v}_i\ , \qquad (L.28)$$

defined relative to a volume-fixed reference frame, which closely approximates the fixed-laboratory frame in which experimental data is acquired. Eqn (L.27) combines with $C_n\overline{V}_n = 1-\phi$ to provide

$$\boldsymbol{X}_i = -(\boldsymbol{\nabla}\mu_i)_{p,T} - \frac{\overline{V}_i}{1-\phi}\sum_{k=1}^{n-1} C_k(\boldsymbol{\nabla}\mu_k)_{p,T}\ , \qquad (L.29)$$

which is identical to the result provided by Batchelor[57] (*cf*. eqn (4.1) of his work). Finally, eqn (L.12) and (L.29) combine to yield

$$\boldsymbol{X}_i = -(\boldsymbol{\nabla}\mu_i)_{T,\mu_n}\ , \qquad (L.30)$$

which describes the driving force for the diffusion of species i in a multicomponent liquid, relative to a reference frame in which the net flux of material volume is zero, and the solvent is force-free according to

$$\boldsymbol{X}_n = -(\boldsymbol{\nabla}\mu_n)_{T,\mu_n} = 0\ . \qquad (L.31)$$

The summation in eqn (L.29) accounts for a contribution to the driving force that acts on component i caused by solvent backflow, which inevitably occurs when a solute gradient is established in an incompressible mixture at constant temperature and pressure in a constant volume diffusion cell. Interestingly, when the same diffusion process is described using the McMillan-Mayer framework, the driving force on component i is given by eqn (L.30) and the solvent backflow contribution is accounted for via an osmotic pressure gradient. One may imagine a 1-dimensional diffusion cell, separated by a semipermeable membrane (permeable only to the solvent) oriented parallel to the flux direction along the diffusion pathway. In this scenario, the membrane separates the multicomponent mixture at each local point from pure solvent, thereby maintaining a constant solvent chemical potential at each point along the diffusion path, so that the solvent is force-free. Here, solvent passes through the membrane into the diffusion cell from the pure solvent reservoir and raises the osmotic pressure locally in proportion with the local solute concentration, thereby enhancing the thermodynamic driving force on component i via a gradient in osmotic pressure, rather

than by backflow of solvent at constant pressure. We note that the McMillan Mayer framework is useful here because of the simplicity of eqn (L.30) as compared with (L.29).

Appendix M: Derivation of R_{90} for binary mixtures of monodisperse micelles with crowding-induced dehydration

In this section, we derive the Rayleigh ratio for a binary mixture of hydrated surfactant (s) and water (w) with a concentration dependent hydration index $n_H = n_H(T, p, C_s)$ and a constant aggregation number m_0. For this system, the total entropy fluctuation at constant temperature T and scattering volume V is given by

$$\delta S_T = -\frac{1}{2T}(\delta\mu_w \delta N_w + \delta\mu_s \delta N_s) \ , \qquad (M.1)$$

where μ_w and μ_s are the chemical potentials for water and hydrated surfactant and N_w and N_s are the respective numbers of moles in the scattering volume V. Imposing constant volume, we have

$$\delta V = \delta[\bar{V}_w N_w + (\bar{V}_s + n_H \bar{V}_w) N_s] = 0 \ . \qquad (M.2)$$

Solving eqn (M.2) for the fluctuation in the number of moles of water provides

$$\delta N_w = -N_s \delta n_H - \frac{(\bar{V}_s + n_H \bar{V}_w)}{\bar{V}_w} \delta N_s \ . \qquad (M.3)$$

At constant temperature, pressure, and volume, the total fluctuation differential in the hydration index is given by

$$\delta n_H = \frac{V}{V}\left(\frac{\partial n_H}{\partial N_s}\right)_{p,T} \delta N_s = \left(\frac{\partial n_H}{\partial C_s}\right)_{p,T} \delta C_s \ , \qquad (M.4)$$

and eqn (M.3) and (M.4) combine to yield

$$\delta N_w = -V\left\{C_s\left(\frac{\partial n_H}{\partial C_s}\right)_{p,T} + \frac{(\bar{V}_s + n_H \bar{V}_w)}{\bar{V}_w}\right\} \delta C_s \ , \qquad (M.5)$$

which indicates that hydrated surfactant displaces free water at constant volume and also adds to N_w via the transfer of bound water from hydrated surfactant to bulk water via dehydration.

Now, using the Gibbs-Duhem relation at constant temperature, pressure, and volume, and solving for the free water fluctuation $\delta\mu_w$ in eqn (M.6) provides

$$\delta\mu_w = -\frac{V}{V}\frac{N_s}{N_w}\delta\mu_s = -\frac{C_s}{C_w}\delta\mu_s \ . \qquad (M.6)$$

The total fluctuation differential in hydrated surfactant chemical potential at constant temperature, pressure, and volume is given by

$$\delta\mu_s = \frac{V}{V}\left(\frac{\partial \mu_s}{\partial N_s}\right)_{p,T} \delta N_s = \left(\frac{\partial \mu_s}{\partial C_s}\right)_{p,T} \delta C_s \ , \qquad (M.7)$$

and eqn (M.6) and (M.7) combine

$$\delta\mu_w = -\frac{C_s}{C_w}\left(\frac{\partial \mu_s}{\partial C_s}\right)_{p,T} \delta C_s \ . \qquad (M.8)$$

Now, combine eqn (M.1), (M.5), and (M.8) with $\phi = C_s(\bar{V}_s + n_H \bar{V}_w)$ and $1 - \phi = C_w \bar{V}_w$ to provide

$$\delta S_T = -\frac{V}{2T}\left(\frac{1}{1-\phi}\right)\left(\frac{\partial \mu_s}{\partial C_s}\right)_{p,T}\left[1 + {C_s}^2 \bar{V}_w \left(\frac{\partial n_H}{\partial C_s}\right)_{p,T}\right]{\delta C_s}^2 \ , \qquad (M.9)$$

Eqn (L.17) reduces for a binary mixture to provide

$$\left(\frac{1}{1-\phi}\right)\left(\frac{\partial \mu_s}{\partial C_s}\right)_{p,T} = \left(\frac{\partial \mu_s}{\partial C_s}\right)_{T,\mu_w} \ , \qquad (M.10)$$

and eqn (M.9) and (M.10) yield

$$\delta S_T = -\frac{V}{2T}\left(\frac{\partial \mu_s}{\partial C_s}\right)_{T,\mu_w}\left[1 + {C_s}^2 \bar{V}_w \left(\frac{\partial n_H}{\partial C_s}\right)_{p,T}\right]{\delta C_s}^2 \ . \qquad (M.11)$$

The master formula for fluctuation theory provides the probability for a fluctuation δC_s in the scattering volume V

$$P(\delta C_s) = \Omega^{-1} e^{\left\{-\frac{V}{2k_B T}\left(\frac{\partial \mu_s}{\partial C_s}\right)_{T,\mu_w}\left[1 + {C_s}^2 \bar{V}_w \left(\frac{\partial n_H}{\partial C_s}\right)_{p,T}\right]{\delta C_s}^2\right\}} \ , \qquad (M.12)$$

and is integrated over all possible fluctuations to determine the normalization constant

$$\Omega = \langle \delta C_S \rangle = \int_{-\infty}^{\infty} d\,(\delta C_S) e^{\left\{-\frac{V}{2k_B T}\left(\frac{\partial \mu_s}{\partial C_s}\right)_{T,\mu_w}\left[1 + {C_s}^2 \bar{V}_w \left(\frac{\partial n_H}{\partial C_s}\right)_{p,T}\right]{\delta C_s}^2\right\}}$$

$$= \left\{\frac{2\pi k_B T}{V\left(\frac{\partial \mu_s}{\partial C_s}\right)_{T,\mu_w}\left[1 + {C_s}^2 \bar{V}_w \left(\frac{\partial n_H}{\partial C_s}\right)_{p,T}\right]}\right\}^{\frac{1}{2}} \ , \qquad (M.13)$$

Using eqn (M.12) and (M.13), the mean square fluctuation in the surfactant concentration is given by

$$\langle {\delta C_s}^2 \rangle = \int_{-\infty}^{\infty} d\,(\delta C_s) \delta {C_s}^2 P(\delta C_s)$$

$$= \Omega^{-1} \int_{-\infty}^{\infty} d\,(\delta C_s) \delta {C_s}^2 e^{\left\{-\frac{V}{2k_B T}\left(\frac{\partial \mu_s}{\partial C_s}\right)_{T,\mu_w}\left[1 + {C_s}^2 \bar{V}_w \left(\frac{\partial n_H}{\partial C_s}\right)_{p,T}\right]{\delta C_s}^2\right\}}$$

$$= \frac{k_B T}{V\left(\frac{\partial \mu_s}{\partial C_s}\right)_{T,\mu_w}\left[1 + {C_s}^2 \bar{V}_w \left(\frac{\partial n_H}{\partial C_s}\right)_{p,T}\right]} \ , \qquad (M.14)$$

In order determine the Rayleigh ratio, we will need the fluctuation in the dielectric constant $\varepsilon = \varepsilon[T, p, C_s, n_H(T, p, C_s)]$, which is expanded in reciprocal space at constant temperature and pressure to provide

$$\delta\varepsilon(\boldsymbol{q}, t) = \left(\frac{\partial \varepsilon}{\partial n_H}\right)_{p,T,C_s} \delta n_H(\boldsymbol{q}, t) + \left(\frac{\partial \varepsilon}{\partial C_s}\right)_{p,T,n_H} \delta C_s(\boldsymbol{q}, t) \ , \qquad (M.15)$$

In eqn (M.15), $\delta C_s(\boldsymbol{q}, 0)$ is the Fourier transform of the local surfactant concentration fluctuation $\delta C_s(\boldsymbol{z}, 0)$, given by

$$\delta C_s(\boldsymbol{q}, 0) = \frac{1}{V}\int d^3\boldsymbol{z}\, e^{i\boldsymbol{q}\cdot\boldsymbol{z}} \delta \hat{C}_i(\boldsymbol{z}, 0) \ . \qquad (M.16)$$

Eqn (M.4) and (M.15) combine to yield

$$\delta\varepsilon(\boldsymbol{q},t)=\left[\left(\frac{\partial\varepsilon}{\partial C_s}\right)_{p,T,n_H}+\left(\frac{\partial\varepsilon}{\partial n_H}\right)_{p,T,C_s}\left(\frac{\partial n_H}{\partial C_s}\right)_{p,T}\right]\delta C_s(\boldsymbol{q},t)\ , (M.17)$$

Using eqn (M.17), the ensemble averaged time correlation function for fluctuations in ε is given by

$$\langle\delta\varepsilon^*(\boldsymbol{q},0)\delta\varepsilon(\boldsymbol{q},t)\rangle=\left[\left(\frac{\partial\varepsilon}{\partial C_s}\right)_{p,T,n_H}+\left(\frac{\partial\varepsilon}{\partial n_H}\right)_{p,T,C_s}\left(\frac{\partial n_H}{\partial C_s}\right)_{p,T}\right]^2\times\langle\delta C_s^*(\boldsymbol{q},0)\delta C_s(\boldsymbol{q},t)\rangle\ . \quad (M.18)$$

Now, setting $t=0$ and using eqn (M.18), the mean square fluctuation in surfactant concentration is given by

$$\begin{aligned}&\langle\delta C_s^*(\boldsymbol{q},0)\delta C_s(\boldsymbol{q},0)\rangle\\&=\langle\frac{1}{V}\int d^3\boldsymbol{z}\,e^{-i\boldsymbol{q}\cdot\boldsymbol{z}}\delta C_s(\boldsymbol{z},0)\frac{1}{V}\int d^3\boldsymbol{z}\,e^{i\boldsymbol{q}\cdot\boldsymbol{z}}\delta C_s(\boldsymbol{z},0)\rangle\\&=\langle\left(\frac{1}{V}\int d^3\boldsymbol{z}\,\delta C_s(\boldsymbol{z},0)\right)^2\rangle\\&=\langle\delta {C_s}^2\rangle\ .\end{aligned} \quad (M.19)$$

Eqn (M.14), (M.18) and (M.19) combine with $t=0$ to provide

$$\langle\delta\varepsilon^*(\boldsymbol{q},0)\delta\varepsilon(\boldsymbol{q},t)\rangle=\frac{k_BT\left[\left(\frac{\partial\varepsilon}{\partial C_s}\right)_{p,T,n_H}+\left(\frac{\partial\varepsilon}{\partial n_H}\right)_{p,T,C_s}\left(\frac{\partial n_H}{\partial C_s}\right)_{p,T}\right]^2}{V\left(\frac{\partial\mu_s}{\partial C_s}\right)_{T,\mu_w}\left[1+{C_s}^2\overline{V}_w\left(\frac{\partial n_H}{\partial C_s}\right)_{p,T}\right]}\ . \quad (M.20)$$

The Rayleigh ratio R_{90} at constant temperature and pressure is determined by combining eqn (34) and (N.20) and $\varepsilon^2=n^4$, and $k_f\approx 2\pi n/\lambda_0$ to provide

$$R_{90}=\frac{I(\boldsymbol{q})L^2}{I_0V}=\frac{4\pi^2n^2}{{\lambda_0}^4}\frac{\left[\left(\frac{\partial n}{\partial C_s}\right)_{p,T,n_H}+\left(\frac{\partial n}{\partial n_H}\right)_{p,T,C_s}\left(\frac{\partial n_H}{\partial C_s}\right)_{p,T}\right]^2}{\left[1+{C_s}^2\overline{V}_w\left(\frac{\partial n_H}{\partial C_s}\right)_{p,T}\right]}\times\frac{k_BT}{V\left(\frac{\partial\mu_s}{\partial C_s}\right)_{T,\mu_w}}\ . \quad (M.21)$$

The surfactant chemical potential derivative $(\partial\mu_s/\partial C_s)_{T,\mu_w}$ is determined using (F.7), reduced for a binary mixture

$$\left(\frac{\partial\mu_s}{\partial C_s}\right)_{T,\mu_w}=\frac{1}{C_s}\left(\frac{\partial\Pi}{\partial C_s}\right)_{T,\mu_w}\ , \quad (M.22)$$

and a general form for the osmotic pressure in a mixture of monodisperse micelles

$$\frac{\Pi}{N_Ak_BT}=C_{tot}Z(\phi)\ . \quad (M.23)$$

where $Z(\phi)$ is the compressibility factor. Eqn (M.21)–(M.23) and $C_{tot}=C_s/m_0$ combine to yield

$$R_{90}=\frac{4\pi^2n^2}{{\lambda_0}^4}\frac{\left(\frac{\partial n}{\partial C_s}\right)_{T,p}^2}{\left[1+{C_s}^2\overline{V}_w\left(\frac{\partial n_H}{\partial C_s}\right)_{p,T}\right]}\frac{C_sm_0}{N_A}\left\{\frac{d[C_sZ(\phi)]}{dC_s}\right\}^{-1}, (M.24)$$

where, according to the chain rule,

$$\left(\frac{\partial n}{\partial C_s}\right)_{T,p}=\left(\frac{\partial n}{\partial C_s}\right)_{p,T,n_H}+\left(\frac{\partial n}{\partial n_H}\right)_{p,T,C_s}\left(\frac{\partial n_H}{\partial C_s}\right)_{p,T}\ . \quad (M.25)$$

Furthermore, using eqn (69), we have

$$\frac{d[C_sZ(\phi)]}{dC_s}=\frac{(1+2\phi)^2-\phi^3(4-\phi)}{(1-\phi)^4}-{C_s}^2\overline{V}_w\left(\frac{\partial n_H}{\partial C_s}\right)_{p,T}\frac{(4+4\phi-2\phi^2)}{(1-\phi)^4} \quad (M.26)$$

A check for the results given by eqn (M.24)–(M.26) is provided by removing dehydration, so that $(\partial n_H/\partial C_s)_{p,T}=0$ and the hydrated surfactant molar volume $\overline{V}_{hs}=\overline{V}_s+n_H\overline{V}_w$ is constant. As a result, using $\phi=C_s\overline{V}_{hs}$ and $m_0\overline{V}_{hs}/N_A=V_0$, eqn (M.24) reduces to

$$R_{90}=\frac{4\pi^2n^2}{{\lambda_0}^4}\left(\frac{\partial n}{\partial\phi}\right)_{T,p}^2V_0\phi\left\{\frac{d[\phi Z(\phi)]}{d\phi}\right\}^{-1}, \quad (M.27)$$

which is consistent with R_{90} or a binary mixture of monodisperse hard spheres.

Acknowledgements

This research was funded by the National Science Foundation (CBET1506474), and from Hatch project 1010420, from the USDA National Institute of Food and Agriculture. N. P. A. acknowledges a Graduate Assistance in Areas of National Need (GAANN) fellowship from the University of California at Davis. All authors gratefully acknowledge Ulf Nobbmann from Malvern for allowing us to borrow a light scattering apparatus for an extended period.

References

1 L. Onsager, Reciprocal Relations in Irreversible Processes. 1, *Phys. Rev.*, 1931, **37**, 405–426.
2 G. I. Taylor, Dispersion of Soluble Matter in Solvent Flowing Slowly through a Tube, *Proc. R. Soc. London, Ser. A*, 1953, **219**, 186–203.
3 R. Aris, On the Dispersion of a Solute in a Fluid Flowing through a Tube, *Proc. R. Soc. London, Ser. A*, 1956, **235**, 67–77.
4 W. E. Price, Theory of the Taylor Dispersion Technique for Three-component-system Diffusion Measurements, J. Chem. Soc., *Faraday Trans. 1*, 1988, **84**, 2431–2439.
5 W. J. Musnicki, S. R. Dungan and R. J. Phillips, Multicomponent Diffusion in Solute-Containing Micelle and Microemulsion Solutions, *Langmuir*, 2014, **30**, 11019–11030
6 W. A. Wakeham, A. Nagashima, J. V. Sengers, *Measurements of the transport properties of fluids*. Blackwell Scientific Publication, Oxford, 1991. 5, 272–294.

7 N. P. Alexander, R. J. Phillips, S. R. Dungan, Multicomponent Diffusion in Aqueous Solutions of Nonionic Micelles and Decane, *Langmuir*, 2019, **35** (42), 13595–13606.
8 N. P. Alexander, R. J. Phillips, S. R. Dungan, Multicomponent diffusion of interacting, nonionic micelles with hydrophobic solutes, *Soft Matter*, 2021, **17**, 531–542.
9 D. G. Leaist, Relating Multicomponent Mutual Diffusion and Intradiffusion for Associating Solutes. Application to Coupled Diffusion in Water-in-oil Microemulsions, *Phys. Chem. Chem. Phys*., 2002, **4**, 4732–4739.
10 M. A. Budroni, J. Carballido-Landeira, A. Intiso, A. De Wit and F. Rossi, Interfacial Hydrodynamic Instabilities driven by Cross-Diffusion in Reverse Microemulsions, *Chaos*, 2015, **25**, 1–10.
11 U. Olsson, P. Schurtenberger, Structure, Interactions, and Diffusion in a Ternary Nonionic Microemulsion Near Emulsification Failure. *Langmuir,* 1993, ***9***, 3389–3394.
12 U. Olsson and P. Schurtenberger, A Hard Sphere Microemulsion, Prog. *Colloid Polym. Sci*., 1997, **104**, 157–15
13 A. Vrij, Concentrated, Polydisperse Solutions of Colloidal Particles. Light Scattering and Sedimentation of Hard-Sphere Mixtures, *J. Colloid Interface Sci*., 1982, **186**, 170–179.
14 P. N. Pusey, H. M. Fijnaut, A. Vrij, Mode Amplitudes in Dynamic Light Scattering by Concentrated Liquid Suspensions of Polydisperse Hard Spheres. *J. Chem. Phys.*, 1982, ***77,*** 4270–4281.
15 A. van Veluwen, H. N. W. Lekkerkerker, C. G. de Kruif, A. Vrij, Influence of Polydispersity on Dynamic Light Scattering Measurements on Concentrated Suspensions, *J. Chem. Phys.,* 1988, **89***,* 2810−2815.
16 W. L. Griffith, R. Triolo, A. L. Compere, Analytical Scattering Function of a Polydisperse Percus-Yevick Fluid with Schulz-Distributed Diameter. *Phys. Rev. A*, 1987, **35** (5), 2200–2206.
17 A. Vrij, Light Scattering of a Concentrated Multicomponent System of Hard Spheres in the Percus–Yevick Approximation, *J. Chem. Phys.* 1978, **69**, 1742–1747.
18 Y. D. Yan, J. H. R. Clarke, Dynamic Light Scattering from Concentrated Water–in–oil Microemulsions: The Coupling of Optical and Size Polydispersity, *J. Chem. Phys.,* 1990, **93***,* 4501–4509.
19 M. Nayeri, M. Zackrisson, J. Bergenholtz, Scattering Functions of Core-Shell Structured Hard Spheres with Schulz-Distributed Radii, *J. Phys. Chem. B*, 2009, **113**, 8296–8302.
20 B. J. Berne, R. Pecora, *Dynamic Light Scattering with Applications to Chemistry, Biology, and Physics*, Dover Publications Inc., New York, 1976, Appendix 10C, 263–272.
21 A. Bardow, On the Interpretation of Ternary Diffusion Measurements in Low-Molecular Weight Fluids by Dynamic Light Scattering. *Fluid Phase Equilib.*, 2007, **251**, 121−127.
22 J. G. Kirkwood, R. J. Goldberg, Light Scattering Arising from Composition Fluctuations in Multi-Component Systems, *J. Chem. Phys*. 1950, **18**, 54–57.
23 R. D. Mountain, J. M. Deutch, Light Scattering from Binary Solutions, *J. Chem. Phys.* 1969, **50** (3), 1103 – 1108.
24 L. Blum, Light Scattering from Multicomponent Fluids, *J. Chem. Phys.* 1969, **50**, 17–20.
25 S. R. de Groot, P. Mazur, *Non-equilibrium Thermodynamics*, Dover Publications, New York, 1984, 3, 23.
26 G. K. Batchelor, Brownian Diffusion of Particles with Hydrodynamic Interaction, *J. Fluid Mech*., 1976, 74, 1–29.
27 G. K. Batchelor, Diffusion in a Dilute Polydisperse System of Interacting Spheres, *J. Fluid Mech*., 1983, **131**, 155–175.
28 G. K. Batchelor, Corrigendum, *J. Fluid Mech*., 1983, **137**, 467–469.
29 P. Schurtenberger, In *Light Scattering: Principles and Development,* ed. Brown, W., Oxford University Press Inc., New York, 1st edn, 1996, 9, 293–326.
30 S. Kaneshina, M. Yoshimoto, H. Kobayashi, N. Nishikido, G. Sugihara, M. Tanaka, Effect of Pressure on Apparent Molal Volumes of Nonionic Surfactants in Aqueous Solutions. *J. Colloid Interface Sci.,* 1980, **73***,* 124–129.
31 Y. Tokuoka, H. Uchiyama, A. Masahiko, Solubilization of Synthetic Perfumes by Nonionic Surfactants. *J. Colloid Interface Sci.*, 1992, **152** (2), 402–409.
32 S. R. de Groot, P. Mazur, *Non-equilibrium Thermodynamics*, Dover Publications, New York, 1984, 11, 246–262.
33 B. C. Stephenson, A. Goldsipe, K. J. Beers, and D. Blankschtein. Quantifying the Hydrophobic Effect. 1. A Computer Simulation–Molecular-Thermodynamic Model for the Self-Assembly of Hydrophobic and Amphiphilic Solutes in Aqueous Solution. *J. Phys. Chem. B*, 2007, **111**, 1025–1044.
34 N. F. Carnahan, K. E. Starling, Equation of State for Nonattracting Rigid Spheres. *J. Chem. Phys.,* 1969, **51***,* 635−636.
35 S. R. de Groot, P. Mazur, *Non-equilibrium Thermodynamics*, Dover Publications, New York, 1984, 4, 30–31.
36 D. E. Koppel, Analysis of Macromolecular Polydispersity in Intensity Correlation Spectroscopy: The Method of Cumulants, *J. Chem. Phys.,* 1972, **57**, 4814–4820.
37 H. L. Toor, Solution of the Linearized Equations of Multicomponent Mass Transfer: II. Matrix Methods., *AIChE J*. 1964, **10**, 460–465.
38 Akcasu, A. Z.; Nägele, G.; Klein, R. Identification of Modes in Dynamic Scattering from Ternary Polymer Mixtures and Interdiffusion. *Macromolecules*, 1991, **24**, 4408–4422.
39 M. Imai, M. Kurimoto, F. Matsuura, Y. Sakuma and T. Kawakatsu, Diffusion of Surfactant Micelles in Fluid and Crystal Phases, *Soft Matter*, 2012, **8**, 9892–9905.
40 A. Shukla, H. Graener, R. H. H. Neubert, Observation of Two Diffusive Relaxation Modes in Microemulsions by Dynamic Light Scattering, *Langmuir,* 2004, **20**, 8526–8530.
41 W. B. Russel, A. B. Glendinning, The effective diffusion coefficient detected by dynamic light scattering, *J. Chem. Phys.,* 1981, **74**, 948–952.
42 W. B. Russel, D. A. Saville and W. R. Schowalter, *Colloidal Dispersions*, Cambridge University Press, New York, 1st edn, 1989, ch. 13, pp. 429–453.
43 G. K. Batchelor, Sedimentation in a dilute dispersion of spheres. *J. Fluid Mech.,* 1972, **52***,* 245–268.
44 M. L. Chichocki, P. Ekiel-Jeżewska, E. Wajnryb, Three–particle Contribution to Sedimentation and Collective Diffusion in Hard–sphere suspensions, *J. Chem. Phys., 2002*, **117***,* 1231−1241.
45 A. J. C. Ladd, Hydrodynamic transport coefficients of random dispersions of hard spheres, *J. Chem. Phys.* 1990, **93***,* 3484–3494.
46 P. N. Segre, O. P. Behrend, P. N. Pusey, Short-time Brownian motion in Colloidal Suspensions: Experiment and Simulation, *Phys. Rev. E., 1995*, **52** (5), 5070–5083.
47 A. J. Banchio and G. Nägele, Short-time Transport Properties in Dense Suspensions: From Neutral to Charge Stabilized Colloidal Spheres, *J. Chem. Phys*., 2008, **128**, 104903.
48 M. Imai, M. Kurimoto, F. Matsuura, Y. Sakuma and T. Kawakatsu, Diffusion of Surfactant Micelles in Fluid and Crystal Phases, *Soft Matter*, 2012, **8**, 9892–9905.
49 G. Nilsson, B. Lindman, Water Self-Diffusion in Nonionic Surfactant Solutions. Hydration and Obstruction Effects. *J. Phys. Chem.,* 1983, **87***,* 4756–4761.
50 H. N. Lesemann, T. P. DiNoia, C. F. Kirby, M. A. McHugh, van J. H. Zanten, M. E. Paulaitis, Self-Assembly at High Pressures: SANS Study of the Effect of Pressure on Microstructure of C8E5 Micelles in Water. *Ind. Eng. Chem. Res.,* 2003, **42***,* 6425−6430.

51 W. G. McMillan, J. E. Mayer, The Statistical Thermodynamics of Multicomponent Systems, *J. Chem. Phys.* 1945, **13**, 276–305.
52 S. Vafaei, B. Tomberli, C. G. Gray, McMillan-Mayer Theory of Solutions Revisited: Simplifications and Extensions, *J. Chem. Phys.* 2014, **141**, 154501.
53 J. W. Tester, M. Modell, Thermodynamics and Its Applications, Prentice-Hall Inc., New Jersey, 3rd edn, 1997, 5, 131.
54 M. Everist, J. A. MacNeil, J. R. Moulins, D. G. Leaist, Coupled Mutual Diffusion in Solutions of Micelles and Solubilizates. *Phys. Chem. Chem. Phys.* 2009, **11**, 8173−8182.
55 M. Tachiya, Kinetics of Quenching of Luminescent Probes in Micellar Systems. II. *J. Chem. Phys.* 1982, **76**, 340−348.
56 S. R. de Groot, P. Mazur, *Non-equilibrium Thermodynamics*, Dover Publications, New York, 1984, 11, 239–246.
57 G. K. Batchelor, Note on the Onsager Symmetry of the Kinetic Coefficients for Sedimentation and Diffusion in a Dilute Bidispersion, *J. Fluid Mech.* 1986, **171**, 509–517.

Supplementary Information: Mathematica Code used for Chapter 3 Derivations.

Section A

The goal of section A is to simplify eqn (I.12) in Appendix I.

$$\frac{\tilde{A}_{0j^*}}{\frac{\pi}{6}{d_0}^3} = \left(\frac{d_{j^*}}{d_0}\right)^3 + \frac{1}{(1-\phi)} + 3\left(\frac{d_{j^*}}{d_0}\right)\frac{\left[1+\left(\frac{d_0}{d_{j^*}}-1\right)\phi\right]}{(1-\phi)^2} + 3\left(\frac{d_{j^*}}{d_0}\right)^2\frac{\left\{1+\left[\left(\frac{d_0}{d_{j^*}}\right)^2-1\right]\phi\right\}}{(1-\phi)^2} + 9\phi\left(\frac{d_{j^*}}{d_0}\right)\frac{\left[1+\left(\frac{d_0}{d_{j^*}}-1\right)\phi\right]}{(1-\phi)^3}. \quad (I.12)$$

```
Clear["Global`*"]
(*Eqn (I.12) from Appendix I*) (*Note,
A0jstarV0 = (1/V0) A0j* , where V0 = pi/6*d0^3*)
```

$$\texttt{A0jstarV0} = \left(\frac{\texttt{dj[Ca]}}{\texttt{d0}}\right)^3 + \frac{1}{1-\phi[\texttt{Ca}]} + \frac{3\left(\frac{\texttt{dj[Ca]}}{\texttt{d0}}\right)}{\left(1-\phi[\texttt{Ca}]\right)^2}\left(1+\left(\frac{\texttt{d0}}{\texttt{dj[Ca]}}-1\right)\phi[\texttt{Ca}]\right) + \frac{3\left(\frac{\texttt{dj[Ca]}}{\texttt{d0}}\right)^2}{\left(1-\phi[\texttt{Ca}]\right)^2}\left(1+\left(\left(\frac{\texttt{d0}}{\texttt{dj[Ca]}}\right)^2-1\right)\phi[\texttt{Ca}]\right) + \frac{9\left(\frac{\texttt{dj[Ca]}}{\texttt{d0}}\right)\phi[\texttt{Ca}]}{\left(1-\phi[\texttt{Ca}]\right)^3}\left(1+\left(\frac{\texttt{d0}}{\texttt{dj[Ca]}}-1\right)\phi[\texttt{Ca}]\right);$$

```
Simplify[A0jstarV0]
```

$$\frac{1}{\texttt{d0}^3\left(-1+\phi[\texttt{Ca}]\right)^3}\left(-3\,\texttt{d0}\,\texttt{dj[Ca]}^2\left(-1+\phi[\texttt{Ca}]\right)^2 + \texttt{dj[Ca]}^3\left(-1+\phi[\texttt{Ca}]\right)^3 - \texttt{d0}^3\left(1+2\,\phi[\texttt{Ca}]\right)^2 + 3\,\texttt{d0}^2\,\texttt{dj[Ca]}\left(-1-\phi[\texttt{Ca}]+2\,\phi[\texttt{Ca}]^2\right)\right)$$

Section B

The goal of section B is to evaluate the second term on the right hand side of eqn (I .7),

$$\sum_{j=0}^{N-1}\tilde{A}_{0j}\left(\frac{\partial C_j}{\partial C_a}\right) = \tilde{A}_{0j^*}\frac{\partial C_{tot}}{\partial C_a} + C_{tot}\left\{\frac{\partial \tilde{A}_{0j^*}}{\partial C_a} - \left(\frac{\partial \tilde{A}_{0j}}{\partial C_a}\right)_{j=j^*}\right\}. \quad (I.7)$$

via differentiation of eqn (I.11)

$$\frac{\tilde{A}_{0j}}{\frac{\pi}{6}{d_0}^3}$$
$$= \left(\frac{d_j}{d_0}\right)^3 + \frac{\left\{1+\left[\left(\frac{d_j}{d_{j^*}}\right)^3-1\right]\phi\right\}}{(1-\phi)}$$
$$+ 3\left(\frac{d_j}{d_0}\right)\frac{\left[1+\left(\frac{d_0}{d_{j^*}}-1\right)\phi\right]\left\{1+\left[\left(\frac{d_j}{d_{j^*}}\right)^2-1\right]\phi\right\}}{(1-\phi)^2}$$
$$+ 3\left(\frac{d_j}{d_0}\right)^2\frac{\left[1+\left(\frac{d_j}{d_{j^*}}-1\right)\phi\right]\left\{1+\left[\left(\frac{d_0}{d_{j^*}}\right)^2-1\right]\phi\right\}}{(1-\phi)^2}$$
$$+ 9\phi\left(\frac{{d_j}^2}{d_0 d_{j^*}}\right)\frac{\left[1+\left(\frac{d_0}{d_{j^*}}-1\right)\phi\right]\left[1+\left(\frac{d_j}{d_{j^*}}-1\right)\phi\right]}{(1-\phi)^3}\,. \qquad (I.11)$$

and (I.13)

$$\frac{\tilde{A}_{0j^*}}{\frac{\pi}{6}{d_0}^3} = \lambda^3 + \frac{3\lambda^2}{(1-\phi)} + \frac{3\lambda(1+\phi-2\phi^2)}{(1-\phi)^3} + \frac{(1+2\phi)^2}{(1-\phi)^3}\,, \qquad (I.13)$$

in Appendix I, in order to acquire eqn (I.17)

$$C_{tot}\left\{\frac{\partial\tilde{A}_{0j^*}}{\partial C_a} - \left(\frac{\partial\tilde{A}_{0j}}{\partial C_a}\right)_{j=j^*}\right\}$$
$$= \frac{1}{C_a}\left\{1 + \frac{\lambda^{-1}(2-3\phi+\phi^3)}{(1-\phi)^3} + \frac{\lambda^{-2}(1+6\phi-6\phi^2-\phi^3)}{(1-\phi)^3} + \frac{\lambda^{-3}\phi(2+\phi)^2}{(1-\phi)^3}\right\} 3\phi\frac{\partial lnR_{j^*}}{\partial lnC_a}\,, \qquad (I.17)$$

```
Clear["Global`*"]
(*Eqn (I.11) from Appendix I*)(*Note, A0jV0 = (1/V0)A0j , where V0 = pi/6*d0^3*)
A0jV0 = (dj/d0)^3 + (1 + ((dj/dj[Ca])^3 - 1) ϕ[Ca])/(1 - ϕ[Ca]) +
  (3 (dj/d0))/(1 - ϕ[Ca])^2 (1 + (d0/dj[Ca] - 1) ϕ[Ca]) (1 + ((dj/dj[Ca])^2 - 1) ϕ[Ca]) +
```

$$\frac{3\left(\frac{dj}{d0}\right)^2}{\left(1-\phi[Ca]\right)^2}\left(1+\left(\left(\frac{d0}{dj[Ca]}\right)^2-1\right)\phi[Ca]\right)\left(1+\left(\frac{dj}{dj[Ca]}-1\right)\phi[Ca]\right)+$$
$$9\,\frac{dj^2}{d0*dj[Ca]}\,\frac{\phi[Ca]}{\left(1-\phi[Ca]\right)^3}\left(1+\left(\frac{d0}{dj[Ca]}-1\right)\phi[Ca]\right)\left(1+\left(\frac{dj}{dj[Ca]}-1\right)\phi[Ca]\right);$$

```
(*Differentiate eqn (I.11) and print the result, i.e. Evaluate B2 = (1/V0){∂Ca A0j}*)
B2 = Simplify[∂Ca A0jV0];
(*Now, using the printed result from the previous line,
replace dj in printed result with dj[Ca],
in order to acquire (1/V0){∂Ca A0j}_j=j*. Then, Store result in B3 below *)
B3 = Simplify[ 1/(d0^2 dj[Ca]^4 (-1+ϕ[Ca])^4) dj[Ca]
    (-9 dj[Ca] (-2 d0 dj[Ca] (d0+dj[Ca]) + (d0^2+3 d0 dj[Ca]+dj[Ca]^2) dj[Ca])
      ϕ[Ca]^3 dj'[Ca] + 3 (4 d0^2 dj[Ca]^2 - 4 d0 dj[Ca] (d0+dj[Ca]) dj[Ca] +
        (d0^2+3 d0 dj[Ca]+dj[Ca]^2) dj[Ca]^2) ϕ[Ca]^4 dj'[Ca] + dj[Ca]
      (d0^2 dj[Ca]^2 + 3 d0 dj[Ca] (d0+dj[Ca]) dj[Ca] + 3 (d0^2+3 d0 dj[Ca]+dj[Ca]^2) dj[Ca]^2)
      ϕ'[Ca] + ϕ[Ca] (-3 (d0^2 dj[Ca]^2 + 2 d0 dj[Ca] (d0+dj[Ca]) dj[Ca] +
          (d0^2+3 d0 dj[Ca]+dj[Ca]^2) dj[Ca]^2) dj'[Ca] + 2 dj[Ca] (5 d0^2 dj[Ca]^2 +
          6 d0 dj[Ca] (d0+dj[Ca]) dj[Ca] - 3 (d0^2+3 d0 dj[Ca]+dj[Ca]^2) dj[Ca]^2) ϕ'[Ca]) +
    ϕ[Ca]^2 ((-9 d0^2 dj[Ca]^2 + 9 (d0^2+3 d0 dj[Ca]+dj[Ca]^2) dj[Ca]^2) dj'[Ca] +
      dj[Ca] (16 d0^2 dj[Ca]^2 - 15 d0 dj[Ca] (d0+dj[Ca]) dj[Ca] +
        3 (d0^2+3 d0 dj[Ca]+dj[Ca]^2) dj[Ca]^2) ϕ'[Ca]))];

(*Eqn (I.13) from Appendix I*) (*Note,
A0jstarV0 =(1/V0)A0j* , where V0 = pi/6*d0^3*)
A0jstarV0 = (dj[Ca]/d0)^3 + 1/(1-ϕ[Ca]) + 3 (dj[Ca]/d0)/(1-ϕ[Ca])^2 (1+(d0/dj[Ca]-1)ϕ[Ca]) +
    3 (dj[Ca]/d0)^2/(1-ϕ[Ca])^2 (1+((d0/dj[Ca])^2-1)ϕ[Ca]) + 9 (dj[Ca]/d0) ϕ[Ca]/(1-ϕ[Ca])^3 (1+(d0/dj[Ca]-1)ϕ[Ca]);

(*Differntiate eqn (I.13), i.e. Evaluate B1 = (1/V0)∂Ca A0j* *)
B1 = Simplify[ ∂Ca A0jstarV0];

(*Now, finally, evaluate the second term on the right hand side of eqn (I.7),
i.e. (1/V0)*{∂Ca A0j*-{∂Ca A0j}_j=j*}*)
Simplify[B1 - B3]
-((3 (-dj[Ca]^3 (-1+ϕ[Ca])^3 + d0^3 ϕ[Ca] (2+ϕ[Ca])^2 + d0 dj[Ca]^2 (2-3 ϕ[Ca]+ϕ[Ca]^3) -
      d0^2 dj[Ca] (-1-6 ϕ[Ca]+6 ϕ[Ca]^2+ϕ[Ca]^3)) dj'[Ca]) / (d0^3 dj[Ca] (-1+ϕ[Ca])^3))
```

Section C

The goal of section C is to combine eqn (I.7)

$$\sum_{j=0}^{N-1} \tilde{A}_{0j}\left(\frac{\partial C_j}{\partial C_a}\right) = \tilde{A}_{0j^*}\frac{\partial C_{tot}}{\partial C_a} + C_{tot}\left\{\frac{\partial \tilde{A}_{0j^*}}{\partial C_a} - \left(\frac{\partial \tilde{A}_{0j}}{\partial C_a}\right)_{j=j^*}\right\} . \quad (I.7)$$

with eqn (I.16)

$$\tilde{A}_{0j^*}\frac{\partial C_{tot}}{\partial C_a} = \frac{1}{C_a}\left\{1 + \frac{3\lambda^{-1}}{(1-\phi)} + \frac{3\lambda^{-2}(1+\phi-2\phi^2)}{(1-\phi)^3} + \frac{\lambda^{-3}(1+2\phi)^2}{(1-\phi)^3}\right\}\left(\phi_a - 3\phi\frac{\partial lnR_{j^*}}{\partial lnC_a}\right). \quad (I.16)$$

and eqn (I.17)

$$C_{tot}\left\{\frac{\partial \tilde{A}_{0j^*}}{\partial C_a} - \left(\frac{\partial \tilde{A}_{0j}}{\partial C_a}\right)_{j=j^*}\right\} = \frac{1}{C_a}\left\{1 + \frac{\lambda^{-1}(2-3\phi+\phi^3)}{(1-\phi)^3} + \frac{\lambda^{-2}(1+6\phi-6\phi^2-\phi^3)}{(1-\phi)^3} + \frac{\lambda^{-3}\phi(2+\phi)^2}{(1-\phi)^3}\right\}3\phi\frac{\partial lnR_{j^*}}{\partial lnC_a}, \quad (I.17)$$

to determine eqn (I.18)

$$\frac{m_0(1-\phi)G_{sa}}{N_A k_B T} = (1-\phi)\frac{1}{C_a}\frac{\partial lnC_0}{\partial lnC_a} + \tilde{A}(\lambda,\phi)\frac{\phi_a}{C_a} - \tilde{B}(\lambda,\phi)\frac{1}{C_a}\frac{\partial lnR_{j^*}}{\partial lnC_a} \quad (I.18)$$

where

$$\tilde{A}(\lambda,\phi) = 1 + \frac{3\lambda^{-1}}{(1-\phi)} + \frac{3\lambda^{-2}(1+\phi-2\phi^2)}{(1-\phi)^3} + \frac{\lambda^{-3}(1+2\phi)^2}{(1-\phi)^3} \quad (I.19)$$

and

$$\tilde{B}(\lambda,\phi) = 3\phi\left\{\lambda^{-1} + \frac{\lambda^{-2}(2+\phi)}{(1-\phi)} + \frac{\lambda^{-3}(1+\phi+\phi^2)}{(1-\phi)^2}\right\}. \quad (I.20)$$

```
Clear["Global`*"]
(*Here, we combine the radii derivative term of eqn (I.16) with eqn (I.17)*)
(* The Radii derivative term from eqn (I.16)
 multiplied by Ca and divided by dlnRj*/dlnCa is given by*)
A = -3 ϕ (1 + (3 λ^-1)/(1 - ϕ) + (3 λ^-2 (1 + ϕ - 2 ϕ^2))/(1 - ϕ)^3 + (λ^-3 (1 + 2 ϕ)^2)/(1 - ϕ)^3);
(* Eqn (I.17) multiplied by Ca and divided by dlnRj*/dlnCa yeilds *)
A2 = 3 ϕ (1 + (λ^-1 (2 - 3 ϕ + ϕ^3))/(1 - ϕ)^3 + (λ^-2 (1 + 6 ϕ - 6 ϕ^2 - ϕ^3))/(1 - ϕ)^3 + (λ^-3 ϕ (2 + ϕ)^2)/(1 - ϕ)^3);
(* The radii derivative expressions of eqn (I.16) and (I.17) combine to provide *)
B = Simplify[Expand[Simplify[A2 + A]]]
(* Note that the term (-2+ϕ+ϕ^2) in the printed result factors into -(1-ϕ) (2+ϕ)*)
```

$$-\frac{3\phi\left(1+\lambda^2\left(-1+\phi\right)^2+\phi+\phi^2-\lambda\left(-2+\phi+\phi^2\right)\right)}{\lambda^3\left(-1+\phi\right)^2}$$

Section D

The goal of section D is to reduce the expressions within the square brackets of eqn (I.25)

$$\frac{m_0(1-\phi)G_{sa}}{N_A k_B T} = -(1-\phi)\frac{\bar{n}}{C_a} + \left[\tilde{A}(\lambda,\phi) + \frac{(1-\phi)(\bar{n}+1)}{\phi}\right]\frac{\phi_a}{C_a} - \left[\tilde{B}(\lambda,\phi) + 3(1-\phi)(\bar{n}+1)\right]\frac{1}{C_a}\frac{\partial lnR_{j^*}}{\partial lnC_a} \qquad (I.25)$$

where

$$\tilde{A}(\lambda,\phi) = 1 + \frac{3\lambda^{-1}}{(1-\phi)} + \frac{3\lambda^{-2}(1+\phi-2\phi^2)}{(1-\phi)^3} + \frac{\lambda^{-3}(1+2\phi)^2}{(1-\phi)^3} \qquad (I.19)$$

and

$$\tilde{B}(\lambda,\phi) = 3\phi\left\{\lambda^{-1} + \frac{\lambda^{-2}(2+\phi)}{(1-\phi)} + \frac{\lambda^{-3}(1+\phi+\phi^2)}{(1-\phi)^2}\right\}. \qquad (I.20)$$

for the tracer limit, in which $\lambda = 1$ and $n = 0$.

```
Clear["Global`*"]
(*For λ=1, eqn (I.19) becomes*)
A = 1 + 3/(1 - ϕ) + 3 (1 + ϕ - 2 ϕ^2)/(1 - ϕ)^3 + (1 + 2 ϕ)^2/(1 - ϕ)^3;
(*For λ=1, eqn(I.20) becomes*)
B = 3 ϕ (1 + (2 + ϕ)/(1 - ϕ) + (1 + ϕ + ϕ^2)/(1 - ϕ)^2);
(*For λ=1 and n=0, the square bracket expressions in eqn (I.25) are givn by*)
Simplify[A + (1 - ϕ)/ϕ]
Simplify[B + 3 (1 - ϕ) ]
```

$$-\frac{(1+2\phi)^2}{(-1+\phi)^3\phi}$$

$$\frac{3(1+\phi+\phi^2)}{(-1+\phi)^2}$$

Section E

The goal of section E is differntiate eqn (I.27)

$$\frac{\Pi}{N_A k_B T} = C_{tot}\frac{(1+\phi+\phi^2)}{(1-\phi)^3} \quad . \qquad (I.27)$$

with respect to solute concentration Ca

```
Clear["Global`*"]
pi[Ca] = Ctot[Ca] (1 + ϕ[Ca] + ϕ[Ca]^2)/(1 - ϕ[Ca])^3;
Simplify[∂_Ca pi[Ca]]
```

$$\frac{-(-1+\phi[Ca]^3)\,Ctot'[Ca] + Ctot[Ca]\,(2+\phi[Ca])^2\,\phi'[Ca]}{(-1+\phi[Ca])^4}$$